Designing Granules for Abrasive Cleaning
(using High-Shear Granulation)

VOLUME I

Robert E Maxim
September 2006

PhD *Chemical Engineering*

Sheffield University – Chemical Engineering Dept **Designing**

IMAGING SERVICES NORTH
Boston Spa, Wetherby
West Yorkshire, LS23 7BQ
www.bl.uk

THESIS CONTAINS

CD

ABSTRACT

PhD Research – Robert Maxim

Designing Granules for Abrasive Cleaning (using High-Shear Granulation)

Abstract:
This work investigates the granulation of fine calcium carbonate powder to form micro-granules (less than 100μm). The influence of formulation and operating conditions on granule properties was investigated. This work analyses experimental data using a database approach to relate granulation conditions to granule properties, to find property-to-property relationships and to investigate the influence on the abrasion of Perspex. It was found that the granulation was undertaken in an unstable regime dictated by the need to produce small granules. As a result, it was not possible to achieve reproducibility in making the granules. For the range of granules produced it was difficult to determine variation in abrasiveness within the experimental errors, a detailed error analysis was carried out. A theoretical relationship between strength and porosity is developed and the factors influencing abrasive wear are investigated.

Two theoretical models are presented: 1) Impact Failure model and 2) Granule Consolidation model. The impact failure model relates dynamic impact strength to static strength, which enables the prediction of a failure distribution curve (how many particles will fail per hundred impacts as a function of velocity). This is done using a "*critical normal impact velocity*" determined from the properties of the granule, properties of the impact surface and experimentally measured granule static strength. The granule consolidation model allows the qualitative prediction of the rate and extent of consolidation from granulation conditions. It models the compaction of a granule by describing the packing of its primary particles within an imaginary internal granule. Sphere packing is discussed with implications for determining the maximum packing of a primary particle size distribution.

PhD Research – Robert Maxim: Designing Granules for Abrasive Cleaning (using High-Shear Granulation)

1 Summary

This research investigates the High-Shear Granulation of calcium carbonate powders to form micro-granules. An investigation of the properties of the influence of properties of the granules on the abrasion of Perspex was carried out. The static strength of granules was related to their dynamic impact strength by the development of a theoretical model. A theoretical relationship between porosity and granule strength was developed together with a mechanistic model describing the influence of granulation conditions and ingredients on consolidation. A data-base approach was used to analyse experimental data in order to relate property-to-property relationships of the granules and the relationships between those properties and how the granulator was operated and what was put in. It was found that in order to produce granules of the desired size the granulator was being operated in an unstable regime; as a result it was not possible to achieve reproducibility in the granules. For the range of granules produced, the range of abrasivity was almost insignificant within the experimental errors. A detailed error analysis was carried out and it was found that several of the techniques used contained large errors. The novel aspects of the research are the investigation of microgranules (less than 100μm) and the use of designed granules as abrasive particles.

It was found that the abrasiveness of a substance containing particles cannot be controlled by using granules as the abrasive particles and subsequently changing the properties of those granules this is because the granulation process is an agglomeration and consolidation process, it produces rounded particles. The abrasivity of a system using

round particles becomes less dependent on the size and properties of the particles as the sphericity of the particles increases. Abrasion is shape dependent, angular particles are the most abrasive and abrasion using angular particles has the most scope for varying the abrasion by changing the particle properties and shape – therefore granulation of an abrasive system is only likely to be useful if it is desirable to reduce abrasion and make abrasion largely particle independent. This research examined the Knoop indent method of measuring particle abrasivity and which was found to be inconsistent. An alternative abrasion test was developed but it is not clear from the results of this research that it is any better than the Knoop indent method.

Working with microgranules is very difficult. It is hard to form them in the first place and if they are formed within a batch of granules they only make up a very small percentage (by mass). Once microgranules are formed there are numerous problems with isolating them for the property testing. It was not possible to reproduce any of the batches of granules produced for this research, even when identical conditions were used.
Depending upon the recipe and ingredients used it is believed that the granulation process can be thought of as falling into one of two regimes, stable and unstable analogous to the Laminar, Turbulent regimes in the Reynolds theory of fluid flow. It follows that there must also exist a transition region between these two regimes.
It is believed that the recipe and ingredients chosen for this research fall into an unstable regime and that is why none of the granulation batches could be reproduced.

Even though granules are not appropriate for use in abrasive systems and the granulation recipe used in this research fell into the unstable granulation regime (these conclusions were not made until near the end of the research) the work on developing designer granules is still valid and very useful. This work led to the development of the impact failure model and the novel granule compaction theory. Additionally the need to relate lots of granule properties to each other and the initial recipe led to the design of a simple, yet useful, relational database. The database is easily transferable to other research using high-shear granulators and opens up the possibility of producing a universal data set incorporating the results of many different granulation trials.

The impact failure model came out of the suggestion that static strength might be used to predict the impact failure strength. If this were the case then static strength might be able to predict the abrasive strength. As it turns out it is shown experimentally that abrasivity of granules is independent of static strength. The development of the impact failure model was done to prove this idea and to develop the skills required to do the analysis on abrasive strength. The impact failure model allows the prediction of the failure distribution curve (how many particles will fail per hundred impacts as a function of velocity) by combining the measured static strength with the physical properties of the granule and the impact surface to define a *critical normal impact velocity*.

The granule compaction theory unites the observations and findings of the work covered in the review of the granulation literature into a coherent mechanistic model allowing qualitative predictions of formulation and processing parameter effects on granule compaction. This is useful because it means confounding effects can be taken into account when analysing results. The theory describes how granule compaction can be modelled and how all the processing and formulation parameters used in this research affect it. Following on from this theory an algorithm has been developed to find the interparticle space at maximum packing for particle size distributions. An analysis of the interparticle space of the packing structure of mono-disperse spheres over length ranges up to 2 particle diameters was also carried out; a general equation is given relating the interparticle space to the packing structure, the particle diameter and the binder layer thickness.

Because of the scope of this research and the power of the relational database to show property to property relationships as well as property to formulation and processing parameter relationships there are lots of apparent trends and conclusions from the work, even though batch reproducibility was a problem. Some of the most important conclusions are included here:

Granulation is not suitable for producing abrasive particles.

Shape and material are the most important particle factors affecting abrasion.

Toothbrush heads should not be used as the counterbody during abrasion testing when a PMMA substrate is used as the toothbrush will cause more abrasion than any particles.

Static strength is generally accepted to be inversely related to porosity, but the porosity is not easy to measure accurately; mercury porosimetry and helium pycnometry are not suitable for measuring the porosity of small granules. Any work relating to porosity should be examined to determine the accuracy of the porosity measurements before believing the conclusions.

Granule compaction is related to porosity and by following the novel granule compaction theory any factors leading to greater compaction will lead to lower porosity and higher strength.

Granule consolidation eventually leads to surface wetness (assuming enough binder is present).
Surface wet granules leads to snowballing.

Increasing the binder ratio increases the static strength. Although binder content was found to be proportional to the binder ratio no relationship between binder content and static strength was found.

Moisture content cannot be assumed constant when determining binder content by thermogravimetric analysis.

Primary particle type affects granule static strength; it is believed that shape is the important particle property as this affects interparticle friction and spatial arrangement during consolidation, which in turn affects strength.

2 Contents

3

3.1 Symbols

Symbol	Definition
$\bar{a}$	Dimensionless area
$\bar{F}$	Dimensionless force
$\bar{t}$	Dimensionless time
a	Contact area
A	Non-dimensionalising area constant
a	Thickness of binder layer
A_{as}	Cross sectional area of abrasion scar
A_o	Normalised cross sectional area of abrasion scar
A_{pb}	Surface area of particle bed
b	Binder constant
B	Constant in Aurbach's equation
b'	Thickness of binder layer at maximum packing of mono-size spheres
b''	Modified binder constant
B_{lbr}	Limiting interparticle space
B_s	Volume of binder on granule surface
B_v	Interparticle space
B_v''	Internal granule interparticle space
B_{va}	Asymptotic interparticle space
B_{va}*	Granule interparticle space at the start of internal granule consolidation
B_{vo}	Interparticle space at end of granulation induction period
c	Parameter in Weibell equation
D	Diameter of granule
d'	Diameter of mono-size sphere
d_g	Actual individual size of granule
d_o	Characteristic length of PPSD (primary particle size distribution)
d_p	Projected diameter
E	Youngs modulus
E_A	Abrasion energy
E_g	Youngs modulus of granule
E_p	Youngs modulus of platen
F	Force
F'	Non-dimensionalising force constant
F_a	Applied load to abrasion plate / head
F_c	Standard force
F_{calc}	Failure load of equivalent single particle
F_{cr}	Critical Load
H	Parameter in Shipway equation
h	Bed height
H	Hardest material (fig 2)
H_a	Hardness of abrasive particle

h_o	Initial bed height
H_s	Hardness of substrate
H_v	Vickers hardness value
K	arbitrary constant in abrasion energy derivation
k	Constant in Laugier equation
k_1	Constant equation (11)
k_2	Constant
k_3	Constant
k_4*	Modified ln (τ/α')
k_5	Consolidation rate constant (Iveson consolidation model)
l	Length or (dimension of length in derivation of abrasion energy)
l_{as}	Length of width of abrasion scar
l_g	Particle (granule) diameter (characteristic size of sample)
l_o	Characteristic length
m	Constant in weibull distribution
M	Medium hardness material (fig 2)
M	Dimension of mass (derivation of abrasion energy)
m_g	Mass of granules added to abrasion plate
m_l	Weighted mass of lower sieve size (taken from PSD)
m_u	Weighted mass of upper sieve size (taken from PSD)
N	Number of undamaged granules per 100 fired
n	Power constant in Aurbach's equation
N_1	Number of segments that a PPSD is split in order to perform the critical packing algorithm
N_2	Number of drum revolutions (Iveson consolidation model)
P	Applied nominal pressure
p	Packing factor
p'	Packing factor used in mono-size sphere analysis
r	Radius of circle of contact
R	Radius of granule (sphere in original Hertzian derivation)
S	Softest material (fig 2)
S_a	Speed of abrasion counterbody
s_l	Lower sieve size
s_u	Upper sieve size
T	Non-dimensionalising time constant
t	Time defined by equation (17)
t*	Time defined by equation (20)
t'	Critical start time of granule consolidation
t''	Time at onset of internal granule consolidation
t_a	Abrasion time
t_{real}	Granulation run time
u	Normal velocity of granule
u_a	Abrasion speed
u_f	Normal failure velocity of granule
v	Velocity of granule
V_b	Volume of binder

V_c Volume of cube
V_{cv} Volume of control volume
V_{db} Volume of density bottle
V_g Volume of granules
V_o Volume of oil
V_p Volume of powder
V_{pp} Volume of $CaCO_3$
V_{pp} Volume of primary particles
V_s Volume of spheres in control volume
W Load
W_1 Mass of bottle + stopper
W_2 Mass of powder + bottle + stopper
W_3 Mass of powder
W_4 Mass of bottle + stopper + powder + oil
W_5 Mass of oil
W_6 Mass of empty crucible before burning
W_7 Mass of crucible + granules before burning
W_8 Mass of granules
W_9 Mass of crucible + granules after burning
W_{10} Mass of empty crucible before drying
W_{11} Mass of crucible + granules before drying
W_{12} Mass of crucible + granules after drying
$x_{i,j}$ Sphere 'i' from segment 'j' of the PPSD
Y Yield stress
z Elevation of centroid of granule above platen
α Pressure coefficient (coefficient of friction)
α' Gradient of slope equation (36)
α'^* Modified α' in equation (35)
γ Surface tension
ε Porosity
ε_o Initial Porosity (Iveson consolidation model)
ε_{min} Final granule Porosity (Iveson consolidation model)
θ Angle of impact with platen (90° being perpendicular)
θ_1 Angle between vertical motion of indenter and the line drawn between the centre of the indenter and sphere
λ Lowest coefficient of friction between indenter and surface
μ Viscosity
ν Poissons ratio
ν_g Poissons ratio of granule
ν_p Poissons ratio of platen
ρ_a Density of particle
ρ_b Density of PEG (true)
ρ_g Density of granule
ρ_o Density of oil
ρ_p Density of powder (bulk density of powder)
ρ_{pp} Density of $CaCO_3$ (true)

σ Stress
σ_c Compressive stress
σ_F Particle failure load (granule)
σ_{max} Maximum stress in contact zone (hertzian)
τ Shear stress
τ'_o Factor $(k_2/k_3)\tau_o$
τ_f Shear failure stress
τ_o Cohesive strength
τ'_o* Modified τ in equation (35)
ψ Sphericity
ω Agitation rate constant (dimensionless agitation intensity per unit time; incorporating energy inputs, rotational velocity and viscous effects in an undefined lumped parameter in eqn. 16 and 19)
ϵ Strain
ϵ_N Natural strain = $\ln (h_o/h)$

3.2 Figures (page)

3.2.1 Plots (from database queries)

3.3 Appendices

Appendix A	Predicting dynamic failure of dense granules from static compression tests (Maxim, et al., [66])
Appendix B	Crushing tests graphs showing qualitative effects of the variables in equations (4), (5) and (6): force, radius and Youngs modulus and k factor. Chart 1 shows total contact area as a function of size and pressure Chart 2 shows the load per particle as a function of particle size Chart 3 shows the effect of particle size on total pressure Chart 4 large to small shows the effect of reduction in size of particles on both the pressure and total contact area Chart 5 Shows he effect of different k values and particles diameter on the contact area
Appendix C	Derivation of analysis of binder content and packing structure.
Appendix D	Abrasion testing report (early copy)
Appendix E	Original drawings for design of abrasion rig
Appendix F	Binder Content Verification
Appendix G	Database – electronic form
Appendix H	Plots from queries from results database
Appendix I	Plots from preliminary testing – Mercury Porosimetry
Appendix J	Theoretical impact failure distribution of granules (Maxim et al. [1])
Appendix K	Modelling effects of processing parameters on granule porosity in high-shear granulation (Maxim et al. [100])

4 Introduction

This thesis is written to fulfil the requirements of a PhD in Chemical and Process Engineering at the University of Sheffield.

This thesis describes the investigation into the design of granules for abrasive cleaning. The granules were made using a high-shear granulator. Different granules were made by changing the way the granulator was operated and the ingredients that were put into it. The granules that were produced were then tested to determine their abrasive strength as well as several other properties. The results of these tests are presented along with proposed relationships between the properties of the final granules and also the relationships between these properties and the way in which the granules were made.

The thesis starts with a background description and literature review of abrasion and abrasive wear, including current testing methods and then moves on to strength and high-shear granulation. Also included are a section on porosity (as this affects strength) and a section on packing (as the theory of packing spheres provides the background to the logic behind the approaches for determining the "critical packing state" – an idea introduced later in the thesis). Three different approaches to consolidation are also described.

The literature review is followed by the Terms of Reference, which describes what the work of this research is aiming to achieve and puts it in context of the existing work described in the literature review.

The Theory section describes the development of a model relating the static strength of granules to the dynamic impact strength of granules. The fact that such a relationship was determined to exist, forms the basis for the hypothesis that the abrasive strength of granules is related to the static strength. It is far easier to measure the static strength than either the dynamic impact strength or the abrasive strength; so having such relationships makes the indirect determination of these strength properties from the static strength far easier than their direct determination. The detailed derivation of this relationship between static strength and impact strength is included in the appendix A.

There is a section describing a novel theory for granule compaction, this gives a mechanistic model for the compaction of a granule and its hypothetical internal granule. The full theory is included in the main report and shows how the way in which a granulator is operated affects this model. An algorithm is then developed for the determination of the maximum possible packing of a collection of primary particles. The appendix relating to this compaction theory gives the analysis of the binder content and porosity of 2 different packing structures. Note that the algorithm and the method described in section 7.3.4 for finding packing density are both un-tested, but are of potential value and should be considered for future work.

There is a section describing the Knoop indent method of determining the abrasive strength and why this is believed to be an unsuitable method. An alternative abrasion test was designed and used for the testing that produced the results upon which this thesis is based.

The experiments section describes the systematic experimental design. It describes in detail the tests that were used to determine the granule properties and the labelling system that was used to trace the batches of granules through the series of tests. This section also describes the constraints that limited the amount of repetition of results. Following this section is details of the theoretical manipulation of the raw data and the programmes that were written to perform this data manipulation.

The results section presents the results that were produced from the experiments. There is comprehensive presentation of all the inter-relations between the properties being measured. There is a section describing the design of the database used for the results entry and how this database allows the easy presentation of a variety of relationships.

The results analysis section describes the meaning of the results and attempts to determine the relationships between the granule properties and the way in which they are made. This section discusses the usefulness of the results obtained.

5 Literature Review

5.1 Overview of Literature

There are several people who claim research in Granulation (and tribology) to be very system specific (this work, Tabor, [2], Sochon, et al., [3], Aulton and Banks, [4]) or that there is "...no general, single, bonding mechanism which is applicable to all particle → granule forming processes." (Sherrington and Oliver, [5]), whose work arose out of the recognition by the Institution of Chemical Engineers in the late 70's that granulation was becoming increasingly important with an extensive literature scattered over a wide range of (principally trade) journals already existing. The work on granulation (like tribology) was mainly empirical production recipes arrived at by a process of trial and error. Even as recently as 2000 (Scott, [6]) and 2001 (Iveson, et al., [7], Litster, et al., [8]) people are still calling granulation an art rather than a science, however it is unclear how many of these empirical procedures actually have a general application being based upon sound principles. Although Iveson et al. claim in their conclusion that such statements are now out of date, their review contains 3 examples of where the system specific nature of granulation research has led to different researchers arriving at contradictory conclusions;

1) The difference between the effect spray nozzle positioning on granule size found by Rankell, et al., [9] and Davies and Gloor, [10], who state that as the nozzle height increases the average granule size decreases, and Schaefer and Worts, [11] who report no change in mean granule height. This particular discrepancy is likely to be due to the combined effect of equipment set-up on the spray flux and the formulation effect on the wetting kinetics.
2) The difference between the dynamic strength of pendular liquid bridges holding granules together found by Mazzone, et al., [12] using viscous binder and Harnby, et al., [13] using water.
3) The effect of binder content on the extent of granule consolidation as a result of the viscosity of the binder.

In another work, Iveson, et al., [14] reiterate their view that granulation has been more of an art than a science. Their statement that "..it is still impossible to predict the granulation behaviour of a new formulation from knowledge of its fundamental properties. Neither is

it known how to vary a formulation in order to obtain a desired change in product properties." seems almost inappropriate in relation to their extensive review on nucleation, growth and breakage. It is correct to say that we have a qualitative understanding of the mechanisms of granule growth, but as the contradictions above highlight it is often difficult to decipher the results and observations of other researchers to get at the fundamental relationships because so much is system specific.
Mort, [15] at the CHoPS 4 conference, claimed that this (not being able to predict behaviour) should no longer be the case. He gives 2 approaches to move granulation from an art to a science by connecting the fundamental models of the microscopic scale to the industrially useful macro scale; one is an approach for process modelling and one is an approach for product design. He argues that if care is taken to develop the meso-scale constitutive models that link the micro-scale to the meso-scale and also the meso-scale to the macro-scale it is possible to link the micro-scale to the macro-scale (as in scale-up or process simulations to predict overall system performance of an agglomeration circuit, including, for example, recycle loops). The alternative is to consider the relevant set of properties or other distributed aspects that are key to making the linkage (although these two methods are essentially the same thing). This is what is currently lacking in the granulation literature; detailed constitutive meso-scale models that will allow existing fundamental micro-scale relationships to qualitatively (and ultimately quantitatively) predict macro-scale properties. The granule compaction theory presented in this thesis (sect 7.3) tries to do just this; provide a constitutive meso-scale model that relates to macro-scale parameters. It takes the relevant set of micro-scale properties (e.g. binder viscosity, surface tension and solid-liquid contact angle), which are aspects of a macro-scale parameter (in this example, the binder type), and forms them into a constitutive meso-scale model relating the macro-scale formulation and processing parameters to the relevant micro-scale properties.

The meso-scale is where the vast majority of the research work is done and produces lots of complicated theories and investigations. It is based on the vast knowledge at this scale that people like Iveson come to the conclusion that granulation can now be modelled accurately and thus make useful predictions, but these models are based on system

specific conditions. It was shown in his own review (and the others discussed later) that the relationships are not only dependent upon the material properties of the binder and primary particles being used, but that the formulation and processing parameters combined with the equipment parameters affect the relationships in ways that prevent them being widely applicable (let alone universally). There is also the problem that much of this work has to be done using "model" systems due to the random nature of granulation and the heterogeneous nature of the produced granules. For example work by Iveson, et al., [16] on consolidation of granules uses hand-kneaded powder as the starting point of the experiments to try to avoid the nucleation stage.

This is changing, Iveson, et al., [7] suggests that it is now possible to make useful predictions about how a material will granulate "provided that the correct material properties and operating parameters are known...". Work at the micro-scale attempts to show micro-scale processes, the properties that are important and how those material properties can be found.

Work in Tribology and wear is also very system specific, Meng and Ludema, [17] investigated lots of wear models and equations and found that "No single predictive equation or group of limited equations could be found for general and practical use. The reasons include the perpetuation of erroneous and subjective expressions for the mechanisms of wear, the slow pace of translation of microscopic observations into macroscopic models of the wearing processes and the paucity of good experiments to verify proposed models." However recent work on maps, both wear maps (Williams, [18], Lim and Ashby, [19]) and granulation growth maps (Iveson, et al., [14]), seem to be providing a way round the traditional system specific work that is done. By finding the operating conditions for transition regions between regimes, experimental work can then be designed to avoid these regions, this means that the equations and models produced will have more general applicability (as long as it is realised that they apply only within a certain region). The actual application of these maps is limited by the parameters used for the X-axis and Y-axis; Ivesons growth maps are limited by the "maximum granule pore saturation", which is a complex function of formulation properties (this is thought to be the equivalent of the limiting interparticle space, B_{lbr}, at the critical packing state described in the section on the novel compaction theory of this report), a wear map

(scratch map) for PMMA described by Briscoe, et al., [20]is limited by the confusing presentation of the map (they use the scratch velocity and a variable called effective strain, which appears to depend upon the indenter geometry, to predict the wear regime and the scratch hardness – which appears to be a material property). This map is not applicable to the granulation wear testing in this work as it is not possible to determine either the strain, load per particle or individual wear track diameter for a multi-particle system. It does however indicate some qualitative trends – that increasing the velocity increases the effective scratch hardness of the PMMA, in other words fast abrasion testing will tend to produce less wear per applied load (this means that any abrasion testing comparing different granules using PMMA as the substrate should use a fixed velocity.) this is assumed to be due to the visco-elastic response of PMMA. The maps for other polymers presented by Briscoe, et al., [20] are all material specific, compounding the argument that much of the work (and applicability of the work) in tribology and wear is system specific.

There are many good reviews and books relevant to the 3 main subject areas covered by this research; granulation, strength and abrasion.
For granulation an article by Knight [21] in the Powder Technology special issue Salman and Hounslow, [22] describes what he considers to be 3 areas of granulation that warrant intensive further investigation; these being strength of wet agglomerates, better models for granule coalescence and the methods of designing mixers that inherently give better control of granulation. The special issue covers aspects of granulation across the length scales, from the micro-mechanistic modelling using real particles sticking to each other to larger scales real impact experiments and numerical simulation of crushing tests. 3 separate articles Bardin, et al., [23], Reynolds, et al., [24] and Fu, et al., [25] show the natural heterogeneity present in granulated products that makes for the challenges considered by Knight and this all links back to the importance of determining the linkages across the length scales as described by Mort, [15] earlier.
A much cited reference on granulation is the review article by Iveson, et al., [7], which covers the main areas of interest in agitated wet granulation (high-shear granulation using binders): Nucleation, growth and breakage. When combined with the book written by the

same researchers a few years later, Litster and Ennis, [26], these 2 sources provide a good start point for anybody working in mixer granulation and are abundant with relevant references to further reading where specific examples of effects of processing parameters and formulations are required. An older book which gives a more general introduction to granulation is by Sherrington and Oliver, [5], this includes an overview of other granulation systems such as spray-granulation and fluidised bed. It also has an interesting section on packing theory; although the first part on packing of equi-sized spheres and the coordination number is better covered by Sloane, [27] the work on packing of continuous size distributions and multi-component mixtures is very useful. It shows that the theoretical packing density is dependent on the ratio of the sizes of the large and small particles (being packed) and can effectively reach infinity if the sequentially smaller particles fit into the gaps between the larger particles (in 2-dimensional packing of circles this is known as a the Apollonian Gasket – the sequential addition of inner "Soddy circles"). The book by Litster and Ennis, [26] includes much of the previous work covered by co-workers such as Tardos et al., [28], Ennis, [29] and Iveson (Iveson et al., [16] and Iveson and Litster, [30]) on granule consolidation and coalescence, these references are nearly always cited in literature reviews covering granulation (especially mixer granulation) Lu, [31], Fu, [32], Azadehnia, [33] and Gabbott, [34]. This work on consolidation and how the operating conditions and formulation affect the rate of consolidation is best covered in the literature reviews of Fu, [32] and Lu, [31] (although the detail is not satisfactory in all cases, for example the evaluation of the empirical exponential decay curve representing the change in porosity of a consolidating granule; which needs to be studied from Iveson and Litster's, [30] original work). Azadehnia, [33] covers the effect of the Stokes Number (ratio of inertial energy to viscous dissipation) on coalescence and sums up the effect as "initial kinetic energy > energy dissipation → particles rebound....initial kinetic energy < energy dissipation → particles coalesce". Fu, [32] also covers granule coalescence and gives 6 different numerical and computer simulations used by a variety of workers to cover situations where the granules have viscous liquid layers, are soft, wet, solid and ways of finding the critical granule size and restitution coefficient. The work using Stokes Numbers was not investigated in detail for this work as several of the necessary variables to determine the Stokes Number were

unknown for the system being considered (e.g. Laplace-young pressure deficiency, thickness of the binder layer and hence the viscous force, as well the sizes of individual granules involved in collisions.) It is better to consider qualitative influences of the variables in the equations and how they are changed by the formulation and operating conditions, for example if a granule grows in mass or the impellor speed is increased then the inertial energy will increase and a greater amount of viscous dissipation would be required for coalescence to occur (this greater dissipation could be realised by greater saturation and surface wetness).

The present author was helped by course notes from the particle science course by Salman, [35]. The notes are written to be used with the textbook by Weideman, et al., [36] on structural materials, together they give the essence of strength and deformation (abrasion is surface deformation); that deformation occurs because of the way the molecules and micro-structures (cracks and impurities) of a material react to forces (tensile, compressive and shear) applied to them and how they dissipate any energy input (plastic or elastic movement and crack growth).

Literature reviews and work that cover strength are those by Gabbott, [34] and Samimi, et al., [37], who concentrate on single and bulk compressions. There is a lack of reviews covering impact strength, but work by Cheong, [38], Maxim et al., [1] and Salman, et al., [39] cover it slightly; with the present author's proposition that abrasion strength might be related to static strength following on from the work by Maxim et al., [1] as impact strength was found to be related to static strength. Ghadiri and Papadopoulos, [40] goes into a lot of detail on impact attrition, covering the strength of the particles slightly but focusing on the damage to the surface (which is typical of most research on impacts). This is effectively thought of as type of abrasion and falls within the remit of Tribology studies. "Solid-Solid interactions" edited by Adams, et al., [41] is a collection of papers and commentaries from the proceedings of a Indo-UK forum in materials science and engineering; it has papers covering wear, strength testing, lubrication and particles (of special interest is the article by Hutchings, [42] on the determination of the critical stress causing failure in the deformation of brittle particles – which applies to dry granules that are considered as being brittle). A general review of research in the field of Tribology (abrasion) is given by Tabor, [2] in his personal account of his research, which includes a

very readable and easily understood book on the subject Bowden and Tabor, [43]. For a more up-to-date and equation light discussion of Tribology the textbook by Hutchings, [44] written for final year undergraduates on engineering courses is the most appropriate. Hutchings, [45] review on wear tests is fairly comprehensive and introduces the useful idea of "tribological intensity" (which is the severity of wear caused by a mechanical stimulus applied over time). "Engineering Tribology" by Williams, [46] is another good book, covering similar topics as Hutchings, but written in a different style – usefully it includes an introduction to wear maps and all the necessary equations of Hertzian elastic contact theory summarised into a single page. Less useful as a general review is Johnson, [47], which is equation heavy and all the applicable deductions from the detailed derivations could be more easily reached using the books by Hutchings and Williams (and other papers such as Conrad, et al., [48]and Laugier, [49]). However this book would be essential for anybody wanting to go into detailed derivation of the contact mechanics involved in impacts and compressions. As this research is aiming to design granules for cleaning purposes, and it is assumed that the thing to be cleaned will be a stain (effectively a thin coating) the section on soft and hard coatings by Holmberg and Matthews, [50] (in the Tribology Series) usefully covers this (including the effect of hard and soft substrate and coating thickness). Schonert, [51]'s work on physics of breakage is an old paper (1979), but importantly he is one of the co-workers of Rumpf and assumes much of Rumpfs work as fundamental (and generally accepted) to the science behind what he covers.

As already described granulation can be thought of as three length scales: Micro-scale, Meso-scale and macro-scale. The micro-scale includes work such as that by Simons, [52] on the modelling of the interaction between a binder droplet and individual granule, this sort of work is mostly very isolated working in model-systems in an attempt to understand fundamentally what is happening within a single granule

At the macro-scale attempts are made to model the relationships between the primary variables, whereas the micro-scale uses secondary variables. Work in the meso-scale uses both primary variables and secondary variables. Work at the macro-scale attempts to

model real granulation systems and make useful predictions (such as in this research), this scale is very system specific and is still very much the "black art". There are some theories such as population balance modelling, Ramkrishna, [53], that are being used in attempts to link together many of the aspects of the meso-scale work and relate them to macro-scale predictions in a quantitative manner. Currently this is not possible. The majority of the work allows qualitative predictions. Much of the macro-scale work in this research uses meso-scale relationships from other peoples macro-scale work to form qualitative relationships, and in the case of the impact theory, a quantitative relationship.

5.2 Abrasion

In David Tabor's, [2] description of his work over the last 25 years he describes the background of tribology. Much of the research work on abrasion and tribology is driven by technology "...to record and if possible classify the results of investigations involving new materials, new lubricants and new surface treatments. The chief objective is to reduce friction....and to minimize wear." There is less emphasis on researching tribological mechanisms in fundamental terms. Sources of fundamental work on tribology is described in texts such as those by Bowden and Tabor, [43] and Hutchings, [44].

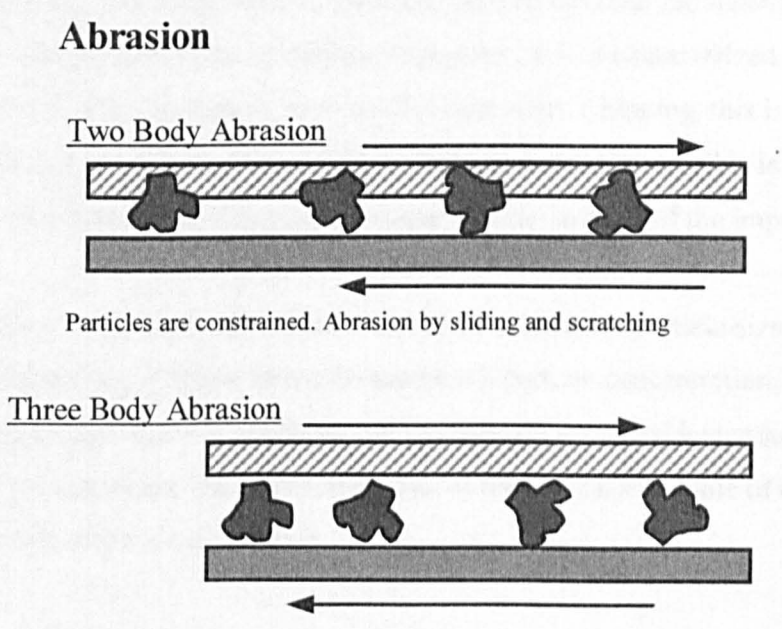

Figure 1 – showing 2-body and 3-body abrasion

Abrasion is defined as the removal of matter by scratching and grinding Chambers dictionary of science and technology Collocott and Dobson, [54]. There are 2 basic forms of abrasion described by Pickles, [55]: 2-body abrasion and 3-body abrasion, shown in figure 1. 2-body abrasion is where only two surfaces are involved, usually with the abrasive particles fixed within the surface of the abrading body. 3-body abrasion is where freely moving abrasive particles are present and forced into contact with the abraded

surface by the 3rd body. An example of 2-body abrasion is the use of sandpaper. An example of 3-body abrasion is using Brasso to clean metal objects. 3-body abrasion is usually less damaging than 2-body abrasion.

The amount of abrasion is influenced by several factors: abrasive particle size Mondal, et al., [56], shape Hamblin and Stachowiak, [57] and strength (hardness) Murugesh and Scattergood, [58], the substrate strength (hardness) Knight, et al., [59], particle concentration Haan and Steif, [60], applied load and tangential velocity of applied load Hutchings, [45], lubrication Hutchings, [61], Bowden and Tabor, [62] and counter-body interactions. There are several forms of abrasive damage / particle motion during abrasion: Tumbling, where the particle rolls and tumbles between the substrate and counter-body causing insignificant damage. Ploughing, this is characterized by the flow of material to the sides and front of the particle impression. Chipping, this is where there is removal of small fragments of material from the substrate. Cutting, this is characterized by material flowing up and forming a lip or separate chip in front of the impression site.

It has been shown by several authors that the effects of abrasive particle size, shape and strength (hardness), the substrate strength (hardness), particle concentration, applied load, lubrication and counter-body interactions can be assessed for individual systems, but the complex interactions means that the current state of the art is not capable of making generalisation applicable to all systems.

5.2.1 Mechanisms of Abrasive Damage

The forces acting on an abrasive particle determine the form of particle motion and abrasive damage taking place. Studman and Field, [63] describe how the original Hertzian theory (1881) predicts the maximum stress, σ, and contact pressure, P, when a sphere is pressed into a flat surface; they show that they are dependent on the radius of the sphere, R, and the load, W:

$$\sigma \propto P \propto \left(\frac{W}{R^2}\right)^{1/3} \qquad (1)$$

They state that the introduction of a single small particle between two surfaces has the effect of reducing the load at which plastic deformation occurs within the surface. However introduction of further particles increases the number of contact points and reduces the stress in the contact region, eventually a stage is reached where the average contact pressure is less than that between two macroscopic bodies.
Studman and Field, [63] go on to describe the geometry of the loads when a spherical indenter is pushed into a flat surface with a single spherical particle trapped between the indenter and the surface. They show that the criteria for a particle slipping out of the way of the indenter occurs if:

$$\frac{\sin\alpha}{1+\cos\alpha} > \lambda \qquad (2)$$

Where, λ, is the lowest value coefficient of friction of either that between the indenter and the particle or the particle and the surface and, α, is the angle between the vertical direction of motion of the indenter and the line drawn between the centres of the indenter and the trapped particle. This shows that the criterion for particle slip is independent of applied load. A critical area of contact is described under which no particle slip occurs; this area is dependent on the size of the indenter and increases as indenter radius increases. This highlights the importance of the relative geometries of the counter-body and the substrate. They also show five possible behaviours when a horizontally sliding indenter contacts a spherical particle (such as in the bristles of a toothbrush): The particle can slip at the contact with the indenter, at the contact with the substrate, the contact of the indenter and substrate; or the particles does not slip leading to either particle fracture or the indenter rolling over the particle. Su, et al., [64] suggest a descriptive model for the forces involved during the sliding abrasion of a micro particle that explains why a reduced downward load would reduce abrasion. Their model indicates that a lower downward force means that a particle is more likely to roll (or tumble) rather than slide (or plough) and as a result there is a less efficient transmission of the energy supplied by the abrading tool to the molecular bonds in the surface of the abraded substrate.

Dwyer-Joyce, et al., [65] investigated the wear of a closed three-body system using diamond particles and a ball-on-disk machine. They found that the nature of the particles affected the abrasion process; ductile particles would flatten and brittle particles would fracture at the inlet to a rolling contact. Small ceramic particles (and diamond dust) would pass through undamaged. Small particles would tumble through the contact whilst large particles ploughed. Abrasive wear was found to increase with particle size and the mass of material worn was found to be proportional to the sliding distance and the abrasive concentration. The concentration in their experiments was measured as mass of abrasive per volume of lubricant. They describe an apparent contradiction between expected behaviour and experimental results; as the particle size decreases the number of abrasive particles increases proportional to the cube of the particle size, whereas the decrease in the cutting area per particle is proportional to the square of the particle size, which would indicate that as the particle size decreases the amount of abrasion should increase. This is in contradiction to their experimental results, which found that abrasive wear decreases as size decreases. Explanations are offered on the basis that larger particles possibly abrade proportionally more material or smaller particles are less likely to be entrained into the contact. (However, as described later, it is the present author's belief that large granules are not abrasive because they are round and smaller particles are more abrasive because of sharp asperities formed from the primary particles). Dwyer-Joyce, et al., [65] suggest that a tumbling-to-ploughing transition size for abrasive particles of approximately 0.88 μm exists below which abrasive wear rapidly drops off with particle size. This size effect at such small sizes can be explained as being the result of spreading the downward load over lots of small particles. Even though the individual force per particle is increased as size decreases, as already described above in the work by Studman and Field, [63], the increased number of particles means the overall load is lowered. A similar effect occurs when a critical concentration is reached for a given size of particle, above which increasing the concentration further reduces the amount of abrasion as the bed of abrasive particles spreads and dissipates the applied load.

The size and concentration effects of the abrasive particles cannot be considered without also considering the nature of the particle. Ductile particles flatten and brittle particles fracture during abrasion. Han, et al., [67] discuss multiple-compression particle breakage and the fatigue failure phenomena in comminution systems. They show that as the compression stresses acting on a particle and the number of compressions increase, the fatigue compression strength decreases. They also showed a dependence on the materials properties. In comminution systems not all the particles are broken down in the first cycle, this is attributed to particles of different size having different strengths (and even particles of the same size having different strength). Particle strength decreases with size; this is mainly due to defects on the surface and micro cracks in the interior of the particle; Samimi, et al., [37]. Larger particles appear to have more defects and are thus weaker, the distribution in number and length of cracks in particles of the same size leads to a strength distribution in particles of the same size. Han, et al., [67] propose that this explains why some researchers have found particle attrition to be independent of particle size Pis, et al., [68] and Veesler and Boistell, [69]. This may not be an important factor where tests use the same homogeneous material, but raises issues about the validity of comparing experiments using granules with those that do not because poorly controlled granules with irregular surfaces and large distributions of internal cracks are likely to have little strength dependence on size. To make the granules more strength to size dependant, and thus make valid comparisons in abrasive properties, the core structure of the produced granules must be homogenized.

As well as the size and concentration of the abrasive particles themselves the nature of the abraded substrate, counterbody and any surface coatings affects the abrasion process. In Holmberg and Matthews, [50] two situations relating to the thickness of a hard coating are described. For thin hard coatings on softer substrates the coating can deform elastically leading to transfer of stresses to the substrate below, often leading to plastic deformation of the substrate and subsequent failure of the coating due to disengagement at the substrate-coating interface. Thick hard coatings remain undeformed as they can support the contact stresses elastically without transmitting the forces to the substrate, failure of thick coatings is generally by a micro chipping or a polishing mechanism.

Montmittonnet, et al., [70] used a finite element model to analyse the indentation of hard faced materials. They also describe circumstances as above where thin hard coatings transmit the deformation to a softer substrate. The depth of penetration into the hard coating is mentioned as the critical parameter referring to a "$1/10^{th}$ rule", Doerner and Nix, [71], which states that the substrate does not affect wear measurements of the coating if the indentation depth is smaller than 0.1 times the coating thickness. For soft coatings Holmberg and Matthews, [50] show that the influence of a hard substrate surface roughness and hard counterbody surface roughness depends upon the thickness of the soft coating compared to the depth of surface roughness.

Hutchings, [72] in his first chapter briefly describes plastic deformation as predicted by the classic Hertzian elastic analysis of a rigid spherical indenter pushed into a plastic half-space (flat platen). Once full plasticity of the platen has been reached the mean contact pressure is independent of the load and remains at 3Y (where Y is the uniaxial yield stress of the material). This appears to be true for other shaped indenters. This means we might expect that when a surface asperity, of any shape, is pressed on to an opposing surface (it does not matter which component yields) the mean pressure over the contact area will always be of the order of 3 times the uniaxial yield stress of the softer material; and the contact area should be directly proportional to the load. In terms of abrasive particles and abrasive cleaning where we have a substrate, a surface layer and an abrasive particle there can be 6 possible combinations of relative hardness's (yield stresses) as shown below. (Where, H, is the hardest, S, is the softest and, M, is in between.)

Referring to Figure 2; when the abrasive particle is harder than the surface, (**b**, **d** and **e**), applying a load will cause significant plastic deformation in the surface without deforming the particle. When the abrasive particle is softer than the surface then the abrasive particle will deform. **f**, is a special case; the surface layer is so thin that it deforms elastically such that the load is transmitted to the substrate and the softer substrate deforms plastically before the particle does.

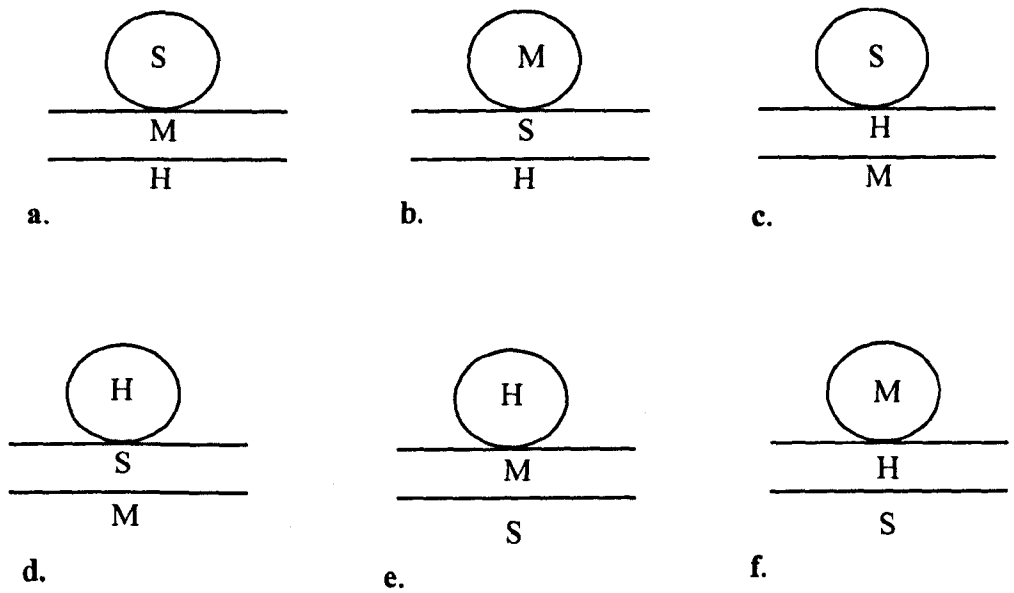

Figure 2 showing different combinations of relative hardness of abrasive particle, substrate and coating layer.

Hutchings, [73] describes something similar in chapter 6 of his book. The ratio of the hardness of the abrasive particle to the hardness of the contact surface dictates the volume wear rate. Particles with hardness much lower than that of the surface cause much less wear than harder particles (see figure 3). When the ratio of the hardness of the particle to the hardness of the surface is greater than about 1.2 then abrasion of the surface will take place and this is often termed *hard abrasion*. When the ratio is less than 1.2, and significantly when it is less than 1, then *soft abrasion* is said to occur. The amount of abrasion occurring with soft abrasion is far more sensitive to the value of the ratio of the hardness's and is largely dependent on whether the particle can sustain a contact pressure high enough to produce plastic deformation in the surface without itself deforming. If the particle fails by flow or fracture before the pressure on the surface reaches 3Y then insignificant plastic deformation will occur in the surface. It should be possible to determine whether a particle will cause significant abrasion by comparing the relative hardness's of the surface and the particle. A problem then occurs: How do you measure the hardness of a micro-granule?

It is evident that the material properties (particularly hardness) are important for determining the abrasive damage. It is therefore important that the correct definition of hardness is used; unfortunately this is not as clear cut as some other material properties.

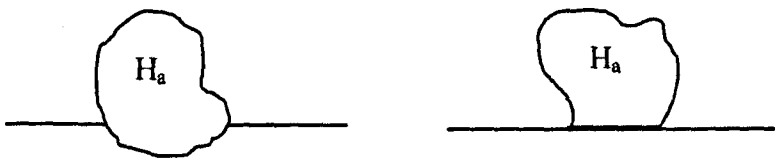

a. $H_a > 1.2\ H_s$ **b.** $H_a < 1.2\ H_s$

Figure 3 Illustration of contact between a) relatively hard particle and soft surface, b) relatively soft particle and hard surface.

Hardness is defined in Chambers dictionary of science and technology Collocott and Dobson, [54] "...signifies, in general, resistance to cutting, indentation and/or abrasion. It is actually measured by determining the resistance to indentation as in Brinell, Rockwell, Vickers diamond pyramid and scleroscope hardness tests... The values of hardness obtained by the different methods are of some extent related to each other, and to the ultimate tensile stress of non-brittle metals.... The resistance that a mineral offers to abrasion. The absolute hardness is measured with the aid of a sclerometer. The comparative hardness is expressed in terms of Moh's scale, and is determined by testing against ten standard minerals: (1) talc, (2) gypsum, (3) calcite, (4) fluorite, (5) apatite, (6) orthoclase, (7) quartz, (8) topaz, (9) corundum, (10) diamond. Thus a mineral with 'hardness 5' will scratch or abrade fluorite but will be scratched by orthoclase."

There are also a variety of hardness tests, Weideman, et al., [36]; scratch tests (Mohs), indentation tests where the size of the impression is measured (Vickers, Knoop and Brinell), indentation tests where the depth of penetration is measured (Rockwell B and C, Shore A) and rebound tests (Shore scleroscope). Each test produces a different number for a given material as there is not a well-defined material property called hardness. These tests all measure different combinations of elastic and plastic deformation. The Vickers hardness test is generally taken as the standard and uses a 136° diamond indenter

pushed into a surface with constant force for a specified time. The hardness is the force divided by the contact surface area of the indentation (kg force mm^{-2}). The Vickers hardness, H_v, bears some relation to the yield stress of a material, but the response depends upon the ratio of Young's modulus, E, to yield stress.
For low Y / E it is found that:

$$H_v \approx 3\,Y \qquad (3)$$

For high Y / E the relationship becomes more complex. Thus the arguments given by Hutchings, [72] do not hold true for all materials.

Gee, [74] describes multiple scratch tests performed on metals and ceramics. Damage to a surface increases with the number of scratch passes but the rate of increase of damage depends upon the nature of the material (hardness / yield stress, visco-elastic dissipation of energy and crack propagation energy / mechanics) as well as the abrasive particle properties (size, shape and hardness / yield stress). The metal surface suffered greater damage for a single scratch, as would be expected as the ceramic is a harder material. However for multiple scratches the ceramic suffered increasingly more damage than the metal and eventually a point is reached where the ceramic material has suffered more damage than the metal for a given number of scratches. This is explained by differences in the contribution of fracture in the development of damage in multiple pass scratches. In ceramic material ploughing and cutting damage per scratch pass do not occur as extensively as in metal, however the multiple passes weaken the surface and lead to significant damage by fracture and chipping.

In conclusion: The nature of the surface and substrate makes more of a difference than the nature of the particle to the amount of abrasive wear. Particle shape and hardness affect abrasion. Granulation cannot significantly affect any of the properties that affect abrasion.

5.2.2 Abrasive Particle Properties (Hardness / Strength / Shape)

Williams, [46], Hutchings, [44] and Dwyer-Joyce, [75] describe how shape affects abrasion. Angular particles cause more abrasion than rounded particles because they are more intrusive into the substrate surface in 2-body abrasion because the contact area is smaller or they are less likely to roll in 3-body abrasion, transferring more of the downward force into the substrate rather than into tangential rolling motion. The relative hardness / strength (as they are related) of the particle and the substrate dictates the amount of penetration of the particle into the substrate before the reactive force of the displacement in the substrate supports the penetration. This penetration and its effect on abrasion is a complex system; the tangential resistance to rolling caused by the frictional forces between the substrate and the particle must be compared to the tangential forces applied by the counterbody. Tangential forces applied by the counterbody differ between 2-body abrasion and 3-body abrasion, if the particle is fixed in the counterbody the tangential force comes from resistance to deformation (strength) of the counterbody and abrasive particle but if the particle is free the tangential force comes from the frictional forces between the particle and the counterbody. This is why 2-body abrasion is generally more abrasive than 3-body; in 2-body abrasion there is only 1 surface where penetration and frictional energy loss occurs, but in 3-body abrasion is occurs at both surfaces.

It was not possible to find any work in the literature attempting to relate the properties of granules and the way those granules are made to the abrasive properties or even to use granulated products as abrasives. That is what this research attempts. The majority of work on tribology investigates how a specific abrasive material affects the wear of a surface by considering operation of the abrasive system or the physical properties of the substrate but rarely the physical properties of the abrasive particles themselves.

5.2.3 Abrasion Testing

Pickles, [76] suggests that when using Perspex as a substrate for abrasion testing using the Knoop indent method (covered in section 7.4.1) the polymer should be left to stand for at least 24 hours before measuring the length of the indent, this is because of the recovery of the elastic component of the deformation. Gauthier, et al., [77] suggests that standard indentation laws can be applied to PMMA (Perspex) but that when determining the elastic relaxation the extent of any plastic deformation will affect this, the effects of the plastic deformation on the elastic recovery was ignored for the purposes of this research and all unrecovered elastic deformation was assumed to be, and measured as, plastic deformation. The fact that PMMA does recover was taken into consideration and is the reason why all measurements on scratched or indented Perspex are taken at least 24hours after testing. This lumping was taken as it is not possible to determine the individual plastic deformation caused by granules of varying sizes, shape and strength and thus it is not possible to determine the effect of the plastic deformation on unrecovered elastic deformation.

Barbezat and Nicoll, [78] describes 3 basic types of abrasion tests. A standard test for 2-body abrasion is the Pin on disk method, whereby a loaded pin is forced against a rotating disk. The pin usually spirals inwards so that only new surface on the rotating disk is used for abrasion. This test can be used to test the wear resistance of the disk or more commonly the wear resistance of a sample fixed to the pinhead. Another abrasion test is the use of high velocity water containing an abrasive particle such as sand – speeds of the order of 170 m/s were quoted as being used. A common 3-body abrasion test is the rubber wheel abrasion test system based on the ASTM Standard G 65-85 – now G65-00e1 ASTM, [79]. This involves a rotating wheel in the vertical plane with a specimen pushed against it by a weighted lever. Abrasive particles are then fed between the wheel and the specimen from a hopper with the abrasive wear being determined by mass loss. Kelly and Hutchings, [80] describe a variation of the rotating wheel tester that uses an abrasive wheel; the abrasive wear is determined by the geometry of the wear scar in this case.

5.3 Strength

Strength is a very general term with no exact definitions, with its meaning varying upon the context in which it is used; e.g. strength of the enemy forces (of numbers), the mans strength was immense (ability to exert a force), a metal ruler is stronger than a wooden one (resistance to damage / failure). This last use is the generally accepted scientific use of strength but even here definitions vary:

"a measure of the ability of a material to support a load"

"the amount of stress an object can receive before it breaks"

One definition draws the distinction between strength of a material and strength of a structure. In material "level of stress at which there is significant change in the state of the material, e.g. yielding or rupture" and in structure "level of loading at which there is significant change in the state of the structure, e.g. inelastic loading, buckling or collapse" [81]. This is important because it draws the distinction between when strength can be defined purely by a load (in structures) and when it needs a reference area in order to define the stress (in material), further the type of failure in the material needs to be defined – whether it is the yield strength or breaking (fracture) strength.

Wikberg and Alderhorn, [82] found that the porosity relates to the static strength, increasing porosity decreases the strength of the granules. It is unclear whether to consider the yield strength of the whole granules, incorporating the porosity, binder type and solid:binder ratio into a single parameter, or to consider them as separate i.e. Looking at the failure mechanism and spread of cracks between pores. Rumpf, [83] is cited, Iveson, et al., [7], as being widely quoted as a model for predicting tensile strength in liquid bound granules. However his model has several drawbacks; it uses 2 major simplifications – that the granule is made of equi-sized spheres and rupture occurs simultaneously across the whole granule, he also uses variables that are difficult to measure directly such as the liquid surface tension and the liquid-solid contact angle. Iveson, et al., [7] also claims that his model underestimates the tensile strength of fine particles with a wide size spread and that it incorrectly predicts the effect of binder content. Work by Kendall, [84] (cited by Iveson, et al., [7]) suggests that strength is

actually proportional to the porosity to the fourth power and that 3-point bending tests are an appropriate way of determining strength. However, as discussed in this thesis the accuracy of conventionally accepted porosity measuring techniques is dubious and papers should not be taken at face value if the exact method of determining the porosity is not given (the experimental work of this thesis shows that the commonly accepted methods are not appropriate for small granules and may not be appropriate for other sizes and shapes of material). Further Weideman, et al., [36] shows how shape affects strength, changing both the compressive and tensile components. Thus it seems inappropriate to use macro-scale tests on different shapes, such as the 3-point bending test, to represent the strength of granules. This may be appropriate for homogeneous large granules, but as this research deals with micro-granules and these are presumed to be heterogeneous a different approach needs to be considered.

Figure 4 shows 3 methods by which cracks could spread within a granule. Very porous granules will have a yield strength depending more on the porosity than the binder content, because the binder will be discrete and cracks won't be able to propagate and the open pores will offer the opportunity for greater granule distortion. Denser granules will have a greater strength dependency on the binder content and type.
As the granules produced by high-shear granulation are generally very dense, it is presumed the strength will relate to the binder content.

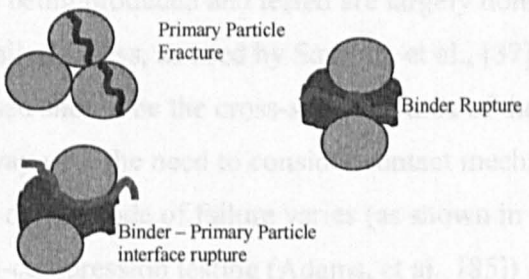

Figure 4 - showing methods of cracking within a granule.

One approach would be to consider the macro-scopic properties of the granules, i.e. to treat the granules as structures and thus relate their strength to an ability to withstand a

load. Conrad, et al., [48] gives a version of the Aurbach equation where the force, F, to crush a granule / particle of diameter, D, is given by the equation:

$$F = B D^n \qquad (4)$$

Where, B, and ,n, are constants, which in the case of granules are thought to represent the lumped effects of porosity, material and binder content.

Preliminary tests crushing individual granules (using a dynamic mechanical analyser and based on the methods in section 7.2.2) showed that small granules fail at a smaller load than larger granules and this fits with the representation given by equation (4) above. It is possible to interpret this as strength increasing with size, but particle strength has been found to decrease as size increases, Samimi, et al., [37]. This apparent contradiction arises because of the different ways of interpreting the strength of a particle; if the strength is taken as the load bearing capacity (as by Conrad and Aurbach) then particle strength increases with size as larger particles can withstand a higher force before failure. If however the strength is taken as the pressure bearing capacity then the pressure at failure may actually be decreasing as particle size increases – because even though the load at failure is increasing the cross-sectional area used to calculate the failure pressure is increasing at a faster rate. This is further complicated by the ambiguity as to whether people are basing the cross-sectional area for determining the pressure on the radius of the particle, R, or the contact radius, r, over which the pressure is being felt.
If the granules being produced and tested are largely homogenous then strength testing based on the failure stress, as used by Samimi, et al., [37], would be the most appropriate and the area used should be the cross-sectional area of the granule (not the contact area – as this does away with the need to consider contact mechanics). If the granules are heterogeneous or the mode of failure varies (as shown in figure 12) then they should be tested by multi-compression testing (Adams, et al., [85]) and considered as structures which means a failure load rather than a failure stress is determined (this is a useful simplification as shown in section 7.2).

An alternative approach to lumping the causes of, and properties affecting, failure together at the macro-scale is to consider the stress intensity fields or crack propagation

energy, in other words the micro-scale causes of the failure. Johnson, [47] gives a detailed mathematical analysis of all aspects of contact mechanics, particularly relevant to determining the stress intensity fields. His work shows how the Hertzian theory on elastic contact can be applied to normal loading, impacts and tangential sliding (abrasion) in order to determine the stress fields. This is useful if the material properties are known and the maximum point stress to induce failure can be determined – because this can then be compared to the maximum stress induced by the loading conditions and geometry concerned. However in terms of heterogeneous micro-granules, where size and mode of failure cannot be determined this usefulness of this work is limited. The derivations and equations that Johnson, [47] does develop that are useful are better illustrated in work such as Laugier, [49], Hutchings, [42] and Shipway and Hutchings, [86]. These enable things such as contact area, pressure and maximum stress to be determined from the granule size and applied loads (which are useful for determining the failure of the granules and the amount of abrasion, as abrasion is dependent on pressure and surface area.)

We know that static strength has a dependency on size, porosity and material Rumpf, [83], Iveson, et al., [7] and Lu, [31]. In the case of granules all of these can change; with the size and porosity depending largely on the processing parameters Knight, et al., [87] (but the formulation parameter: solid:binder ratio, has some effect Van Den Dries, et al., [88], indirectly as it affects granule consolidation). The material property (or yield strength) is related to the surface interactions between the binder and primary particles as well as the ratio of solid:binder.

Laugier, [49] gives a relationship for the force acting on a sphere in contact with a surface:

$$F = \frac{3}{4} r^3 \frac{E}{kR} \qquad (5)$$

Where F is the applied force, r is the contact radius, R is the particle radius, E_g is the Youngs modulus of the particle and k is a material factor given by:

$$k = \frac{9}{16}\left[\left(1-\upsilon_g^2\right)+\left(1-\upsilon_p^2\right)\frac{E_g}{E_p}\right] \qquad (6)$$

Where E_p is the Youngs modulus of the platen, υ_g and υ_p are the Poissons ratio of the particle and platen respectively.

This equation by Laugier requires (relates) the material properties of the particle and the surface, notably the Youngs modulus and the Poissons ratio. It can be imagined that porosity and binder content will affect both of these values for a granule (the porosity affecting the ability to take-up strain and the binder content affecting the ability to absorb energy in viscous dissipation - if liquid).

A small value for the Youngs modulus of the contact surface results in a larger k value and thus a larger contact area per applied force. Increasing the particle size (or radius R) decreases the force per unit area.

5.4 High-Shear Granulation

High-Shear Granulation is the use of shearing forces, due to a mixer blade, to produce the granulating effect. There are 2 levels of variables that need to be considered when reviewing the literature: Primary variables and secondary variables. An example of a primary variable is the binder type, it is a primary variable because it is something that can be changed in isolation and something a machine operator can easily adjust. Viscosity is a secondary variable, because it is dependant on a combination of primary variables: the binder type and temperature.

5.4.1 Types of Granulation

There are different types of granulation for example; fluidised bed and shear-mixing. This research will only deal with shear-mixing.

5.4.2 Processes (Nucleation / Growth / Breakage)

High-shear granulation uses shearing forces to combine and distribute a binder with solid primary particles. The granulation process can be thought of in three stages (Litster and Ennis, [26]):

1. Nucleation or wetting stage – this is where the binder contacts the powder and forms the initial interaction.
2. Consolidation and growth – this is where the binder and particles get packed closer together and granules grow by layering of fine powder on the surface or coalescence with other granules.
3. Breakage and attrition – this is the process of weakening in a granule, surfaces are stripped away by contact with other granules and the equipment or the granules fail and fracture.

The nucleation and wetting stage is dependent on the addition method Scott, [89]. There are three choices for adding the binder: Pour-on, melt-in and spray-on.

Fu, [32] claims that other workers claim (and show) that the addition method is the most important stage in the granulation as it affects the initial nucleation of the granules. It is shown that the initial nucleation and size distributions at nucleation affect the final properties and size distribution of the granules. Knight, et al., [87] showed that at extended run times the high-shear mixer homogenizes and the initial addition method becomes less important. At extended run times it is the balance between the competing processes of "consolidation and growth" and "breakage and attrition" that become important.

An analysis of the method used to produce granules using a High-Shear mixer showed that it can be broken down into 2 distinct types of parameters: FORMULATION parameters and PROCESSING parameters. The formulation parameters are the ingredients and the ratio of the ingredients used to make the granules. The processing parameters are the way the high-shear mixer (Rota-Junior) is used, the equipment settings and recipe.

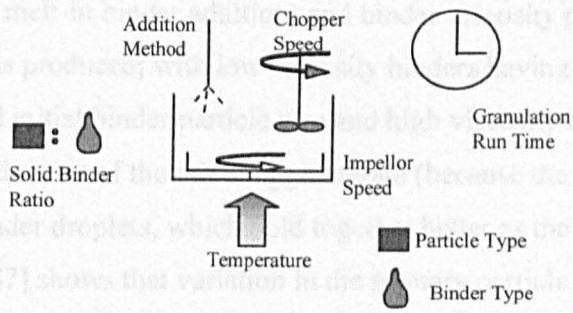

Figure 5. – Processing and Formulation Parameters affecting High-Shear Granulation

5.4.3 Formulation and Processing Parameters

The **formulation parameters** (primary variables) that can be investigated are:

- Primary Particle Type
- Binder Type
- Binder : Primary Particle Ratio

The **processing parameters** (primary variables) that can be investigated are:

- Addition method
- Impellor speed
- Chopper speed
- Temperature
- Granulation Run time

The important formulation and processing parameters are shown in figure 5.

5.4.4 Control and Operation

Bardin, et al., [23] highlights the existing difficulties with control of particle size distribution using high-shear mixers. They show that considerable irreproducibility exists between batches using identical processing conditions, they hypothesise that a major source of poor experimental reproducibility is batch to batch variation in the distribution of the liquid in the wet mass. Schaefer and Mathiesen, [90] show that variation in binder particle size (of melt-in binder addition) and binder viscosity produce variations in the size distributions produced; with low viscosity binders having little relation between granule size and initial binder particle size and high viscosity binders having a greater dependence on the size of the initial agglomerate (because the powder immerses in the large molten binder droplets, which hold together better as the viscosity increases). Knight, et al., [87] shows that variation in the primary particle size produces variations in the granule size distributions, and additionally that these distributions vary with time. As differences are observed in the granule size distribution due to variations in size of primary particles, binder particles and granulation time at the batch to batch level, it is a fair hypothesis that Bardin, et al., [23] propose that these size variations will exist at the scale within a batch, this has been found to be the case Reynolds, et al., [24] This is as a result of variations within binder and primary particles of a single batch combined with the varying times of agglomeration start points.

This demonstrates the problems with testing models of granule coalescence (that there is no single start point and no single model that describes the different interaction behaviour of viscous and non-viscous binders on particle size), and why people like Knight, [21]

express the need to develop better models for granule coalescence. A consolidation model needs to have variables for which the qualitative (if not quantitative) changes can be predicted for a specific combination of formulation and processing parameters. The model must also have enough variables such that any changes (or combinations of changes) to the formulation and processing parameters will have an appropriate variable that they will affect. The Granule Compaction Theory presented in this thesis tries to do this; for example it has variables that allow it to describe the changes in primary particle type (size distribution affects the critical packing state – changes the value of, d, in eqn 16 and ultimately, B_{lbr},)

Knight, et al., [87] showed that the addition method is important during the early stages of granulation; presumably because the different addition methods will have different binder droplet / particle sizes and rates of distribution (start times.) Where the addition method is the most important stage there has been some useful work using the idea of a spray flux Litster, et al., [8] – this relates the rate and size of binder droplet addition to the rate of surface powder renewal. It describes how to predict the different ways that the batch might granulate by the level of saturation of the powder surface with binder. Spray addition is largely accepted as the most suitable method of addition for controlling the process, this is because it is possible (in theory) to measure and control such things as the droplet size, surface area targeted, rate of addition and rate of surface powder renewal – these parameters all form part of the spray flux and thus controlling the spray flux allows certain predictions on expected behaviour (of course you need to know how the spray flux value relates to behaviour for your specific system, in the case of this research the level of control attainable on the sprayer meant that attempting to use the spray flux theory was pointless).

Watano, et al., [91] describe the use of an on-line monitoring system linked to a fuzzy control system to control granule growth. Their work highlights two problems with high-shear granulation; 1) that it is very sensitive to even minor changes in initial moisture content, amount of binder and the operating conditions. 2) that determining the desired

end point is tricky because no reliable tools exist to monitor granule growth directly (and there is a time lag after changing operating parameters during which growth continues.) Their on-line monitoring of granules using image processing allows the progress of the granulation to be monitored continuously and they claim that fuzzy control solves the problem of the lag-time and can control granule growth with high accuracy. This on-line monitoring is probably generally applicable to most granulation processes to some extent, but the claim "...with high accuracy..." is comparative to the use of control by on-off switching of the liquid feed pump. However their assertion that the conventional control technique is by on-off switching of the liquid (binder) feed pump and the statement that high shear granulation is very sensitive to moisture are both misleading because they are system specific observations that are written as if they are generalisations. This is typical of much of the work in granulation; many papers are very system specific and as a result can be misleading. The on-off switching control technique is only applicable to systems where the binder is sprayed throughout the granulation and applies to short granulation times (relative to the granulation times used in this research). The statement that granulation is very sensitive to moisture content is based on work by Holm et al., [92]. Both sets of research used binders in aqueous solutions or water as the binder, meaning that sensitivity to moisture content should really be stated as a sensitivity to binder content, which is the more generally accepted trend. Sochon et al., [3] found that increasing binder content increased the final size of Zinc Oxide granules, and it was also thought to affect the strength (but this was inconclusive because of the confounding effects on size due to the binder content). Iveson et al., [7] suggests that increasing binder content increases the strength, up to the saturation point.

As already mention much of the work in granulation is system specific and the trends that are drawn from the work are often a combination of trends applicable only to the system and the more generally applicable trends. This means that work can get referenced in a misleading way, such as the case with the sensitivity to moisture content by Watano et al., [91] and Lu, [31]'s interpretation of the effects of surface tension (when referring to the contradictory findings of Iveson and Litster, [30] and Ritala et al., [93]) that increasing surface tension increases porosity. The work by Holm et al., [92] states that

"..granulation of a particular material in a high-speed mixer can be very sensitive to even minor changes in moisture content.." and the paper referenced by Watano et al., [91] appears to show that granulation has sensitivity to moisture content because changes in the moisture content affected the results they were getting. Their results were based on the temperature changes as a function of the energy input, and a change in moisture content will mean a change in mass and specific heat capacity of the granulator contents and thus a change in the temperature response to a given energy input. It was reported that preliminary experiments showed that moisture content is the main parameter of the granule growth process. This should really be that the liquid saturation is the main parameter of the granule growth process, as the binder they were using was an aqueous solution and largely water. The reality of the generalisation they had observed is that binder content is the main parameter of the granule growth process, but because it was convenient for them to measure the moisture content of the final granules they reported that as the main parameter rather than determine the binder content. In this system specific work the growth process is very sensitive to the moisture content, meaning the moisture content as a result of the aqueous binder content not the moisture content due to humidity (which is how Watano, et al., [91] are believed to have interpreted it as they wrote "..moisture content, amount of binder and.." as if the moisture content is totally different from the amount of binder). This illustrates how system specific work can cause misinterpretations, particularly where the investigation is of secondary variables (e.g. surface tension and moisture content) that are dependent on the primary variable of binder type. This highlights the need for an overall understanding of the granulation processes (such as the granulation compaction theory in chapter 7.3 of this thesis tries to do: to show how various formulation and processing parameters interact to affect granule consolidation, they cannot and should not be considered in isolation without considering the confounding and compounding affects of other parameters). The work by Holm, et al., [92] does show, indirectly, that granule growth is affected by energy input. Impellor speed does not itself affect granule growth; it is the change in energy input as a result of changing the impellor speed that affects granule growth. Most of this energy goes into heat generation. These conclusions are inferred by measuring the power consumption needed to maintain a given impellor speed and the change in temperature over time as the

granules grow. This suggests that in order to control granule growth and make designer granules the energy input conditions should be controlled (for example the impellor speed, chopper speed and the run time) as well the rate of heat loss (so the granulator jacket temperature and heating rate would need to be adjusted for mass used and ambient temperature.)

There does not appear to be any literature that specifically investigates the effect of humidity on the granulation process in high-shear granulation. There are several papers investigating the effect in fluidised bed granulation, such as Hemati, et al., [94] and Rambali, et al., [95], in these cases humidity does affect the granulation process. It is believed that humidity will affect fluidised bed granulation more because the particles and binder are being agitated in air and the humidity of that air will affect the mass transfer of aqueous binder by changing diffusion coefficients of water between the binder and air and the granules and air, whereas in high-shear granulation mass transfer to and from the air is probably a lot less important. The other effect that humidity will have is on the moisture content of the primary particles; a high humidity will mean the primary particles will have higher moisture content – in fluidised bed granulation this will affect the powders fluidisability due to tiny particles sticking together, whereas in high-shear granulation it won't make as much difference due to the larger mechanical mixing forces. The likely effect of a higher humidity on high-shear granulation will be a change in the specific heat capacity of a powder charge and a change in the strain resistance of the powder to shearing, in other words the energy input from a given impellor speed. Humidity was cited as the cause of the spread in reproducibility of granule batches, Westerhuis, et al., [96], this is a possible cause for the non-reproducibility of results in the work presented in this thesis. Westerhuis, et al., [96] also investigated the effects of moisture in the granules on their tableting properties (but their conclusions in this respect were not clear).

There have been many studies on the effects of a single or few mixer operating or formulation parameters on a single or few granule properties e.g. Davies and Gloor, [10] and Van Den Dries, et al., [88]. There have also been many studies on the relationships

between a single or a few granule properties and other granule properties e.g. Schaefer and Mathiesen, [90] and Wikberg and Alderhorn, [82]. These studies often do not allow for (or qualify) the confounding and compounding effects of other parameters and properties on the property being investigated. This research attempts to put in place a general experimental protocol, and database for storing the results so that any relationships that are investigated can be done in conjunction with the analysis of any confounding and compounding effects. Unfortunately there is no way of getting round the fact that it will be system specific, but intelligent experimental design (such as used by Rambali, et al., [95]) means that the database will allow any and all the primary variables associated with the specific equipment and formulation to be varied and analysed.

Even though much of the work that has been done are stand alone relationships, that are quantitative for the specific system studied they do allow qualitative predictions to be applied to other systems. The most notable is the relationship between porosity and strength Rumpf, [83]; that a granule gets weaker the more porous it becomes – there are several reasons why such theories and relationships are not quantitatively useful in all systems. This is evidenced by the number of studies that confirm this qualitative relationship but there are some reports that Rumpf's equation overestimates the strength of large granules Gabbott, [34]and Iveson et al., [7]. This is because it is not a simple relationship; it is compounded with the effects of the size of the granules, the stress-strain history and presence of pores within the granules. It is also complicated by different measuring techniques used for finding the strength and the porosity (the errors associated with these will be discussed later in the thesis and it will be shown that this is a very likely cause for some researchers reaching differing conclusions).

The following relationships have been taken from the papers on granulation listed in the bibliography and the books and reviews on granulation mentioned at the start of this literature review (but mainly from the reviews by Iveson, et al., [7], Lu, [31], Scott, [89] and Fu, [32]).

A relationship exists that allows static failure strength to predict dynamic strength Salman, et al., [39], therefore it seems sensible, and is proposed by the present author,

that there may also be a relationship between static strength and the abrasive strength. So to test this notion the static strength and the abrasive strength must be investigated.
The static strength is related to the porosity of a granule Wikberg and Alderhorn, [82] (strength decreases as porosity increases), so the porosity must be measured and investigated.
Porosity is related to the consolidation of the granule (porosity decreases as a granule consolidates and becomes denser) so the factors that affect consolidation must be investigated. The agitation within the granulator affects the consolidation (greater agitation leads to greater consolidation in an exponential decay curve - Iveson and Litster, [30]), the agitation is a combination of the mixing time and the energy put in.
The energy put into the system has been related to the power of the mixing (more energy means greater impellor speeds which means more mixing) Holm, et al., [92], which comes from the impellor and chopper so their effect will have to be investigated.
The static strength is related to breakage and it has been shown that at high impellor speed breakage and layering occurs Capes and Danckwerts, [99]. As well as the direct relationship between impellor and porosity (increasing impellor speed leads to lower porosity) there is the subsequent indirect relationship between impellor speed and strength (as lower porosity means higher strength). The direct relationship to strength caused by the limiting effect of breakage related to the impellor speed needs to be investigated.
The run time needs to be investigated as it has been shown that at small run times the addition method is important (spray flux affecting the regime of initial granule growth, the size distribution and the binder distribution - Litster, et al., [8]) and at long run times the granules consolidation increases. At short run times the addition method will have to be investigated to determine the changes it causes to the binder content and size of the granules, this is because some workers have shown there is a relationship between size and strength with larger granules becoming weaker.
Also linked to the size is the relationship between abrasion and shape, specifically the angle of contact (due to shape) between an abrading particle and the surface being worn (angular particles are more abrasive) Hamblin and Stachowiak, [57]. Thus size needs to

be investigated because not only do larger particles become more regular and spherical, larger spheres have a smaller contact angle.

The binder content affects the final porosity of the granules, Iveson, et al., [16] and as porosity is important to strength, and that is something we need to know about, the binder content becomes an important parameter to investigate.

The binder type, in other words the viscosity and surface-chemistry interactions with the primary particle, affects the consolidation process. More viscous binders require greater agitation to produce a given consolidation. So the binder type needs to be investigated.

As the surface-chemistry interactions are dictated not only by the binder type but also the primary particle type the primary particles need to be investigated. Another reason for this is the nature of the primary particles - their shape, affects the closest possible packing state and the frictional resistance to packing as well as the abrasive properties of individual particles and particles imbedded on the surface of a granule.

All of the above relationships are in the literature (either in the main reviews by Iveson, et al., [7], Lu, [31], Scott, [89] and Fu, [32] or the sub-references within those papers – notably Iveson, et al., [16], Tardos, et al., [28], Knight, et al., [87] and Ennis, [29]) but they are not all together in one place and they do not all relate to the same system. And as already said granulation processes are system specific so it is very unlikely that quantitative trends from any of the literature would be applicable to this research and it is quite possible that even some of the qualitative trends might not be applicable (or confounded). For this reason a lot have not been detailed.

5.5 Granule Porosity

Porosity, ε, is a physical property of the granules and is defined as the ratio of: the volume of pore space to the total volume. The porosity of granules depends upon the formulation of primary particles and binder used and the operating conditions of the granulator. Using identical formulation it is possible to get granules of different porosity by changing the processing method, Wikberg and Alderhorn, [82].

Porosity within granules and granulated products, such as tablets, can be considered at three length scales:

- INTRA-PARTICULAR: On the smallest level the pores within the primary particles. Pores within primary particles become more important as the particles get larger or when using porous designer particles such as Zeolite, which have a hollow structure.

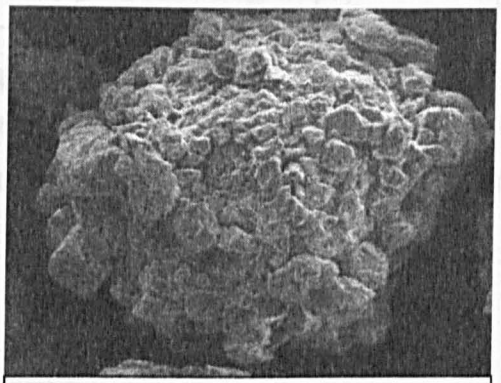

Figure 6 – TEM image showing intra-granular pores (Care of Unilever – Port Sunlight Lab)

- INTRA-GRANULAR: (see figure 6) relates to the intra-granular pore space within an agglomerated granule. If a granule is not saturated with binder and has a funicular or pendular structure then it will have air pockets or pores within the structure. It is imagined that some of these pores will have entrances on the surface of the granule and others will be completely enclosed – this has ramifications on the porosity measurement techniques discussed later.

- INTER-GRANULAR: (see figure 7) the third length scale relates to the inter-granular pore space between processed granules such as in tablets. It also relates to the pore space between discrete granules that have formed into an aggregate, either due to surface attractive forces (on very small granules) or, more likely, due to surface binder (on saturated granules forming weak inter-granular bridges).

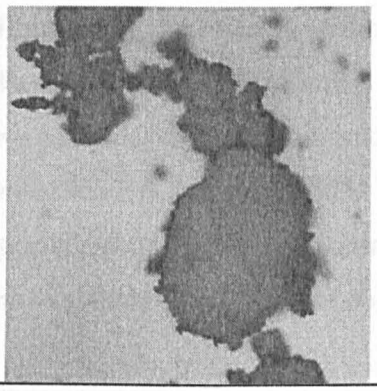

Figure 7 – Inter Granular pores (Sheffield University – Chem. Eng. Dept.)

5.5.1 Formulation effect on Porosity

The above description of the 3 length scales of porosity allows us to see how changes in the formulation might affect the overall porosity of the granule and indeed which length scale becomes important.

5.5.1.1 Binder-solid ratio:

The binder-solid ratio of the formulation will affect the saturation of the produced granules, which in turn dictates how much intra-granular pore space is present. Low binder-solid ratios will result in granules of funicular and pendular nature and thus understanding of intra-granular porosity is important, as the binder-solid ratio decreases further the chances of enclosed pores within the granules decreases. High binder-solid ratios will result in granules of a capillary or saturated nature. This increases the chances of a wet saturated surface and the formation of inter-granular bridges increases, thus inter-granular porosity length scales become more important as binder-solid ratio increases. Knight, et al., [87] showed that as the binder-solid ratio increases the porosity

decreases, (however it is believed this conclusion ignored their observed effects of run-time, which is shown to affect consolidation and consequently porosity Iveson and Litster, [30], Maxim, et al., [100]).

5.5.1.2 Binder type:

Liquid binders will tend to flow amongst the spaces of the primary particles and reduce the intra-granular porosity. However very viscous binders or those with a low surface wetting affect (on the primary particles) may not flow amongst all the pores spaces. Using high binder-solid ratios of binders that are liquid at room temperature is far more likely to produce saturated granules that will have few intra-granular pores and will form inter-granular bridges and thus the third length scale of porosity becomes important.

5.5.1.3 Primary particle type:

The type of the primary particle will dictate the primary particle size distribution and particle shape, which may affect how the granules form and their subsequent porosity. Primary particles formed by comminution, e.g. ground $CaCO_3$, will have rough, squared shapes with a wide size distribution that will have different granulating properties than neatly formed precipitated particles over a narrow size distribution. Some primary particles such as zeolites will have internal pores that will add to the overall porosity of the granule if the binder cannot seep into these intra-particle pores. Particle type also affects surface wetting and must be considered in conjunction with binder type.

5.5.1.4 Primary particle size:

The size and size distribution of the primary particles will have an affect on the porosity of the granules formed. Smaller primary particles will have a larger surface to volume ratio and thus use up more binder – so for a given binder-solid ratio the use of smaller size particles should produce a more porous structure. However this is balanced by the fact that small particles can pack very close together so the space between primary

particles within a granule that needs to be filled with liquid gets smaller and the amount of binder needed to form saturated granules is reduced, and therefore the porosity decreases. Obviously playing a large role in this is the shape of the primary particles and the size distribution; a large size distribution will tend to have a lower intra-granular porosity as the smaller particles can fit into the packing spaces between larger granules. Very irregular and needle-like primary particles will tend to pack in an irregular manner and thus have larger spaces between particles than more regular spherically shaped particles.

5.5.2 Operating conditions effect on Porosity

The processing parameters most likely to affect the porosity of granules are the binder addition method, impellor speed and run time.

5.5.2.1 Binder addition method:

Work by Scott, [89] compared different binder addition methods; pour-on binder addition produced granules with lower porosity than melt-in binder addition. Spray addition of the binder was not investigated. The effect of binder addition on porosity is dependent on the manner in which the binder contacts the primary particles. For pour-on addition the binder is completely liquid to start with and is a continuum compared to the droplets of spray addition and to the primary particles themselves. Thus the primary particles imbed themselves in the binder, which is free to flow into all the small spaces and cover the entire surface of the primary particles. Because the melt-in process relies on heat transfer from the bulk to the solid binder flakes it does not produce an instantaneous continuum of liquid binder, rather the surface melts whilst the core of each binder flake is solid. As a result there is not enough liquid binder to flow smoothly over the entire surface of the primary particles and it gets stripped from the solid binder core by primary particles contacting the surface, picking up a small amount of liquid binder and breaking free under the influence of the impellor. Spray addition will probably produce granules of porosity half way between the two other addition methods, due to it being completely

liquid, but at the same time if the droplets are sufficiently small they may not have enough binder to flow around the primary particles.

5.5.2.2 Run time:

The method of binder addition is unimportant when a large run-time is used. Knight et al., [87] show that granule size distributions tend towards a uniform monomodal distribution regardless of addition method, the differences occur in the early stages of granulation and in the time taken to achieve the monomodal state. This is because the addition method affects the initial distribution of the binder amongst the primary particles; this is inferred from the fact that different addition methods have markedly different initial porosities. As all the binder distribution is dependent on the degree of mechanical mixing, and as time progresses the batch becomes evenly mixed the porosity will tend to a steady value. What is interesting to note is that the results from Knight et al. suggest that the final porosity is not only independent of addition method but also the initial mean primary particle size and initial binder-solid ratio. However this is misleading as they only report the porosity of large granules, 1000μm - 1400μm, and not the smaller granules that are produced. This is important, as Scott, [89] points out, because small granules are made up of a smaller number of larger primary particles and tend to have a lower binder-solid ratio than large granules. Even though, as run time progresses, the granule size distribution tends towards a monomodal size the primary particle distribution and binder content of individual granules at the large and small end of the monomodal peak are different.

5.5.2.3 Impellor speed:

Impellor speed will have a similar effect on porosity as the run time, Jaegerskou et al., [101] found that increasing impellor speed reduced the intragranular porosity. Increasing impellor speed will negate the effects of addition method because increasing the impellor speed increases the mixing intensity and the batch should reach an evenly mixed state faster. However increasing the mixing intensity might produce granule breakage, Van

Den Dries, et al., [88] and better redistribution of primary particles and binder within the granules of the monomodal granule size distribution. Van Den Dries, et al., [88] states that formulation parameters such as viscosity and the particle size determine a granules final strength (a transition between breakage and non-breakage formulations occurs), that a balance between granule strength and impact force determines whether breakage occurs. Increasing the impellor speed increases the impact force, but this will only make a difference to the amount of breakage if the formulation is near the transition point between breakage and non-breakage. It is imagined for a given run time a higher impellor speed would tend to give a tighter size distribution with a less noticeable difference in the primary particle size and binder content between the small end and the large end of the distribution. Knight, et al., [97]found that increasing the impellor speed from 450 rpm to 800 rpm did produce a tighter distribution and increase in average particle size, but at 1500rpm the distribution widened again and the average size was lower than at 800 rpm – they put this down to growth being limited to breakage.

5.6 Packing of Spheres

Packing of spheres has been studied for centuries as far back as 1611, when Kepler famously hypothesized that close packing is the densest possible and this assertion is known as the Kepler Conjecture. Subsequently the problem of finding the densest possible packing of spheres (not necessarily periodic) has been known as the Kepler Problem (Mathworld, [102]). Sloane, [27] reports that the commonly accepted densest possible packing arrangement of equi-sized spheres, being the face-centred-cubic packing, has never been mathematically proved to be maximal. The face-centred-cubic packing fills just over 74 percent of the volume of the space. Sloane, [27] and others Edmondson, [103], Hales, [104], Mathworld, [102] cite the wok of Rogers, [105] who proved that no packing of spheres can have density greater than about 0.7796, however Rogers proof offers no construction of a packing that will reach this density.

Closely associated with the Kepler conjecture is the concept of the "kissing number". In 2 dimensions it is the maximum number of equi-sized circles that can fit around a central circle and in 3 dimensions it is the maximum number of equi-sized spheres that can be placed touching a central sphere. In 2 dimensions the kissing number is found to be 6 (this happens to be the arrangement of the planes of spheres in the face-centred-cubic packing structure and the centres of any 3 spheres form an equilateral triangle). In 3 dimensions the kissing number is 12, but this leaves a significant amount of free space (but not enough to fit a 13th sphere) Mathworld, [106].

Edmondson, [103] explains how Fuller (R. Buckminster Fuller) used a continuous looped necklace made from solid lengths of dowel connected by small pieces of tubing to demonstrate, by the sequential removal of single lengths of dowel, that the triangle is the only stable polygon. Edmondson then goes further to describe why the Tetrahedron is the smallest stable structure (contrary to the belief that cubes are stable, cubes are only given stability by the introduction of stabilising triangles and tetrahedrons – often hidden within solid walls of a cube). Sloane, [27] notes that another way to consider the complexities of sphere packing is to consider the tetrahedron packing arrangement of 4 spheres, this is the densest possible packing of 4 spheres and it is the only arrangement where 4 spheres each touch each other (it is analogous to the triangular arrangement in 2 dimensions). It is

emphasized that this must not be confused with the kissing number, which is the maximum number of spheres touching a central sphere (not necessarily touching each other). It seems that a logical progression from Fullers arguments that triangle and tetrahedron are the most stable structures that the densest possible packing would also be the most stable and be formed from a recurring tetrahedron arrangement. It initially seems sensible that a tetrahedron should be able to form a repeating geometric unit with each tetrahedron sitting congruent to all neighbouring tetrahedron. In reality they do not (this is because the tetrahedron is not a perfectly repeating volume, as the angle between 2 faces is approximately 70.5^0 rather than 72^0 – which is what would be needed to pack 5 tetrahedrons axially around a central spine). The kissing number of 12 is achieved through a series of tetrahedral arrangements of spheres packed together, but eventually a gap appears. In order for all twelve of the touching spheres to be touching 3 others on the surface (and thus form an Icosahedron) the radius of the internal sphere has to be reduced, thus meaning the packing structure is now pyramidal rather than true tetrahedral. Robert, [107] shows an Icosohedron with equi-sized spheres packed around a central sphere, this shows how the centroids of the spheres rest at the apex of pyramids on the outside surface of the Icosohedron, there are 20 pyramids forming the Icosohedron but because of the packing arrangement there are only 12 spheres surrounding the central sphere. The spheres all appear to be touching perfectly (which is contrary to packing of mono-disperse spheres), however Robert, [107] quotes the internal sphere as having a radius smaller than the external spheres.

Sloane, [27] points out that the sort of packing using tetrahedral unit cells does produce densities higher than that found to be the limit by Rogers when considering mono-disperse spheres packed with overall packing structure lengths of the order of magnitude of a few sphere diameters. But when greedy algorithms are used to pack in a tetrahedron structure they eventually become undone and the density falls below this limit as more are added (because the tetrahedron is not a perfectly repeating volume as described above and greedy algorithms are based on making the best immediate option without considering the long term effects). It is proposed (here) that if the basis of the density of packing spheres was taken as the tetrahedron being the control volume the maximum packing density values may be different (as suggested by Sloane [27]), and this present

work shows this to be the case when analysing the interparticle space associated with different packing structure (see section 7.3.2.2 and appendix C) – Note: the analysis performed in this work makes the over assumption that the portion of a sphere contained at the apex of a tetrahedron unit cell can be approximated from the portion of a sphere contained at the apex of a pyramid forming an Icosahedron – this results in an over approximation of the maximum packing density. It could be argued that because of the number and spread in the sizes of the primary particles in granules the smallest possible repeating structure (the tetrahedron – over length scales of the order of a few diameters) could be used as the unit cell for determining the porosity. It can also be argued that the way that binder (liquid) rests between spheres along the centre lines between the spheres that any packing density need not consider edge effects (i.e. calculate the density based on the volume taken between centre lines of packed spheres). Additionally as already mentioned by Sherrington and Oliver [5], the theoretical packing density is dependent on the ratio of the sizes of the large and small particles (being packed) and can effectively reach infinity if the sequentially smaller particles fit into the gaps between the larger particles.

This work takes 2 theoretical approaches for determining the maximum packing of a primary particle size distribution. One that is an algorithm based on the idea that the tetrahedron and a tetrahedral type packing will produce the densest possible packing structure and the other is based on the analysis of the interparticle space described in appendix C. It uses a modified equation with the variables being undefined functions of the characteristic length of a size distribution, the spread of the size distribution and the binder content. It is unknown what value there is in trying to describe the packing of a size distribution using a model based on mono-disperse spheres. The algorithmic approach using the tetrahedral type packing should overcome the limitations of packing mono-disperse spheres as the spheres get progressively smaller and will be able to fill gaps in the structure.

5.7 Existing Models for the Consolidation Process

The work on consolidation is quite extensive, for example Iveson, et al., [14], Iveson, et al., [16], Iveson and Litster, [30], Knight, et al., [97] and Tardos, et al., [28].
Consolidation is the reduction in porosity caused by rearrangement of the particles and squeezing binder and air-pockets out of the granule. This rearrangement is caused by energy input from mixing and influenced by the energy dissipation characteristics of the binder and resistance to rearrangement due to particle shape. The models described in this section rely on knowing physical properties that quite often can't be measured for granules in situ – surface tension, wetting angle, viscous dissipation. Even the model presented in this thesis requires parameters that cannot yet be quantified (agitation rate constant and limiting interparticle space), but these types of model are useful for making qualitative predictions.
There are three existing models for the consolidation process that need to be discussed prior to the proposal of the new model for granule compaction in this thesis (section 7.3). The first is a stochastic approach by Ouchiyama and Tanaka [98], where they consider force balances between impact forces and resistive negative capillary pressure forces. The second is an energy based approach by Ennis et al. [29], relating the kinetic energy of collision to the viscous dissipation of that energy. The third is a by Iveson et al. [16], [30], and moves away from the previous limited approaches of trying to model upwards from microscopic fundamental physics, but rather models on a macroscopic level that better relates operating and processing variables to granule consolidation.
Although the application of the consolidation models by Ouchiyama [98] and Ennis et al. [29] is of limited use to this work they are included here to show those limitations and because the paper by Iveson [30] claims they are the only 2 prior existing models in the literature to describe the consolidation process and they still reveal some very important fundamental processes.

5.7.1 Ouchiyama & Tanaka

The work by Ouchiyama and Tanaka [98] is a stochastic approach and uses force balances and capillary negative pressure to relate porosity, strength and operating condition (extent of granulation and speed).

Their model is based on mono-dispersed spheres where the porosity is related to the packing of the spheres by the coordination number (of touching spheres). It is a stochastic approach because it relates the rate of increase in the coordination number (the packing ergo the consolidation) to the frequency of applied external forces and the probability that the applied force is greater than the resistive force. The resistive force is modelled on the capillary negative pressure. The greater the coordination number the greater the capillary negative pressure and thus the resistive force meaning it becomes less likely an externally applied force will be large enough to lead to a larger coordination number and further consolidation. The conclusion is this leads to decay in the rate of consolidation with time and that there is a finite limit to the model based on the coordination number of packing monodisperse spheres.

Note: this assumes a random packing and thus fractional coordination numbers can exist. They also "discard the effects of de-neighbouring spheres".

They model the applied force per particle as the averaged (per particle) force of a deformation force resulting from the kinetic energy transfer to deformation work in an impact. The resistive force is a force balance of frictional forces, capillary negative pressure and normal forces. The maximum force is taken as being at the limit when two particles cannot withstand separating apart from each other. This includes the un-defined "function of coefficient of sliding friction". The frequency of applied external forces is related to the rotating speed thus managing to incorporate at least one macroscopic variable. The derivations and discussions are difficult to follow and confusing, introducing another un-defined term: the "function of saturation".
They do however appear to show that the model produces trends between porosity, strength and dimensionless retention time that are backed up by observations in their

cited work of others. They theorise that their model should be able to describe the effects of increasing impellor speed, decreasing feed rate and increasing liquid content (all of which reduce porosity) and they test this experimentally; but it fails on the prediction of the effects of liquid content. Iveson [16], believes this is because of the complex inter-relations of viscous energy dissipation, capillary pressure and frictional energy dissipation (which Ouchiyama and Tanaka appear unaware of).

5.7.2 Ennis, Tardos & Pfeffer

The work by Ennis et al. [29] covers two distinct areas, granule coalescence and granule consolidation, using the concept of the Stokes Number. However the emphasis is with the effects of inertial energy and viscous dissipation on granule coalescence during impact rather than on granule consolidation. Ennis only briefly describes the effect that an increased viscosity will increase the resistance to rearrangement and thus reduce the consolidation rate.

They describe two separate approaches to granulation relationships that existed at the time – microscopic fundamental relationships and macroscopic level using population balance modelling (which is limited by the inability to describe growth and breakage kernels in the required equations). Their work focused on determining regimes with granule coalescence and consolidation limited to a consideration of the influence of dynamic pendular bridge strength. They introduce the viscous nature of the binder meaning that energy dissipations have to be considered, rather than force balances, for granule coalescence and consolidation (except in cases where the static capillary strength is larger than the viscous dissipative *strength*). This explains the divergence between results and theory in the Ouchiyama and Tanaka model.

They propose a model based on the dissipation of kinetic energy due to viscous dissipation within a binder forming dynamic pendular bridges within a granule. The model uses viscous binder around spherical particles, ignores frictional forces and discards capillary dissipative energies through analysis. The premise for the model relating the inertial energy to the viscous dissipation is promising; that coalescence occurs if the inertial energy is insufficient to overpower the viscous dissipation. Otherwise granule rebound occurs. It should be useful that quantifiable regimes and

boundaries appear to exist for what they call non-inertial coalescence, inertial coalescence and layering, however the presentation of the theory masks this and the current author was unable to follow it.

The consolidation section relates the rate of change in the velocity of 2 particles within a granule moving together to the viscosity such that high viscosities have a high rate of change and thus low rate of consolidation. They state that an increasing inertial energy, number of contacts and reduced viscosity all increase consolidation, but they do not state their reasoning. They define a critical stokes number, related to the granulation system and properties of the powders and binders used (the physical basis and derivation is unclear). To this the actual stokes number of the impact is compared. For a stokes number much smaller than the critical stokes number non-inertial coalescence occurs and is independent of kinetic energy and viscous dissipation instead relying on presence of binder for coalescence. In this regime the consolidation is affected by the viscosity and inertial energy. As the stokes number increases and becomes larger than the critical stokes number then inertial coalescence occurs, where coalescence becomes dependent upon the viscosity as this determines whether viscous dissipation of the kinetic energy occurs. In the inertial coalescence regime the consolidation is still affected by the viscosity and the inertial energy but additionally as more impacts will be taking place (due to rebounding and subsequent further collisions) the rate of consolidation will greatly increase. The final regime occurs when what they call the "spatially averaged stokes number" equals the critical stokes number, in this regime they claim no consolidation occurs and coalescence is by layering as particles break on impact. The current author is not satisfied with their brief description and reasoning for this regime (although undoubtedly layering and runaway growth does occur in real systems).

Their work is important because it highlights the importance of considering coalescence and consolidation separately when determining granule growth; that depending upon the regime determined by the stokes number the viscosity and kinetic energy will always affect consolidation but may or may not affect coalescence. Their experimental results are also useful because they show that rate of consolidation and extent of consolidation are

independent, something they do not mention but Iveson [30] highlights. This is because the extent of consolidation is controlled by the rate of cooling, whereas rate of consolidation is affected by impacts.

5.7.3 Iveson, Litster & Ennis.

Iveson et al.'s [30] description of Ouchiyama's model implies that it relates the final (minimum) porosity to the rate of consolidation and the general expression uses 2 unclear terms: a function of coefficient of sliding friction at particle contacts and a function of granule saturation and particle assembly. As Iveson [30] points out the extent of granule compaction and the rate of compaction are independent but both depend upon the binder content and the viscosity of the binder, something which Ouchiyama and Tanaka, [98] doesn't highlight.

Iveson et al. [16] presents a model for compaction that uses a minimum porosity, $\varepsilon_{min,}$ as the material end point; this has to be determined experimentally (whereas in the granule compaction theory presented in this work its equivalent, B_{lbr}, is proposed to be determined theoretically).

$$\frac{\varepsilon - \varepsilon_{min}}{\varepsilon_0 - \varepsilon_{min}} = \exp(-k_5 N_2) \qquad (7)$$

Iveson's model also uses a consolidation rate constant, k_5, (also used in the Ouchiyama model and similar to the agitation rate constant, ω, in the granule compaction theory presented in this work). The other parameters in Iveson's model are porosity, ε, initial porosity, ε_o, and drum revolutions, N_2.

The model presented by Iveson et al. [16] is an empirical model based on as many of the operating and formulation variables as they determine are needed to describe the consolidation process. They argue that although the fundamental work at the microscopic scale is important it has only partially been successfully modelling the effects of operational parameters, Ennis et al. [29]. Exact relationships between microscopic processes and macroscopic granule consolidation are not clear (and sometimes contrary)

due to the complex interactions. These complex interactions limit the previous models because important parameters cannot be determined. Thus an empirical approach should be used, which is what Iveson et al. [16] used.

The experimental work by Iveson et al. [16], concentrates on the effects of binder content and binder viscosity on the minimum porosity (extent of consolidation) and the consolidation rate. Iveson et al.'s [30] later work presents a mechanistic model (drawing on the fundamental principles from previous workers) that describes their experimental results; consolidation within the granule is thought of as being controlled by three forces: capillary, viscous and inter-particle friction. Inter-particle friction and viscous forces resist consolidation and capillary forces act to pull a granule together. They show that the relationship between binder content and consolidation is complex; increasing the binder content decreases the inter-particle friction, but increases the viscous effects. For low viscosity binders increasing the binder content increases the extent of consolidation because inter-particle forces dominate, whereas increasing viscosity for high-viscosity binders where the viscous forces dominate decreases the extent of consolidation. They found that a transition region exists where the consolidation extent of binder of a given viscosity is independent of the binder content. "Unless the relative magnitudes of the viscous and frictional forces are known, it is impossible to predict beforehand the effects of changing binder content, even qualitatively." They did find that increasing viscosity does decrease the rate of consolidation. This consolidation model appears to be useful for predicting the effects of some processing and formulation parameters, but needs to be combined with experiments to determine the effects of the viscosity and to determine the minimum porosity end point.

5.7.4 Maxim (New theory)

The model proposed in this work for the consolidation of a granule assumes that the granule is made up of binder and primary particles that exist as an overall structure that is trying to consolidate to a finite end state, which is only dependant upon the primary particles and their distribution. The model assumes that this final end state of the primary particles, and the binder required for it to be perfectly saturated, can be thought of as an

internal granule existing within the overall structure. Excess binder over and above that which is required for the internal granule to be in a saturated state will be expelled to produce surface wet granules as the internal granule consolidates. Resistance to reaching this end state comes from the physical shape, size, size distribution and actual arrangement of the primary particles as well as resistance from viscous effects due to the presence of binder. Exponential decay curves are used to represent the consolidation towards these end points, with the end points and the variables describing the curves being affected by changes in primary variables (i.e. the things that can be changed by the operator directly).

This model is limited in the same fashion as those by Tanaka [98] and Ennis [29], because it uses functions that cannot as yet be determined (in this case the limiting interparticle space, B_{lbr}, at the end point). Three approaches for determining this end point are proposed: 1} adapting the general equation (13) for describing the interparticle space of mono-disperse spheres over short length scales, 2} converting a primary particle size distribution (PPSD) into spheres and using the packing algorithm (section 7.3.3), 3} using a random packing model.

The advantage that Iveson et al.'s [30] approach has over the granule compaction theory presented in this work is that the end point is able to be determined (albeit experimentally) and the mechanistic model describes the effects of viscosity more readily, however the model presented in this work deals with all the primary variables rather than secondary variables that cannot be varied directly (such as viscosity and surface tension). This work attempts to theoretically determine the end point. By theoretically determining the end point rather than experimentally granules are one step closer to being designed a priori.

The previous models by Iveson et al. [16] and Ouchiyama et al. [98] are essentially the same as the model presented in this work in the way they describe consolidation as an exponential decay in porosity, but differ in the way they describe end point (Iveson [16] calls it an end porosity but gives no indication of how it might be determined or the consequences of the internal compaction on surface saturation that this model describes). They also differ in the way the agitation intensity is accounted for, Iveson et al. [16] measures the drum rotation, whereas this model measure time and impellor speed, which

allows the influences of other energy rates to be more easily included – such as rate of heat transfer.).

The theory presented here has the following advantages over that posed by Iveson [16], [30]; it presents the idea of the consolidation of the entire granule and the minimum porosity being related to a critical packing state that describes the porosity in terms of the packing of the particles and enables the onset and extent of surface wetting to be predicted as a result. The theory presented here also has time as a parameter rather than drum revolutions meaning that it is easier to incorporate rate dependant factors in the future (such as heat transfer) and it allows the qualitative effect of all the primary parameters (processing and formulation) to be predicted by their effect on the individual variables in the equations (something which Iveson [30] does not try to do). The advantage of Iveson's model is the simplicity of visualisation of the equations meaning and the fact that it accounts for the complexities of binder viscosity and binder content quite well.

6 Terms of Reference:

6.1 Research Brief

Investigate the abrasive properties of microgranules with a view to being able to produce microgranules designed in such a way that the abrasive strength can be controlled by the manufacturing process. The microgranules are made using a high-shear granulator – the Rota Junior, lab scale.

6.2 Interpretation of the Research Brief

In order to make designer granules with controlled abrasive strength you need to know how to make microgranules using a high-shear granulator and the properties of those microgranules. Once this known the property-to-property relationships and the property-to-production method relationships can be found. Knowing and quantifying these relationships is the key to making designer granules.

6.2.1 Properties of Granules

The aim is to find out how the properties of the granules relate to each other. Once this is known the aim is to try to determine how the processing and formulation parameters affect the properties. Hopefully the end result is that the property-to-property relationships and the property-to-granulator parameter relationships are known. The ultimate aim is to know quantitatively how the high-shear granulator formulation and processing parameters affect the properties of the granule and how those properties affect the abrasive strength. The high-shear granulation process can then be manipulated to produce granules which have designer properties, in terms of their abrasion behaviour.

6.2.2 Properties of Interest

The properties of the microgranules that were decided to be investigated, and find inter-relationships for, are:

- Porosity
- Binder Content
- Abrasive Strength
- Size
- Static Strength

6.3 Justification of Work

Most of the granulation work presented in this research has been done by others, but not on the same system and so in that respect alone it is valid; as others have found many of the relationships in granulation to be very system specific.

The work relating abrasive properties to granule properties and the parameters making those granules is completely novel. As there was no evidence in the literature of trying to design granules specifically to be used for abrasive cleaning.

The idea of the critical packing state and the associated packing algorithm are novel. The exponential decay curve and the associated equations were formed from the interpretation of many stand alone relationships affecting consolidation described by different workers and covered in the literature review. It is indicative of a sensible interpretation of the physical processes involved in consolidation that the decay curve presented here is similar to the empirical consolidation model proposed by Iveson et al., [16] (which was discovered after the theory presented in this thesis was produced), it reinforces the validity of this work as both this work and Iveson et al. independently arrived at mathematically similar relationships describing the consolidation process. Both use an exponential decay curve and use a multiplier of "e" raised to the power of a double variable (incorporating the effective energy input) to describe the change in porosity from an initial value towards an end point.

The novel consolidation theory in this work is incomplete, but it contains some very useful ideas unifying a lot of other peoples work and allows qualitative predictions on granule consolidation. The algorithm given for determining the critical packing state for a population of spherical particles highlights a problem: It is this authors belief that it sensibly gives the densest possible packing of the spheres (and this aligns with Edmondson, [103]'s description of Fullers Synergetic theories and the tetrahedron being the most stable 3-dimensional shape) but it has not been proved rigorously mathematically and nobody has used computer modelling to transform the algorithm into a useful program. If it is found to not work or be an appropriate method for determining the critical packing state then this will have shown that consolidation modelling is best done empirical methods where the end point has to be determined experimentally. As such it would show that granules cannot be designed a priori.

A problem exists with the impact failure theory – it has been derided as being "not a new concept to propose a relationship exists between static strength and dynamic strength" Referee, [110] – but the novel aspect of the work presented in this thesis is that it takes a crude theoretical relationship and shows exactly how it can be used to predict dynamic failure from the measurements of a few static compression tests and no literature was found that explicitly presents this, seemingly obvious, proposal. A catch 22 situation therefore exists, it is not possible to prove the non-existence of the previous work relating static strength to dynamic failure, but without the references being given it is impossible to know whether they actually exist or not and thus disprove the referees' comments.

7 Theory

7.1 Critical Impact Velocity: Relationship between Static Strength and Dynamic Impact Strength

The work by Maxim, et al., [1] shows how the static strength can be used to determine the dynamic impact strength of granules. The full derivation is given in appendix A, Maxim et al. [66]. The fact that such a relationship exists, forms the basis for the hypothesis that the abrasive strength of granules can be related to the static strength. It is far easier to measure the static strength than either the dynamic impact strength or the abrasive strength.

7.1.1 Impact Experiments: 2-parameter Weibull Distribution

Salman, et al., [39] characterised the failure of spherical granules of fertilizer by firing them at a rigid platen at various velocities, v, and incident angles, θ (90^{o} being perpendicular).

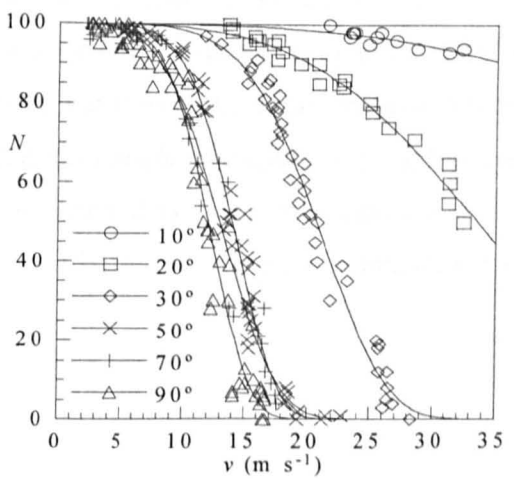

Figure 8 Undamaged granules, N, as a function of impact velocity and angle (From original work by Salman et al. [39])

Experiments tested 3 granule sizes; 3.2mm, 5.3mm and 7.2mm, with the number of undamaged granules, N (out of every 100 fired), being counted and plotted against impact velocity for each incident angle. Figure 8 shows a typical set of data and the Weibull

distribution curve fits for, N, undamaged granules as a function of velocity, v, and impact angle,θ.

A 2-parameter Weibull distribution (with, c, and, m, as parameters) is used to relate the number of undamaged granules, N, to the impact velocity, v, as given below:

$$dN = 100\exp\left[-\frac{v^m}{c}\right] \tag{8}$$

7.1.2 Theoretical Model

Impact failure rate of low porosity granules on a surface the failure rate is dependent on:

Impact Velocity

Angle of Impact

Physical Properties of the Granule

The 2-parameter Weibull distribution can be fitted to experimental data and it can be used to predict the failure using the impact velocity, v, if the correct values for the parameters, m and c are known. Parameter, m, describes the width of the distribution and was found not to vary with impact angle or granule size and has a weighted average value of 4.77. Parameter, c, is interpreted as the critical impact velocity required to induce 63.2% failure, further related to the critical normal impact velocity, u_f, and the angle of impact, θ, by:

$$c = \frac{u_f}{\sin\theta} \tag{9}$$

Maxim, et al., [1] define the critical normal impact velocity, u_f, as a function of material properties and particle size. For granules undergoing elastic failure with no plastic deformation the elastic failure theory defines u_f as a function of:

- ***(Fcr)*** **Static Critical load**
- ***(ρ_g)*** **Density**
- ***(E_g)*** **Young's Modulus of the Granule**

- ***(k)*** **Constant**
- ***(R)*** **Radius of Granule**

$$u_f = \left[\frac{F_{cr}}{1.835R^2} \left(\frac{k^2}{\pi^3 E_g{}^2 \rho^3} \right)^{1/5} \right]^{5/6} \qquad (10)$$

Where *Fcr* is the static critical load of failure, this is found using a modified version of Aurbach's Law developed by Conrad, et al., [48] relating critical load to particle diameter *D*.

$$F_{cr} = B\, D^n \qquad (4)$$

The constants, *B*, and, *n*, are found from experimentally measured static fracture loads. So the failure distribution curve can be found by measuring the static fracture loads and finding the critical load of failure (eqn 4). This then allows the critical normal impact velocity to be found if the physical properties of the granule are known (eqn 10). The critical normal impact velocity combined with the angle of impact gives the, c, parameter (eqn 9) in the weibull distribution which uses the velocity of impact to predict the failure (eqn 8).

The derivation of, u_f, is based on Newton's laws of motion and predictions by Laugier, [49] that relate the force, *F*, of impact in a platen to the radius, *R*, of an impacting sphere and the contact radius, *r*.

$$r^3 = \frac{4kFR}{3E_g} \qquad (5)$$

Where, *k*, is a constant relating the Young's Modulus, *E*, and Poissons ratios, υ, of the sphere and platen (subscript $_g$ is the sphere, subscript $_p$ is the platen:

$$k = \frac{9}{16}\left[\left(1-\upsilon_g^2\right) + \left(1-\upsilon_p^2\right)\frac{E_g}{E_p} \right] \qquad (6)$$

7.1.3 Experimental Verification

Section 7.1.1 showed that the experimental data from impact experiments can be fitted using the 2-parameter Weibull equation. Section 7.1.2 showed how it is possible to predict the distribution using the Weibull equation if the critical normal impact velocity, u_f, can be found.

This theory was verified by conducting static compression experiments using similar granules to those used in the original impact tests. The static failure loads were then used to calculate the critical normal impact velocity using the equation for u_f above. Figure 9 shows the failure loads for experimental data and their curve fit using the modified Aurbach equation (4) (produced by the present Author using original data from the work by Salman et al. [39]).

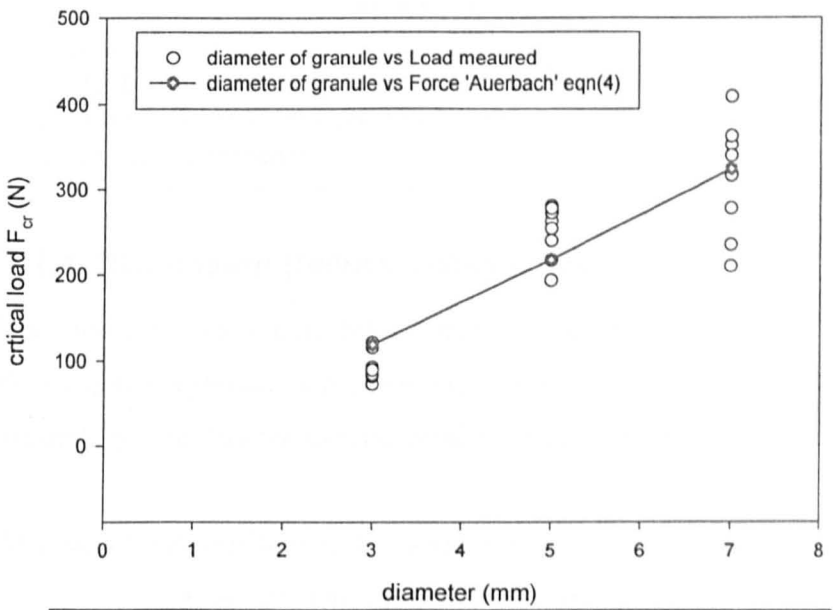

Figure 9 – Static failure loads – experimental data and Aurbach curve fit (Produced by current Author from original data used by Salman et al [39])

Critical velocity was plotted against diameter to verify the theoretical model for finding u_f from material properties and static compression tests. Figure 10 clearly shows that calculating the critical normal impact velocity using the theoretical model and static failure loads (fitted using the modified Aurbach equation) satisfactorily match the

experimentally derived c-parameter values (and subsequent u_f) (produced by the present Author from original data used by Salman et al [39]).

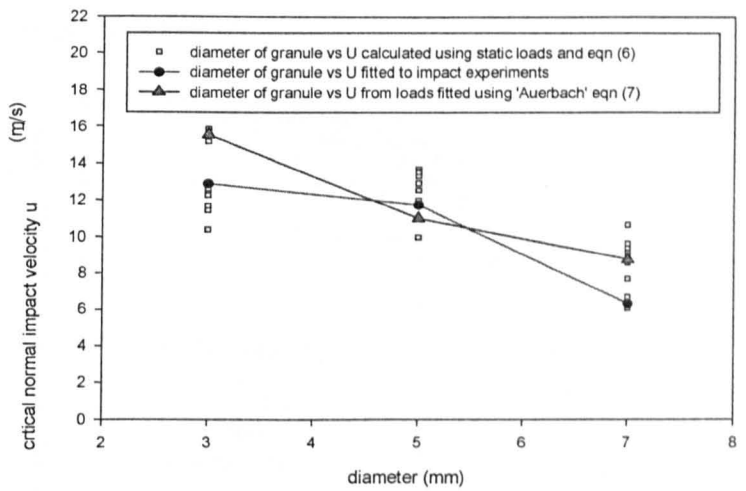

Figure 10 – comparison of critical normal impact velocity fitted from static load experiments and impact experiments

7.1.4 Discussion (failure criterion model)

The failure distribution model is suitable for predicting the failure rate of dense granules (< 3% porosity) based on granule size and impact velocity. The Weibull equation accurately describes the experimental distribution of impact failures.

The theoretical distributions of impact failure can be found by:

1. Conduct static compression tests
2. fit data using modified Aurbach equation (4)
3. Calculate the critical normal impact velocity eqn. (10)
4. Use the critical normal impact velocity and impact angle to find the c-parameter eqn (9) .
5. Use the Weibull equation (8) to find the failure distribution.

A fairly good agreement between the theoretical critical velocity calculated using eqn 10 and values obtained from impact experiments supports the applicability of the theory – this is shown in figure 11 (produced by the present Author [1] from original data used by Salman et al [39]).

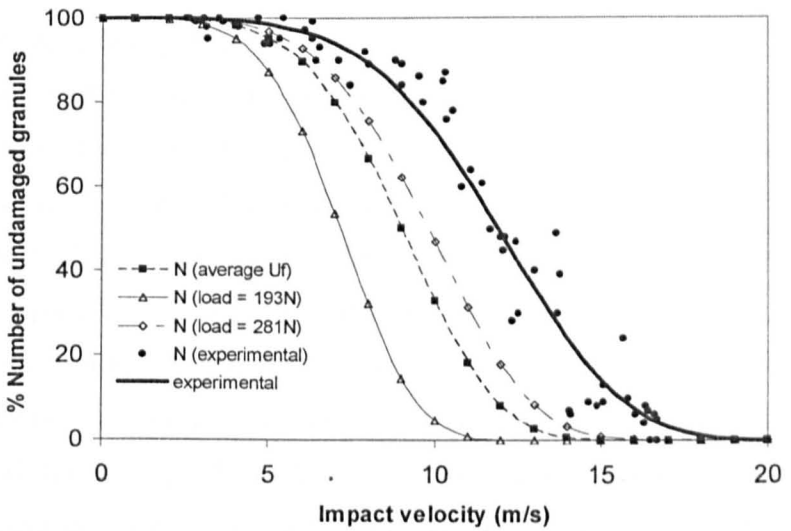

Figure 11 – Distribution fitted from impact experiments compared to theoretical fit from static compression testing.

7.2 Granule strength – crushing individual granules and multiple granules

7.2.1 Theory of Granules Strength

For granules / particles sandwiched between 2 plates. The total contact area for a given force will vary with the size of particles and the number of particles. It is expected to get a relationship between the failure load and size. It is expected larger granules will withstand a greater load than smaller granules and for multiple granules to withstand a greater load than single individual granules. This was tested using single granule compression and multiple granule compression of real granules. . The applied load at failure during the preliminary trials was measured using a dynamic mechanical analyser, (during multiple crushing tests using the theory of uniaxial compression the tests were performed using a Zwick© compression tester). A theoretical analysis based on the equations given in section 5.3 Laugier, [49], Conrad, et al., [48] and Studman and Field, [63] (which are themselves based on the Hertzian theory) was carried out to determine the import factors that will affect strength testing and need to be considered when designing a "fair" test.

The equations (4), (5) and (6) in section 5.3 can be plotted to give simple qualitative trends in the way particles and system properties will respond in crushing and abrasion systems to changes in the particles properties (density, Youngs modulus, Poisons Ratio and Aurbach's constants) and operating conditions (mass of particles, applied force). For the granules considered in this research the values of Youngs Modulus and Poisons ratio for the granular material cannot be measured (and thus k-value cannot be determined). To graphically illustrate the effects of varying the other particle and system properties the equations are applied to an imaginary sample of mono-disperse spheres and the k-value and Youngs modulus were assumed. Note that choosing appropriate values for the Youngs modulus and Poissons ratio of real granules is important if quantitative contact areas and pressures during crushing / compression are needed. The graphs are shown in Appendix B and show normalized values for y-axis values.

Chart 1 (figure 12) shows the effect of varying mass dose (the mass of particles being crushed) and the size (of the mono-sized spheres in a single layer) on the total contact area as a function of particle size. As the particle size gets larger the number of particles decreases, the contact area of individual particles increases but the reduced number means that the overall contact area decreases when the dose is kept at constant mass. Increasing the mass of the dose increases the total contact area; this assumes that all particles are in contact with the surfaces and not stacked on top of each other. The total contact area affects the amount of abrasion; a larger contact area means more abrasion (but this needs to be considered in conjunction with the particle shape, mode of abrasion and applied load). So in terms of an abrasion test increasing the mass dose or decreasing the average size of the particles should result in more abrasive wear.

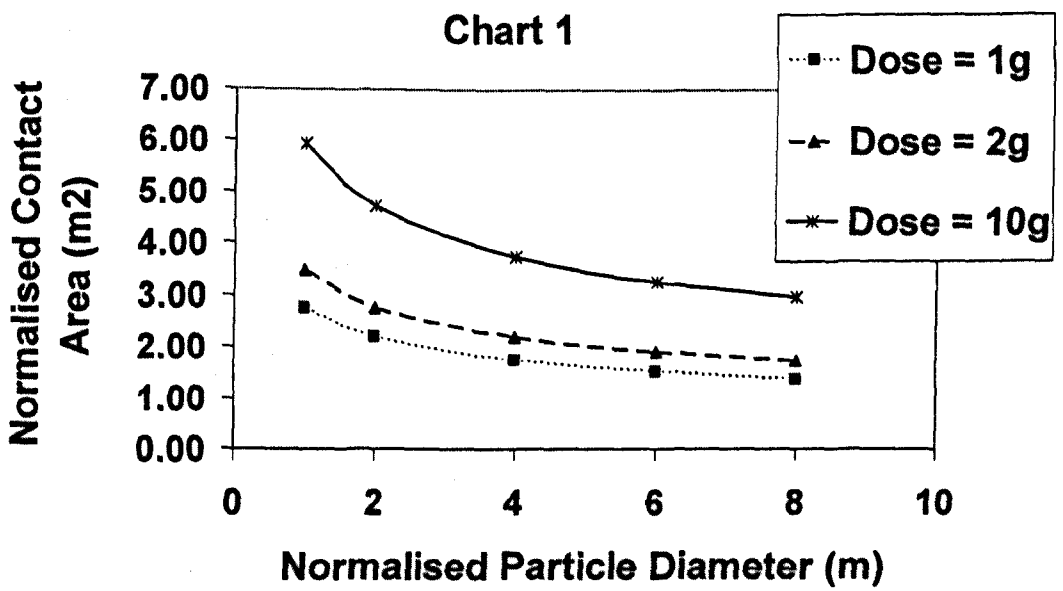

Figure 12 – Chart 1 Effects of Mass dose and particle diameter on the total contact area of particle being crushed

Chart 2 (figure 13) shows the load per particle as a function of particle size for a constant mass dose and constant applied load. This shows that the load per particle rises as the particle size increases; this is due to there being fewer granules as the size increases. As

can be seen doubling the particle size more than doubles the load per particle. If the Aurbach constants in equation 4 are known for the granular material then the line representing the failure load as a function of particle size could be plotted on the same graph; any points where the 2 lines crossed would be a transition size between particle failure and no-failure- where the representing failure load is below the line shown in Chart 2 the granules would fail in an abrasion or crushing system with that given load and dose.

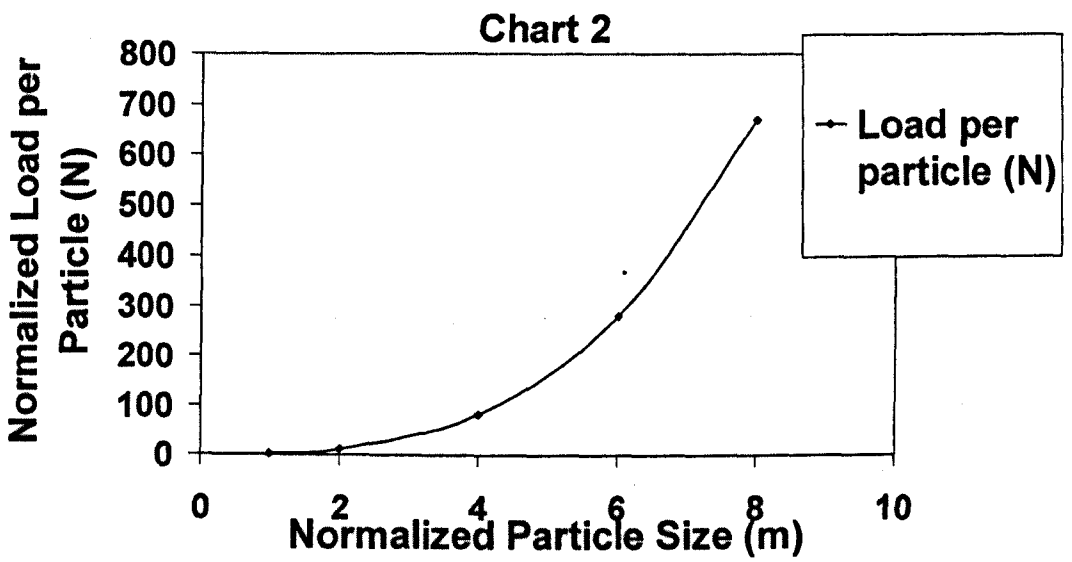

Figure 13 - Chart 2 – showing Load per particle as a function of size – constant dose mass

Chart 3 (figure14) shows that the total pressure increases as particle size increases, this is sensible as the total load remains constant and the total contact area is decreasing. Note that the rate of increase in total pressure decreases as the particle size increases. This is because of the relationship between the contact area, r, and the particle radius, R. The total number of particles is proportional to $1/R^3$, r^3 is proportional to FR (from eqn. 5) and F is proportional to the total number of particles. This means that the contact area, r, is proportional to $1/R^{2/3}$. In terms of an abrasion system this means that if the mass of particles being used is kept constant that decreasing the particles size used as an abrasive

will be expected to reduce the amount of abrasion, because a lower pressure means lower stress intensities and lower efficiencies in transfer of abrasive energy.

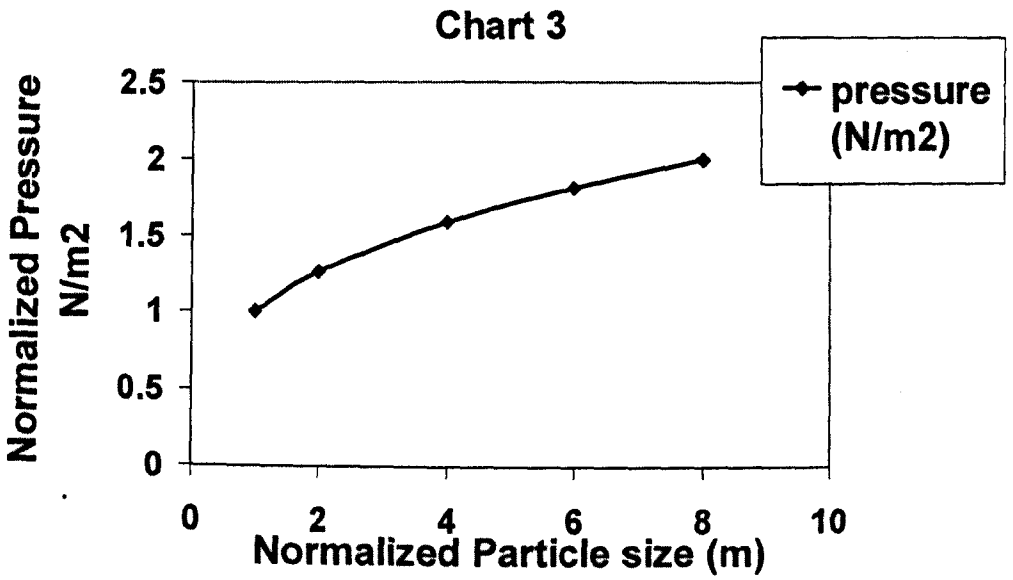

Figure 14 – Chart 3 showing Total Pressure on substrate as a function of size (constant dose mass)

Chart 4 (figure 15) shows the effect of reduction in size of particles, as if the surface was being eroded as a result of abrasion. The number of particles stays constant, as does the applied load but the size of the particles reduces. It shows that the total contact area decreases almost linearly but the pressure increases exponentially as the particle size decreases. The effect of this on an abrasion system will be confounding as a reduced contact area will reduce abrasion, whereas an increased pressure could be expected to increase damage to the substrate and increase abrasion. For mono-disperse systems under constant applied load that undergo surface erosion reducing the particle size; the particles will eventually reach a size at which the load per particle is enough to cause failure. The size at which the particles fail depends on the applied load and the mass dose of particles. Again, if the line describing the failure load as a function of particle size is plotted using the Aurbach equation (as described above for Chart 2) then the size at onset of crushing

failure as a result of abrasion erosion of the particle surface can be determined. This relies on accurate determination of the Aurbach constants.

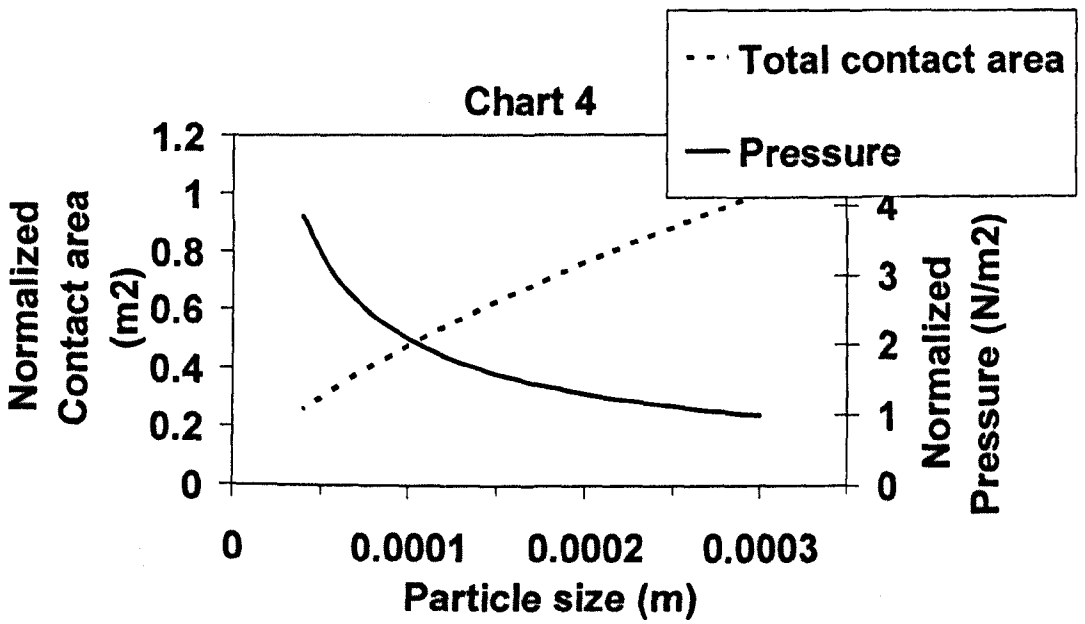

Figure 15 – Chart 4 showing effect of Total Contact Area and Pressure for particle changing size from large to small (constant number)

Chart 5 (figure 16) shows the effect of total load on the contact area (both for constant mass dose). It shows that as the load increases so does the total contact area, but importantly it shows that at low particle sizes the contact area is larger than at large particles sizes and it increases by a larger amount when the load doubles. What this means for abrasion systems is that if smaller particles are being used then the sensitivity of the system, in terms of abrasive wear, to changes in applied load will increase (assuming that wear is related to contact area).

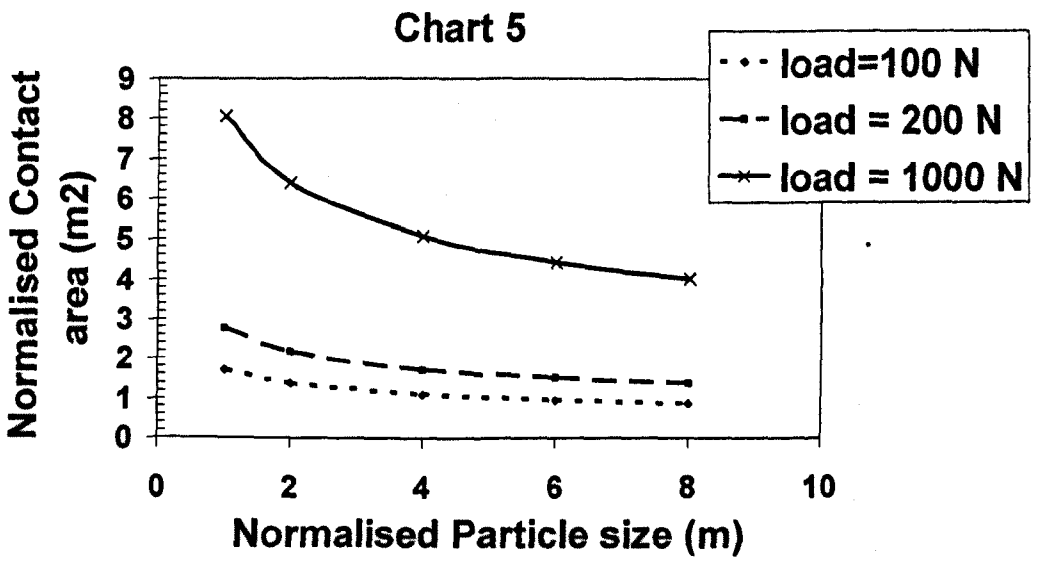

Figure 16 – Chart 5 – Contact area as a function of particle size and applied load.

For a real system of multiple particles being crushed the particles will not be mono-disperse and the number of particles in contact will vary with time, initially not all the particles will be in contact with crushing surfaces meaning that the load per particle may be high enough to cause some failure or compaction. Particle failure will increase the pressure on remaining particles, possibly leading to further failure. Compaction will reduce the gap between the substrate and the crushing surface bringing more, smaller, particles into contact and thus reducing the pressure. Real crushing tests on individual granules taken from a sieve cut 300 – 355 um, in figure 17, shows that there are 4 types of crushing curves (probe position as static force is increased). The forces required to

induce the types of curve also vary, this variation in shape and failure force is probably due to the variations in the physical make-up of the granules and the fact that the granules are not exactly the same size but vary from 300 to 355 um. In any case it suggests that crushing tests involving multiple granules will contain particles that will fail by the four mechanisms and at different force loadings. Defining these modes of failure and investigating the different causes is beyond the scope of this research, it is satisfactory to note that granules of a given size will fail by different mechanisms and different loadings – that this is probably due to the heterogeneous nature of the granules.

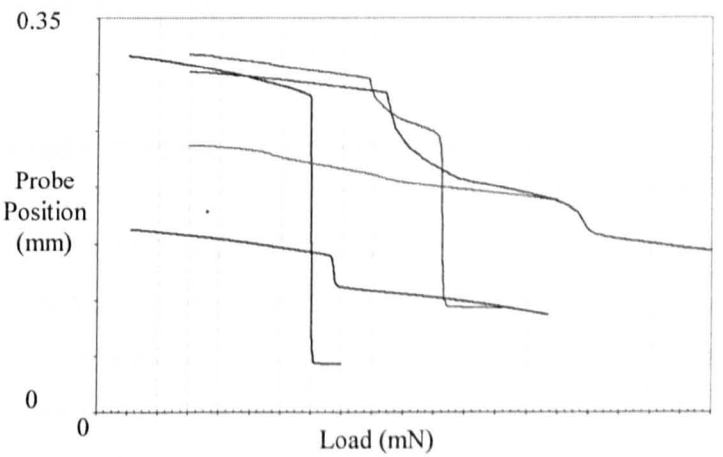

Figure 17 - showing individual granule crushing failure modes.

The charts (1-5) show qualitative predictions of what happens in a system of particles when the applied load and numbers of particles are changed. They show that particle properties (size) are also important and necessary for quantitative predictions (Youngs modulus and Poisons ratio). The potential to determine transition points between regions of failure and no failure is possible if these material properties are known and the constants in the Aurbach equation can be determined. This is only relevant to large granules (on which individual crushing tests can be performed). However, as Figure 17 shows, there are many modes of failure meaning that many individual crushing tests would have to be performed to determine the Aurbach constants. This is inappropriate to micro-granules due to the difficulty in isolating them (see next section). Additionally the

material constants will either have to be assumed (for small granular material) or measured on larger pieces of material in test such as the 3-point bending test (for material that can be formed into appropriate shapes for such testing). What these graphs show is that several of the factors affecting abrasive wear (surface area, pressure and number of abrasive particles) are likely to change simultaneously in addition to the material properties of the abrasive granules when different batches are tested. Thus in order to design a fair abrasion test where granules from different batches are tested on a like for like basis controlled changes to the abrasive system (load, concentration and wear time) need to be made with an understanding of the particle and substrate properties. An attempt at this is made in section 7.4.4.

7.2.2 Compression Testing - preliminary

In this report two ways to assess the strength of granules are used: abrasion testing and static compression testing. Compression testing involves putting the granule between two plates and slowly ramping up the static load until the point of failure. This is conventionally done using a Dynamic Mechanical Analyser (DMA), which when used in the static stress scan mode progressively increases the load applied whilst measuring the displacement of the crushing plate. The point of failure can be determined by a sudden jump in the load-displacement scan. The preliminary compression testing was done using a DMA and attempted to find the static strength of individual granules by crushing individual granules. Section 7.2.3 covers multiple compressions using a uniaxial compression test.

It would ideally be possible to compress individual granules in order to determine the exact relationship between strength and the granule structure. The granule structure can vary due to the porosity, binder ratio, granule size and primary particle size. Section 5.2 has already shown that porosity and binder content are important to strength. How operating parameters and formulation variations can be used to alter the porosity is described qualitatively in section 7.3. By compressing individual granules it would be possible to get a better understanding of the relationships involved, but there are a number of difficulties relating to crushing individual microgranules.

It is very easy to isolate single granules that are upwards of about 500μm and to then perform crushing tests on them. Some tests were performed on slightly smaller individual granules crushed using the (Dynamic Mechanical Analyser) DMA the force to crush granules was assumed to be 900 mN (this is based on the mid-range of 300-355 μm granules produced using impellor speeds of 400 and 800 rpm.) Unfortunately the granules concerned with this research are far smaller, often 1000 times smaller by mass. This makes the granules very difficult to handle and impossible to isolate individually with the equipment and expertise that was available as they tend to stick to each other and any implement used to isolate them. Due to the size, individual granules are not visible to the naked eye so all this has to be done using microscopes.

The current author suggests that to test individual granules is too difficult with the equipment and expertise that was available for this work and Adams et al [85] suggests that strength tests could be conducted on a bed of granules – unfortunately the way the mechanical analysers work (applying a continuous load against displacement) causes problems. If there are 2 granules on the same sample plate, A and B: A has a diameter larger than that of B, thus the loading head will not come into contact with B until A has either been crushed or compressed to the point where its height is equal to B. This will produce variations in the stress displacement scan, especially if there are many granules of various sizes (heights) on the sample plate. This suggests that either a layer of mono-sized particles or individual granules should be used. This situation is further complicated by the fact that the heterogeneous nature of granules means they do not fail by the same mechanisms (as shown in figure 17) – suggesting that either lots of individual tests need to be carried out to find the mean failure stress or if multiple granule crushing of a mono-layer is performed then some granules will fail before others.

Isolating Granules

In order to test the static failure strength of granules using the DMA individual granules need to be isolated. As the granules are very small, ~ 30 - 100μm, they cannot simply be picked up and placed on the sample head of the DMA.

Several approaches have been considered:

a) Using a very fine wire to pick up a small cluster of granules up.
b) Sequential diluting of granules in some liquid until a small number of granules is present.
c) Charging a collector and placing near the granules

Methods

a) Using a very fine wire is good in theory but finding a wire or tip small enough is very difficult – a fine needle is about 5 times too big. Another problem is the human hand is constantly twitching and these shaking movements equate to about 10 length scales of the granules being picked up. With the equipment available it was not possible to pick up a single granule, they just get shunted around with none sticking to the pick up tool.
b) Sequential diluting appears to work but it is very labour and equipment intensive. An initial test using 5 stages; an initial mix and 4 subsequent dilutions produced some reasonable results. 2ml of vegetable oil was placed into 5 cuvettes. A small amount of granules was poured into the first cuvette and shaken to disperse the granules. 0.5ml was removed using a needle syringe and added to the next cuvette and the contents shaken to re-disperse the granules. This was repeated for a total of 4 dilutions (all using the same needle syringe – which may have caused contamination of more granules in later stages). After 3 dilutions excess of 50 granules were present in 3 drops of oil when examined under microscope, after 4 dilutions about 10 granules were present in 3 drops of oil. However a number of clusters of small particles were present after 3 and 4 dilutions, these clusters resembled clusters formed by crushed granules. There were more of these clusters in the 4^{th} dilution sample.
c) The third method of using a charged probe to collect individual samples has not been investigated.

The one approach to isolating individual granules that did meet with some success is the sequential dilution of a small mass of granules in oil (oil has to be used as water dissolves

the granules). A microscope set-up beneath a crushing probe should enable a slide with the diluted granules to be positioned such that the crushing probe tip is immediately over a single granule and a crushing test can be performed.
There are a number of concerns with this process. Firstly the dilution process appears to produce granule breakage - clusters of bodies similar in shape and pattern to crushed granules appear more frequently as each step in the dilution takes place. Secondly it was not possible to manoeuvre individual granules to underneath the probe tip. Lastly there is concern about the layering effect of the oil and how much of the crushing force will be taken up by the oil and not the granule

It is apparent from the initial tests on the dilution method that breakage of the granules occurs – larger volumes of oil could be used with larger pipettes but this would produce very large amount of contaminated oil. Use of a water insoluble binder would allow water to be used as the diluent in as large a volume as necessary.

7.2.3 Compression testing – multiple granules – uniaxial lumped parameter compression

It is more convenient to measure the compressive strength of multiple granules than to test individual granules. There are 2 reasons for this; it is too difficult to isolate individual granules in the size ranges considered in this report and there is always a spread of fracture loads in any batch of granules of the same size made using nominally identical conditions (this is explained by the theory of multiple nucleation start points – within section 13.4). The simplest way to do multiple compression is to compress the granules in a rigid fixed cylinder; this is known as uniaxial compression. Because this process lumps together the failure of many granules simultaneously by measuring the compaction of the granules in the cylinder and this compaction can be the result of elastic or plastic deformation, frictional sliding and plastic or elastic failure it is known as a uniaxial lumped parameter compression.
The particles are placed into a cylinder and tapped to remove any spatial re-arrangement prior to loading, in the case of very small granules as used in this report simply tapping

the cylinder will not induce complete spatial rearrangement and the initial compressive loading will involve some rearrangement. The theory and method used is based on the work by Adams, et al., [85]. This models the particle bed as a series of columns which take up the load once complete rearrangement has taken place. As the compressive force increases the load bearing "columns" (or granules) will fail and the probe will displace downwards and take up further load bearing columns, thus the stress and strain will be increasing. It is the initial part of the compression curve (after rearrangement) that is of interest as this is the region that reveals most about the strength behaviour of individual granules – it is imagined that as the compression progresses that granules that have already failed will come back into play and start to support the load (this is because the fracture particles have nowhere to go and in turn will themselves become load bearing.)

The method involves measuring the stress and strain of the load. The linear region of a logarithmic plot of the stress against strain is then used to find 2 parameters that are used in a theoretically derived equation that should describe the shape of the whole curve. 1 of these parameters is then adjusted incrementally until the theoretical curve matches the plotted results on a least squares basis. The second parameter is then used to find the failure load of the granules; however this is a lumped parameter and incorporates a constant that can only be determined accurately by measuring single granule compression. Essentially this method can be used to quantitatively predict individual granule strength by compressing multiple granules but only if the constant is determined experimentally from individual granule crushing. The method can be used to qualitatively compare the granule strengths of multiple granules but only where it is believed that the constant will not vary a great deal. As the granules being tested in this report are all of the same order of magnitude, use the same binder type and are made from the same raw material (albeit of different sizes and there are a few exceptions to binder type and material type) and with no realistic alternative it is acceptable to assume the constant of conversion to individual granule strength is constant. Another point of view is that the individual granule strength is unimportant due to the vast variability in crushing strength and failure mode within a single batch, as already mentioned, combined with the fact that

this research is interested in the relationship between static strength and abrasive wear (which ultimately uses multiple granules not individuals).

The theory by Adams lumps the compressive strength into an *Fcalc* value in the form below:

$$Fcalc = k_1 \tau \qquad (11)$$

Where *Fcalc* is the estimate of the compressive load at failure of an individual granule, k_1, is a constant combining the granule diameter, the universal *Pi* constant and presumably the material properties. τ, is the modified value of the 2nd parameter found from fitting a theoretical equation describing the stress-strain profile of multiple granules to the actual measured stress-strain curve using a least squares method.

NOTE: within this report the reported value of *Fcalc* is a lumped value and includes the, k_1, constant as it was not possible to determine a value for k_1. It is therefore not an absolute value (as in Adams original work) but a relative value. *Fcalc* is not a strength it is a failure load. Thus strictly where this report talks about granule strength derived from the multiple compression testing it should be referring to failure load – however this is not a problem where comparisons are being made within the same size class as strength is load per area (and area isn't changing).

7.3 Granule Compaction Theory

This is split into 2 major parts; section 7.3.1 describes the initial thought process behind the concept of a critical packing state and the limiting binder ratio. The 2nd part of section 7.3 is a version of the published paper "Modelling effects of processing parameters on granule porosity in High-Shear Granulation" by Maxim, et al., [100], giving the derivation of the theory. The last 3 sections of 7.3 include the full algorithm for finding the critical packing state from a Primary Particle Size Distribution (PPSD), an un-tested method for using the critical packing model and some considerations about shape and moisture content.

7.3.1 Theoretical relationship between porosity and granule strength – proposal of the critical packing state

Porosity is the key property to the strength of the granule. The strength is independent of primary particle material (only true if the primary particle material is weaker than the binder or the binder-particle interface) and only depends on the inter-particle bonds (binder bridges and binder-particle bonds) and the porosity of the granule. Wikberg and Alderhorn, [82] show how the porosity affects compaction strength of a granule. High porosity granules have lower compaction strength than low porosity granules.
It should be possible to control the porosity by manipulating either the processing parameters (e.g. mixer speed / duration), the formulation (binder-solid ratio, binder type and primary particle size, shape and distribution) or by manipulating the processing parameters and formulation simultaneously.

The effects of various processing parameters and formulations on porosity have already been discussed in section 5.5. A high mixing intensity and long processing time tend to produce low porosity, saturated granules Fu, [32], Lu, [31]. Low binder-solid ratios will lead to high porosity granules, increasing the binder-solid ratio will provide more binder to cover all the surfaces and fill the gaps between primary particles and leads to larger less porous granules. It is thought that binder-solid ratio is the biggest factor affecting the porosity of a granule, closely followed by the packing of the primary particles.

The packing of primary particles is dependent upon the primary particle size, shape and size distribution as well as being affected by the mixing time and mixing intensity (both of which should reduce the porosity by encouraging better packing of the primary particles) (Fu, [32], Iveson, et al., [7]). Consider a mono-size batch of granules with low porosity and low packing density made up of mono-size primary particles, better packing of the primary particles has the possibility of resulting in 2 cases; a reduction in number with the granules being less porous but having the same binder-solid ratio and remaining the same size, the same number of granules being less porous and having the same binder-solid ratio but a smaller size. For a real batch of granules there is a distribution of granule sizes with larger granules tending to have smaller primary particles, higher binder-solid ratio and a lower porosity. There will also be a spread of primary particle size distributions and binder ratios (and thus porosity) within a selection of granules of a given size, Reynolds, et al., [24]. Where the primary particle distribution within a granule cannot be altered by improved packing without breaking and reforming granules the granule size and binder-solid ratios can be altered.

It is proposed:
By progressing the batch using processing parameters such as higher mixing intensity and longer mixing time that encourage better packing the granules will tend towards a critical packing state.
The critical packing state is a function of the mass of primary particles and their size distribution within a granule; the critical packing state will have a limiting binder ratio dependant on the size distribution of the primary particles within the granule and a size that is then defined by the mass of primary particles and the binder ratio. Note that this assumes the critical packing state is one where there are no intra-granular pores. We define the limiting binder ratio as that which leaves no pores within the body of the granule and only just produces a capillary state.

To find a fundamental way of predicting the strength of granules an understanding of how the critical packing state affects granular strength needs to be determined. To do this

an expression for the critical packing state needs to be found and then related to strength and further the extent to which the critical packing state is reached (porosity) can then be related to granular strength. Once this is known it should be fairly straightforward to quantify the processing parameter and formulation effect on granular strength.

This theory helps to explain why high-shear granulation can be thought of as existing in 1 of 3 regimes (unstable, stable and transition) depending upon the formulation and processing parameters; It seems sensible that there cannot be a situation where all granules have reached the critical packing state. Even if all granules are such that the primary particles within them have reached the critical packing state some will have a deficit of binder and be below the limiting binder ratio and others will have an excess of binder above the limiting binder ratio. This is because when a granule reaches its critical packing state as much binder as can be is expelled to the surface, excess binder will produce a granule in the saturated state and this will tend to be stripped off by other granules in a non-saturated state that can use the binder to fill pores.

It might initially seem desirable to select a formulation binder-solid ratio that matches the critical packing state binder-solid ratio of granules having the same primary particle size distribution as the formulation primary particle size distribution. But as a number of workers (Scott, [89],Schaefer and Worts, [11] and Litster and Ennis, [26]) and preliminary experiments for this research have shown the initial granules will be different sizes with different primary particle size distributions, binder-solid ratios and thus different critical packing states and extents to which those critical packing states have been reached.

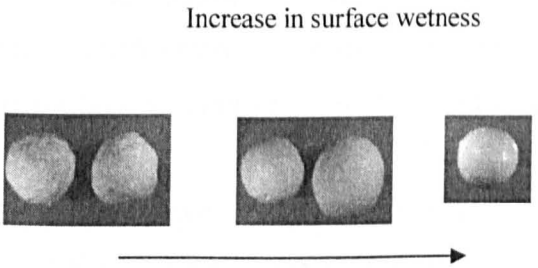

Figure 18 – showing the increase in surface wetness with granulation time

In an ideal world the mixing caused by the impellor and run time would lead to all granules tending towards their critical packing state all with the limiting binder-solid ratio. It is imagined that in a real high-shear system as mixing progresses the packing gets closer and closer to the critical packing state and as it does the granules expel binder to the surface, this produces lots of saturated granules. These saturated granules will either combine with other saturated granules or non-saturated granules producing larger granules whilst at the same time changing the primary particle distribution and thus the critical packing state and limiting binder ratio. This is kind of evident from observations that a longer run time and / or increased impellor speed produce larger granules with a smaller size distribution. This is also backed up by the observations of Knight, et al., [87] which show that as time progresses granules tend towards a very low limiting porosity and that experiments had to be halted due to granule surface wetting, which is caused by expulsion of the binder due to better packing of the primary particles within the granules. This is shown above in photos of granules taken out of the granulator as time progressed (figure 18).

Knight et al. also showed that as time progressed the granule size distribution became tighter. Scott, [89] points out that this unimodal size distribution is not necessarily indicative of a tendency towards a single primary particle size distribution within the granules, even citing evidence to the contrary – that granules at the large size end have a larger number of smaller primary particles and granules at the small size end have a smaller number of larger primary particles. This could be indicative of a granular system naturally finding a balance of granules containing different primary particle size distributions and thus having different critical packing states and binder-solid ratios. Equally it could be indicative that the theory is limited and unable to account for other factors influencing the redistribution of primary particles or the equilibrium state has not been reached.

There is also the issue of fragile, low porosity granules that are far from their critical packing state. These may break and smear their primary particles onto larger saturated granules changing the critical packing state.

7.3.2 Unabridged version of paper "Modelling effects of processing parameters on granule porosity in High-Shear Granulation"

When trying to meet the final product specifications for porosity of granules made using high-shear granulation there are many choices for the formulation and processing conditions. Section 7.3.2.3 presents the concept of a Critical Packing State of the primary particles forming a granule and the associated Limiting Binder Ratio, which allows granule consolidation to be modelled.

The effect on consolidation of varying the following processing parameters is explained: Mixing intensity, mixing time and binder addition method. The effects of varying the following aspects of the formulation recipe are explained: Primary particle type, shape and size distribution, binder type and binder: solid ratio.

Granule porosity is an important end product specification in many granulation processes as it affects the density and strength of the granule, Wikberg and Alderhorn, [82], as well as the dispersal properties of active ingredients. There are a lot of experimental observations from a number of sources (Fu, et al., [111], Holm, et al., [112], Scott, [89], Knight, et al., [87] and reviews mention in literature review) giving the effect of varying processing conditions and formulation recipes on the granule porosity when using high-shear granulation.

This paper describes granule consolidation and how a surface wet granule can be thought of as having a granule core surrounded by excess binder. An analysis of the interparticle space between primary particles within a granule is given followed by the concept of a critical packing state, which is used to describe the interparticle space of the granule core. A model is then presented to predict granule consolidation. This is followed by a description of the effect on the model of varying processing parameters and the formulation recipe used. Similar work modelling consolidation using an empirical model has been carried out by Iveson et al., [16] and has been covered in section 5.7. The section on Granule Consolidation in the review by Iveson et al., [7] gives a good alternative description of the processing parameter and formulation recipe effects that are covered in this section.

7.3.2.1 Granule Consolidation

Granules are generally made up of three phases, solid primary particles, liquid binder and air. As the granules collide with other granules and the process equipment the primary particles pack closer together squeezing out the air and binder. The extent of granule consolidation affects the surface wetness and interparticle space of the granule product. The interparticle space is defined as the fraction of the granule occupied by binder and air. Fig. 19 shows how granule consolidation with time affects the interparticle space. Curve A represents the consolidation of the whole granule, shown in Fig. 20. Curve B starts at the onset of surface wetting and represents the continuing consolidation of the primary particles. This can be imagined to represent the granule core consolidating towards its limiting interparticle space, squeezing out binder and making the granule more surface wet; this is shown in Fig. 21.

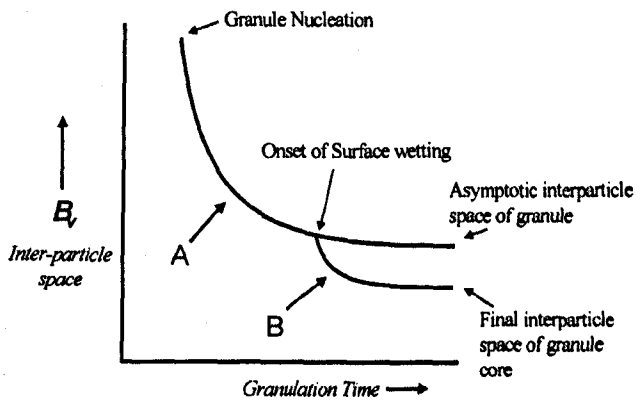

Figure 19 – Effect of granule consolidation with time on the interparticle space of the whole granule (curve A) and the imaginary internal granule (curve B)

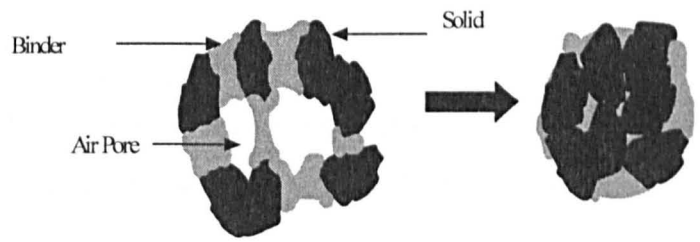

Figure 20 – Consolidation of the whole granule (represented by curve A in fig. 14)

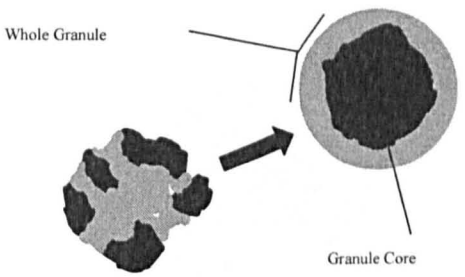

Figure 21 – Consolidation of internal granules (represented by curve B in fig.14)

7.3.2.2 Analysis of interparticle space

An analysis of the binder content associated with two different packing structures (body-centred cubic and a tetrahedral control volume) of mono-disperse spheres was done, shown in Fig. 22. This yields a general equation, Eqn (13), for the interparticle space, available for binder and air, in terms of the packing structure, particle diameter and interparticle binder layer thickness. The interparticle space, B_v, is defined as:

$$B_v = 1 - \frac{V_s}{V_c} \qquad (12)$$

where V_s is the total volume of the spheres within the control volume and V_c is the volume of the control volume. The control volume is found in terms of the diameter of the spheres, d`, and the thickness of the binder layer, $a$`, at the minimum separation of the spheres. The general equation for the interparticle space of a packing structure is:

$$B_v = 1 - \frac{k` d`^3}{(d` + a`)^3} \qquad (13)$$

where $k`$ is a factor dependent on the packing structure of the control volume; for body-centred cubic packing $k` = \pi\sqrt{3}/8$ and for a tetrahedral control volume (approximation) $k` = \pi\sqrt{2}/5$.

The full derivation is given in appendix C .

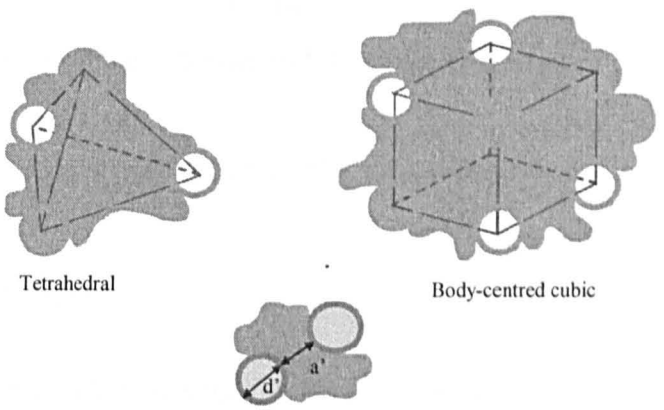

Figure 22 – Tetrahedral and Body-centred cubic unit cells used for the analysis of the interparticle space (d' – particle diameter, a' – binder layer thickness)

Note: The tetrahedral packing structure is only applicable over short length scales. As described in section 5.6, tetrahedrons packed using greedy algorithms progressively lose volume as the packing progresses as they cannot be packed in a repeating structure indefinitely. The approximation on the k' value for a tetrahedral packing structure comes from the approximation of the tetrahedral packing around a single point to an Icosohedron (see appendix C) – the value quoted here is an under-approximation.

7.3.2.3 Critical Packing State

The critical packing state is defined as the closest packing of solid particles forming a granule. For any primary particle size distribution (PPSD) there exists a theoretical state

(critical packing state) in which the primary particles are packed as close as they will ever get. The critical packing state has an associated minimum interparticle space. When binder is added the existence of a minimum binder layer between particles will expand the structure increasing the theoretical interparticle space. For any given PPSD and binder combination there is a corresponding interparticle space at maximum compaction defined as the limiting interparticle space, B_{lbr}. If this space is completely filled with binder then the limiting binder ratio can be found from:

$$Limiting\ Binder\ ratio = \frac{V_b}{V_p} = \frac{B_{lbr}}{1 - B_{lbr}} \tag{14}$$

where, V_b, is the volume of binder and, V_p, is the volume of primary particles forming a granule.

It can be expected that Eqn (13) might be used to describe the limiting interparticle space such that:

$$B_{lbr} = 1 - \frac{k d^3}{(d+a)^3} \tag{15}$$

where, d, is a characteristic length of the PPSD, k, is a packing factor taking into account the shape of the particles and the spread of the PPSD and, a, is the binder constant equivalent to the minimum binder layer thickness. Surface roughness and solid-binder wetting properties are accounted for in the binder constant. The problem with this is that it introduces, as yet, unknown functions (and as such is more use than the models by Tanaka et al. [98] and Ennis et al. [29]).

The limiting interparticle space can also be found by splitting the PPSD into segments, converting the segments into spheres and packing these into a 3D shape – the critical packing state, this is shown in Fig. 23. The limiting interparticle space is the fraction of the total volume that is not spheres. The effect of the minimum binder layer thickness is accounted for by increasing the diameter of each sphere before packing. The full

algorithm for this is given in section 7.3.3.

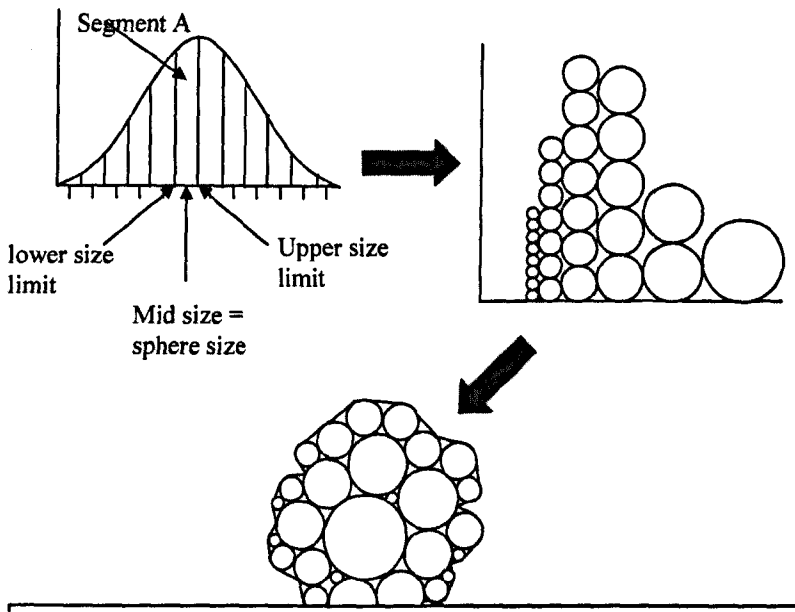

Figure 23 – Find the critical packing state by: convert a PPSD into segments, then these into spheres then pack the spheres into a 3D shape

7.3.2.4 Predicting Granule Consolidation

Fu et al., [111] and Knight et al., [87] show that granule porosity decreases to an asymptotic value as a batch granulation progresses. The interparticle space decreases to an asymptotic value as shown in Fig. 19, as the granule nears this value the granule becomes more surface wet as the granule core continues consolidating. The concept of the critical packing state and the analysis of the interparticle space allow the prediction of the limiting interparticle space of the granule core, B_{lbr}. This is an imaginary end point that the granule is trying to reach, squeezing out the air to reduce the porosity then squeezing out excess binder to form surface wet granules. In reality it is not possible for the primary particles to reach the critical packing state because the random way that particles move in the consolidation process means they do not all orientate exactly as required.

Iveson et al., [16] give an exponential decay model for predicting the effect of granule consolidation on porosity based on a consolidation rate constant and the number of drum

revolutions. A similar general rate equation is defined here for the interparticle space, B_v, of the whole granule representing consolidation along curve A with time.

$$B_v = (B_{v0} - B_{va})e^{-\omega t} + B_{va} \quad (16)$$

where, B_{va}, is the asymptotic interparticle space, ω, is the agitation intensity rate constant (a parameter representing the dimensionless agitation intensity per unit time, it incorporates energy inputs, rotational velocity and viscous effects in an undefined lumped parameter) and, B_{v0}, is the interparticle space at the end of the formation period, defining the critical start time, $t`$, such that:

$$t = t_{real} - t` \quad (17)$$

where, t_{real}, is the granulation run time.

By comparing the limiting binder ratio to the binder ratio of the start system we can modify the binder constant in Eqn (15) to a modified binder constant, $a``$, accounting for the extra thickness between primary particles. This gives an expression for the asymptotic interparticle space:

$$B_{va} = 1 - \frac{k d^3}{(d + a``)^3} \quad (18)$$

Once the granule has reached the asymptotic interparticle space then further agitation will result in the primary particles getting squeezed closer together in an attempt to reach the maximum packing state, this can be thought of as the primary particles forming an internal granule with its own associated interparticle space, $B_v``$. This results in excess binder being squeezed out and producing a surface binder layer. This phase of granule consolidation can be modelled by an adapted version of Eqn (16) such that:

$$B_v`` = (B_{va}{}^* - B_{lbr})e^{-\omega t^*} + B_{lbr} \quad (19)$$

where $B_{va}{}^*$ is the point considered to be the start of internal granule consolidation resulting in surface wetness occurring at time, $t``$, thus t^* is defined by:

$$t^* = t_{real} - t`` \quad (20)$$

The amount of binder on the surface, B_s, is equivalent to the difference between the asymptotic interparticle space and the consolidated internal granule interparticle space:

$$B_s = B_{va} - B_v`` \quad (21)$$

Fig. 24 shows Eqn (16) as line A and Eqn (19) as line B with the important associated times and interparticle spaces marked out.

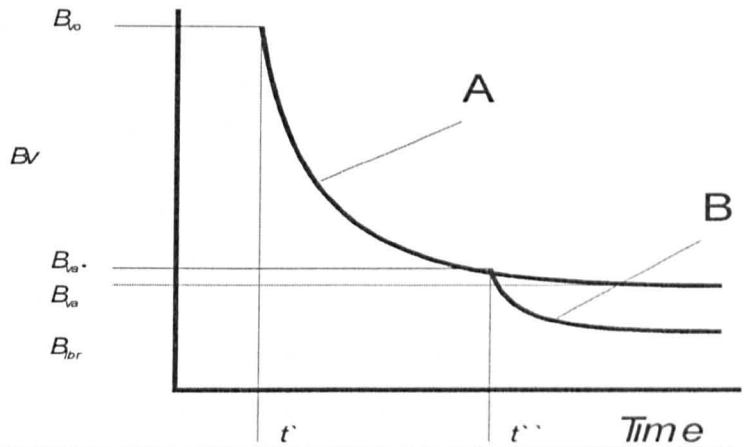

Figure 24 – Granule consolidation - Graphical representation of Eqn. 16 (line A) and Eqn 19 (line B)

7.3.2.5 Qualitative effect of processing parameters and formulation

In high-shear granulation formulation parameters and processing parameters can be varied in an attempt to alter the interparticle space of final granules. Many of these parameters act interdependently, for example the binder type and temperature act together to determine the viscosity and surface tension of the binder, this in turn combines with the primary particle material to give the wetting characteristics of the binder.

Primary Particle Type

The primary particle type dictates the material, the shape and the size distribution of the primary particles. If particles are very spherical in shape then the orientation during packing will not affect the final interparticle space. Flat plate-like particles or needles will have a much greater dependency on the orientation of the particles. If they align parallel to each other then the final interparticle space will be very low and the value of, k, will be high. If they align perpendicular or at angles then the final interparticle space will increase and the value of, B_{va}, will increase. The size distribution will affect the final interparticle space. It is thought that a wide size distribution will increase the value of, k,

due to the smaller particles fitting into the spaces between large particles. The particle material dictates the chemistry of its surface and importantly the surface free energy, when this is combined with the chemistry of the binder it determines the wettability of liquid binder on the solid. Iveson, et al., [16] report that a non-wetting liquid will not spread or form a film, but stay as discrete bridges. This will have the effect of increasing the value of the binder constant, a, in the general packing equation, which in turn will increase the value of B_{va}.

Binder Type

The binder type has several important properties, viscosity, surface tension and wettability. The wettability depends on the chemistry of the binder and primary particle material as already described. Changing the viscosity of the system will change the magnitude of the agitation rate constant, ω. The viscosity varies as a function of temperature and shearing forces. Generally the viscosity will decrease with temperature. For Newtonian binders reducing the viscosity will reduce the consolidating effects of any agitation and reduce, ω. For shear-thinning binders the effect is compounded with agitation intensity; increasing agitation intensity will increase the value of, ω, but will also decrease the viscosity further increasing the magnitude of, ω. For shear-thickening binders the effect is confounded. It is assumed that binder type also affects the thickness of the minimum binder layer between particles at their maximum compaction, this is reflected in the value of the binder constant, a. It can be visualised that this is dependent on the molecular arrangement of the binder when squeezed into very thin films between two surfaces. It is assumed that surface tension will affect the stability of air pockets within the granule and the net force felt by binder bridges (as oppose to continuum) during compaction, increasing the surface tension would reduce the net force and reduce the value of the agitation intensity rate constant, ω.

Binder Ratio

We define binder ratio as volume of binder per unit volume of primary particles. For any given PPSD and binder type there is a binder ratio at maximum packing defined as the limiting binder ratio. If the initial feed binder ratio is the same as the limiting binder ratio

then theoretically all the granules could consolidate to their maximum compaction and there would be no air phase within the granules. In reality this does not happen, if the initial binder ratio is less then either granulation will not occur or a portion of the internal space must be occupied by air. If the initial binder ratio is greater than the limiting binder ratio then the value of, $a``$, will increase and if it is assumed that no air is present at the onset of internal granule compaction, when $t = t^*$, then, $a``$, scales as:

$$a`` = d^3\sqrt{k\left(\frac{V_b}{V_p}+1\right)} - d \qquad (22)$$

If air is present then the asymptotic interparticle space must be increased appropriately. When the binder ratio is greater than the limiting binder ratio then as the granule consolidates it will squeeze binder out to the surface and produce surface wet granules. The extent of surface wetting is modelled by Eqn's (19), (20) and (21). When a granule is surface wet it will attract more fines and grow by layering, thus changing the volume of primary particles and the granule binder ratio – this will continue until the binder ratio has reached a stable value and the surface is no longer wet. Growth and stabilisation can also occur by coalescence with other surface dry granules, but coalescence of 2 surface wet granules will lead to a less stable state.

Run Time

The effect of granulation run time is accounted for by Eqn's (16) and (19), increasing the run time increases the extent of agitation and thus the extent of consolidation and production of surface wet granules. It is important to note that this model predicts a region before, $t`$, when granules will be highly porous. When high binder ratios are used long run times will lead to formation of large surface wet granules.

Agitation Intensity

Increasing the mixer speed will increase the agitation intensity and increase the value of the agitation rate constant, ω, leading to faster consolidation. However it must be noted that there is a limit to this effect, at elevated intensities breakage of granules occurs limiting the size of granule growth. When surface wet granules collide with other granules such that the combined size is greater than the stable size it is thought the

surface binder will be stripped away by the impacting granule rather than absorbed by the coalescence.

Binder Addition Method

Work by Knight et al., [87] suggests that granule porosity is independent of addition method at extended mixing times, it is proposed that individual granule interparticle space is independent of addition method after time $t``$. The addition method will affect time, $t`$, the modified binder constant, $a``$, and the initial interparticle space, B_{v0}, of individual granules. Spray addition will have a large spread of, $t`$, values compared to say pour-on addition, but might have a narrower spread of values for, $a``$, and, B_{v0}.

7.3.2.6 Conclusion to Critical Packing theory

A model has been proposed to represent firstly the reduction in porosity of a granule with time and secondly the subsequent consolidation and squeezing out of binder to form surface wet granules. The model allows the theoretical prediction of the amount of binder on surface wet granules as a function of time, Eqn (21). This model allows qualitative predictions of how changes in the granulation process and formulation will affect the consolidation rate and final surface wetness. The practical value of the model for quantitative predictions is currently limited by the determination of appropriate values in Eqn (15) and by the absence of a computer code for the algorithm converting a PPSD into a critical packing state. Experimental verification will be difficult due to the heterogeneous nature of any granulation system, realised in the model by the spread of values for, B_{v0}, $t``$, and $a``$, as a result of the addition method. Further work combining this models prediction of surface wetness with existing growth and breakage rate models should make experimental verification possible and subsequent determination of the various constants.

7.3.3 Algorithm for Packing Spheres

It is proposed that the maximum packing of spheres of a PPSD with given mass can be determined by doing the following:

The PPSD is first converted into a finite number of different sized spheres. This is achieved by:

Split the PPSD into n segments.

Find the area of each segment $x_1, x_2 \ldots x_n$ as a fraction of the total area of the PPSD.

Convert the fraction into a mass by multiplying by the total mass.

Convert the mass in each segment into a finite number of spheres each having a diameter equal to the mid-point of the segment. (shown in figure 25) For ease we will uniquely label each sphere alphabetically starting with the largest (see figure 26)

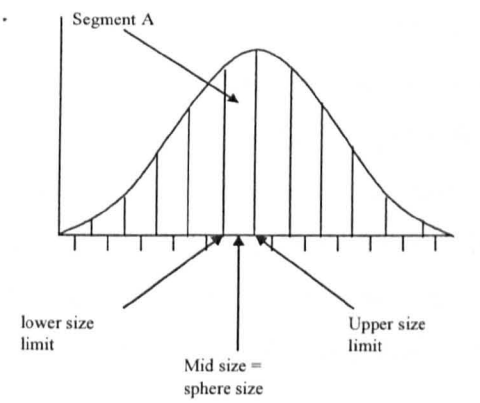

Figure 25 – size distribution / segmentation

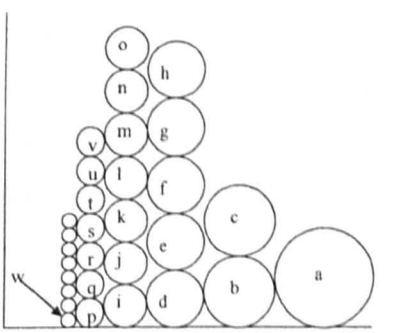

Figure 26 – PPSD converted to spheres

The greater the number of segments, n, and the greater the mass the more accurately the finite number of spheres will represent the real PPSD.

The next step is to pack the spheres into as dense a packing structure as possible – that is the theoretical maximum packing (minimum porosity). It is believed that a tetrahedral packing structure is the closest possible packing of mono-disperse spheres over length scales of a few spheres. It follows that if the structure is bi-disperse such that the second size was small enough to fit into the interstices then the porosity would be much smaller,

but still retain the tetrahedral shape. The idea is to maintain the tetrahedron structure when packing the spheres and to fill the gaps when a particle is small enough to fit inside (along the lines of an Apollonian Gasket). It seems plausible that the small length scales over which the packing occurs in a granule and the reducing size of the spheres will negate the effects of volume loss / incomplete packing that occurs with mono-disperse spheres packed in a greedy algorithm using tetrahedral structure.
This needs to be solved in 3 dimensions as the tetrahedral packing structure does not arrange in planes and so is not repeating in a planar sense and cannot be solved in 2 dimensions.

The algorithm is thus.
Start with the largest sphere, ***a***, as the central body.
Take the next largest sphere, ***b***, and add this to ***a***.
Subsequent spheres are added in descending size order and added such that they touch the largest sphere if possible, then move around the surface of that sphere until they come into contact with the next largest sphere, it then moves around that surface (remaining in contact with the initial sphere) until it contacts the next largest sphere – this should produce a tetrahedral type structure. If it is not possible to fit the sphere into a space such that it touches the largest sphere, ***a***, then move on to the next largest, ***b***, and so on until space is available. (This is shown in figures 27a. and 27b)

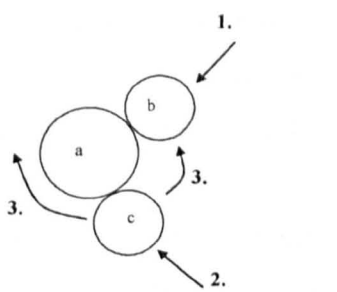

Figure 27a – 2D packing starting with large sphere

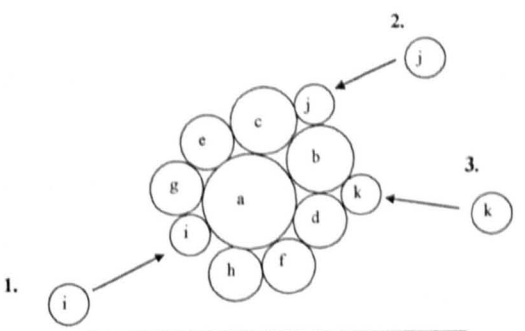

Figure 27b – 2D packing of spheres (4th set)

A situation will occur at the very small sizes of sphere where it will be able to touch the largest sphere by fitting into the gaps between larger spheres, in this case the same criteria applies: the sphere must touch the largest sphere and then move such that it is touching the next biggest and so on.

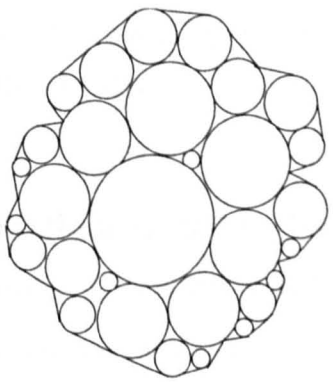

Figure 28 – control volume based on packed spheres

Once all the spheres have been packed the porosity can be calculated – this is done based on the definition of a saturated granule that is 'all the internal spaces are filled with liquid and the surface is only just wet'. The porosity is defined as 1 – fraction of the total volume occupied by spheres. The volume occupied by the spheres can be found from the sum of the individual volume of the spheres, the total volume can be found by taking a control volume based on the external spheres and joining the surface by a tangential line (shown in fig 28)

People working in similar areas on the packing of particles are Stepanek K. (UCL) and Gan M. (Leeds University).

Gan, et al., [113] described the use of DIGI-PAK, a computer programme designed for constructing packing of random shapes in ordered or random packing arrangements. It is the steric hindrance (or geometry) that dictates the packing – most relevant to non-sticking particles. The method involves digitising the particles, the packing space and the particle movement. This programme can be used for random packing, sticking particles to a surface and to model compaction. Gan claims that rough irregular shapes have a lower packing density than spheres. This computational approach might be used to predict flow channels within a granule by knowing the contact points, as well as allowing calculation of the stresses within and the stability of a structure (this would be useful for predicting the flow of binders during compaction of granules in the critical packing theory presented

in the current work). It is unknown whether Gan's algorithm can pack random shaped particles from a PPSD to give a packing density (thus allowing the determination of critical packing state for a PPSD).

7.3.4 Un-Tested method for using the Critical Packing State Model (Recommended scope for future work)

This method is un-tested in the sense that it is currently not possible to determine many of the values or exact relationships. This work has not been taken further than the conceptual stage as it would be a whole new project to try and determine the methods of finding the values and relationships. However the qualitative description of the model presented in section 7.3.2 remains useful in unifying and making sense (one possible interpretation) of all the results form the wide variety of different researchers upon which the work was based (from the reviews covered at the start of the Literature Review) for an alternative interpretation see the work by Iveson et al., [30].
Probably an easier approach to find the critical packing state would be to write a computer program that uses the algorithm in section 7.3.3, this would probably allow experimental design that would enable some of the other parameters to be found empirically.

The un-tested method is thus:

1) Determine the primary particle size distribution using any standard method.
2) Determine the shape factors, a_s, b_s and c_s that describe the spheroids equating to the typical primary particle shape.
3) Determine the k-value for the primary particle size distribution based on the shape factors (a_s, b_s and c_s) and the spread of the PPSD.
4) Use the k-value to determine the theoretical porosity, B_v', of the critical packing state.
5) Decide on a characteristic length, d', that describes the size distribution. I propose that mass-mean size be taken as the characteristic length.

6) Determine the binder constant, a, for the binder used and the temperature to be used.

7) Use the k-value, the characteristic length and the binder constant to determine the porosity of a granule at maximum compaction.

8) The porosity at maximum compaction can be used to find the limiting binder ratio.

9) By comparing the limiting binder ratio to the binder ratio of the start system, or otherwise determine the asymptotic porosity value, B_{va}, for the system.

10) Determine the agitation intensity rate constant, ω, based on the impellor speed to be used and the binder properties at the temperature to be used.

11) Determine the porosity, B_{vo}, at the critical start time, t'.

The porosity of granules as a function of time can now be determined by the general rate equation:

$$B_v = (B_{v0} - B_{va})e^{-\omega t} + B_{va} \qquad (16)$$

Where $t = t_{real} - t'$ (17)

Thus a hypothetical model is presented where it is possible to produce granules of a known porosity. Knowledge of the primary particle size distribution, the shape of the primary particles, the binder used and how the binder properties of viscosity and surface tension vary with temperature should allow the prediction of the porosity at maximum compaction. It is supposed that a knowledge of the binder ratio used in the feed and the shape of the size distribution will allow the prediction of the asymptotic porosity value. The addition method, initial operating conditions and binder ratio will determine the critical start time. The run time and the agitation intensity then determine to what extent the granules reach the asymptotic porosity.

Note: that none of this is currently possible as many of the steps in the un-tested method outlined above are either not possible yet (or not widely common knowledge). It may not even be possible to find some of the relationships, for example step 3 assumes that it is possible to convert a particle described by 3 spheroids into a single k-value that describes

the packing arrangement. As it currently not possible, after centuries of work, to rigorously prove Keplers Conjecture for packing mono-disperse spheres it seems very unlikely that packing of irregular shapes will be any easier. It thus appears that the best route will be done with computer simulation and determination of the critical packing state by conversion into spheres and packing them sequentially as proposed by the algorithm in this work.

7.3.5 Effect of Shape and Moisture Content on packing

Puri, [114] gave a talk at CHOPS 4 entitled *Bulk Mechanical properties as influenced by particle shape, moisture and sphagnum peat using the cubical triaxial tester.* Apparently increased moisture increases the packing of particles, but this only has an affect on rounded particles and angular particles. Moisture has no effect on spherical particles as these generally have a packing density close to their maximum. The effect of moisture is more pronounced with rounded particles than with angular particles, presumably because it helps the rounded particles slide over each other and re-arrange into a dense packing, in the case of angular particles the sharp edges get in the way and the effect is not as noticeable. Puri also noted that where the liquid between particles is compressible then the shape of the particles makes no difference to the rearrangement.

7.4 Abrasion

7.4.1 Knoop Indent Method

At the inception of this research the abrasion testing was to be carried out using a method based on the 'in vitro abrasivity testing using indented Perspex blocks – K2 project – Unilever report number PS 01 0514'. This abrasion test was originally designed to test and compare the abrasivity of toothpastes and remove the need for testing using bovine enamel. The test is a simplified version based on the British Standard 5136:1981.

The test uses Perspex blocks that are indented in 4 locations on the surface using a Knoop indenter in accordance with Unilever GCP SOP 129 01. The indents are measured using a microscope and the lengths recorded prior to abrasion. The Perspex blocks are then abraded using 1 of a variety of abrasion rigs (each having a slightly different set-up). This causes the surface of the Perspex to be worn away; as it does it reduces the length of the Knoop indent in proportion to the depth of wear. The diamond shaped geometry of the indent means that as the surface wears away the 2D size of the Knoop indent decreases. The length of the indent is then re-measured and the depth of abrasion determined. This is interpreted as a relative measure of the abrasive strength of the granules. This theory is sound, but as will be shown in section 7.4.2 there are flaws in the practical application of this method to testing the granules produced for this research using the equipment that was available. It is believed that the alternative abrasion testing method described in section 7.4.3 is superior to the Knoop indenting method as it removes the human "judgement" error in determining the end points of the Knoop indent after abrasion (these can be easily hidden by striations caused by granules or the linear motion of the abrasion rig).

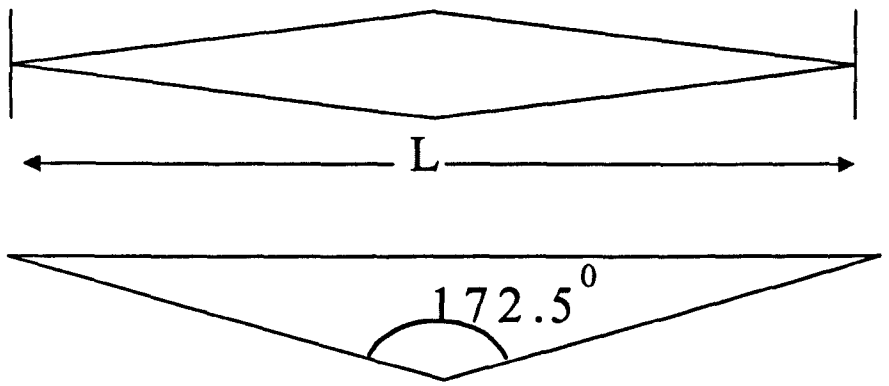

Figure 29 – Knoop indent geometry

A knoop indent is a diamond shaped indent produced by indenting a perspex block (or other material) using a micro-hardness tester. The geometry of a Knoop indent is such that it allows quantitative calculations of the amount of abrasion taking place in terms of depth of material removed by simply measuring the length of the indent before and after abrasion. The geometry of the knoop indent is shown in figure 29:

When a knoop indent is made in Perspex it needs to be left for 24hrs before the length of the indent is measured due to elastic recovery of the perspex, the angle at the base of the indent of 172.5^0.

The depth change in abraded material can be calculated by:

$$\Delta d = \frac{0.5\Delta L}{\tan 86.25} \qquad (23)$$

Where Δd is the depth change as shown in figure 30:

ΔL is the length change of the indent and Δd is the depth change that is calculated.

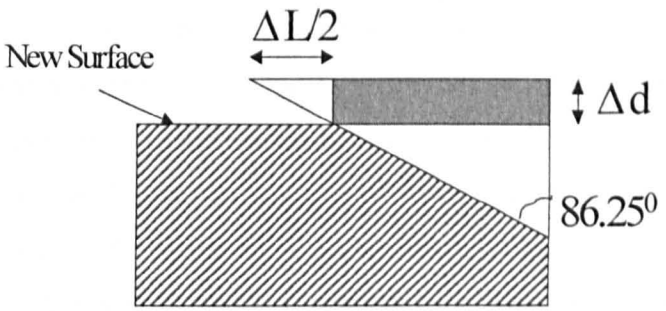

Figure 30 – Abrasion depth change

7.4.2 Rejection of Knoop Indent method of quantifying particle abrasion

There were 4 abrasion rigs that were used to do the initial abrasion testing using the Knoop indent method and appendix D shows an early report into the different types and also the effects of using a toothbrush as the counterbody.

The 4 rigs were 2 linear reciprocating motion, 1 hand-held toothbrush and a Lissajous (figure of eight) motion. The initial testing used a toothbrush as the counterbody and the amount of wear generated was measured by the reduction in the length of a Knoop indent.

There are a number of problems with abrasion testing using the Knoop indent and toothbrush as counterbody. The amount of wear (ignoring granule dependent factors) is dependent on the pressure applied to the toothbrush head, the nature of the bristles, the diluent used, the grade of the perspex used, number of brush strokes and intensity of brush strokes. These are all rig dependent characteristics and mean that results from different test rigs cannot be directly compared as the loading and brushing characteristics are different, these variations can be minimised by using a single rig and it was decided to use an In-house purpose built rig for the tests described in later sections of this report. This meant that some of the abrasion test data is non-comparable.

A greater concern than comparing results from one rig to another is the accuracy of measurements of the length of the Knoop indent before and after abrasion within the results from a single rig. It was found that the measurements of the indents vary

depending upon what microscope is used to measure them. A test using two different microscopes to measure indents produced differences between the two of between –25μm and +148μm with a standard deviation of 41μm, equating to an average error of ± 23% of the measured length. Thus the same microscope should be used before and after indentation. There is a lot of variation in the measured length of a single indent even if the same operator measures it several times using the same microscope. This is due to the difficulty in determining exactly where the indent starts and finishes as shown in figure 31. (It is even more difficult to determine the start and finish point when the ends are masked by striations caused by the abrasion testing).

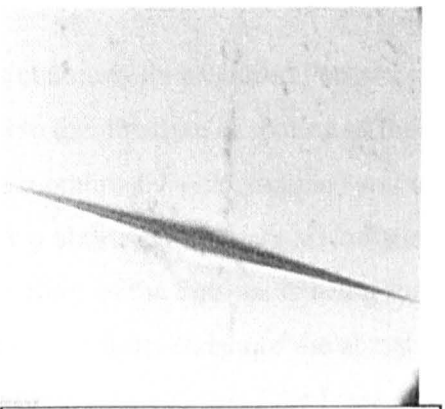

Figure 31 – showing fuzzy ends of typical Knoop indent

A test measuring 12 indents and then re-measuring them using the same microscope found an estimated average error of ± 12%. This is an error on the measurement of the length of the Knoop indent before and after, which when combined in quadrature gives an error of ± 44μm on the length change of the indent. This is the smallest error based on the precision of measuring a clearly identifiable Knoop indent, the error will be larger when using toothbrushes or a linear motion as the scratches and gouges created from these obscures the ends of the indent and makes it difficult to determine where the length should be measured to.

There is a real concern that the precision of the measurements of the Knoop indent is not tolerant enough to pick up the subtle differences in the amount of abrasion caused by different granules made using the variety of processing and formulations investigated in this research. The range of errors for the calculated wear using the Lissajous rig was from ± 6% to ± 81.5%, with an estimated average error of ± 16.1% (this will be even greater for linear motion abrasive wear because of striations running perpendicular to the Knoop indent and obscuring the ends). This error is greater than the differences between the average wears for different types of granules, so even though the results appeared to give a trend in the amount of wear these could easily be because of the random nature of the errors in the precision of the measurements of the Knoop indents.

Tests using a toothbrush as counterbody produced Perspex plates with many striations in the surface running parallel to the direction of motion of the toothbrush. Further tests using different loads on the toothbrush (with granules) and using the toothbrush with oil only showed that the resulting abrasive marks are all indistinguishable. Thus any striations and wear on the surface of the Perspex is being formed by abrasion due to the toothbrush only and is completely independent of the abrasive material.
These tests imply that the results obtained using the Lissajous abrasion rig at the Unilever Port Sunlight research facility are flawed - that the majority of the abrasion in those cases is due to the toothbrush bristles and not the abrasive media.

The theory of basing the level of abrasion on the length change of a Knoop indent is sound - however the practice of using this approach is inaccurate and more so when toothbrushes are used. Measurements are based on the size of the Knoop indent but the human error in determining the length of the indent before and after is very large compared to the amount of abrasion taking place.

The experimental fact that the abraded surface looks identical with and without granules indicates that the toothbrush bristles are producing the abrasion in the linear forward-backward motion abrasion rigs using toothbrushes as a counterbody. This is further

supported by the fact that when the abrasive block was replaced with a piece of jay-cloth covered cork the striations were significantly reduced.

It is experimental fact that the reproducibility of measurements of the length of the Knoop indents is poor due to human error judging the end tips of the indent.
However, the results from the Port Sunlight facility did seem to indicate that material type for the granule alters the abrasiveness and that abrasiveness does in-fact increase when abrasive particles are present. This could just be a random anomaly due to the small number of tests involved and the human error aspect combined with the effect of striations "cutting off" the end of an indent. More tests using the Knoop indent would need to be carried out to give any confidence in an observed trend, but it is consistent with the observations from the results of subsequent testing using an alternative abrasion method (see section 12.3.1).

Note – details of the experiments described in this section have not be included in this report as they are not comparable with the results contained in the results database and were obtained using a method that is inconsistent with the current work.

7.4.3 New experimental procedures – ABRASION TESTER

As the Knoop indent with toothbrush counterbody method of abrasion testing was found to be unsatisfactory a new test method needed to be devised. It was decided that a completely new abrasion test rig would be built in-house with a reciprocating motion (as this was the simplest to construct in the limited time available).
There are a number of different abrasion tests currently used to either assess the abrasive resistance of a surface or the abrasiveness of different particles. There are 3-body and 2-body abrasion tests, but the most common are 3-body abrasion with a slurry of fresh abrasive particles being fed between the counterbody and the substrate. The most popular type of test is the ball-cratering or rotating disc type, whereby a wear scar is produced with similar geometry to the counterbody (circular in the case of ball-cratering and rectangular in the case of rotating disc). This type of test was not used in this research, as it needs a continuous feed of abrasive particles; the limited batch size of the produced granules and the sieving time required to produce enough abrasive particles for a

continuous fresh feed would have limited the number of achievable tests. A method based loosely on (British Standard) BS 5136:1981 was developed.

A new method of measuring the wear was needed as the Knoop indent was too inaccurate. Pickles, [115] of Unilever Oral Care research group, suggested blanking off two strips either side of an exposed central strip on a piece of Perspex. Then measuring the surface depth profile across the exposed section after abrasion and somehow relating that to the wear. This was the approach that was taken. Sellotape was used to blank off the surface of a Perspex abrasion plate leaving a roughly 3mm wide strip running along the length of the plate. The Perspex plates are abraded, the Sellotape removed and the surfaces cleaned. The surface underneath the Sellotape act as a datum and the perpendicular profile across the wear scar is measured using a profilometer, a standardised length of this profile is then used to calculate the cross-sectional area of the wear scar and this is taken as a relative measure of the abrasivity of the particles. Toothbrush heads could not be used as the counterbody as they produce wear scars even when abrasive particles are not present and they push the particles to the sides of the sample holder and away from the area being abraded. A solid metal block covered in a soft cloth such as jay-cloth was the answer. This was tested without granules and did not produce measurable scratches and gouges in the surface of the Perspex. It was hoped, by using a flat block and a cloth, that when the counterbody is lowered into a slurry of oil and granules on the Perspex plate that the weight of the counterbody and the fibres in the cloth would hold enough granules in place to abrade the Perspex substrate. This is assumed to cause both two-body abrasion (with granules held in the fibres of the cloth) and three-body abrasion (with granules escaping and rolling around under between the cloth and the Perspex). Observations show most of the granules are still pushed to ends and sides of the sample holder and take no part in the abrasive test, but examination of the underside of the counterbody after testing shows that granules are trapped there and must therefore be taking part in the abrasion.

Appendix E shows the original abrasion rig design and estimates on the operating conditions. A change to this design is the toothbrush counterbody was replaced with a

metal block of dimensions 11mm x 11mm x 28mm, around which the cloth could be wrapped (this allowed fresh cloth to be used for each test without destroying the metal counterbody). The rig consists of 2 metal plates placed on top of each other – the base plate (shown on page 3 of appendix E) and the top plate (shown on page 4). The bottom plate has 5 sample housings into which the 5 removable sample plate holders can be placed. Perspex blocks 54mm x 54mm x 5mm are blanked off with sellotape and placed into these sample plate holders. The top plate moves in a reciprocating motion on a set of runners and is attached to a geared motor (shown on page 5 of appendix E) – the speed of the motor is fixed and resulted in a change to the speed from 150 cycles per minute to 81 cycles per minute. The top plate contains the toothbrush holders (metal counterbody holders) with the option of adjusting the angle of abrasion to either 10^{o} or 25^{o} (this is a change from the original abrasion rig design) – for the purpose of the abrasion testing in this report the angle was fixed at 10^{o}. The counterbody holders have the option of adjusting the vertical load by the addition of a weight on the spindle.

The abrasive particles are dosed by mass; it is the easiest method without the need for calculations. If the abrasive granules are dosed by keeping surface area or number constant they will still need to be weighed, the calculations required to work out the mass required to keep the surface area or number constant will be an estimate based on the size cut and the size distribution within that size cut. This is because the exact surface area or number of the particles used cannot be known due to the spread of granular sizes within a sieve cut.

1.5grams of granules used.
5ml of Oil is added as a diluent
The combined weight of the counterbody and abrasion block is 125g ± 2.5g (No additional weight is added onto the spindle of the counterbody holder)
The test is run for 5 minutes.

figure 32 below shows the abrasion rig and figure 33 shows the sample plate and holder, metal counter body and the counter-body holder.

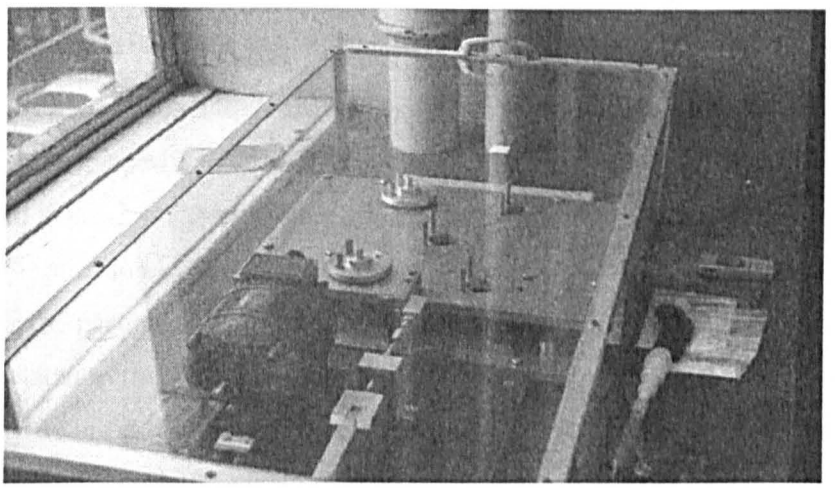

Figure 32 – In-House Abrasion Rig

Figure 33 – Counterbody Holders (top), CounterBody (centre), Sample plate (bottom left) and Sample Plate holder (bottom right)

7.4.4 Dimensional Analysis of Abrasion Testing (an attempt to develop a new hypothesis)

This section describes a dimensional analysis of the abrasion process, specifically relating to the test developed in section 7.4.2. The current knowledge and theories of abrasion described in section 5.2 were used to help determine the factors believed to affect the amount of abrasion in the specific case investigated by this research. Included in the factors is the particle failure load, as we are trying to test the theory that static strength can be related to the abrasive strength it makes sense to include this parameter somewhere (and it feels intuitive that a stronger granule will produce more abrasion – it can wear for longer before it is destroyed).

The abrasion testing machine (abrasion rig) is used to produce abrasive wear in Perspex plates by 3-body abrasion. The substrate is a square Perspex block which is rigidly fixed in a sample holder. The abrasive particles are granules of Calcium Carbonate and PEG made using a High-Shear Granulator. The counter-body is a metal block covered with Jay-cloth.
The Perspex sample is fitted into the sample holder. A mass, M_g, of granules is added and topped up with oil (carrier fluid). The counter-body is then lowered into the granules / carrier fluid and forced into contact with the Perspex substrate by an applied load, F. The counter-body is then moved backwards and forwards at speed, S_a, for a total time, t_a.

For the purposes of this dimensional analysis the following is accepted: That size of an abrasive particle affects the amount of wear; whether this is smaller particles producing more wear or larger particles producing more wear or a size-wear relationship that varies with size is unimportant at this stage. The applied load will affect the amount of wear; it seems obvious that if you push harder you are more likely to scratch the surface. The abrasive speed will affect the wear; a faster abrasive block moving in a single direction will cover more distance in a given time and therefore a larger surface that is worn away and thus more worn material, for a reciprocating motion it makes sense that the wear from the additional strokes is just layered on top and adds to the depth of the wear in that

spot. Abrasive time will therefore affect wear for a similar reason; a longer time means a greater distance travelled for a given speed or a greater number of total abrasive strokes and if the abrasive wear per stroke is assumed constant then there will be greater wear. The particle (granule) failure load is assumed to affect the wear, if the downward force is greater than the fracture load of the granule then it will fail and fragment, the abrasive wear caused by these fragments will be negligible as the downward force of the abrasive block will be supported by the remaining granules. The granules will not fail immediately the force is applied but their failure load will change as the abrasion test goes on, this is because the abrasion process is believed to erode the surface of the granules and thus reduce their size and in turn the failure load. There is also the consideration of repetitive strain, it is known that repeated loading and unloading will reduce the failure load, as the granules are in 3-body abrasion they are rolling with the downward force acting in a continuously changing meridian – this puts a continuous cycle of tension and compression on the granule as it flexes due to the rolling and changing meridian stress. (it is assumed that fracture fragments are too small to affect the wear process – but this could be very wrong and a conflicting theory of this work is that the abrasive wear is more dependent on the size, and material, of the primary particles than on any macroscopic properties of the granule agglomerate). The mass added and the density of the particles (granules) are also assumed to affect the abrasive wear, but not directly; they act together to change the number of abrasive particles and the total surface area that is causing abrasion. It is thought that the surface area is the ultimately important factor but this would need to take into account the shape and size of the primary particles and the formation of the granules surface including binder content, but these are not quantifiable in terms of a dimensional analysis and cannot be directly varied in terms of the abrasion test. Adding more mass is a measurable option for the abrasion test and it is assumed that it would increase the number of particles and thus the abrasive particle surface area abrading the Perspex leading to more abrasive wear, the density works against this and is changed along with the size and failure load when a different granule is used. An increasing density will lead to a lower number of abrasive particles for a given mass loading and thus a smaller abrasion. There is a limit to this added mass effect, too many abrasive particles can form layers on top of each other and reduce the force transfer from

the downward load of the abrading counterbody to the abrading particles on the surface of the substrate.

Some of the above can be generalised by the following:

More granules => more abrasion
Larger granules => weaker
Smaller granules => more abrasion
For given mass => if smaller => more granules => more abrasion
Same number =>if smaller => less mass => probably less abrasion

So for the purpose of the dimensional analysis the factors that affect the amount of abrasive wear in the substrate are thought to be:

- Particle (granule) failure load σ (N)
- Particle size l (m)
- Mass of particles added M_g (kg)
- Density of particle ρ (kg / m^3)
- Abrasion time t_a (s)
- Applied load F (kg)
- Abrasion speed S_a (m / s)

Based on the Buckingham $\prod$ theory a dimensional analysis of the problem was performed.

Before conducting the analysis it was decided to combine the abrasion time, applied load and abrasion speed into a single (new) term, Abrasion intensity (or Abrasion Energy), E_A.

$$E_A = F.t_a.S_a \qquad (24)$$

Thus we have 5 variables with 3 independent physical dimensions (M – mass, L – length, T – time) as shown below:

Variable	Dimensions
Particle strength	$\frac{ML}{T^2}$
Particle size	L
Mass of particles added	M
Density of particle	$\frac{M}{L^3}$
Abrasion energy	$\frac{ML^2}{T^2}$

The Buckingham $\prod$ theory states that 5 (variables) – 3 (dimensions) = 2 dimensionless parameters are needed. These were found by choosing 3 repeating variables and non-dimensionalising the remaining variables. The variables chosen were, Particle strength, Particle size and Particle density (it is advantageous that these are all fixed by the type of granule / particle used, i.e. they are formulation variables). The remaining 2 variables that need to be non-dimensionalised were Abrasion energy and Mass added (both of which are operating variables and can be easily changed by varying the operating conditions of the abrasion test).

The 2 Π groups that represent the dimensionless Added mass and dimensionless Abrasion energy respectively are:

$$\Pi_1 = \frac{M_g}{\rho l^3} \quad (25)$$

$$\Pi_2 = \frac{E_A}{\sigma l} \quad (26)$$

Now the bit where a new hypothesis is attempted to be made:
The purpose is to devise a fair abrasion test that takes into account all the measurable factors that affect abrasion and removes their influence on the amount of abrasive wear. A test was wanted such that the wear due to a few big strong dense granules could be measured and compared, on a fair (like for like) basis, against the results for lots of small weak porous granules to find which was the most abrasive (this isn't possible without some form of dimensional analysis).

The Π groups are now combined into a final dimensionless function.

try :

$$0 = \Pi_1 \pm \Pi_2$$

$$0 = \frac{M_g}{\rho l^3} \pm \frac{E_A}{\sigma l} \quad (27)$$

By multiplying both sides by l and the fact that increasing the value of Π_1 and / or Π_2 increases the amount of abrasion (making the sign of the $\pm$ change to -) this simplifies to:

$$0 = \frac{M_g}{\rho l^2} - \frac{E_A}{\sigma} \quad (28)$$

If it is assumed that the above equation is correct: By using this equation as the basis for determining the values of the variables in any given abrasion test abrasiveness can be compared directly, in other words a fair test.
i.e. if there are 2 different sets of granules, A and B, that are made such that they have different formulations (strengths, densities and characteristic lengths) a suitable set of operating conditions (added mass and abrasive energy) needs to be determined for the abrasion test such that the results can be compared directly. In the case of the abrasion rig it is the simplest operating method to keep the abrasion energy fixed and vary the added mass.

A test calculation (using equation 27) based on the current (arbitrary) abrasion test protocol was done to check the validity of the chosen order of magnitudes of the variables used. As particle strength is currently the hardest variable to determine accurately experimentally this was the variable whose order of magnitude was determined.
The current test protocol uses:

Load (mass)		0.01032 kg
Speed		0.1025 m / s
Time		300 s
Added mass		0.0025 kg
Characteristic length	$\approx$	2×10^{-4} m
Density	$\approx$	2265 kg / m^3

Putting these values into equation (27) gives a desirable particle strength of 0.1150 kg which is the equivalent to 1128 mN (which is within the range of a set of experimentally tested granule strengths of between 400 – 1500 mN); found from static strength tests. The orders of magnitude for the test conditions seem appropriate based on equation (27)

***NOTE** – the value of the added mass used in the experiments later in this report is less than the value quoted here as it needed to be reduced due to the lack of material available for testing.*

However the equation below (in the full dimensionless form) does not seem completely satisfactory.

$$0 = \frac{M_g}{\rho l^3} - \frac{E_A}{\sigma l} \qquad (29)$$

The first term, Π_1, is effectively the number of particles. The top half of the second term is the energy supplied by the abrasion process and the lower half is a force x length (or work done or energy), which can be thought of as the energy needed to cause failure in a particle size l. This means that the second term, Π_2, can be interpreted as the number of broken granules (it is effectively the ratio of abrasion energy (input) to another form of energy – probably the energy required to crush a granule). The reason why the equation with this combination of Π's does not seem appropriate is that an increase in abrasive energy would increase the 2nd term, but to keep the equation equal to zero then the mass added needs to be increased. Increasing both would be expected to lead to an overall increase in wear, by the argument above this would mean that the particles being analysed are more abrasive (but they are really the same).

To counter this, the following equation is proposed.

$$\frac{M_g}{\rho l^3} \cdot \frac{E_A}{\sigma l} = K \qquad (30)$$

Where, K, is an arbitrary constant that is kept the same for all experiments. In this equation it is no longer clear what the meaning of the L.H.S. is (no. of particles x some measure of the destruction of the particles).

It is not known whether this equation holds true. It is known that there are trends in some of the parameters for certain material, such as the failure load increases with size.

The combination of Π parameters that correctly describes the abrasion test can be used to directly compare granules. If it is kept constant for various abrasion tests (by changing the appropriate factors – probably mass added to balance the changes due to other granule dependent factors) a larger volume of worn material indicates a better transfer of abrasive energy to material removal. In other words if granules A and B are tested such that the real (currently un-defined) $f(\Pi)$ expression is constant and it is found that A produces twice as much wear as B then A is twice as efficient at transferring input energy into

energy to damage the substrate surface. (This would be due to granule properties that we currently do not know about or cannot quantify such as shape). These equations have not been tested or verified.

7.4.5 Determining the value of the length term from a sieve cut

For both the abrasion testing hypothesis and the critical packing concept a value for the size of the granules being considered is needed. A single value is preferable as it reduces the need for complicated maths and iterations.
The real physical process of sieving a sample to get a sieve cut will produce a range of granules of different sizes within that cut, single size values will probably not be identical even if several sieve fractions are taken from the same batch because of the random nature of sampling.

Consider 3 sieves with nominal ranges 63-106μm, 106-212μm and 212-300μm. We are interested in testing the properties of the sieve cut 106-212μm and the analysis of our data requires that we need a single length value to represent this. One could just choose either of the end points as an estimate of the size, using the mid-point would be better but a mass-weighted length is even better. Even this is not ideal as the actual sizes will be skewed because of the physical limitations of sieving. This mid-size sieve will not contain any particles larger than 212μm (assuming the sieve is made properly) as these cannot physically fit through the holes in the upper mesh. The 106-212μm sieve will probably contain some particles smaller than 106μm. This is because these particles will not necessarily fall through the holes and may stick by aggregation to the larger particles (this is observed to happen in the granules used in this research – see figure 34 below – v.small particles stick electrostatically, larger particles stick by weak binder bridges)

To get a mass weighted length a mass-based size distribution of the particles is produced (e.g. using a Camsizer© – particle sizer based on digital analysis of photos of projected area of particles). The upper sieve size is chosen, S_u, and the lower sieve size is chosen,

S_l, that correspond to the edges of the sieve fraction being used. The weighted mass, m_u, corresponding to the upper sieve size and the lower sieve size, m_l, are found from the mass-based size distribution.

The characteristic length can then be estimated from:

$$L = \frac{S_l m_l + S_u m_u}{m_l + m_u} \tag{31}$$

8

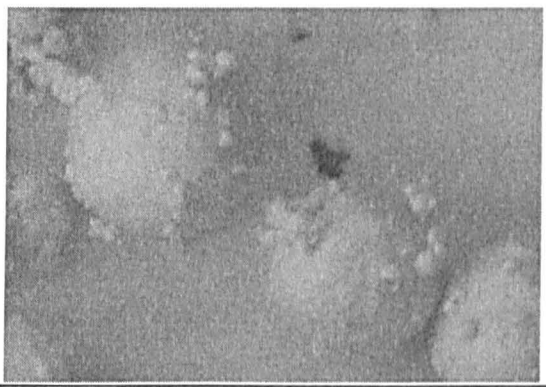

Figure 34 – Showing tiny particles stuck to larger granules by aggregation. (Small particles approx. 0.5mm)

Experimental Methods

8.1 Experimental Design

The principles of experimental design that were used in this research and the methods used to design the experiments and tests are:

- List all experimental parameters that will affect the output
- For each parameter that can be described by a numerical value choose a set of values (ideally a minimum of 5 values with the mid-value being the nominal value)
- For each objective parameter that cannot be described by a number the set is dictated by the different objects (e.g. binder addition method has 3 variables; spray-on, melt-in and pour-on)
- Combine all the sets of values for the different parameters into a matrix of experiments such that all possible combinations are listed – this is the "ideal" experimental design
- Each combination should ideally be repeated a minimum of 5 times

This can produce an unfeasibly large number of experiments, and when this is combined with the property tests that need to be performed on each experiment and the replication of these tests for validity purposes (to remove random error) you get an unrealistic number of total tests: 5,299,200 tests!

Intelligent experimental design was applied to reduce the number of tests required. This involved designing a standard experiment and varying 1 parameter at a time and reducing the number of variations of each parameter. This gave a total of 21 experiments. Opting for minimal reproduction of experiments and tests (see section 8.1.1 for difference between an experiment and a test) due to time constraints meant that the following reduction in repetition was done:

- Experiments 5 down to 1
- Sieve cuts 5 down to 1
- Strength tests 5 down to 1

- Abrasion tests — 5 down to 3
- Profilometry (of abrasion test) — 5 down to 3
- Binder content — 5 down to 3
- Moisture content — assumed fairly constant
- GSD — 5 down to 1
- Density — 5 down to 1

This is far from ideal – but was necessary due to the sieving sample preparation stage being the rate limiting step and other tests taking a long time to perform. In order to check the validity of the results (i.e. attempt to estimate the effect of random spread) 1 experiment was repeated 3 times to determine if granules of the same property could be produced using the same protocol. After initial tests on 1 sieve cut (106-212 μm) they were repeated for another sieve cut (212-300 μm). Once the initial experimental sweep was completed it was intended to duplicate results to improve accuracy.

It should be noted that it was later concluded that the experiments were being attempted in an unstable combination of operating and processing parameters – that it was in fact not possible to reproduce a single granule experiment that was considered for this report. The repeated tests referred to were chosen from initial granule batches that looked like they had a tight size distribution and were well formed in the sizes of interest – this turned out to be misplaced faith as these batches were just as irreproducible as the others, it is assumed to be the random nature of granulation in the unstable regime that they formed as they did on the first attempt.

8.1.1 "Experiments" and "Tests"

In this work there is a difference between an experiment and a test. "Experiment" refers to the way in which the High-Shear granulator was operated in combination with the formulation of the ingredients used. Thus repeating an experiment means making a batch of granules using an identical method to one already used. The term "test" refers to the procedures or tests carried out on the granules, which are produced from any given experiment, in order to determine the properties of the granule.

For example: Batch No. BN/04/01 is made according to experiment number 1. The granules that are made are then tested using the following tests: sieving, GSD, static strength, abrasion, profilometry, binder content and porosity.
This distinction is drawn because we are ***experimenting*** with the way a High-Shear granulator is used to make different granules with the intention of determining how to make granules of specific properties, in order to characterise those properties we have to ***test*** the granules that are produced.

8.1.2 The "Standard Experiment"

In order to reduce the overall number of experiments and tests a standard experiment was chosen and one parameter at a time was changed to determine the effects of that parameter on the granule properties. The parameters for the standard experiment were chosen based on a set of values that were known to produce granules, when using 65μm primary particles. It was assumed, without any indication to the contrary, that they would produce satisfactory granules using 5um primary particles. The parameters were varied one at a time to produce each new experiment. For each parameter a higher than standard value and a lower than standard value were chosen so that crude trends for the parameters could hopefully be determined. Where a parameter did not have a value then variation were used (e.g. addition method or primary particle type). It was decided to do this "2-Dimensional" experimental design rather than "3-dimensional" design of varying several parameters in unison, because the large numbers of parameters and the numbers of tests associated with each experiment would make a 3-D experimental design impractical.

The standard experiment used the following parameter settings (these will be explained in section 8.2).

Primary Particle Type	-	Omyacarb 2AV
Binder Type	-	PEG 1500
Primary Particle Mass	-	2000g
Binder Mass	-	300g
Addition method	-	Spray-On

Impellor speed	-	400 r.p.m
Chopper speed	-	1400 r.p.m
Temperature	-	60°C
Run Time	-	30 minutes

NOTE:
The full list of experimental recipes is detailed in the experiments sheet of the Database (in computer form) and given in Appendix J.

8.1.3 Limitations on research

The research presented in this report was conducted in the following order:

1. Properties of interest to be tested were decided
2. Preliminary tests were carried out
3. Test protocols were designed
4. The processing and formulation parameters to be varied in the experimental design were decided
5. The overall experiment was designed
6. The results database was designed and made
7. Experiments and their respective tests were conducted
8. Data was captured, manipulated and entered into the results database
9. The results were analysed

This is shown schematically in diagram 35 below.

As described in earlier sections there was not a satisfactory standard method for testing the abrasive strength of small particles or for determining the static strength of very small particles that cannot be isolated. It is a major limitation of this research that some of the property tests involved are in a developmental stage. Another significant concern is the fact that it was not possible to reproduce a batch of granules using identical experimental recipe – but, there is not a single controllable operating or formulation parameter that is not dictated and controlled by the experimental recipe. Thus it is assumed that either another unknown and uncontrolled parameter is affecting the granulation process or it is

possible that granulation behaves in a way analogous to Reynolds theory of fluid flow; having regions of unstable and stable granulation with a transition region in between.

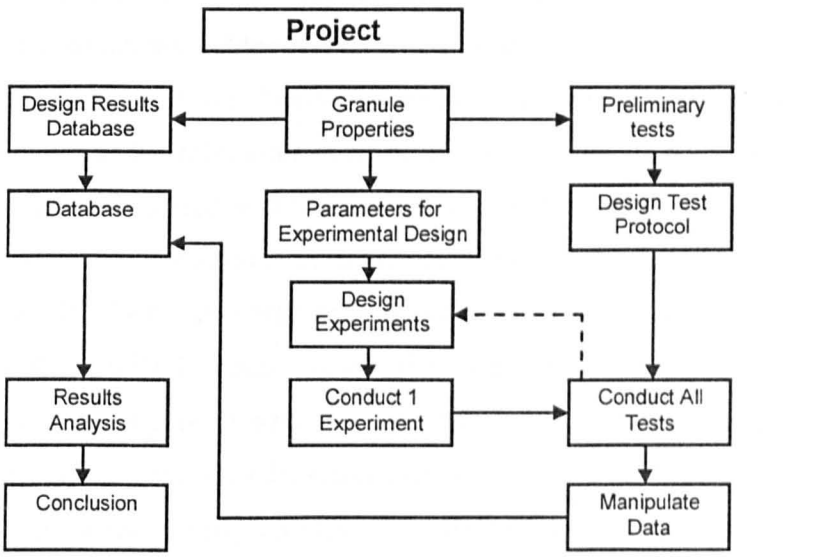

Figure 35 – Flow Diagram of the steps involved in this research project

It is possible that step 4 "The processing and formulation parameters to be varied in the experimental design were decided" does not include all the necessary parameters to control the properties of the produced granules, and the fact that 2 identical granule batches could not be produced using identical experimental protocols suggests this. The only thing that can be thought to have varied that was not controlled or measured is the moisture content of the binder and primary particles (due to the humidity in the air). Other parameters such as surface tension are dependent parameters, in other words they are fixed by the choice of the primary parameters that are dictated within the experimental recipe; surface tension is fixed by the binder type and the operating temperature of the mixer.

8.1.3.1 Spraying Binder

The sprayer used in this research was purpose built in-house and did not work for most of the research so the pour-on method of binder addition was used for the majority of

batches. When the sprayer did work there were several limitations: There was no accurate way of determining the exact amount of binder that had been added, the spraying device needed to be calibrated before every test and would generally run for 1 maybe 2 tests before giving an unreasonable reading. It is thus plausible that the mechanical counter within the spraying unit was slowly clogging up every time PEG was run through it, this means that even as the calibration is going ahead the flow rate being measured and the actual real flow rate would be drifting apart. This effect would be continuous so the first run after calibration is not likely to be an exact flow – the effect of this is that in reality slightly more PEG will have been added to each batch than is actually recorded.
Another problem with the sprayer is that there was little control over the dimensions of the spray cone or the droplet size. The size of the spray cone could be altered qualitatively and the extent of the changes gauged by eye, but this was very crude – this limited the use of the Spray-Flux theory for controlling granule nucleation discussed earlier. Additionally the size of the droplets was unknown.

A problem with granulation processes using high shear mixers and fluidised bed granulation appears to be the generation of small droplets. In order to produce <40um granules a combination of microscopic primary particles and microscopic binder particles is required (binder as droplets or ground-up particles).
If the primary particles are too large then obviously they cannot agglomerate to form small granules.
If the liquid binder droplets are not small enough then the small primary particles will immerse into the binder droplet. Thus reducing droplet size appears to be important in reducing the critical granule size.

There is a limit to the size which droplets can be reduced to by using a compressed air sprayer. Generating droplets from small orifices and trying to break them apart using high flow gas streams will not generate small enough droplets. Firstly reducing the orifice size reduces droplet size to a limit; the droplets grow at the orifice and 'Stick' until the dislocating force is greater than the sticking force. This sticking force is due to surface

electro-chemical properties and the surface tension. Increasing the pressure of delivery only increases the material through the nozzle (not the ultimate droplet formation size). Blowing the droplets off by a tangential gas stream may produce slightly smaller droplets but coalescence due to increased turbulence will probably negate these effects.

8.1.3.2 Particle Separation (Classification)

The granules that are produced are generally powdery and it is very difficult to make out individual granules with the naked eye. The size range of these granules can be from the size of the primary particles (~ 2-5 μm) up to 400 – 500 μm granules. Some batches, where the granulation is extensive, produce only large granules visible with the naked eye with very little powder.

Separation of most granule batches is relatively easily done using sieves with size fractions of <63 μm, 63 – 106 μm, 106 – 212 μm, 212 – 300 μm, 300 – 355 μm and >355 μm. Some of the batches do not separate using the sieves; the smaller particles (primary particles and small granules) aggregate together, stick to the sieve wires or larger granules and thus do not fall through into the correct size cut. This means that for some batches the sieve cuts 63 – 106 μm and 106 – 212 μm contain lots of smaller particles; it is not a problem for the <63 μm sieve cut as this will only contain the small particles anyway, it is not a problem for the >300 μm sieve cuts (it is assumed that the apertures are big enough to allow the small particle aggregates to fall through easily, medium size granules falling through the apertures take the powder with them and the bouncing of large granules prevents too much powder sticking to them or the sieve wires). This was a particular problem for the Zeolite primary particle based granules.

Another problem with the sieving of the granules was the time involved to get a large enough sample for further testing, this stage of sample preparation was the major rate determining step in the Critical Path analysis of the experimental procedures.

Alternative approaches to sieving that were considered include using cyclones, electrostatic plates and settling tanks. Cyclones and electrostatic plates required specific technology that was not available and may not be appropriate to the small scales required for testing. Settling tanks require an additional liquid, which gives further separation problems – especially as the components of the granules are water-soluble.

8.2 Making Micro-Granules: High-Shear Granulation

The High-Shear Mixer that was used in this work is a Rota-Junior (Zanchetta®). A schematic is shown in figure 36.

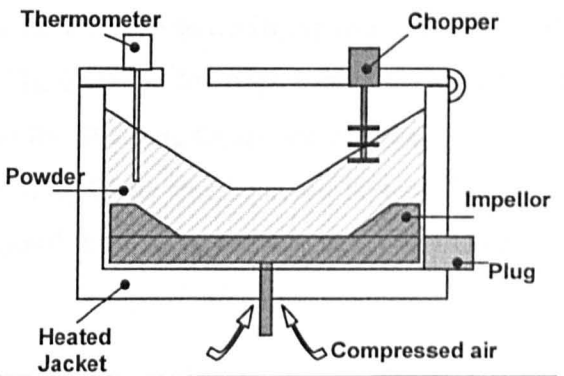

Figure 36 – Rota Junior: High Shear Granulator

The Rota-Junior is a circular, batch based mixer with a vertical axis impellor (mixing blade). There is a water heated jacket (using water from an integral boiler unit). There is a removable plug for removing granules. Ingredients are added via a hinged lid with removable temperature probe and chopper (the chopper motor is built into the lid); an opening is present through which the binder is added by either pouring or into which the sprayer nozzle is placed.

Compressed air flows up through the impellor drive shaft to prevent powder and liquid ingress. The impellor speed, chopper speed, boiler water temperature and water circulation are all operated electronically with current settings and powder temperature being displayed on an integrated control panel. The impellor rotates in a clockwise direction and the chopper rotates in a counter clockwise direction (when viewed from above). The impellor blades rest flush to the bottom and sides of the mixer and have a 15cm radius, 5cm depth and a single fin on each vane set at an angle to the direction of travel. The chopper consists of 15cm shaft with 3 sets of blades each 1cm apart and at 90^0 rotation to each other around the axis (when viewed from above); the blades are 1cm long with a thickness of 2mm and an angled edge. The impellor blade rotates in a stirring motion contacting the granules across the whole width of the blade. The chopper blades

rotate in a cutting motion contacting the granules across the thin angles edge of the blades.

When the mixer is operated the impellor blade sweeps through the granules forcing them round in a rotational motion about the axis of the impellor. Centrifugal forces cause the granules to move axially outwards whilst the angles fins force the granules up and over the rotating blade. The Granules fall back behind the sweep of the impellor blade under the influence of gravity. Shearing forces occur at the walls of the mixer, between granules and between the impellor blade and the mixer bottom. The chopper blades cause granules from the upper edges of the sloping mass to be redistributed towards the central axis of the mixer.

8.2.1 General High-Shear Granulation Method

Below is the standard method used to make the granules using the High-Shear mixer (Rota- Junior). This method ensures that all the parameters that could affect the granulation process are controlled (with the exception of humidity as mentioned in section 8.1)

1. The High-Shear mixer is cleaned
2. Compressed air is turned ON (Low flow rate through impellor shaft to stop small particles clogging working parts – negligible mixing effect)
3. The boiler temperature is set to 60°C
4. The granulator jacket heating is turned on
5. Primary Particle powder is weighed out (to nearest g)
6. The powder is put into the Furnace at 100°C for 5 minutes
7. The powder is added to the HSG
8. The impellor is turned on to 40 rpm
9. Leave to heat powder (until it reaches desired experimental temperature measured using a thermometer probe fixed to the mixer lid and protruding into the powder)
10. Spray system is set up
11. The impellor speed is set to batch requirements
12. The Chopper speed is set to batch requirements

13. The timer is started and the PEG is sprayed on (or poured as appropriate)
14. The PEG sprayer is removed and mixing continued for a time according to batch requirements
15. The granules are collected on metal trays via the sample plug
16. The granules are kept lightly agitated on metal trays as they cool to room temperature
17. Granules are left overnight before being bagged and labelled

Variations

If the experimental batch requires a temperature of 40°C then the boiler temperature is adjusted and the powder is not preheated in the furnace.

If the PEG addition method is pour on, it is melted and poured straight through one of the openings in the HSG lid. The experimental run time is started às soon as the binder starts to be added.

For Melt-in the PEG is added as a solid powder through one of the openings in the HSG lid. The experimental run time is started as soon as the binder starts to be added.

Standard protocol

Impellor – 400 rpm

Chopper – 1400 rpm

Temp. – 60°C

Run time – 30 mins

Spray-on - 450ml

Powder – 3kg

8.2.1.1 Binder : Primary Particle RATIO

The Binder : Primary Particle Ratio is a formulation parameter.

The binder ratio is calculated by mass and is given as a percentage; this is mass of binder added as a percentage by mass of the primary particles that are added (NOT percentage of the total mass – so it is not a true percentage.) This does mean that the total mass in the mixer varies between experiments with different binder ratios.
3 choices of binder ratio were chosen, 15% binder was taken as the standard and 2 further experiments use different ratios of 12% and 13.5%. It was chosen to test lower binder ratios and not higher ratios as preliminary testing at 15% showed that increasing the agitation constant (see critical packing theory) led to very surface wet granules. A test with 18% binder produced a sloppy mess. It was expected that lower binder contents would lead to smaller granules with weaker structures.

8.2.1.2 Primary Particles

The Primary Particle Type is a formulation parameter.

Calcium Carbonate was chosen as the basic primary particle as it has been used in a wide variety of high-shear granulation modelling and it was a cheap easily available material with a large variety of sizes ($CaCO_3$ grown from crystals can be grown in different conditions that change their crystal shape and properties). The Calcium Carbonate used is crushed calcium carbonate of nominal size. Size analysis of a variety of powders was done in the preliminary testing, Omyacarb 2av was chosen as it had a very small mean particle size (less than 10μm) and a relatively narrow size distribution compared to other powders such as Durcal 5. A powder with a small mean size is needed as the initial aim of the research was to investigate the properties of microgranules, with the intention of making and testing granules of approximately 40μm. In order to make granules of this size they need to be made from primary particles that are smaller (preferably as small as possible).

In order to assess the effect of particle physical properties such as surface energy, shape and hardness different materials were chosen as primary particles. This was also done to see how it affected the granulation process and whether they would produce smaller, larger or more uniform granules. Wessalith, a type of Zeolite, was chosen as it had very

narrow size distribution and it was thought it would produce relatively uniform granules compared to the other primary particle types. Zeolite however did not granulate except in 1 of the preliminary experiments and this could not be reproduced using the conditions (or variations of) described in this report. Two other forms of Calcium Carbonate were used, Durcal 65 and Pacal H. Pacal H was a precipitated Calcium Carbonate and had a mean size slightly larger than Omyacarb, but a tighter distribution (it was not chosen for all experiments because of cost). Durcal 65 was chosen because it had a very wide distribution and its mean size was about 60microns greater than Omyacarb – this meant it was not suitable for making granules of the order of 40μm but it was used to investigate the effects of primary particle size on the properties of interest (and as preliminary tests showed it was not possible for us to make 40μm granules and that 106-212μm were the smallest useable producible size it was thought not to matter).

8.2.1.3 Binder

The Binder Type is a formulation parameter.

PEG 1500 was used as the standard binder. This a long chain polymer of PolyEthyleneGlycol with an average molecular weight of 1500. PEG is used in many commercial granulation applications and it is solid at room temperature and melts easily (liquid at 45+ °C). This means it could be used for melt-in addition experiments and by melting it in a microwave it could be used in pour-on and spray-on.
PEG 1000, which is liquid at room temperature and has a molecular weight of 1000, was used to test the effect of liquid binder bridges on the final granule properties and the effect of reduced viscosity on the granulation process. PEG 6000, which is a solid at room temperature and melts at 50+ °C with a molecular weight of 6000, was used to test the effect of supposedly stronger binder bridges (due to greater van der walls forces and cross-linking) and the effect of increased viscosity on the granulation process. The viscosities were not measured quantitatively.

PVP (Polyvinylpyrolidone) was used as another alternative binder. This was chosen because it is another widely used commercial binder and has different properties to PEG.

However it could not be made to granulate under the operating and formulation conditions required and an alternative formulation that would cause granulation could not be found.

8.2.1.4 Impellor

The impellor speed is a processing parameter.

The impellor speed is an important parameter in the processing of the granules. An impellor speed of 400 revolutions per minute was used for the standard experiment; this equates to tip speed of approximately 6 m/s. This is not the relative speed of the blade to the granules. They move around with the blade (but not quite at the same speed) which imparts momentum to the granules. The granules are also moving relative to the walls and floor of the granulator. The energy required to consolidate the granules and cause mixing and breakage comes from the impellor, but it is not clear whether granule impacts with the impellor or granule impacts with the wall are responsible for the greater transfer or energy. It is believed that the chopper does not impart significant energy into the granules as even at maximum speed of 1400 r.p.m. it has a tip speed of approximately 1.5 m/s.

Other impellor speeds were investigated to change the agitation intensity rate constant, speeds of 200, 600 and 800 r.p.m. were used. The 600 r.p.m test was combined with an extended run time to see if it would produce granules similar to those made with an impellor speed of 800, as these should have similar agitation intensity rate constant, and to see what the differences were. It was surmised that at 800 r.p.m. there would be greater breakage, whereas at 600 r.p.m or 400 r.p.m with extended mixing time there would be a slower steady agglomeration and consolidation.

8.2.1.5 Chopper

The chopper speed is a processing parameter.

It was believed that the chopper was a largely vestigial component of the high-shear granulator, and it certainly didn't "chop" the granules. With a maximum tip speed about 4 times lower than the nominal impellor speed it is far less likely to be causing breakage than the impellor. It is believed that the only purpose was to add turbulence to the flow patterns of the granules by distributing granules in the radial direction.

A nominal impellor speed of 1400 r.p.m. was used as the standard experiment, with variations at 700 r.p.m and with the impellor completely turned off and removed.

8.2.1.6 Temperature

The temperature setting on the high-shear granulator is a processing parameter.

A temperature of 60°C was chosen as the nominal experimental temperature as this was enough to keep the PEG molten and prevent premature solidification during the granulation process. If lower temperatures were used then solidification of binder droplets might have occurred before proper distribution in the powder bed and the results could not be used to test the Novel consolidation theory presented in section 6.5 as this relies on the binder being able to flow between the primary particles within a granule. A lower temperature would also have led to imperfect granulation from melt-in addition as the binder would only be combined with the primary particles by smearing and compressive forces.

In order to reduce thermal shock the powder bed was heated for 30 minutes prior to the addition of the binder to ensure that it did not solidify the binder on contact with a cold bed of powder.

An experiment at room temperature and at 40°C were performed to assess the effects of using a reduced temperature and thus an accelerated solidification, it was assumed that

this would lead to a very wide size distribution of granules and granules with high binder contents.

8.2.1.7 Run Time

The experimental run time is a processing parameter.

A run time of 30 minutes was used, this was completely arbitrary. Extended run times of 1 hour, 1 ½ hours and 2 hours were done to investigate the theory of run time increasing the overall agitation (ωt in eqn. 16) as described by the granule compaction theory in section 7.3. Experiments were also done where the granulator was stopped at regular intervals and photographs of the granular bed were taken.

It is believed that 30 minutes is long enough that if the processing and formulation parameters lie in a regime that undergoes an induction period that induction period is elapsed and proper granules are formed. There was however an uncorroborated report of one batch of granules forming large homogenous granules early on, then the granules disappeared and a bed of powder appeared to be present, this then subsequently turned into large homogenous granules again. This apparently happened in the space of a few minutes. The 3rd year undergraduate student working on this project who witnessed this claims that he had previously come across a small reference in some literature somewhere remarking on this type of behaviour but could not remember the source. The observations were attempted to be reproduced but could not be verified. It is possible that this behaviour was chaotic (unstable regime), indicative of granulation behaviour in a formulation / processing regime that is in a transition zone similar to the transition zone between turbulent and laminar fluid flow or it could be indicative that the granules are behaving in an induction regime meaning that the transition is a 2-step process: size reduction followed by rapid size re-enlargement.

8.2.2 Experiment (Summary of Variables)

Primary Particle

Omyacarb 2AV	OMYA (Saint Gobain)	2 μm Nominal
Durcal 65	OMYA (Saint Gobain)	65 μm Nominal
Aluminium Oxide Zeolite	Unilever	5 μm Nominal

Binder

PVP (Polyvinylpyrolidone)	United Chemicals	
PEG 1000 (Polyethyleneglycol)	ICI	MR 1000
PEG 1500 (Polyethyleneglycol)	ICI	MR 1500
PEG 6000 (Polyethyleneglycol)	ICI	MR 6000

Binder Ratio

12 %
13.5 %
15 %
18 %

Primary Particle Mass

2000 g

Addition Method

Spray – on	19 L/min atomising air	4 Bar reservoir pressure
Melt – in	2 mm nominal pellets	
Pour – on	5 second addition rate	

Impellor Speed (rpm)

200
400
600
800

Chopper Speed (rpm)

0
700
1400

Temperature of HSG jacket and powder bed (degrees C)

60
40

Run-Time (minutes)

20
30
60
120

This gives a total of 24 different experimental combinations as shown in the database in Appendix G (contained on CD or file as appropriate) and in Appendix J. At least three

attempts were made to make batches using each of the combinations, in some cases more. Out of 77 recorded attempts only 37 batches successfully granulated with no experiments producing batches that were reproducible (in terms of the visible appearance). Most batches that failed to granulate were not recorded.

8.2.3 SPRAY-ON binder addition

Below is a detailed step-wise explanation of the spray-on method (this is included here for accurate reproducibility of the spray-on method). The spray-flux could not be calculated and was not used as a variable parameter because the spray unit used was not reliable enough to vary settings and take measurements with any certainty (it is even dubious whether it produces reproducible spray rates using identical settings.)
The sprayer consisted of an enclosed unit housing a heater, all the working parts and the controller. A binder inlet with a sintered brass microfilter and isolation valve allowed molten PEG to be added to the PEG reservoir, which is surrounded by an insulated jacket and contains a heating element. The reservoir is connected to via a control valve to externally supplied compressed air to allow reservoir pressurization. The molten PEG is forced into a rotary pump connected to the control panel, which allows the rate of rotation of the pump to be controlled and thus the flow rate – the total flow is determined by the number of pump revolutions (after the pump is calibrated – it is believed that this method for determining the total PEG delivered is unsatisfactory as it appears that the amount of Peg delivered per rotation varies and decreases with each rotation.) The molten PEG is pumped along heated piping (heated by hot compressed air) into the spray nozzle unit – there is a section of unheated PEG piping that requires heating manually with a hot air gun. The molten PEG is forced out of the sprayer nozzle and the hot compressed air is blown across the aperture to aid droplet formation.

The primary particles are added to the mixer as outlined in 8.2.1 and heated until they reach 60 degrees centigrade. 400g of binder is melted in a microwave, sieved through a 40 micron sieve and added to the spray unit. The unit is then calibrated before every experiment to ensure the flow meter is working properly before spraying the binder into the High-Shear mixer through an opening in the lid. The PEG spraying unit is a purpose

made unit with an adjustable cone spray nozzle (changes angle of cone) and adjustable air pressure and reservoir pressure (to change the atomising effect and PEG flow rate). Identical settings were used on the spray unit each time, but the time taken for the spray to add 300ml of binder would vary from experiment to experiment (suggesting that there was something inherently wrong with the sprayer).

The atomising air pressure is adjusted until the flow is 19 litres per minute; the reservoir pressure is set to maximum (safe limit) of 4 bar. 300ml of PEG is sprayed onto the powder bed through a hole in the mixer lid. The hole is approximately 10cm from the outer rim of the mixer. The timer for the experiment is started at the onset of spraying. The spray unit is not very consistent. The time taken to spray 300mls of PEG could vary from as little as 30 seconds to several minutes and seemed to be independent of the setting of the reservoir pressure from one experiment to the next (for any given experiment increasing the reservoir pressure increased the spray rate). It is known from the work of Litster et al.,[8] that the spray rate affects the spray flux and that the spray flux is an important factor in the formation of granule nuclei and in turn the resulting granulation and ultimately the final granules. The angle of the cone was not measured, but the nozzle was adjusted by a ¾ turn from closed (an approximation of the angle can be taken from the spray contact area being roughly 4" diameter from roughly 4"height)

8.2.4 MELT-IN binder addition

Solid binder particles are weighed and mixed in with the weighed, cold primary particles. These are both added to the pre-heated mixer. Melting of the PEG particles will occur as the whole powder bed heats up. The start point for timing the experiment is when the powder and PEG are added to the mixer. The protocol is probably not very appropriate because there will be a significant thermal lag before the bed of primary particles reach 60 degrees centigrade (the 30 minute granulation time may have even elapsed before this occurs and granulation starts properly). With hindsight it would have been better to heat the primary particles for 30 minutes before adding the PEG particles by pouring into an agitated bed of primary particles (this would have reduced the thermal lag that is caused by the heating up to the melting point of the PEG of cold primary particles). If the

primary particles had been pre-heated the 30 minute granulation run would be expected to produce granules of different properties and sizes than when binder is added to a cold bed of primary particles; either way is a valid method for assessing an alternative to spray-on addition.

8.2.5 POUR-ON binder addition

Primary particles are weighed and added to the mixer and heated to 60 degrees centigrade for 30 minutes prior to binder addition. 300 ml of binder is melted in a microwave and poured through a hole in the mixer lid. The binder is poured in as quickly as possible without spillage, typically taking about 5 seconds.

8.2.6 Special Procedures

For some of the granulation experiments (mostly in the preliminary testing stage) different special procedures were used.

The first example is: it was proposed that by dissolving the PEG binder in water just to the point of solubility and then adding this to the hot primary particle bed the granules would form in a similar fashion to when an equivalent amount of pure binder was added; except that the water would then evaporate leaving formed granules with a lower than normal binder content and thus hopefully with a weaker structure. This did not happen; a sticky mass was formed in the mixer and no granulation occurred. It is thought that the primary particles partly dissolved in the water based binder (as $CaCO_3$ is soluble in water). Similarly tests using water alone were useless.

The second example of a special procedure is BN/04/X3D (This is an example of a unique batch code used to identify which experimental recipe is being followed and what repetition number of that recipe it is – this is explained in section 8.4.1 – the full list of batch codes is given in the electronic database), this used 1000g of Pacal H (a form of $CaCO_3$ grown from solution rather than crushed from rock and which has a tighter size distribution than Omyacarb 2AV). The binder in this case was added in 2 lots, 250mls at the start and a further 50mls after 30minutes. The granulation was left to run for a total of 1 hour.

BN/04/X1A and BN/04/X1B are actually the same batch, except that the granules tested as BN/04/X1A were removed after 30minutes and those tested as BN/04/X1B were removed after 1 hour. Only a small amount of granules were removed after 30 minutes so as to hopefully not disturb the granulation process of the remaining powder. BN/04/X1A was a fine powder, indicative of the induction period. After 1 hour the granules appeared much larger with a few much consolidated granules.

BN/04/X15B and BN/4/X15A do not use the chopper; this was done to determine if the chopper had any affect whatsoever on the granulation process. It is this author's view that the chopper on the Rota-Junior had no effect because its position is up out of the powder bed and its tip speed is a lot lower than the tip speed of the impellor. It is a misrepresentation to call it the chopper as it appears to just get clogged up with powder and binder in a sticky mess – a more appropriate name might be "redistributor". BN/04/X15B was run for 1 hour and stopped at 2, 10, 20, 40, 50 and 57 minutes to take photographs of the contents of the mixer. It appeared that there was a gradual build up of cake on the mixer walls, possibly due to the absence of the chopper. This was not a problem isolated to this batch and occurred in most of the batches with the impellor on and was the main cause of batch granulation failure.

BN/04/X21A was run for 2 hours, but it was stopped every 15minutes to take a photo of the contents of the mixer.

Some experiments were recorded as void because they snowballed into very large granules (up to 2cm in diameter) whilst others produced masses of caking in the mixer rather than forming discrete granules. BN/04/X16C2 was binned because it formed massive snowballs. This batch was observed to undergo a curious transition during granulation; after 10minutes the powder formed fine granules that subsequently turned back into a fine powder before turning into granules a second time. After the second time the granules were formed they continued to grow rapidly forming large snowballs that were inappropriate for property testing.

Another experiment that was recorded as void was BN/04/14, this used an impellor speed of 200 rpm, this formed a sticky mass on the sides and base of the impellor and no granulation occurred.

Two attempts at making granules according to the experimental recipe of BN/04/22 were abandoned; in the first case because large weak granules formed that fell apart during cooling, in the second case because all powder/ PEG / Granules had formed a solid cake stuck to the walls. This highlights a major problem with this research; something was obviously not being accounted for in the parameters that affect high-shear granulation or the Rota-Junior (high-shear mixer being used) was not accurate.

Three attempts using HPC as the binder resulted in caking on the mixer walls and this was abandoned as an alternative binder type.

Four attempts were made to granulate using Pacal H before and after the successful granulation of BN/04/X3D. The initial attempt used 2000g of powder and 300ml of binder and this didn't granulate so a further 100ml was added after 30minutes and the impellor speed increased to 600 rpm for 20minutes but granulation still did not occur, a further 100ml was added and after 5 minutes the powder had snowballed. An attempt was made using 150ml of binder and this didn't granulate and an attempt was made using 350ml of binder and this rapidly formed a cake on the sides of the mixer. An attempt to replicate BN/04/X3D was made but using 150mls for the first 30 minutes and a further 30mls for the second 30minutes, no granules formed in the first 30 minutes (the primary particles remained a fine powder) and during the second 30 minutes large granules were formed in excess of sizes suitable for property testing. This suggests that the general high-shear mixer experimental protocol that was chosen for this research is very unstable, particularly with certain combinations of powder and binder. It is thought that this is due to accidentally choosing an operating region that is analogous to the unstable or transition zone between laminar and turbulent flow based on Reynolds number or it is due to an external parameter that is beyond the control of the investigator.

8.3 Tests – collection of raw data for properties

8.3.1 Sieving

In order to perform the property tests on the granules that were produced they first needed to be sieved into appropriate size cuts, ideally these wanted to be as narrow as possible as it is known that properties such as static strength vary with size (and it is assumed that other properties such as porosity and abrasive strength will also vary with size). By testing the samples in narrow size cuts the effects of size can be accounted for. If wide size cuts are used it is not really applicable for getting property to property relationships because we will not know exactly what sizes of granules are in the specific cut being tested; for example if 2 (wide) sieve cuts of a given batch were made and one was tested for static strength and one was tested for porosity, but the granules in the sieve cut used for the static strength happened to be nearer the large end and the granules in the sieve cut used for the porosity happened to be nearer the small end then the true relationship between porosity and static strength would be hidden. This effect is reduced by narrowing the width of the sieve cuts. However there is a practical limit to how narrow the sieve cut can be taken, this is limited by the testing time to carry out multiple tests on lots of sieve cut sizes combined with the fact that as the sieve cuts get narrower they produce less sample per sieving run, thus more time has to be spent sieving. It was decided that the optimal compromise was to use the following set of sieve cuts:
Base collector, 63μm, 106μm, 212μm, 300μm and 355μm

Sieving method:
Mechanical Sieve machine (Ro-Tap®) is set up using a base collector, 63μm, 106μm, 212μm, 300μm and 355μm sieves
Amplitude intensity set to 1.5 (1.5mm travel per oscillation)
Interval Sieving is set to ON (stop and starts to help redistribution of granules by gravity)
Interval time set to 15 seconds
Total run time is set to 5 minutes

2 level teaspoonfuls (approximately 25ml) of granules are added to the top sieve (dry granules were put sequentially through a set of rifflers to obtain a representative sample, this was done 10 times before scooping granules)
Metal holding plate is secured
The sieving machine is turned on and left to run
Powder left on each sieve is collected and put into appropriate labelled bags
The sieves are cleaned and the process repeated, adding powder to bags already containing powder.

Care needs to be taken not to contaminate a bag containing lots of powder that has already been sieved – it is very easy for contamination to occur (accidentally adding the wrong size sieve cut to a bag or adding a sieve cut that contains flakes of metal / cleaning brush bristles).
The powder is added to the bags using a metal funnel clamped to a stand – the funnel is cleaned between each use by using a vacuum cleaner and cloth.

Cleaning sieves

To clean the sieves between sieving soft brushes are used carefully on the underside of the sieve. Compressed air is then blown through the upper side of the sieve after using the brush to ensure no contamination due to broken bristles has occurred.
Cleaning the sieves at the end of a session uses hot water in the sink (calcium carbonate and PEG granules will dissolve in water). Sieves are rinsed thoroughly and dried using either compressed air or the oven in the particles lab (on low setting so as not to damage the rubber seal between sieves).
Care is needed when cleaning the sieves with fine mesh as they are easily damaged and easily contaminated.

8.3.2 Granule Size Distribution (GSD) Test

The size distributions were measured using a combination of sieves and the Camsizer (a digital camera imaging device – Retsch Technology Inc.®); this was because the sieving of the samples at small sizes would have taken too long to get an accurate size distribution and the width of the sieve cuts were too narrow to use by themselves. The Camsizer could not be used by itself as the sizes of the particles under consideration had large amounts that were smaller than the smallest size that the Camsizer could deal with – the Camsizer is quoted as being able to measure down to 35μm, but in this work it was only used down to 63μm (and there is even doubt about the accuracy at this level as explained in the errors section).

The Camsizer has vibrating angled feed tray onto which the particles are poured; they are then moved along the tray and fed through an opening by the vibrations. The particles then pass between a backlit screen and a digital camera. The size analysis is taken from the projected area captured by the digital camera.

In order to get the whole size distribution the granule sample is first sieved to remove the particles below 63μm; both the upper and lower sieve fractions were weighed before repeating the sieving with fresh granules. All the upper sieve fractions from the separate sieving were combined before being run through the Camsizer – a schematic of the process is shown in figure 37.

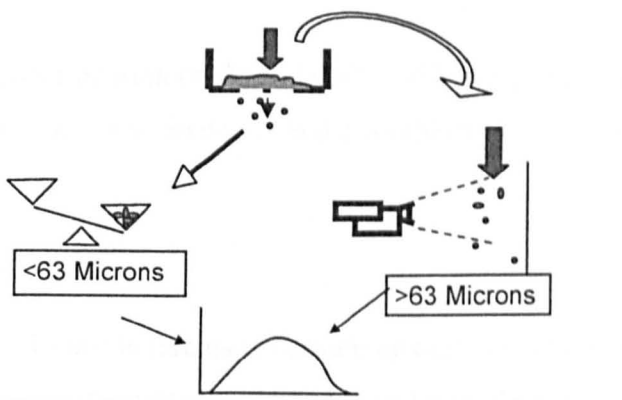

Figure 37 - showing how the GSD is found by combining sieving and the Camsizer

Sieving

The sieve machine (Ro-Tap) is set up using a base collector, 63μm sieve and a 355μm sieve.

The base collector is weighed – record empty weight

The 63μm sieve is weighed – record empty weight

Amplitude intensity is set to 1.5 (1.5mm travel per oscillation)

Interval time set to 15 seconds

Run time is set to 5 minutes

2 level teaspoonfuls (approx. 25ml) of granules are added to the top sieve

Metal holding plate is fitted

Sieves are run

Carefully:

The base collector is weighed – record powder weight (by difference)

The 63μm sieve is weighed – record powder weight (by difference)

The upper fraction is put into a labelled bag

The bottom fraction is put into a labelled bag

Sieves are cleaned

This is repeated 2 more times

All the powder >63μm is combined

Use combined upper fraction (>63um) to get a GSD using the Camsizer. The total weight of this combined fraction is needed as is the combined weight of their corresponding lower fractions.

Camsizer Method

The Camsizer is cleaned before use to ensure no particle or dust is on the lenses.

Camsizer is turned on (button in middle of box at rear of Camsizer)

"Camsizer 2.4E beta version" is selected

Task File "Maxim2004.afg" is loaded through the options menu (this describes the settings by which the Camsizer will be operated)

The 'Measure' menu is selected

On the pop-up screen:

Size class file "maxim2004.gkl" is selected (this selects the imaginary sieve sizes into which the particles will be sized)

Material : "granules"

Density "1.9 g/cm^3"

Excel-readable English (*.xle), tick-box is selected

For the "File name" – the batch number corresponding to the granules being tested is entered

For the "File number" - the tick-box is selected and the number of the Camsizer run for that batch is entered.

Granules (upper size fraction) sprinkled evenly over the feed-tray on top of the Camsizer

The Camsizer is started and data collected automatically

The data is checked to ensure it has saved in C:\programfiles\camsizer beta\CAMDAT\maxim2004

The Camsizer is cleaned after use (Taking care not to scratch the lenses or leave dust particles on them – as this will affect future size measurements)

8.3.3 Abrasion Test

The abrasion test was designed specifically for testing the amount of abrasive wear that the different granules produce, the specific development of this test is covered in section 7.4. Three abrasion tests were carried out per sieve cut per granule batch that was produced.

1. Perspex sample plates are labelled on the reverse side with the abrasion test ID. This is a code which contains information in 3 sections: the first letter is the sieve cut being analysed (W is 300-355, Y is 63-106 and Z is 212-300 μm – if none of these letters are present and it begins in a number or an X then it corresponds to the sieve cut 106 – 212 μm), the second section of the ID gives the batch code and is simply the *x* part of the batch code BN/04/*x*, the last section of the ID is a letter corresponding the number of the abrasion test for that batch and sieve cut – so if it

is the 3rd abrasion test of 63-106 granules from batch X5A then the abrasion test ID would be YX5AC (Y => 63-106, X5A => batch no. BN/04/X5A, C => 3rd abrasion test), an ID ending in A is the 1st, B the 2nd and so on...

2. A wear strip and datum are marked off using sellotape, ensure gap is approximately 3mm wide and runs down the centre of the sample plate (see figure 32).
3. Labelled and marked-off sample plates are put into the sample plate holders (these are removable plastic holders designed to hold the sample plates in the correct position on the abrasion rig with a flush fit to prevent oil seepage and a hole in the bottom to aid sample plate removal at the end of tests).
4. The abrasion rig is isolated at the mains power supply
5. The shaft retaining pin connecting the top plate to the motor drive arm is removed (allowing the top plate to be completely removed)
6. The top plate is slid back on the runners (depress the ratchets to slide fully back)
7. 1.5 grams of granules is added to each of the sample plates – the granules form an even mound in the centre of the sample plate (a record of which batch number and sieve cut corresponds to which sample plate is made)
8. 5ml of vegetable oil is added to each sample plate
9. Sample plate holders are placed into the slots on the base plate, ensuring the wear strips run parallel to the direction of motion of the top plate.
10. A single strip of cloth (fine-weave Jaycloth-type material) is wrapped around the aluminium abrasion blocks.
11. Cloth-wrapped abrasion blocks are mounted into the counterbody holders and the locking nuts are tightened using an Allen key.
12. Top plate is moved back to the start position and attached to the drive shaft using the shaft retaining pin (ensure the securing screw is fitted and thumb tight)
13. The numbered abrasion block holders are mounted on the appropriate securing pins on the top plate, the abrasion block holders should slide smoothly down the pins and the cloth-wrapped abrasion blocks should slot through the holes and rest on the mound of granules on the sample plate below.

14. Each abrasion block is firmly pressed into the granule sample and left to rest under its own weight.
15. Safety cover is replaced
16. Abrasion rig is started
17. Start the stop watch and time for 5 minutes
18. Abrasion rig is turned off
19. Safety cover is removed
20. Shaft retaining pin is removed
21. Counterbody holders are removed
22. Top plate is slid back (depress the ratchets to slide fully back)
23. Sample plate holders are removed
24. Waste oil and granules are poured into the Winchester waste bottle for recycling
25. Sample plates are removed from their holders.
26. Sample plates are cleaned carefully using warm soapy water – care not to clean off the label.
27. Any spilt oil on the abrasion rig is cleaned off
28. Top plate and safety cover are replaced.
29. Cloth on the abrasion blocks is replaced

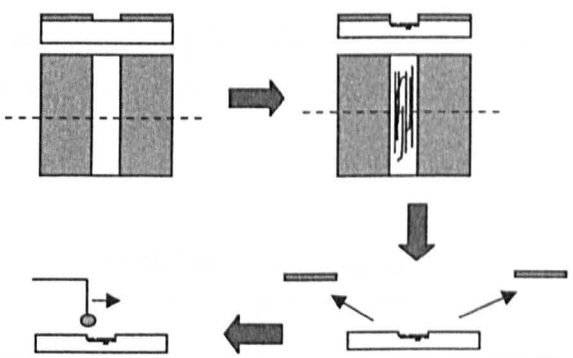

Figure 38 - showing Datum Abrasive Wear

Above is figure 38 showing the schematic of the datum for the Abrasive Wear that is created by the use of sellotape. The dark is the sellotape which is attached to the surface of the Perspex sample plates. The sellotape prevents the surface below from being

scratched so when it is removed it reveals the un-abraded surface of the sample plate which then forms the datum surface for the profilometry test.

1.5 grams of granules added
5ml of rapeseed vegetable oil
125 grams loading (counterbody plus abrasion block and cloth)
Run time 5 minutes
81 cycles per minute
Abrasion block set at 10^0 off from the direction of travel

8.3.4 Profilometry Test

In order to find the profile of the wear scar it was necessary to have a datum to measure the wear depth against. The Perspex abrasion plates were sectioned off using Sellotape; this was laid in 2 even strips along the length of the plate, roughly 3mm apart and parallel to the motion of the abrasive wear. The sellotape prevented wear of the Perspex plate either side of the wear channel, thus producing the datum.
Profilometry ID codes were used in accordance with the abrasion test ID codes (see section 8.3.3) except that an extra letter was added on to the end of each code corresponding to the number of the profilometry test in the same manner that multiple abrasion tests are added – i.e. the first test adds an "A" onto the end, the 2nd ends in a B, the 3rd a C and so on… (only 3 profilometry tests were performed except in special cases).

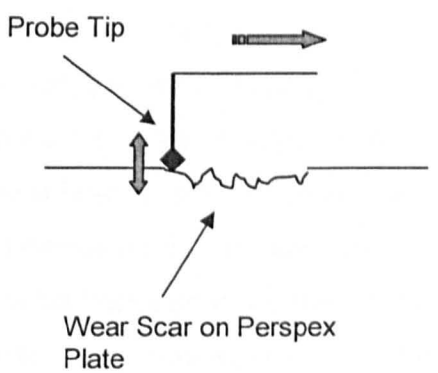

Figure 39 - showing Profilometry

The profilometry was done using a Sloan® Dektak3, a needle probe profilometer (see figure 39)

1. The sellotape is removed from the Perspex sample plates
2. "gummy" bits are cleaned off using iso-propanol. – taking care not to remove the abrasion test ID label on the reverse side.
3. The Dektak scanning program is opened from the attached desktop computer.
4. The Scan Routine is adjusted to the following settings:

ID	-	0
Meas. Range	-	655 ka
Profile	-	"square above and below profile"
Length	-	5000mm (see note below)
Data resolution	-	High
Speed	-	Low
Stylus Force	-	10 mg
Soft Touch	-	Selected

NOTE: The actual distance travelled by the probe tip is not 5000mm, it is 50mm. There is an error in the units and programming of the interface, but it didn't affect the running of the Dektak or the accuracy of the results.

A stylus diameter of 2.5 micrometers was used.

5. "display" and then 'Sample Positioning' are selected (a video image of the sample surface can then be seen)
6. Using the joystick on the machine to move the sample, it is positioned such that the probe tip is hovering to above the datum (unscratched) area of the sample plate and the direction of motion is perpendicular across the wear scar.
7. The probe tip is then lowered onto the Perspex plate and the test is ready to run
8. A single scan is performed using the automatic run function on the Dektak
9. Once the scan data has been captured it needs to be levelled (as it is often not a horizontal profile but has downward or upward slopes to it that need to be

smoothed out) by moving the [M] and [R] cursors on the screen to opposite ends of the wear scar (on flat line) and selecting 'level' from the command functions.

10. The depth of individual 'valleys' in the wear profile could be examined by moving the [M] cursor over the point at the base of the valley.
11. The linear position and depth data are then saved to file and exported to excel for data manipulation.
12. The wear profile is repeated so that 3 profiles were taken for each abrasion plate.

Steps 9 and 10 are simply operational steps for the particular Dektak machine used in this research. It was the standard procedure advised by the technicians and researchers who used the equipment daily.

This meant that in theory there was 3 wear profiles for each abrasion plate, so there was 3 different amounts of wear per abrasion test used to calculate the average abrasive wear. For each granule batch there was supposed to be 3 abrasion tests so the abrasive wear is then the average of the average abrasive wear.

8.3.5 Static Strength Test

Earlier in this report the importance of static strength and how it can relate to other granules properties was discussed. There was a section describing how the static strength can be related to the critical velocity for impact failure of a granule, this was followed by the preposition that static strength might be related to the abrasive strength of granules as well. In order to test this abrasive strength needed to be tested as already described in 8.3.3 and 8.3.4, but also the static strength of granules from the same batch and size cut needed to be determined.

Section 6.4 described in detail the theory of static strength and difference between crushing individual granules and multiple granules. Preliminary single crushing tests were performed using the Dynamic Mechanical Analyser (Rheometrics® Solids Analyzer RSA3); the aim was to develop a satisfactory test protocol that would produce reproducible results. This testing method was not used for the bulk of the results on which this report is based but it did yield useful information that suggested that multiple compression testing was the most appropriate testing method.

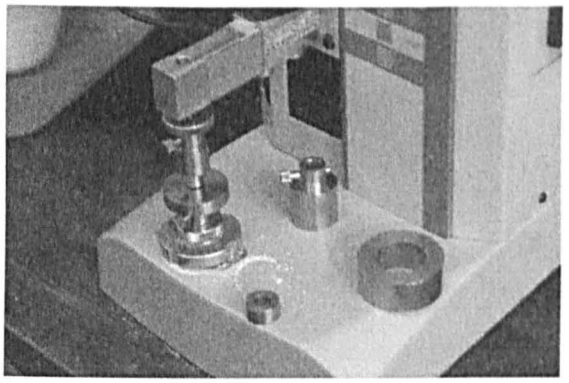

Figure 40 - showing the Zwick Compression Tester torsion bar and 2 sizes of crushing probe and cylinders

A multiple compression test based on the method suggested by Adams, et al., [85] was used. This is a uniaxial confined compression test. A Zwick® Compression Tester was used. 2 different sized cylinders and close-fitting pistons were made for the purpose of testing, however only the smaller size container was used due to limitation on the sample sizes. The cylinder / container had a diameter of 10mm and a depth of 9mm (although the depth of the bed of granules placed in the cylinder varied in depth and was approximately 7mm) and was made from polished stainless steel. Figure 40 shows the base plate, torsion bar, crushing probes and cylinders that were used with the Zwick compression machine.

Method:

The appropriate measurement programme is selected from the Zwick software, TestExpert©, according to the guidelines in the instruction manual (a program with all the required settings was saved to ensure the same system setting were used for each test).

A 500N torsion bar (strain-gauge) is fitted.

The crushing probe is screwed onto the torsion bar (this is a specially made piston that fits snugly inside the cylinder holding the granule sample)

The cylinder / sample holder is placed around the crushing probe and the whole thing lowered to close to the base plate.

The crushing probe and cylinder are lowered until the whole unit is close enough that the sample holder can be released and left to drop under its own weight onto the base plate

whilst still remaining in contact with the crushing probe. This ensures that the crushing probe will align with the sample holder when crushing commences.
The crushing probe is then raised away from the base plate and sample holder.
Carefully (so as not to knock the sample holder and misalign it with the crushing probe) granules are added to below the rim of the sample holder, leaving a small gap.
The crushing probe is then lowered again until it is just within the sample holder (thus holding the sample holder in the correct position).
The base plate is then tapped to settle the granules within the sample holder.
The crushing probe is lowered onto the granules (under the control of the crushing machine) and the start height recorded.
The crushing experiment is then run by pressing start using the measurement programme.

The crushing probe is driven down into the granule sample at a rate of 0.5mm / minute and the force – displacement data is recorded and output to an excel file for manipulation as described in section 9.3.

8.3.6 Binder Content Test – Furnace

There is a need to determine the liquid binder to solid ratio of individual granules in order to determine if there is an even distribution of binder in all sizes of granules or if there is a change in the ratio of solid-liquid as the granule size changes.

For the analysis of the system $CaCO_3$ and PEG an experimental protocol has been suggested on the basis that PEG burns completely leaving no residue at 600°C whilst $CaCO_3$ remains unaffected.

Method (based on Fu, [123]:
The mass of an empty crucible is recorded W_6.
A scoop of granules is added to the crucible and weighed W_7
The crucible and granules are placed in an oven at 600°C for 1hr.
After heating the crucible is placed into a desicator until cool.

The crucible and content are then re-weighed W_9 – the mass of Calcium Carbonate left in the crucible can now be found by difference, and the weight that has burnt off is the PEG and moisture.

The percentage binder by mass is given by:

$$Binder = \left(\frac{W_7 - W_9}{W_7 - W_6} \times 100\% \right) - moisture\% \qquad (32)$$

The binder : solid ratio by mass could then be given by:

$$= \frac{Binder\%}{100 - Binder\%} \qquad (33)$$

NOTE: This assumes that:

A) The binder completely volatilises at 600°C

B) No decomposition of $CaCO_3$ takes place at this temperature.

C) All moisture is surface moisture and none is bound up in the granules

D) No volatilisation of PEG occurs at 105°C (the temperature used to determine the moisture content)

8.3.7 Moisture Content Test – Furnace

In order to determine the Binder content of granules the PEG needs to be burnt off at 600°C. But, this will also be removing any moisture that is in the granule. So a sample of granules from the same batch needs to be tested at the same time to determine what weight that is burnt off at 600°C is actually moisture.

The moisture content of the granules needs to be determined:

The mass of an empty crucible is recorded W_{10}

A scoop of granules is added to the crucible and weighed W_{11}

The crucible and granules are placed in an oven at 105^0C for 1 hr.

The crucible and content are then placed in a desicator until touch cool.

The crucible and content are then re-weighed W_{12}

The percentage moisture by mass is given by:

$$Moisture = \frac{W_{11} - W_{12}}{W_{11} - W_{10}} \times 100\% \qquad (34)$$

NOTE: this test method was originally proposed by Peter Knight and adopted as a standard protocol within the PPG group at Sheffield University; however there is no evidence of it being verified as a legitimate method. Appendix F outlines some experiments that were performed to validate this test method.

8.3.8 Porosity Bottle Test

In order to find the porosity of a particle you need to know the envelope density (that is the density of the particle including the pores and spaces connected to the outside world) as well as the true density (the density of all the solid material within the envelope of the particle but ignoring pores and spaces trapped within the envelope or connected to the outside world). It is not necessary to know the skeletal density, which does not account for pores and spaces that are trapped within the internals of the particle.

A combination of mercury porosimetry and helium pycnometry is often quoted as the most accurate method of finding the porosity of particles. The mercury porosimetry finds the envelope density by forcing mercury around the surface of the particles and then as the pressure is increased it is forced into the pores that are open to the outside world. This is fine if there is a single large particle that is being analysed and this can give information about the size of pores and numbers within the granule. However if the test is to find the porosity of very small granules (as is the case in this report) then it is not a satisfactory approach as it is not possible to isolate a single granule for testing and a sample of many particles have to be used. The problem with this is that the output of the

mercury porosimeter is a pressure-volume curve and it is very difficult (if not impossible) to determine the point at which inter-granular pores become intra-granular pores – which is the point at which the envelope density can be found (see graphs of output curves in appendix I). Helium pycnometry produces similar pressure-volume curves but it flows easily into the pores within the particles that are open to the outside world, thus it can be used to find the skeletal porosity (even for a collection of very small particles). It is necessary to know the mass of material in order to find the skeletal density and the envelope density using the helium pycnometry and mercury porosimetry respectively. The problems with this method of determining granular porosity are that it is often very difficult to determine the envelope density, as already described, using mercury porosimetry and the Helium Pycnometry is not capable of measuring enclosed pores. An initial trial attempting to find the porosity using a combination of Helium Pycnometry and Mercury Porosimetry failed as it was not possible to see any transition point. It was decided to use a combination of density bottles, to find the envelope density, and thermogravimetric analysis, to find the true density. This was done using the method described by Fu, [123].

The envelope density is found using density bottles. A 25ml density bottle (Gay-Lussac type) was used (it is not know whether the bottles used were pre-adjusted or not, no calibration of the volume was performed – this is a potential source of error). Tests were carried out in environmentally controlled labs at 25°C. The vegetable oil was calibrated to determine its density using the density bottles actually used for the tests.

1. The empty porosity bottle + stopper is weighed W1
2. Powder is added and the bottle and powder + stopper re-weighed W2
3. Weight of powder is calculated (by difference W2 - W3) W3
4. Oil is added to the porosity bottle, stopper inserted and excess oil wiped off
5. Powder, bottle and oil are weighed W4
6. Mass of oil is calculated (by difference between W4 – W2) W5
7. Volume of oil based on density of 0.9148 kg/l is calculated V_o
8. Volume of powder is calculated (by difference 25ml – V_o) V_p

9. Density of powder is calculated (by using V_p and W3) ρ_p

The density calculated in 9 is the envelope density of the granules; this is more accurate than the mercury porosimetry as long as the oil completely wets the surface of all the powder. To ensure this happens the contents are shaken to free any trapped air bubbles which would increase the apparent volume of the powder.

The true density is found from the results of the binder content test combined with the true (known) density of Calcium Carbonate and the true (known) density of PEG. The binder content test gives the ratio by mass of $CaCO_3$ to PEG, when the weight of the powder is known the actual mass of $CaCO_3$ is found and the actual mass of PEG is known. The true density of these constituents are then used to give the actual volume of PEG and actual volume of $CaCO_3$ within the powder contained in the density bottle, knowing these volumes the volume of solid material within the powder is known.

The porosity is then simply the difference between the volume of the powder and the volume of the solid material contained within the powder (this is better than combining mercury porosimetry and helium pycnometry as it takes into account enclosed pores.)

8.3.9 Summary of Tests

Tests were carried out on all successful batches that could be sieved. Not all the batches produced granules that were suitable for subsequent testing. Failed tests where the granules were not suitable, a large enough sample could not be produced or the test either produced none or corrupted data were not recorded. Successful tests that produced useful data were recorded and the details are in Appendix G (database on file or attached CD as appropriate).

TEST	TESTS	SUCCESSFUL
Granule Batches	77	37
GSD (Camsizer)	47 (111)	(47)
Abrasion	168 (235)	112
Profilometry	336 (504)	307
Binder Content	156 (235)	128
Porosity	52 (235)	(51)
Strength	51 (80)	51

Note: "TESTS" Performed – is the number of tests that were attempted on the produced granules; it includes cases where a test either produced no data or corrupted data was recorded. The number in brackets is the ideal number of tests that should have been carried out based on successful batches from the previous step. The ideal number was not done because of either limited granules in the appropriate size ranges for testing, limitations due to testing time, equipment and procedures or, in the case of Profilometry, limited useful results carried forward from Abrasion testing. In the case of GSD and Porosity the tests were stopped once it was determined that the procedure was likely to be unsuitable or containing errors.

8.4 Data Capture

For the some of the tests the data is captured automatically by computer and then exported to excel for data manipulation. For others the data has to be measured manually and recorded by hand before manipulation. Data for the abrasion profiles (profilometry test), static strength tests and Camsizer were all captured electronically (no data is produced from the abrasion tests, the sample plates generated are subsequently used in the profilometry tests). The data from binder content, moisture content and porosity testing as well as the sieving element of the GSD's have to be collected and recorded by hand before data manipulation to give the results.

8.4.1 Labelling system / tracking system

As all the testing techniques used in this report are destructive (with the exception of the GSD analysis) representative samples.from a given batch of granules have to be used in each test. In order to allow easy and accurate comparison of results from granules within a given batch and between granules from different batches a detailed labelling and tracking system needed to be used.

Every batch of granules that was made using the High-Shear Mixer was given a unique code, even if a batch didn't turn out correctly it was assigned a unique code and the observations about why the batch failed were recorded (this was so best operating practice on the HSG could be maintained and all granules in the labs could be traced back to a date, time and operator.) The batch code uses an easily identifiable coding system that allows it to be instantly recognised as the unique batch number and allows for easy identification of the experimental recipe (see section 8.1.1) upon which the batch was based.

The batch code consists of 3 sections separated by a ' / ', the first section is always BN (representing Batch Number and makes it instantly recognisable as a unique batch code), the second section gives the year in which the granules were made (most of the useful batches used in the results of this report were made in '04), the last section gives the experimental recipe that the batch follows. For the first batch produced, which exactly follows an experimental recipe, this last section is simply the number of the experiment.

Subsequent batches or those which follow a slight change from the experimental recipe (for example using Pour-On addition method instead of Spray-On because the sprayer was broken) have a last section which starts in an X (meaning an "extra" batch) and ends in an alphanumeric letter (A = 1st, B = 2nd, C = 3rd and so on...).

Once the batch is made it needs to be sieved (sample preparation) into the following size cuts: <63 μm, 63<106μm, 106<212μm, 212<300μm, 300<355μm, >355μm

Each of these size cuts is bagged up and labelled:

Date	-	e.g. 29/06/04
Batch number	-	e.g. BN/04/1
Impellor Speed	-	eg Imp 1400
Chopper Speed	-	e.g. Chp 400
Run time	-	e.g. 30min
Addition method	-	e.g. Spray
Binder type and weight	-	e.g. PEG 1500 / 311ml
Powder type and weight	-	e.g. Omyacarb 2 / 3kg
Sieve cut in bag	-	(1 of) <63 μm
		63<106 μm
		106<212 μm
		212<300 μm
		300<355 μm
		>355 μm

The sieving is repeated several times, with each sieving of the same size going into the same bag, until enough of a sample is generated in the size cuts of most interest (106-212 and 212-300). The bags are labelled with the batch no., size cut, date, impellor speed, chopper speed, binder type and content (by mass) and primary particle type and content (by mass).

The granules used in each of the subsequent destructive testing test for abrasion, static strength, porosity and binder content are taken from these bagged and labelled sieve cuts.

For the abrasion tests each Perspex sample plates was labelled on the reverse side with a unique abrasion test ID. This is a code which contains information in 3 sections: the first letter is the sieve cut being analysed (W is 300-355, Y is 63-106 and Z is 212-300 μm – if none of these letters are present and it begins in a number or an X then it corresponds to the sieve cut 106 – 212 μm), the second section of the ID gives the batch code and is simply the *x* part of the batch code BN/04/*x*, the last section of the ID is a letter corresponding the number of the abrasion test for that batch and sieve cut – so if it is the 3rd abrasion test of 63-106 granules from batch X5A then the abrasion test ID would be YX5AC (Y => 63-106, X5A => batch no. BN/04/X5A, C => 3rd abrasion test), an ID ending in A is the 1st, B the 2nd and so on...

The unique profilometry ID code for the data from the profilometry tests was labelled in accordance to its corresponding abrasion test ID, except that an extra letter was added on to the end of each code corresponding to the number of the profilometry test in the same manner that multiple abrasion tests are added – i.e. the first test adds an "A" onto the end, the 2nd ends in a B, the 3rd a C and so on... (only 3 profilometry tests were performed except in special cases).

For the Granule Size Distributions the label is simply the batch number followed by a dash and a number corresponding to the number of the run through the Camsizer. The ID code used in the results database is just a simple number used as an identity key in Access.

For the binder content and porosity tests the label is just the batch number, as they are not inter-dependent on other tests (as the abrasion and profile are).

8.5 Other Experiments

8.5.1 Preliminary testing of New abrasion rig

A series of preliminary abrasion tests were carried out to determine if the experimental technique was valid and to test the abrasive difference between granules and the powders that make up those granules. The experiment was done using 2g of powder in 5ml of oil and an abrasion time of 5 minutes. The Perspex abrasion plates were blanked off using sellotape as in the normal abrasion experiments. For these tests the solid metal abrasion block wrapped in cloth was used in place of the toothbrush counterbody as the purpose was to determine if the counter body alone would cause significant abrasion.

2 tests were done using oil only and no abrasive particles – these were labelled Abra11 and Abra10.

3 tests were done using Wessalith Powder (a form of Aluminium zeolite) – labelled Abra16, Abra17 and Abra18.

3 tests were done using Wessalith Granules (106-300um) – labelled Abra: ,7,8 and 9.

3 tests were done using Durcal 5 powder (small particles of crushed $CaCO_3$) – labelled Abra13,14 and 15.

3 tests were done using Durcal 5 (Standard granules) but only 2 of these came out – Abra5 and Abra6.

8.5.2 Testing of abrasion of toothbrush and granule breakage

Square Perspex sample plates were used without Knoop indents. A suspension of 106 – 300 μm granules in oil made up using 0.5 grams in 2 ml of oil was dosed onto each sample plate. The abrasion rig was then run for 10 minutes at 81 strokes per minute. Tests were run with a total downward load of: 103.2 grams, 153.2 grams, 203.2 grams and 303.2 grams. The samples were then removed and the damage observed under a microscope. A separate test was conducted using oil only without granules and a total downward load of 103.2 grams.

These tests were done using the toothbrush head rather than the solid abrasion block.

8.5.2.1 Size analysis before and after abrasion

A suspension of 63 – 106 μm granules in oil was made up using 0.6 grams in 5 ml of oil. This was stirred using a pipette to agitate the granules and keep them in suspension. 2 separate samples were taken and measured using the Sympatec® (Rodos laser scattering particle size distribution device) in a 6 ml cuvette that was stirred by hand. A separate sample was taken and measured using the Sympatec in a 25 ml cuvette that was stirred mechanically. Roughly 3 ml of the granule suspension was then abraded for 3 minutes using the Hand-Held abrasion rig (an electric toothbrush held by hand, pushing into the slurry of granules and oil). The abraded particles were measured using the Sympatec, 2 samples using the 6 ml cuvette and 1 using the 25 ml cuvette.

9 Data manipulation

9.1 Granule Size Distribution

The data for the granule size distribution was obtained from a combination of sieving and image sizing using the Camsizer. The sieving removed and weighed the particles of sizes below 63μm; the remaining particles were weighed and run through the Camsizer, which allocated the particles according to imaginary sieve cuts. The data that comes out of the Camsizer is equivalent to results that would have been obtained from sieving; it gives the distribution on each theoretical sieve as fraction based on volume.

In order to get the overall size distribution the following data manipulation is performed:

1. The total weight of the particles that are below 63μm is found
2. The total weight of the particles that are above 63μm (and go through the Camsizer) is found.
3. The total weight of all the particles is found by adding (1) and (2)
4. The fraction of the total distribution that is above 63μm is found by (2) / (3)
5. The raw data from the Camsizer as the fraction on each sieve cut is recorded
6. The fraction in each sieve cut is found by multiplying the fractional result for that sieve from the Camsizer data by the fraction of the total that went into the Camsizer (5) x (4)
7. The cumulative undersize is found by starting at the fraction on the sieve cut below 63μm and entering that value from (6), the value under the next sieve cut is the total so far plus the respective value for that sieve cut from (5). This is done for all the sieve cuts until the total fraction equals 1.
8. These distributions are plotted
9. The weighted distribution is then found using the values from (6) and dividing them by the width of the sieve cut upon which they are based. e.g. the weighted value for the sieve cut 71microns to 80microns would be divided by 9 [80-71 =9]
10. This weighted distribution is then plotted

9.2 Average Abrasive Wear

There are 2 forms of average abrasive wear that are quoted in the results of this research. There is the average abrasive wear for the wear scar produced on a single Perspex abrasion sample plate from a single abrasion test, the average is the average wear from the 3 profilometry tests associated with that particular abrasion sample plate. The second average abrasive wear is really an average of the average abrasive wear. For example for sieve cut 212-300um from BN/04/01 there were 3 successful abrasion tests with ID Z1A, Z1B and Z1C. Each of these had 3 profiles of their wear scar taken and the average of the x-sectional areas of the successful profiles was used to give an average abrasive wear for each of those abrasion tests. The average abrasive wear of the each of these abrasion tests were: Z1A = 65000, Z1B = 91,000 and Z1C = 80000. Thus to find the abrasive wear (strictly abrasivity) for granules from BN/04/01 it is the average of these 3 values. This could be taken one step further and the average abrasivity of all batches made using the same experimental protocol could be found (except that reproducibility of batches made in the HSG was found not to be possible).

The cross-sectional wear area (that is taken as a measure of the relative abrasivity so the units of abrasive wear should be quoted in metres squared) needed to be calculated from the profilometry data points produced by the Dektak. The profiles needed to be converted into a wear area for comparison, and needed to be standardised. It was not possible to ensure that the width of wear scar was the same for each abrasion test so a section of the wear profile was measured to obtain the abrasive wear rather than taking it across the whole of the exposed section. To ensure that the same length of section was analysed each time the profile used to calculate the wear area was taken as the area starting at the 1000^{th} data point and ending at the 4000^{th} data point, these were chosen because in all tests they fell within the wear scar.

In order to get a value for the abrasive wear for a given profile the following data manipulation was done:

1. The Dektak profiler was run perpendicularly across the wear scar (this produces data that is in a diagonal form due to systematic errors in the profilometer)

2. The diagonal profile was levelled by moving 2 cursors points to parts of the profile that correspond to the datum (or the un-abraded surface of the Perspex), preferably on either side of the wear scar, and set the profile to horizontal
3. The data for the profile was output to Excel (the data is in the form of a data point number and its corresponding depth from the datum in nanometres)
4. These values are then plotted to give the wear profile
5. The values of the depth are then compared to zero prior to integration, if they are positive (i.e. a peak) they are set to zero so that they do not reduce the value of the subsequent integration of the wear area. This is valid because some material will be pushed up in peaks as granules plough through the Perspex and if they were not zeroed it would mean that a plate with no abrasion would give the same abrasive wear result as one where all the material was ploughed up above the datum.
6. The values from (5) are used to find the average depth between consecutive points, the average depth of wear between 2 points is taken as the sum of the point before and the next point divided by 2.
7. The total standardised wear is then taken as the sum of the values calculated in (6) between the 100^{th} and the 4000^{th} data points
8. This relative wear from (7) is then multiplied by 7814 (as this is the approximate distance in nanometres between each data point)
9. These values are normalized by dividing all the relative abrasive wear values by the smallest value so they are seen on a scale as multiples of abrasion of the least abrasive case.

9.3 Static Strength – multiple compression testing

The data for the multiple granule compression testing and analysis using the method described by Adams, et al., [85] was obtained using a Zwick compression tester. This recorded the initial bed height, h_o, and then the standard travel (from which the actual bed height, h, was found) and the corresponding standard force, F_c. These data points were exported into an excel spreadsheet and the natural strain (Є), $\ln(h_o/h)$, was then found for each data point. The cross-sectional area (surface area of bed) is known to be 7.85×10^{-5}m and was used to find the applied nominal pressure, P, in the bed and the Log of this was taken for each data point.

Adams theory derives the following equation:

$$\ln P = \ln\left(\tau_o'/\alpha'\right) + \alpha' \epsilon + \ln\left[1 - Exp\left(-\alpha' \epsilon\right)\right] \qquad (35)$$

This provides a pressure-volume relationship for confined uniaxial compression (it is a not a dimensionally balanced relationship). At large values of Є, a plot of ln P as a function of Є should be linear with a slope of α' and an intercept of $\ln(\tau_o'/\alpha')$, from which τ_o' can be calculated. τ_o', is a parameter that allows the calculation of the failure load of equivalent single particle, F_{calc}, to be determined from multiple granule crushing tests.

To find the slope and the intercept the last 10% of the data points for the ln stress (ln P) and natural strain are used (it is assumed that this is the linear region as otherwise there is no standard way of comparing the results and the consequential values of F_{calc} vary so wildly that they are meaningless). A gradient, α', of the slope is determined by taking:

$$\frac{\ln P_{100\%} - \ln P_{90\%}}{E_{100\%} - E_{90\%}} = \alpha' \qquad (36)$$

The intercept, $\ln(\tau_o'/\alpha')$, is then determined using this value of the gradient and the $\ln\sigma_{100\%}$ value. The value of, τ_o', can then be determined. These values of α' and τ_o' are then used in equation (35) above combined with the original values for the natural strain to determine new theoretical values for the stress terms. These new stress terms are compared to the original data on a squares difference basis.

A goal seek scenario was then set up to find modified values of , α', and τ_o'. The value of , α', is altered using the goal seek function in Excel to minimise the least squares difference between the original data and the data obtained by using equation (35) above

and the goal seek value of, α'. The last 10% of values of these new data points are then used to find a modified, α'^*, and a modified $\tau_o'^*$, from the gradient and intercept. This determined value of modified $\tau_o'^*$, is the equivalent to the single granule failure strength multiplied by a constant. Unfortunately as already described this constant cannot be determined without comparing to data from single granule failure tests, which are not practically feasible on the granules considered in this report. For the purposes of this report the modified $\tau_o'^*$, is the equivalent of F_{calc}.

Summary of data manipulation method:

1. Capture force and displacement data using Zwick machine
2. Export to spreadsheet
3. Convert force to stress, using bed surface area and take logs.
4. Convert displacement to natural strain ($\ln(h_o/h)$)
5. Find the initial value of, α', from the gradient of slope of last 10% values
6. Find the value of, τ_o', from the intercept of the slope of the last 10% values and the, α', found in (5)
7. Use the values of, α', τ_o', and the initial values of the natural strain in equation (35) above to determine theoretical stress values
8. The squares difference between the theoretical values stress values and the original data is calculated
9. The value of, α', is then incrementally changed to find new theoretical stress values using the goal seek function such that the sum of the squares difference between the theoretical stress value and the original data is minimised (least squares basis)
10. Once the theoretical stress data has been determined on a least squares basis modified α'^*, is found from the gradient of the slope of last 10% values
11. Modified $\tau_o'^*$, is found from the intercept of the slope of the last 10% values and the modified α'^*, found in (10)
12. Modified $\tau_o'^*$, is the same as F_{calc} in the results section of this report and is the equivalent to the single granule failure stress multiplied by a constant.

9.4 Binder Content

The binder content has very simple data manipulation. The difference between the weight of crucible containing granules before and after burning is recorded and divided by the mass of granules placed in the crucible (following the test protocol outlined in section 8.3.6).

The percentage binder by mass is given by:

$$Binder = \left(\frac{W_7 - W_9}{W_7 - W_6} \times 100\%\right) - moisture\% \qquad (32)$$

Where W_6 is the weight of the empty crucible, W_7 is weight with granules before burning and W_9 is the weight after burning.

An excel spreadsheet was set-up to input these values with the moisture content was assumed constant (the average of several moisture content tests was taken, see section 9.5). The Binder content calculation was then automated.

9.5 Moisture Content

Performing moisture content experiments was time consuming when done in unison with binder content experiments so a series of tests were done to determine the extent of the moisture content variation. These were performed over several days (including a wet day) so it was assumed that if the moisture content varied a lot due to atmospheric conditions it would show up in the results. 3 different batches were tested and the moisture content was determined for each according to the protocol in section 8.3.7

The percentage moisture by mass is given by:

$$Moisture = \frac{W_{11} - W_{12}}{W_{11} - W_{10}} \times 100\% \qquad (34)$$

Where W_{11} is the mass of granules and crucible before burning, W_{12} is the mass after burning and W_{10} is the mass of the crucible without granules.

The results of these tests indicated that the percentage moisture was less than 1% and typically between 0.3 and 0.7. The average moisture content over these 3 days and 3 different batches was taken as a value to be used in the determination of the binder content of all the granules; as the calculated binder content with this percentage moisture was typically around 16% the moisture accounted for less than 5% of the binder content.

The average moisture content was found by:

1. The average moisture content of 7 samples of BN/04/X2 was found to be 0.37% with a standard deviation of 0.18
2. The average moisture content of 4 samples of BN/04/01 was found to be 2.33 % with a standard deviation of 1.82
3. The average moisture content of 6 samples of BN/04/10 was found to be 0.23% with a standard deviation of 0.04
4. These were then averaged to find the average moisture content of 0.78% with a standard deviation of 1.19
5. It was assumed that the variations in the moisture content would be insignificant.

Note: with hindsight it is now believed that this could be a substantial error in the quoted values of the binder content and ultimately the porosity content (as these use the binder content values)

9.6 Porosity

To find the Porosity of the granules requires the use of the data collected from the density bottles (Porosity tests) and the binder content (which itself combines the binder content test and the moisture content test).

The density calculated from the porosity bottle test is the envelope density of the granules. The true density is found from the results of the binder content test combined with the true (known) density of Calcium Carbonate, 2.7 g/cm^3, and the true (known) density of PEG, 1.093 g/cm^3. The binder content test gives the ratio by mass of $CaCO_3$ to PEG, when the weight of the powder is known the actual mass of $CaCO_3$ in the sample is found and the actual mass of PEG in the sample is found. The true densities of these constituents are then used to give the actual volume of PEG and actual volume of $CaCO_3$ within the powder contained in the density bottle. By knowing the volume of PEG and the volume of $CaCO_3$ the volume of solid material within the powder is found.
The porosity is then the ratio of the volume of the empty space contained within the powder (found by difference between envelope volume of powder and the combined volume of binder and solid) to the volume of powder found from the porosity bottle test (this is better than combining mercury porosimetry and helium pycnometry as it takes into account enclosed pores.)

The porosity was found by the following.

1. An excel spreadsheet was set up to automate the calculation of the envelope density.
    a. The mass of the bottle, W_1, is subtracted from the mass of the bottle plus granules, W_2, to give the mass of granules, W_3.
    b. The mass of the bottle plus granules, W_2, is subtracted from the mass of the bottle, granules plus oil, W_4, to give the mass of oil in the bottle, W_5.
    c. The volume of oil, V_o, is then found by multiplying the mass of oil by its density (0.9148 g/cm^3).

d. The volume of the granules, V_p, is then found by subtracting the volume of oil from the volume of the density bottle.

e. The envelope density of the granules, ρ_p, is then given by $W_3 \div V_p$

2. The envelope density is fed into another spreadsheet that contains the information from the Binder Content tests.
3. The information from the Binder Content test is used to find the volume of the $CaCO_3$ and PEG within the powder.
    a. The volume of $CaCO_3$, V_{pp}, is the weight of the granules, W_{pp} ($W_9 - W_6$), divided by the density of $CaCO_3$ (2.7 g/cm^3)
    b. The volume of PEG, V_b, is the weight of the PEG, W_b ($W_7 - W_9$), divided by the density of PEG (1.093 g/cm^3)
4. The volume of the granules, V_g, in the Binder Content test is then found by dividing the mass of granules, W_8, by the envelope density, ρ_p.
5. The porosity, ε, is then found by dividing the volume of space ($V_g - V_{pp} - V_b$) within the granules by the envelope volume of the granules, V_g.

10 Results Database

As already discussed in section 8.1 (experimental design) there is a massive number of results that were to be generated from the tests associated with each of the experiments and then further results from the duplication of these tests and duplication of the experiments. An efficient means of storing and relating all this data is to use a relational database. It was decided to use Microsoft Access as the basis for the database as this is a very simple and powerful database and it is widely available (meaning greater possibility for the dissemination of the database and data). The database is included in appendix G (as an attached file or CD as appropriate)

10.1 Design and Purpose of Results Database

- Designed to make the analysis of results easier
- Maximise plots of *Property – Property* and *Property – Experimental Parameter* relationships
- Easy to move between, and see, different sets of results
- Easy and quick data entry
- Transferable to other projects

The database was designed after the experimental design and the preliminary tests had been performed so very little of the data from these tests is entered into the database (often because it was not in an appropriate form). The development of the database was done in parallel with the early testing and the information obtainable from the database was used in feedback to the continuous development of the testing procedures to ensure that the correct, useful, raw data was being collected. The information from the testing was used in a similar fashion to dictate the fields and relationship keys within the database during its design process. This means that some of the data in the database is not completely useful, but the finished database is perfect for adding further information in the study of granule properties and their relationships to each other and the High-shear mixer operating and formulation parameters. The database has been set-up in such a way

as to allow easy navigation and data entry and to allow data sets from other experimentalists to be added for direct comparison to my data.

The queries were written to include all the most important relationships and to present the data in a form ready for manipulation in Excel or other spreadsheets.

10.1.1 Sequence of testing (background for database design)

A High Shear Granulation batch is performed according to the protocol of the unique experiment number. This High Shear Granulation batch is given a unique batch number code such as BN/04/1; where BN stands for batch number, 04 stands for an experiment performed in 2004, the 1 means it was made according to the protocol of experiment number 1. Subsequent batches are labelled with an X preceding the last number (meaning it is an extra batch) and a letter after it (increasing sequentially for each extra batch), so BN/04/X14B is the 2nd extra batch to be produced according to Experiment number 14. Each batch (with its unique batch number) then has a Granule Size distribution (GSD) performed on it. The batch is then sieved into size cuts ready for further testing. The further testing includes porosity testing using a density bottle, burning the granules in a furnace and crushing them in a force-displacement machine. Each individual test produces results that need to be entered into their own spreadsheet and then manipulated to give a value. For example burning the granules produces 3 weight readings which are then manipulated to give the binder content as a percentage; the strength testing gives a data set of about 6400 values that are plotted graphically and a single value of *Fcalc* (pseudo crushing force) is derived. The density bottle test produces a density for the powder which, when combined with binder content, allows the porosity to be calculated as a single value.

The sieve cuts from the batch (with its unique batch number) are also run through an abrasion rig, this does not produce any results but the operating conditions of the abrasion rig need to be recorded. The abrasion test produces a series of Perspex plates that are each labelled with a unique abrasion test ID. These Perspex plates are put through a profilometry tester that produces a data set of about 6000 values corresponding to the

cross-sectional profile of the wear scar on the surface of the Perspex plate, 3 cross-sectional profiles are taken per plate and converted into a single value representing the average abrasive wear for that unique abrasion test for a given sieve cut from that unique batch.

10.1.2 Requirements for Database design

A database was wanted such that the data from the different tests could be entered into their own tables. These tables needed to be linked together in a useful fashion. Separate tables for each of the experiment types with the headings for the information (fields) required within the table were written. Data entry forms were required such that the data for all fields for a given record in a given table can be entered one record at a time. These forms needed to be set-up in such a way as to minimise data entry mistakes. It was required to be able to view all the data on a given table and to sort the data according to different fields.

The main table is the High Shear Granulation (HSG) test table, this lists all of the High Shear Granulation experiments that have been performed (ie. All the different batches that have been made). There is a unique record entry for each batch of granules made (identified by its Batch No. and this is the tables Primary Key). There is an entry for the experiment number that the batch corresponds to (even though this is included in the batch no. code there are some discrepancies and some anomalous batch numbers, but all batch numbers are unique). The exact way the batch was made is also recorded with a box for observations / comments – this is because even though a batch is made according to the protocol of a unique experiment number it is not always possible to get all the operating conditions exactly the same as the protocol when actually making a batch. A separate table called Experiment Number records the ideal experimental protocol for each unique experiment number whilst the High Shear Granulation test table records the unique batch number with the exact conditions that were really used (with a link to the experimental number table so that the ideal conditions can be easily viewed).

5 Sub tables are linked to the High Shear Granulation (HSG) test table using the unique Batch No. primary key in the HSG test table and including the Batch No. as a field in each record in each sub table. The sub tables are:

GSD (granule size distribution)

Porosity

Binder Content

Strength

Abrasion

The abrasion sub table has a further table called Profilometry linked to it; this is so that for each abrasion test the 3 cross-sectional areas corresponding to the unique abrasion test ID can be stored. This is shown schematically in the figure 41 below with tables and relationships between tables shown in red, real physical processes are shown in black and data transfer is shown in green.

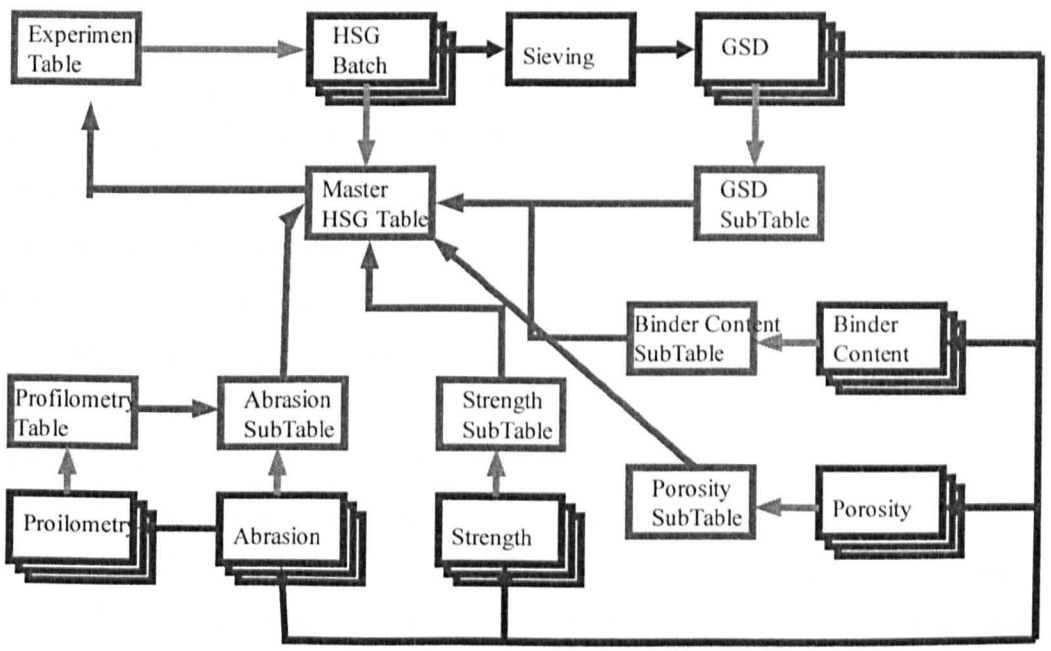

Figure 41 - schematic of the results database.

The GSD sub table includes fields for the Batch No. being tested, a unique GSD ID, the mode size of the granules, the mean size of the granules, X50, X10 and X90 (the mean, mode X10, X50 and X90 are all derived from graphs in individual excel worksheets for each Batch No.). A single Batch No. could have several GSD tests performed on it, but each one of these would have its own GSD ID. This table is set up such that only GSD tests for a single Batch No. or selected group of Batch No's can be viewed together or such that all the GSD tests can be viewed together.

The Porosity sub table includes fields for the Batch No. and size cut being tested. This table is set up such that only Porosity results for a single Batch No. or selected group of Batch No.'s can be viewed together or such that all the porosity results can be viewed together. The table includes the following fields; Batch No., size cut, Density of powder and a unique Porosity Test ID. If several tests are performed on the same size cut from the same batch number then each test will be allocated a unique Porosity Test ID.

The Binder Content sub table includes fields for the Batch No., Size cut, Binder content and a unique Binder Content Test ID. This table is set up such that only binder content results for a single Batch No. or selected group of Batch No.'s can be viewed together or such that all the binder content results can be viewed together. If several tests are performed on the same size cut from the same batch number then each test will be allocated a unique Binder Content Test ID.

The Strength sub table includes the fields for the Batch No., Size cut, pot size, Fcalc and a unique Strength Test ID. (The Fcalc value is derived from graphs in individual excel worksheets for each Strength Test ID). This table is set up such that only strength test results for a single Batch No. or selected group of Batch No.'s can be viewed together or such that all the strength test results can be viewed together. If several tests are performed on the same size cut from the same batch number then each test will be allocated a unique Strength Test ID.

The Abrasion sub table includes the fields for the Batch No., Size cut, sample holder, mass of granules added, mass of oil added, abrasion time, a unique Abrasion Test ID and the average abrasive wear. Each sample plate tested using the abrasion rig must be given a unique Abrasion Test ID, this corresponds to the unique label written on the Perspex Sample plate in order to identify its particular test conditions. Each unique sample plate is tested by profilometry 3 times (and thus each unique Abrasion Test ID will have 3 corresponding entries in the Profilometry table). The average abrasive wear corresponds to the average of these 3 values. This table is set up such that only abrasion test information for a single Batch No. or selected group of Batch No.'s can be viewed together or such that all the abrasion test information can be viewed together. It is also be set up such that it links to the profilometry table such that the 3 entries corresponding to each unique Abrasion Test ID can be viewed.

The Profilometry sub table (which is linked to the Abrasion sub table and NOT the HSG main table) includes the fields for the Abrasion Test ID, the cross-sectional area of the profile and the unique Filename corresponding to the 1 of the 3 profiles that the cross-sectional area relates. This table is set up such that only Profilometry information for a single Abrasion Test ID or selected group of Abrasion test ID's could be viewed at the same time.
The figures below show the user interface screen from the view tables menu and the tables that are brought up as a result. The second diagram shows the main HSG table in the background with tables corresponding to the abrasion tests carried out on and associated with individual batches, the foreground tables show the profilometry results associated with a single entry in the abrasion sub-table.

With all the tables and their relationships set-up data entry is done in such a way that minimises errors, so data entry to the sub tables is done using lists that only allow you to select specific values of batch no's that correspond to the main High Shear Granulation table. The High Granulation Table has drop down lists for entries in certain fields that allow easy sorting (otherwise "Spray-on" and "Spray On" might be typed as 2 different

entries in the addition method field and these would not be grouped together if the records are sorted by Addition method "Spray On".

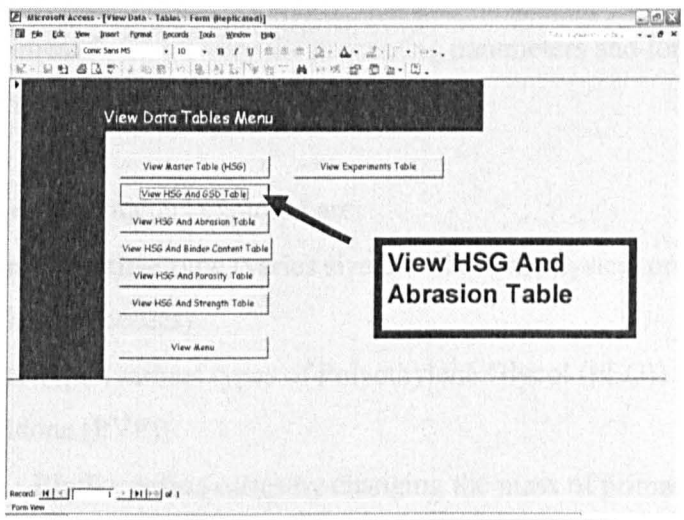

Figure 42 - showing the user interface menu from the results database

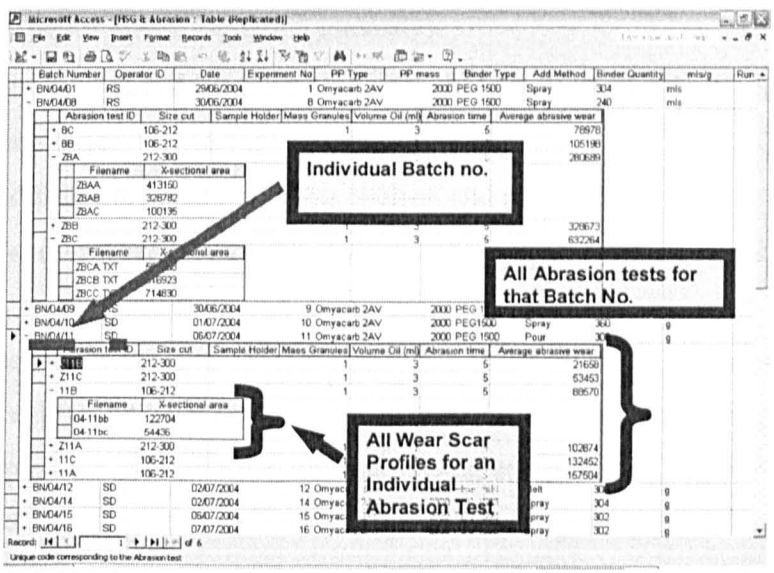

Figure 43 - showing the Abrasion sub-tables and their associated profilometry tables

10.2 Property to Property Relationships / Property to Processing Parameter Relationships

Batches are produced using the High-shear granulator according to a given recipe from a list of "experiments". These vary the processing parameters and formulation parameters to produce granules.

The formulation parameters explored are:

- **Primary particle type** (varies size distribution, physical properties and surface chemical properties)
- **Binder type** (various types of Polyethylene Glycol (PEG)) and Polyvinyl Pyrolidone (PVP))
- **Solid : Binder ratio** (varies by changing the mass of primary particles and the mass of binder added)

The processing parameters explored are:

- **Impellor speed** (agitation intensity)
- **Chopper speed** (to determine if this has an effect or not)
- **Run time**
- **Addition method** (spray-on, melt-in and pour-on)
- **Temperature** (affects the viscosity of the binder and the state of the binder)

It was intended to design a standard batch and then vary one of the 8 parameters at a time to produce different batches to determine the effects of that particular parameter. It has not been possible to do this due to experimental equipment failing (notably the binder spray system) or a given combination of parameters does not produce granules suitable for further testing (because of the combination of Processing parameters and formulation parameters falling into the unstable regime).

The granules produced from successful batches were tested to try to give the following granule property information:

1. Granule size distribution (**GSD**)
2. **Binder content** of granules in the sieve cuts 106-212 microns and 212-300 microns
3. Static **compressive strength** of multiple granules in the sieve cuts 106-212 microns and 212-300 microns
4. **Abrasive strength** (abrasivity) of multiple granules in the sieve cuts 106-212 microns and 212-300 microns
5. **Porosity** of granules in the sieve cuts 106-212 microns and 212-300 microns

10.2.1 Desirable relationships

It is important to consider the interaction of the properties of the granules (these are determined from the 5 experimental tests: abrasion, static strength, porosity, binder content, GSD). Once the interaction and interdependency of granule properties is established it then becomes important to determine how these properties can be controlled. To do this comparisons will be made between a given granule property and its formulation and processing parameters.

As an example consider the following 2 batches BN/04/11 and BN/ 04/22, both are made with exactly the same experimental recipe except that BN/04/11 uses Omyacarb 2AV as the primary particle and BN/04/22 uses Durcal 65. The batch using Omyacarb 2AV produces very small granules whereas the Durcal 65 produces large granules; so considering only these 2 granule types a plot of static strength against size might reveal that strength increases with size. Based on this it could be assumed that primary particle type affects the size of the particle produced and thus the strength. However further testing of the granules from BN/04/11 and BN/04/22 that are within the same size class might reveal that there is still a difference in static strength and this can no longer be linked to size of the resultant granule. An analysis of these granules comparing static strength against porosity might show that the granules that are less porous are stronger

and that these happen to be made from Durcal 65. So from an experimental recipe point of view granules made with Durcal 65 will be stronger, whether this is due to porosity or size would not be clear until further testing on other granules.

It was decided that the following trends would be of interest:

Trend 1 How does the abrasivity vary with the static strength?
To determine this requires plotting abrasivity (in terms of worn material under constant conditions) of various granules of all size cuts against their static strength. To take this one stage further needs a plot of the abrasivity of granules within the 106-212 sieve cut against the static strength data of the same granules in the 106-212 sieve cut. This is because it is believed that size has an effect on abrasivity and static strength. To test the effect of size on static strength needs plots of static strength against size for all granules, thus plots of static strength against size for granules from 1 batch but with several sizes cuts. To test this effect of size on abrasivity requires plots of abrasivity against size for all granules and a plot of abrasivity against size for granules from 1 batch but with several size cuts.

Trend 2 How does the abrasivity vary with granule type?
To determine this requires plotting the abrasivity of the granules within a single sieve cut against the type of granule; i.e. the way the granule was made and what the granule is made from. Some variation in the abrasivity produced is expected. This needs one plot for all granule types in the size cut 106-212 microns and another plot for all granule types in the size cut 212-300 microns. Another plot showing the variation in abrasivity for ALL abrasion tests performed is useful.

Trend 3 What affects the static strength of granules?
To determine this requires plotting the static strength of granules within a single sieve cut against the type of granule; i.e. the way the granule was made and what the granule is made from. Some variation in the static strength is expected. This needs one plot for all granule types in the size cut 106-212 microns and another plot for all granule types in the

size cut 212-300 microns. It needs a plot showing the variation in the static strength for all strength tests performed, a plot of static strength as a function of porosity (for 106-212 micron sieve cut and the 212-300 micron sieve cut) and a plot of static strength as a function of binder content (for 106-212 micron sieve cut and the 212-300 micron sieve cut). These plots will give an idea of the granule properties that affect its static strength and how those properties affect it, but plots relating these properties to the processing parameters will also be needed in order to know what processing and formulation variables affect the static strength.

10.2.2 Plots / graphs from Data

Below is a list of all the plots that will be carried out.

1. Abrasivity against Static Strength (all granules all sizes)

2. Abrasivity against Static Strength (106-212 micron granules only – all granule types)

3. Abrasivity against Static Strength (212-300 micron granules only – all granule types)

4. Abrasivity against size (106-212 microns and 212-300 microns as the size cuts – all granule types)

5. Abrasivity against size (<63, 63-106, 106-212, 212-300 and >300 as the size cuts – single granule type)

6. Abrasivity against granule type (106-212 microns – all granule type)

7. Abrasivity against granule type (212-300 microns – all granule type)

8. Abrasivity against granule type (all sizes – all granule type)

9. Abrasivity against Porosity (all granules all sizes)

10. Abrasivity against Porosity (106-212 micron granules only – all granule types)

11. Abrasivity against Porosity (212-300 micron granules only – all granule types)

12. Abrasivity against Binder Content (all granules all sizes)

13. Abrasivity against Binder Content (106-212 micron granules only – all granule types)

14. Abrasivity against Binder Content (212-300 micron granules only – all granule types)

15. Static strength against granule type (106-212 microns – all granule type)

16. Static strength against granule type (212-300 microns – all granule type)

17. Static strength against granule type (all sizes – all granule type)

18. Static strength against porosity (106-212 microns – all granule type)

19. Static strength against porosity (212-300 microns – all granule type)

20. Static strength against porosity (all sizes – all granule type)

21. Static strength against binder content (106-212 microns – all granule type)

22. Static strength against binder content (212-300 microns – all granule type)

23. Static strength against binder content (all sizes – all granule type)

24. Static Strength against size (106-212 microns and 212-300 microns as the size cuts – all granule types)

25. Static Strength against size ((<63, 63-106, 106-212, 212-300 and >300 as the size cuts – single granule type)

26. Porosity against granule type (106-212 microns – all granule type)

27. Porosity against granule type (212-300 microns – all granule type)

28. Porosity against granule type (all sizes – all granule type)

29. Porosity against size (106-212 microns and 212-300 microns as the size cuts – all granule types)

30. Porosity against size ((<63, 63-106, 106-212, 212-300 and >300 as the size cuts – single granule type)

31. Porosity against binder content (106-212 microns – all granule type)

32. Porosity against binder content (212-300 microns – all granule type)

33. Porosity against binder content (all sizes – all granule type)

34. Binder Content against granule type (106-212 microns – all granule type)

35. Binder Content against granule type (212-300 microns – all granule type)

36. Binder Content against granule type (all sizes – all granule type)

37. Binder Content against size (106-212 microns and 212-300 microns as the size cuts – all granule types)

38. Binder Content against size ((<63, 63-106, 106-212, 212-300 and >300 as the size cuts – single granule type)

39. Size against granule type

10.2.3 Writing the *Microsoft Access* Queries

The *Microsoft Access* queries generate tables of linked data that is exported to excel for further manipulation if necessary before turning into graphs.

The queries for these plots were written in Access using the query wizard and pull the data straight out of the database holding the data. The exception is the data for plot 33, Binder content against porosity, this data was taken from the excel spreadsheets used for the Binder content and porosity calculations – this was done to see if there was a trend between binder content and porosity but also because it meant the individual matching pairs could be plotted as the binder content is used in the porosity calculations.
NOTE: - these queries are embedded within the computer file containing the database, Graphs of the queries are shown in appendix I and in the results section next to the relevant discussions.

The queries were written using the design wizard which allows easy manipulation of the data and ensures that the, *x*, and, *y*, data that is being plotted is actually related by the unique batch number in the master table. There are 2 basic types of query that were generated:

1) A query linking 3 tables together such as Query 23, which generates a table showing 3 useful columns (and 2 more confirming that the sizes are correct) showing the batch number from the Master HSG table in the first, and in this case a second column containing the average of the FCalc values for that batch and size cut and a third column containing the average of the binder content for that same batch and size cut. This type of query results in an x-y scatter plot.
2) A query linking 2 tables together such as Query 17, which generates a table showing 2 useful columns (and 1 more confirming the sizes) showing the batch number from the Master HSG table in the first and in this case a second column containing the average of the FCalc values for that Batch and size. This type of query results in a bar chart type graph.

There are 2 variations of the first type of query, those where the values for a given batch and variable are not averaged before display in the output table and those where the variable is averaged. There are advantages from a results analysis point of view for using both; by averaging the variable for a given batch it reduces the number of data plots generated from a batch where several tests were done by averaging in the x and y values separately – this also removes the effect of weighting the trend lines due to multiple points. The problem with this is that by averaging it hides any anomalous data points within the average and these can make the average completely unrealistic and subsequently give false trends. Where possible these anomalous data are removed from the query before averaging.

There is 1 variation on the 2nd type of query. Query 39 showing granule size against type combines 4 columns for each granule type. There are three columns for the Averages of X_{10}, X_{50}, and X_{90} for that granule plus a final column for the mode size.

11 Error Handling

There are well established mathematical principles for defining and handling errors in scientific experiments. There are 4 generally accepted forms of error; precision, systematic, random and human. Unfortunately definitions of these errors are not always clear and consistent between error textbooks and the way in which scientists apply the mathematical principles for handling these errors varies. The definitions and error handling methods are explained clearly in this section so as to avoid ambiguity in interpreting my results. However some key points on error handling should be stressed:

1. The person performing an experiment probably had some "gut feeling" and "hung" an error on the result primarily to communicate this feeling to other people. Common sense should always take precedence over mathematical manipulations.
2. Correct error analysis in complicated experiments can indicate where further work needs to be done to improve the accuracy or the precision of the results.
3. There is virtually no case in scientific experimentation where the correct error analysis is to compare the obtained value to a standard value in some book. A correct experiment is one that is performed correctly, not one that gives agreement with other measurements.
4. The best precision possible for a given experiment is always limited by the apparatus.

An accurate experiment is one which contains no human errors (i.e. The operator doing something wrong, this is different from precision and systematic errors produced due to the precision of the human eye and human reaction times which are legitimate experimental errors). An accurate experiment must also be set-up and controlled correctly, such that no external unwanted factors influence the experimental readings.

When assessing errors 2 questions must be asked:

1. Is the experiment accurate? – did it work properly and were all the necessary factors taken into account?
2. What is the numerical error range in the quoted value? – is it due to precision errors in the measuring device, systematic error in the device or the method or random (indeterminate) errors resulting from natural variation.

This section on error analysis was drawn from the information on 5 website, [117], [118], [119], [120], [121].

11.1 Precision Errors

A precision error is how close to a value an instrument or measuring device can measure a value due to the increments in markings (or the digital output of an electronic device). An example of a precision error from this work is the readings taken for the mass in the binder content experiments; the machine used weighs to ± 0.00005 grams. The machine reads to 4 decimal places and assuming that the engineering is correct it will round values up or down to the nearest 0.0001 gram (thus its precision is ± 0.00005 grams). However as already mentioned it is sometimes necessary to "hang" an error on a certain measurement, in this case the reading on the scales fluctuates and varies with time as it is very sensitive to people walking about in the lab and to air currents passing over the device so the error is more likely to be about ± 0.001 grams (and thus the feel for the value of the reading will probably mean that the results are more indeterminate and the error becomes more likely to be random rather than precision). It is important to note that the accuracy to which a human can judge the value is considered a legitimate precision error, but is more likely to be accounted for within the random or indeterminate error.

11.2 Systematic Errors

A systematic error is an error inherent in the experimental set-up which causes the results to be skewed in the same direction every time i.e. always too large or always too small. An example of a systematic error in this work is in the reported porosity values, the results show that the porosity varies from -2.043 to 0.1731. This is not possible as the porosity cannot be negative so it is very likely that this is the results of a systematic error. However as the porosity is not measured directly but calculated by manipulating data from 2 separate tests (binder content and porosity bottle) it is possible that the apparent systematic error is a result of random errors being combined in the parent experiments.

11.3 Random (indeterminate) Errors

All experiments have random error, which occur because no measurement can be made with infinite precision. Random errors will cause a series of measurements to be sometimes too small and sometimes too large. Random errors can occur because of indeterminate errors and variations within an experimental set-up or factors beyond control or measurement. Random error also results from the random way a series of values is rounded as a result of the equipment precision or the human judgement in reading a non digital value. An example of a random error in this work is the spread of values in the binder content for granules of size 106-212 μm from batch BN/04/01. The values are spread from 15.44 to -4.16 (as a percentage fraction of the total). Unfortunately because you cannot have a negative fraction there must have been some sort of problem in the experimental method or the errors combined in such a way to give a negative result in these negative cases.

11.4 Statistical methods used

11.4.1 Standard Deviation

Standard deviation is used to analyse the random error in a set of repeated tests. There are several formulas for the standard deviation. If an infinite number of samples is taken then the definition of standard deviation can be used to find the appropriate formula: the root mean squared variance from the mean. However this gives a biased result when a non infinite number of samples are tested. A modified, unbiased, variation of the formula that will be used in this work is:

$$Std.Dev = \sqrt{\frac{\sum_{i=1}^{n}(x_i - \bar{x})^2}{n-1}} \qquad (36)$$

Where, x_i, is the 'i'th number, $\bar{x}$, is the average value and, n, is the total number of samples tested. This formula is for determining the standard deviation of a set of samples from the whole population.

When a series of test values is used to calculate the standard deviation the error is usually reported as plus or minus the standard deviation, i.e. the random error. If a systematic or precision error is greater than the random error, then it should be quoted instead of the standard deviation. In general it is difficult to tell if the error is systematic, precision or random when there is no basis or standard to compare against.

If we can find a standard value or get a feel for a standard value (the real world value of that test) from the results then we can use an analysis of the standard deviation to help determine the type of error that is present in each result. Firstly the percentage error (difference) between the mean of the result under consideration and the "standard value" is found (based on the standard value being 100%). The standard deviation of the result under consideration is then found and the difference between the "standard value" and the mean of the result in terms of number of standard deviations is calculated:

$$number\ of\ stnd.\ deviations = \frac{mean\ of\ result - "stnd.value"}{\sigma} \qquad (37)$$

If the standard value is more than 2 or 3 standard deviations away from the mean of the result then the error is mainly systematic. Specifically if it is 1 standard deviation away then there is a 68.3% chance the error is systematic rather than random, this increases to 95.4% at 2 standard deviations.

We can summarize the analysis below:

- Small % error, standard value within 1 or 2 σ: small, mainly random errors
- Small % error, standard value not within 3 σ: small, mainly systematic errors
- Large % error, standard value within 1 or 2 σ: large, mainly random errors
- Large % error, standard value not within 3 σ: large, mainly systematic errors

11.4.2 Standard Error

The standard error takes the analysis of random errors one stage further; it is a measure of the precision of the estimate of the mean related to the original measurements. The more measurements upon which the mean is based the more accurate its estimation is.

The standard error is found from the standard deviation and the number of measurements used to find the average by using the following formula:

$$S\tan dard\ error = \frac{stnd.\ dev.}{\sqrt{no.\ of\ measurements}} \qquad (38)$$

Where applicable the average of the results is quoted with the standard error and the number of measurements on which the standard error is based, in the form:

Value ± *standard error* (mean, ± s.e.; n = *number of measurements*)

The standard error can be used to find the standard deviation of the sample set simply by multiplying by the square of the number of measurements. The standard error also allows us to calculate the confidence limits of the mean by using standard t-table values. The t-tables were used to find the 95% confidence limits (in other words the ± range within which the mean of another set of measurements of the variable would fall 95% of the time). As the majority of the results in this report are based on 2 or 3 measurements (and in a very few cases 4 or 5) the t-table values needed to multiply the standard error to find the confidence limits are:

- 2 measurements t = 12.71
- 3 measurements t = 4.3
- 4 measurements t = 3.18
- 5 measurements t = 2.78

Where a variable was measured and only one useful data point was collected then it is not possible to allocate confidence limits and just the data point by itself will be plotted.

11.4.3 Combining errors using quadrature

Usually, errors are probabilistic. This means that the actual value of a parameter is probably within a specified range. When combining measurements we want the error in the combination to preserve this probability. If you subtract 2 measurements to find the mass of material the true ultimate range of possible value would be the calculated value ± the total of the errors. But this assumes the very unlikely scenario that the quoted result might be the combined value either the lowest possible value of the low end with the highest possible value at the high end or the highest possible value at the low end and the lowest possible value at the high end. Obviously this is not very likely so instead of simply adding the absolute errors they are more correctly combined in quadrature, thus keeping the range in which the result will probably be.

For example when determining the binder content the mass of original granules is found by weighing the empty crucible (W_6) (which has an error of ± 0.001 grams) then adding the granules and finding the combined weight of the crucible and granules (W_7) (which has an error of ± 0.001 grams). The mass of the granules is thus $W_7 - W_6$. If the masses were 10.000g and 5.000g respectively then the mass of granules would be 5.000g. The absolute highest possible value would be 5.002g and the absolute lowest value would be 4.998g suggesting that a quoted result should be 5.000 ± 0.002g, but this is not very likely and should only be used to test if a series of results are possible or not (as opposed to probable or not). It is far better to quote the result by combining the errors using quadrature which will give the range over which the value is probably going to be. In this

case because it is simple subtraction then rule 2 (below) of combining errors implies the error is:

$error = \sqrt{0.001^2 + 0.001^2}$ = 0.001

Thus using the rules of combining errors using quadrature the correct (probable) precision error for the mass of granules would be 5.000 ± 0.001g.

The quadrature of a set of values (errors) is the square root of the sum of the squares:

$$= \sqrt{a^2 + b^2 + c^2} \quad (39)$$

For the simple combinations of the raw data in this report there are 3 standard rules that are applied to find the correct probable error. Δ_x, Δ_y, Δ_z will stand for the errors in precision of x, y and z. These rules assume x and y are independent of each other.

1. Addition and Subtraction

   If $z = x + y$ or $z = x - y$

   Then $\Delta z = \sqrt{\Delta x^2 + \Delta y^2}$ (40)

   (the error in z is the quadrature of the errors in x and y)

2. Multiplication and Division

   If $z = x*y$ or $z = x \div y$

   Then $\frac{\Delta z}{z} = \sqrt{\left(\frac{\Delta x}{x}\right)^2 + \left(\frac{\Delta y}{y}\right)^2}$ (41)

   (the fractional error in z is the quadrature of the fractional errors in x and y)

3. Raising to a Power

   If $z = x^n$

Then $\Delta z = n x^{(n-1)} \Delta x$ or equivalently => $\frac{\Delta z}{z} = n \frac{\Delta x}{x}$ (42)

The overall precision error for results that are found from the combination of several measurements have to be found by carefully combining and applying these 3 rules of quadrature. The precision errors for each measurement are found individually and then combined in a stepwise manner using these rules in the same sequence that the measurements are combined to find the result.

11.5 Accuracy of Test procedures

This section describes the accuracy of the experimental test procedures and how non-quantifiable errors might affect the data collected and the results derived.

11.5.1 Sieving

The sieving of the granules is the preparation stage for the other tests, it is not really a test but the procedure has some errors associated with it. The purpose of the sieving is to split the sample of granules into a variety of size cuts with a large enough quantity of powder being collected for each sieve cut to allow further testing. The sieves used to collect the size cuts were 63μm, 106μm, 212μm, 300μm and 355μm sieves as well as the base collector (< 63μm).

There are 3 major problems with sieving granules in order to split them into size cuts.

- Sliming of the mesh
- Aggregation of very small granules and ungranulated primary particles
- Breakage of weak granules due to mechanical agitation

Sliming of the mesh occurs at small sieve sizes (212μm sieves and below) and is due to small particles getting stuck in the holes in the mesh and preventing other smaller particles from falling through and into the sieve cut in which they belong. The error associated with this is that a prepared sample of a quoted sieve size 63-106μm, 106-212μm and 212-300μm will contain a portion of particles that are actually smaller than that sieve cut. This problem is dependent on the sieve size (for smaller sizes it is a larger problem), the nature of the granules and powder being sieved and the amount of material added to the sieves. To minimise the effect of sliming a small volume of granules is added to sieves for each sieving run, but this has to be balanced with the need to generate enough of a sample for further testing. As sieving was the limiting step (time-wise) in the critical path analysis there was a trade off between sliming and getting a large enough sample without contaminating it too much with small size particles.

As well as sliming, aggregation leads to smaller sized particles being present in a sieve cut than should really be there. The aggregation of the primary particles to each other and larger granules occurs because the sizes being used in this research are so small that they clump together and are attracted to larger granules, presumably by electrostatic forces. Some of the smaller granules are aggregated with the larger granules during the granule cooling process after the granules leave the high-shear granulator, if any granules are even slightly surface wet then they can aggregate together as the wet binder forms weak bridges between them as it cools and solidifies (these are not real granules and are not what I am trying to analyse in this research). To reduce the aggregation of primary particles to each other and the aggregation of granules forming weak bridges the sieving intensity needs to be increased or the sieving time increased. This will reduce the errors in the sieve cuts associated with retained particles of a smaller size than should actually be present, but there is the 2 problems associated with this; time is limited and increasing either the sieving time or intensity too much will lead to increased breakage of weak granules which leads onto the third major problem with sieving.

Mechanical agitation or extended sieving times will lead to breakage of weak granules, this means that the fragments of these breakages will possibly fall through the holes in the sieves and contaminate smaller sieve cuts. Also it means that the granules on a given sieve plate will have already had weak particles filtered out, the properties that are being measured in the subsequent tests are deemed to be very strength dependent or affect the strength of the granules. By losing granules that are weak from a particular sieve cut or having additional fragments of weak larger granules within a small sieve cut could possibly lead to errors in the relationships between granule properties being tested. The amount of error resulting from granule breakage in this form is unquantifiable, the only course of action is to reduce the sieving time and agitation but this has the effect of increasing errors due to sliming and unwanted aggregation. By examining the particles from several sieve cuts it is my belief that the set of conditions described in the sieving protocol minimise the combined effects of sliming, aggregation and breakage.

11.5.2 Granule Size Distribution (GSD)

The approach taken to find the Granule Size Distribution of the granules is not very robust. Because of the small sizes involved it is not possible to do the size analysis using just a single method or measuring machine; this is problematic because particle size analysis is renowned for its lack of consistency between measuring devices largely down to the fact that the size is generally inferred from some other particle property. The Camsizer, which was used for the large end of the size cut has a supposed lower measuring limit of 32μm, so it cannot measure the size and quantity of particles smaller than 63μm as this would include sizes smaller than its measuring limit. By using sieves to first separate the lower sizes out it is possible to produce an overall size distribution by converting the fraction below 63μm into a form useable with the output from the Camsizer.

This method is reasonably sensible as the sieves measure the size based on the projected area, as this is the area that will fall through the wire mesh on the sieve. The fact that the sieve is a physical process means that it is impossible for any particles larger than the wire mesh to be present in the base collector, in other words the particles in the base have to be less than 63μm (unless the sieve has been incorrectly made). It is possible that smaller particles are present in the upper sieve fractions (due to sliming and aggregation as described in section 11.5.1). The Camsizer also measures the size based on the projected area, it takes a photo of the image and converts the area of the projected shadow into a particle size. In both cases it is assumed that the particles are spherical in order to present sizes on a by volume or mass basis – thus they should be interact able.

However analysis of the data and conversion into size distributions shows that something is very wrong with the Camsizer. The Camsizer program for analysing the size and the selected sieve cuts and all the parameters are appropriate but the size distribution that it produces does not appear to be correct. This experimental method is not accurate (or at least in most of the cases).

Consider the data for the first test of Batch BN/04/01. The initial sieving produced a weight of 20.79grams of powder in the base collector and 25.277grams on the sieves of

size 63μm and above, this means that 45% by mass of the granules are less than 63μm. The remaining 55% was put through the Camsizer and produced the following data:

Upper Size	Fraction
0.071	0
0.08	0
0.09	0
0.1	0.0001
0.112	0.0001
0.125	0
0.14	0.0001
0.16	0.0001
0.18	0.0002
0.2	0.0005
0.224	0.0034
0.25	0.0082
0.28	0.0174
0.315	0.03
0.355	0.0645
0.4	0.1189
0.45	0.1635
0.5	0.1521
0.56	0.1337
0.63	0.0874
0.71	0.045
0.8	0.0438
0.9	0.0203
1	0.0077
1.12	0.0029
1.25	0.0093
1.4	0.0204
1.6	0.0197
1.8	0
2	0.0223
2.24	0.0284
2.5	0
2.8	0
3.15	0
3.55	0
4	0

This data shows that there are no particles between the size of 63 and 100μm and very little particles are present until it gets to over 300μm. When this exact same selection of particles was run through a collection of sieves of size 63, 106, 212, 300, 355, 425, 500

and 1000μm it was found that the physical quantities and numbers present on the sieves did not match, or come anywhere near, the size distributions found using the Camsizer. There were countless particles in the 212-300μm range, about 300 particles from 300-355, about 45 particles in the 355-425μm range, 20 in the 425-500μm range and less than 10 up to 1mm, No particles were present over 1mm (as the Camsizer indicated there should be). This is shown graphically in figure 44 below.

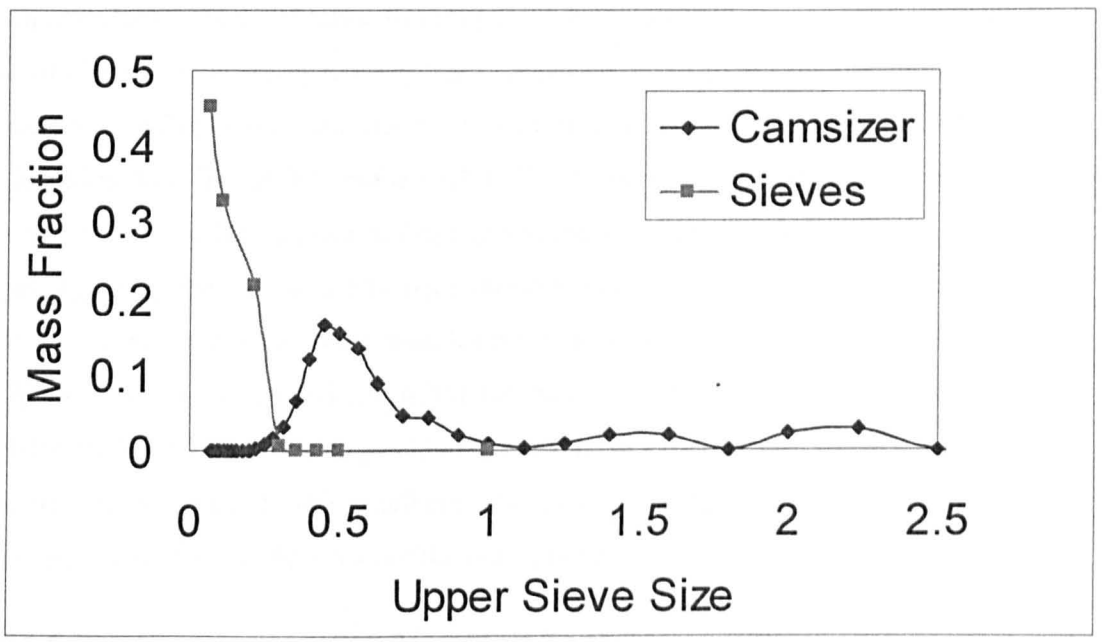

Figure 44 – Graph showing unreliable Camsizer data against actual data for same granule sample measured through sieves

The conclusion from this was that the Camsizer was not being used properly or that it was not accurate enough to deal with small particles in the approximate range 63-750μm. But about 10 of the Camsizer outputs did seem reasonable and produced nice shaped distributions; however the accuracy of these distributions is thrown into doubt because of the consistent failure of the Camsizer to pick up particles in the lower size range in over three quarters of the experiments that were run through it. It is my belief that this is a systematic error in the way the Camsizer was operated, because of the presence of small fines (due to sliming and aggregation in the sieving process) these would float about as they fall through the Camsizer and "stick" to both the glass screen and other particles – the result of particles sticking to the glass screen is that they will obscure areas of the

image taken by the Camera in the Camsizer and the computer program that analyses these images will believe they are larger particles or part of large particles. This problem was confirmed by running a very precise experiment where care was taken to keep the glass screen clear of fine powder build up – the results from this showed a much more realistic shaped curve from the same set of powder.

The results for the GSD taken from the Camsizer should be considered very carefully, it is not however necessary to completely disregard the GSD information as the fractional masses found by sieving are still very valid, and the following GSD's seem to have valid shaped curves: BN/04/XB and BN/04/X3B. The other curves are valid for comparing the relative size distribution within this experimental context, but they are not valid for getting a true feel for the actual sizes. Repetition of the experiments was not possible as GSD's were performed on the samples prior to sieving preparation and they were very time consuming, if full analysis of the results had been possible at the time of carrying them out it would have been possible to change the experimental procedure to ensure extra care was taken to stop small particle build-up on the glass screen – it is still not definite that this was the cause of the inaccuracies.

11.5.3 Accuracy of Abrasion Test

As already discussed in an earlier section the abrasion test adopted in this research is a new test procedure developed for testing the abrasion of microgranules. Part of the purpose of generating the data in this thesis is to test the accuracy of this abrasion test. The test is designed to determine if the abrasive wear in a substrate (Perspex in this case) is affected by the nature of the abrasive (granules in this case). The experiment is un-accurate if any abrasion caused by other means masks the abrasive wear caused by the granules. It is possible that wear is occurring due to the cloth counterbody that is used to hold the granules in place, but a test in the development stage suggested that this is not the case.

It was observed during the testing that the counterbody and cloth tend to push the abrasive particles (granules) to the front, back and sides of the counterbody and away

from the contact zone. Even particles that are initially trapped between the counterbody and the substrate tend to migrate towards the edges of the counterbody and come out of the contact. This is countered to a small extent by ensuring that a large amount of particles is piled up immediately beneath the counterbody when it is initially lowered onto the substrate, but this migration of particles happens within about 15 seconds of testing. Initial trials were stopped every 30 seconds to re-distribute the particles, the counter body was raised up and the particles pushed so that they were underneath it. This was not a satisfactory technique as it was impossible to judge how much of the particles had been re-distributed and whether it was done evenly, it was very time consuming and the timing of the whole experiment became very tricky (more than double the number of successful tests had to be thrown out due to stopping the rig at the wrong time or missing one of the sample plates for re-distribution. It was decided that to keep the repeatability of the experimental procedure the experiment would run for 5 minutes continuously without stopping to redistribute the granules.

There is no doubt that wear is taking place on the Perspex substrate using this technique and that this wear is due to the presence of the granules. The Perspex plates were examined before and after abrasion with and without granules; before abrasion there were no marks on the Perspex. After abrasion there were parallel grooves running in the direction of the counterbody motion, there were a lot more grooves and the grooves were deeper for abrasion tests using particles than those just using the cloth counterbody (as already mentioned the cloth counterbody on its own produced very little wear).

It is difficult to determine whether the fact that most of the particles are pushed out of the abrasive zone makes this test any less accurate for determining the abrasive wear of the particles. It is sensible that very small particles will not feel the applied load of the counterbody if the counterbody is being supported by larger particles, this would mean that the smaller particles would roll about and be free to escape the abrasive zone during the reciprocating motion. In this case all the abrasive wear would be occurring due to the larger particles. As these fail and fracture either the pressure would increase on the remaining particles leading to further fracture and further increasing the load, until

eventually a situation could be imagined where all the larger particles initially holding the counterbody away from the surface are fractured. In this case the fragments would then continue causing the wear, probably with increased wear characteristics as the fragments would be angular and we know that angular shapes cause more wear. But this might not be the case, the cloth counterbody might have enough "give" in it to hold the larger particles and at the same time hold smaller particles. Not enough is known about the motion of the particles between the counterbody and the substrate in this particular abrasion set-up to comment on this further and to try and make predictions on the wear mechanism, observations of the wear particles do however give us some insight.

Images of the granules taken using a microscope show that the granules are round, but rough before abrasion (figure 45). After abrasion the granules appear to be the same size as before abrasion, with no evidence of fractured granules, but they are much smoother and there is a massive increase in the number of very small angular particles within the oil (figure 46). This suggests that the abrasive particles are probably just rolling about and that the small particles are primary particles on the surface of the granules that are worn off by attrition or they were aggregated with the granules by weak bridges and the abrasive motion separated these bridges. Another possibility is that the granules that were observed in the microscope slides were not involved in the abrasive wear at all, that they were the granules that were pushed to the sides of the counterbody as described above. This is likely as visibly the number of particles outside of the counterbody is thousands of times more than the number remaining trapped underneath at the end of the test.

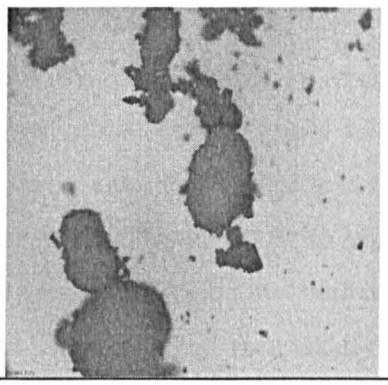

Figure 45 - showing granules before abrasion – note rough surface (x25 mag.)

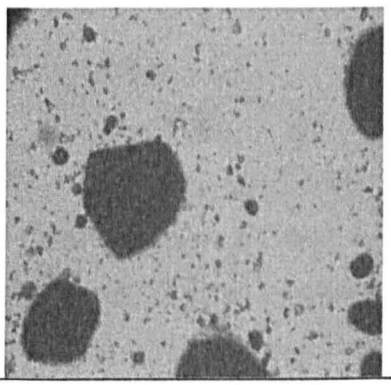

Figure 46 - showing granules after abrasion – note the smooth surface and lots of small particles (x25 mag.)

Both images were taken at x25 magnification, although shown not to scale the large granule in the centre of figure 46 is approximately 1mm in diameter.

Preliminary tests comparing the abrasivity of granules to the primary particles forming those granules showed that the primary particle powder on its own produced as much if not more wear than the granules, but these tests were not conclusive as 1 of the granule tests produced as much wear as the primary particles and 1 of the powder tests produced as little wear as the granules. As there were only 2 successful granule tests (in the preliminary testing) it is hard to say whether the low or high abrasive wear is typical of granules, but tests with another material show the same sort of trends; wear being roughly equal for granules and their primary particles with the exception of 1 anomalous result for both the powder and granules in which the abrasive wear was much lower.

11.5.4 Accuracy of Profilometry Test

The profilometry test is the second test that has to be performed in order to find the abrasivity of the granules. Once a Perspex sample plate has been abraded using the abrasion rig then it is cleaned and run through a Dektak profilometer. The profilometer works by running a microscopic probe tip over the surface of the Perspex and recording the vertical displacement at regular intervals. These vertical displacements are then presented graphically for manipulation using the Dektak software before being exported as data to an excel spreadsheet.

As it was observed that the wear scars caused by the abrasion tend to run nearly the full length of the exposed strip it was deemed necessary to take only 3 x-sectional profiles of the wear scar, the first being in the middle and the next 2 being about 5mm above and below this. This was done to ensure that the profiles were all comparable, that they were measuring the region that was continuously under the abrading counterbody. If the 2^{nd} and 3^{rd} profiles had been taken near the extremes of the exposed strip then it would not be representative of the wear as in these regions the Perspex is not feeling the presence of the abrading particles and the counterbody continuously during the abrasion experiment due to the reciprocating motion of the abrasion rig. This was what was supposed to happen, but due to difficulty in visually identifying suitable start points for the profile and lack of awareness of this issue by some of the people performing this experiment I do not believe that all the measurements consistently measured the profile in this central zone.

The sample preparation stage is a possible source of error, as the sellotape forming the sides of the exposed strip need to be removed and all the gum thoroughly cleaned off this step has the possibility of scratching the surface further and making deeper wear scars. Alternatively if not all the gum was removed it could clog the probe tip (this wasn't believed to have happened as great care was taken to clean the sample thoroughly). Another problem with the cleaning was that the soap used to remove the gum also removed the permanent marker that was used to label each sample plate. Only results that could be accurately identified and traced were recorded.

As the profiles were to be converted into a wear area for comparison they needed to be standardised. It is not possible to ensure that the sellotape strips are exactly the same distance apart (to the degree of precision required to not mask the wear profile) so the section of the wear profile measured to obtain the abrasive wear was not taken across the whole of the exposed section. To ensure that the same length of section was analysed each time the profile used to calculate the wear area was taken as the area starting at the 1000^{th} data point and ending at the 4000^{th} data point, these were chosen because in all tests they fell within the wear scar.

A serious problem with this method is the way the Dektak collects and reports the data. Because the sample table onto which the sample is placed is not correctly aligned (and very difficult to do so) the data needs to be re-aligned once it is collected. Essentially this means that the profile that is initially produced by the Dektak looks like a diagonal slope with lots of little troughs in it, this diagonal slope needs to be made horizontal by manually selecting two datum points on the slope and making the line between them the zero datum. This process is very tricky and user dependent, it cannot be automated and introduces the possibility of unquantifiable errors in the wear profiles. It is more accurate if the datum points are selected on either side of the wear scar (this was obvious when you examined the majority of profiles). For profiles with very little wear or wider than normal wear scars this was not as easy.

If the direction of travel of the probe tip is not aligned exactly perpendicular with the wear scar then it will produce an incorrect wear profile and subsequently the calculated abrasivity will be wrong. This is because the greater the angle the greater the influence of individual wear grooves on the overall profile calculated, so if there is 1 especially large or especially small groove within the profile then it will throw the overall calculated wear in that direction (relatively greater wear for large grooves, relatively smaller wear for small grooves). It is worth noting that if the wear grooves within a wear scar are all exactly the same width and depth then changing the angle by a few degrees will make no difference (except to the start point of the calculation).

11.5.5 Accuracy of Static Strength Test

To find the static strength of granules and particles they are generally crushed under uni-axial compression and the force at failure combined with the particle size used to calculate the static strength. Unfortunately because the particles being investigated in this research are so small it is not possible to isolate them individually and perform individual crushing tests. Therefore tests had to be performed on multiple granules.

The test procedure was based on work by Adams, et al., [85]. The theory requires that the stress-strain curve for the behaviour of the granules during crushing is measured and the

initial curve analysed. Granules are put into a crushing pot of dimensions such that the diameter is large compared to the depth; this is so that the wall-particle frictional forces do not have a significant effect on the results. By tapping the granules before the crushing test begins the majority of compression due to rearrangement will have occurred, continued rearrangement and packing will take place in the initial stages of the test and this is accounted for by using the linear region of the stress-strain curve (not the initial section). It is assumed that once the packing has finished that the granules will start to take up the load, as granules fail the number of load bearing granules will change and should increase as new granules take up the load in compression.

After running the tests it was not obvious that any crushing or failure of the granules had occurred at all, because the granules were so small it was impossible to see if failure had occurred – the theory uses the initial stages of the stress-strain curve (after rearrangement) to derive the effective strength of the granules and in this region very few of the granules will have failed. When taken to extreme loads the granules did eventually fail in bulk, but the graphical data is meaningless at this level of compression and cannot be used to find the static strength. The theory indicates that an effective crushing strength, *Fcalc*, is found from the multiple crushing and that single granule crushing on the same material needs to be done in order to find the conversion factor from the multiple crushing value to an individual static strength. However as individual crushing was not possible on the samples used in this report this conversion was not possible and all static strength values have been reported as the multiple granule crushing strength, *Fcalc*. This does not make the experiment inaccurate as these values can easily be compared to each other to find the relative strengths of the granules and allow trends of strength-other granule property to be analysed.

11.5.6 Accuracy of Binder Content (and Moisture Content)

It was assumed that the moisture content was constant for the majority of the tests that were conducted, this was because the majority of the tests were conducted over 2 months in the summer and initial trials to see if the moisture content of the granules changed

because of moisture in the air revealed that there was no difference between a rainy day and bright sunny day.
The essence of the binder content and moisture content experiments is to use thermo gravimetric techniques. In other words to weigh a sample, burn it in an oven to remove either the moisture or the binder and then reweigh the contents and calculate the binder / moisture content by mass loss.

A section in appendix F highlights a problem with the experimental protocol for finding the binder content. At 600 °C there is some degradation of the Calcium Carbonate and when it is mixed with PEG binder the mass loss is increased, probably due to carry out of fines with the PEG vapours. Granules made with zeolite cannot be assessed using this technique as the zeolite degrades significantly at 600 °C. No alternative temperatures were tested to find their suitability as this problem was not realised until late into the research and it was decided that the degradation and carry-out are fairly small only equating to a few % at most. This causes a systematic error in the reported binder contents, the real values are all slightly lower than the values that are quoted.

11.5.7 Accuracy of Porosity Bottle Test

The porosity bottle test actually uses Density bottles to find the density of the granules and then by combination with the results of the binder content experiments it is possible to calculate the porosity. A series of trials were run using the density bottles, by other researchers within the department, to find the most accurate and it was found that the calibration of the volume of one of the bottles was incorrect. It is believed that the other bottles that were actually used for the tests were accurate in this respect.

It was hoped that the porosity of the granules would be found using the density bottles and the results compared to a control tested using mercury porosimetry and helium pycnometry. However these supposedly more accurate techniques for finding the porosity were not applicable to the granules produced for this research due to the varied nature of the granules, it was not possible to determine the transition from inter-granular pores to intra-granular pores. The density bottle results had to be taken as the porosity values of

the granules. Tests conducted within the department have found that the results obtained from the density bottles vary a great deal within a given batch of granules, whether this is a result of the experimental method or a true physical phenomenon of the granules is unclear. Poor repeatability in the experiments might be due to incomplete wetting of the granules in the bottom of the density bottles, this would mean that air pockets would remain present and the calculated porosity would be higher than the real porosity. Care had to be taken to ensure the granules are sufficiently agitated to release any trapped air. It is not believed that the oil will penetrate into the intra-granular pores due to the pores being too small, the granules are very dense due to be made using a high-shear granulator (microscope analysis does not show any surface pores). The limiting pore size that oil would penetrate into for the temperatures and pressures used has not been calculated, it is not believed to be important as the surface chemistry (and thus wetting characteristics) of all the granules is similar and so the limiting size will be the same on all granules. This would only be an issue if a sample of granules had lots of surface open pores of a size larger than this limiting size. This would mean that a granule that was porous in reality would actually appear less porous as the oil would occupy the pores.

The calculation method used to find the porosity ignores the moisture content of the granules, but instead combines the mass loss due to moisture evaporation into the mass loss due to PEG being burnt off. This means that the mass of PEG used in the calculations will be 0.78% (by mass) higher than it really is. However, this is not likely to make very much difference as the density of PEG, 1.093 g/cm^3 is very similar to water, $\approx$1 g/cm^3, so the actual volume change will be very small. What this means is the calculated volume of PEG will be slightly lower than reality, thus the calculated volume of pore space in the granule will be slightly higher than reality so the quoted values of the porosity will be slightly higher than reality. This moisture is likely to be mostly surface moisture so as it is taken into account as a volume of the PEG it will be increasing the porosity relative to reality. The overall effect of this is that the small amount of moisture content will make a very small difference to the systematic error of the calculated porosity. Another advantage of ignoring the moisture in this way is that the error in the moisture estimate is not carried into the precision accuracy of the Porosity calculations.

11.6 Errors in the Results

11.6.1 Method used to find the error

To find the error in the results the following general procedure was used:

1. Find the raw data (which produces the results in the database)
2. Determine the precision in the raw data
3. If raw data is combined (summed, multiplied, powered or averaged) then apply the appropriate quadrature / error rule to find the precision error in the results.
4. Find the mean of the results
5. If all the results fall within ± (1 x the precision error) of the mean then the error is quoted as (mean ± p.e.) ;this means that the results are not limited due to the randomness of the nature of the variables or the accuracy of the experimental set-up but limited by the randomness generated in the precision of the measuring instruments.
6. If any of the results are further from the mean than 1 x precision error then: Find the standard deviation in the repetition of the results of a single test for a given variable from a single batch (this will usually be 1, 2 or 3, but sometimes 4 or 5 results)
7. Find the standard error and quote the results as (mean ± s.e., no. of measurements)
8. Calculate the 95% confidence limit using the standard error and the appropriate t-table value
9. Plot the mean of the results with the 95% confidence limits (or the precision error) whichever is applicable for each step in the variable
10. Attempt to estimate a standard value and trends from the shape of the curve to enable the analysis of whether any individual result is systematic, precision or random.

11.6.2 Error in the Granule Size Distribution (GSD)

It is not possible to calculate the errors in the graphical representation of the GSD's, and inaccuracies in the experiment due to the Camsizer have already been mentioned. But the values of Mean (X_{50}), X_{10} and X_{90} are taken from the cumulative undersize graphs, the

error is thus in the precision to which these can be read from the graph combined with a feel for the width of the sieve cuts that were used to produce the graphs. It is felt that the likely plausible error is ± 50μm, but more likely to be about ± 25μm.

The mode size is quoted as the sieve cut below which the mode exists; this is because for the vast majority of the samples the mode size is below 63μm, which is the lowest sized sieve cut. It is thus impossible to say at what point between 0 and 63 the mode exists and it is wrong to quote the mid-point.

11.6.3 Error in the Abrasive Wear

The profiles taken using the Dektak are measured in linear data steps of approximately 7814 nanometres. The depth of the profiles is quoted to 1 nanometre, but it is not clear that this is the precision to which the machine is capable of measuring. As already mentioned in the discussion about the accuracy of the experiment the problem of setting the datum and ensuring the profile is taken perfectly perpendicular to the wear scar mean that the precision will never be this low, as variations in the chosen position of the datum can make depth values fluctuate.

When the wear profile is not very deep it is even harder to determine the datum and so some of the values of the profiles come out as positive, this is no good for calculating the wear as when they are integrated the positive quantities will reduce the negative wear material. To counter this all positive wear values were rounded to zero, this is justified because if the material is pushed upwards out of a wear track then the edges will be raised – if they were considered it would be as if the material had not been worn at all.

In essence it is not possible to accurately determine the precision of the wear profiles so I have decided to hang an error onto the calculated values which takes into account the feel of trying to get the datum level and its effect on the profile. It is likely that the datum could fluctuate by as much as 25μm up or down and so this is taken as the depth variance, but if it is applied across the whole width (3000 points from the 1000^{th} to the 4000^{th}) then it equates to a precision in the calculated wear of ± 586μm.

For each value of average abrasive wear for a given batch there are typically 2 to 3 abrasion tests and each of these abrasion tests will have 2 to 3 profiles taken across them. Calculations for the standard deviation from just 2 or 3 values is not very valid, but as we have lots of tests we can find the average standard deviation and also an average standard error (this is not strictly a correct method but gives a feel for the actual values rather than quoting about 30 different standard errors.)

The average value for the standard deviation in the measured profiles of single Perspex abrasion test samples is: ± 45560 um^2 this gives an average standard error of 26875 on a basis of 2.9 measurements (numbers of the measurements were averaged in order to find the standard error from the average standard deviation).

When these measured profiles are combined with the average wear from profiles taken from other Perspex Plate abrasion tests the average standard deviation in the average wear is ± 68926 um^2, the standard deviation in the results is on average 56% of the value of the average wear. That is to say for a wear of 100000 um^2 the standard deviation would be ± 56000 um^2, the average standard error is 27798um^2 based on 6 measurements. So with 95% confidence limits this has a t-value of 2.45, this means that a series of wear readings based on my experimental procedure and these results of 100000 um^2 has a lower limit of 32000 um^2 and an upper limit of 168000 um^2. This is the range in which 95% of the average values of the wear would fall.

It is safe to say that the random errors associated with the experimental technique are far larger than the precision errors of the instrument and the calculations. It is not possible to determine if there is systematic errors associated with this as there is not a standard value or a series to put into a trend in order to estimate the standard value.

11.6.4 Error in the Static Strength

The static strength was measured using the Zwick compression tester with a 500N load cell. The Zwick compression tester had a drive system resolution of 0.226μm with a positioning of ± 0.5μm (repetition accuracy – reversal). It is not clear what this means but it is assumed that whatever the reading on the gauge it is accurate to ± 0.226μm when driven in a single direction, and that upon reversal the reading becomes accurate to ±

0.5μm. As the measurement for the initial bed height and the subsequent height are in a singular direction then the error is just ± 0.226μm as the machine will measure any error in the same direction (unlike a human reading a ruler – who would add the precision error at both ends.) The load cell is quoted as having an accuracy of ±0.4% of the nominal value or ± 2N. This is taken to mean that the reading is accurate to ±0.4%, as strain gauges are progressive resistance measuring devices.

It is not possible to calculate the effects of these errors on the overall result by the simple method explained in section 11.6.1 as the final determined value of F_{calc} is found by an iterative process automated by Excel. However in order to guess at the likely value of the error the effects of these precisions were investigated for the strength measurements of BN/04/X11A sieve cut 106-212μm second run of measurements (this was chosen at random from the set of successful measurements and was accepted as the shape of the stress-strain graph matched the desired shape discussed in original paper by Adams, et al., [85] on which the multiple granule compression testing was based.)
The value of the initial bed height was altered by a value of – and + 0.266μm and the load was altered by – and + 0.4%, the effect on the F_{calc} was found with and without the iterative process.
The original value of F_{calc} was 4520000 and the highest value from the possibilities due to precision was 4547000 (lower bed height reading and a higher load reading combined with iteration) and the lowest possible value was 4507000 (lower bed height and lower load without iteration). This equates to a maximum error of ± 0.6%.
However, as the determination of F_{calc} is largely effected by the chosen position of the linear section of the graph and this is open to human interpretation and will vary from person to person (and even within a single graph if it is repeated) it was decided that the same data points would be used each time to allow comparison (and speed up the calculation process as by using fixed points the process could be easily automated). By moving the data points over which the gradient of the slope is calculated by 10% results in a variation in the final F_{calc} of 3.2%. This means that the error in F_{calc} can be as much as 5 times greater as a result of picking the wrong data points than the error caused by the precision of the machine measuring the compressive load and compressive strain. This

also highlights the problem with assuming that the last 10% of data points collected are the most appropriate – the actual error in comparing two values of F_{calc} from 2 separate experiments is unquantifiable. It is assumed it is larger than the 3.2% error in the variation of 1 experiment on its own and thus an error of 4.5% is hung on the quoted values of F_{calc} to allow for comparisons (3.2% / $\sqrt{2}$) – the square root of 2 was used on the denominator because dividing by the root of the number of observations combined in an error is the accepted method of finding the likely error, and as the F_{calc} has to be used relatively then the minimum number of observations has to be 2 determined values of F_{calc}.

11.6.5 Error in the Moisture Content

The moisture content is found using the equation:

$$Moisture = \frac{W_{11} - W_{12}}{W_{11} - W_{10}} \times 100\% \qquad (34)$$

The precision error in the weight measurements, W_{10}, W_{11}, and W_{12}, are all accurate to 3 d.p. (this is a hung error on the scales due to fluctuations). So in terms of a value the precision is ± 0.0005 g.

To find the overall precision error the individual errors are combined in quadrature.

Error in the top line is:

$$\sqrt{0.0005^2 + 0.0005^2} = 0.000707$$

Error in the bottom line is:

$$\sqrt{0.0005^2 + 0.0005^2} = 0.000707$$

The error in the individual moisture content values is then found using the rules of quadrature for dividing values, i.e. the fractional error of the top and bottom is used to give the fractional error in the moisture content, and the absolute error in a single calculated moisture content is given by:

$$MoistureCalc \times \sqrt{\left(\frac{0.000707}{W11-W12}\right)^2+\left(\frac{0.000707}{W11-W10}\right)^2} \qquad (43)$$

For the range of moisture contents that were used to calculate the average moisture content the range of errors was from ± 0.0167% to ± 0.0459% (these are percentage moisture in the granule not percentage error in the quoted value) with typical values being around ± 0.003%

The error on the quoted average of the moisture content is found by using quadrature rules of summation and division on the individual errors making up the average, this was done on an automated excel spreadsheet. Note: The division rule could be ignored as the number that is being divided by is a constant number not a variable (the number of terms being averaged).

$$\text{Error in average} = \sqrt{(err_1)^2+(err_2)^2+.....+(err_n)^2} \qquad (44)$$

As the average moisture content was based on 17 values the n-terms is 17, this gave an overall precision error in the quoted average moisture value of ± 0.1212%

So the average moisture content of the granules quoted has a value of 0.78% moisture by mass, precise to ± 0.1212% moisture by mass.

BUT, the measured values of the moisture do not fall within 1 x precision error, this means that the results are not limited by the precision of the weighing scales but by the random spread of moisture contents within the granules. The standard deviation of the values used to find the average moisture content is 1.19. This is based on 17 results so the error is quoted as the standard error:

Moisture content is 0.78% ± 0.2884% ; n = 17

In order to calculate the error in the binder content calculation (and subsequently the error in porosity) the appropriate error needs to be chosen for the moisture content. For combining errors you should use the larger of the precision error and the standard deviation, thus the error in the moisture content in these other dependent tests is 0.78 ± 1.19 percent by mass. (This means that the value of the moisture content can be negative when the error is taken into account; this is impossible as there is no physical meaning to negative moisture content in a granule. This large error in the moisture content could possibly explain why some of the calculated porosity values come out negative, because the error is carried through)

11.6.6 Error in the Binder Content

The binder content is found by using the equation:

$$Binder = \left(\frac{W_7 - W_9}{W_7 - W_6} \times 100\% \right) - moisture\% \qquad (32)$$

The precision error in the weight measurements, W_6, W_7, and W_9, are all accurate to 3 d.p. (this is a hung error on the scales due to fluctuations). So in terms of a value the precision is ± 0.0005 g.

To find the overall precision error the individual errors are combined in quadrature. The error in the left hand term needs to be found and combined with the error for the moisture found in section 11.6.5. The left-hand term combines is the total binder content and moisture content.

Error in the top line of left-hand term of eqn 32 is:

$\sqrt{0.0005^2 + 0.0005^2}$ = 0.000707

Error in the bottom line of left-hand term of eqn 32 is:

$\sqrt{0.0005^2 + 0.0005^2}$ = 0.000707

The error in the individual total content values (left-hand term) is then found using the rules of quadrature for dividing values, i.e. the fractional error of the top and bottom is

used to give the fractional error in the left-hand term, and the absolute error in a single calculated value of the total content is given by:

$$Total\ Binder\ and\ Moisture\ Calc \times \sqrt{\left(\frac{0.000707}{W7-W9}\right)^2 + \left(\frac{0.000707}{W7-W6}\right)^2} \quad (45)$$

These error terms are then combined with the error from the moisture content using quadrature as follows:

$$Total\ precision\ error = \sqrt{(error\ l.h.\ term)^2 + (1.1893)^2} \quad (46)$$

Note – the standard deviation error is used from the moisture error as this is the largest of the random error and precision error.

Each of the calculated binder contents will have a different precision error because of the way in which the errors are based on the absolute calculated value of the left-hand term when they are combined in quadrature for terms that are divided. The average precision error in the Binder Content is ± 1.1941%, with a maximum precision error of ± 1.2564% and a minimum precision error of ± 1.1898 %. When this total error is compared to the contribution from the error in the moisture content it is clear that the majority of the precision error in the Binder Content is as a direct result of the errors in the moisture content.

To find the standard deviation, the random error due to the properties of the granules, the standard deviation should really have been calculated for every set of granules and quoted individually for each set. This is because the standard deviation in the results for binder content of granules sized 106-212um in batch BN/04/01 will be different from granules sized 106-212um from BN/04/X2. As the majority of the sets of results for a given size cut from a given granule batch only have 2 results it is fairly meaningless to try to take the standard deviations and try to get a feel for the average standard deviation. Thus 6 different sets of size cut and batch number combinations with 3 or more results for their binder contents were chosen at random to find their standard deviations. The standard

deviation in the Binder Content varied from 0.05398 to 7.5262 (but this last value was caused by 2 extreme results). The estimate of the standard deviation of the binder content is based on the average of these 6 standard deviations and is ± 1.42% which has it own standard deviation of 2.9991 (this is the standard deviation in the estimate of the random error). If we use this estimate of the random error (which is quite rough) then we can say that the estimated error in the Binder Content is random and is ± 1.42%.

It is not appropriate to quote the error as standard error in this case as the quoted random error is itself an estimate and does not use the entire population of binder content values.

What this error analysis does show is that the error in the Binder Content is attributable more to the randomness in the properties of the granules rather than the error in the precision caused by carrying through a large error due to the randomness in the moisture contents. In other words it is justified to use the average moisture content of 0.78%

11.6.7 Error in the Porosity

The porosity is found by combining measurements from the density bottles with the calculated Binder Content, so the error from the Binder Content tests will be carried through into the precision of the porosity calculations.

The porosity is found by using the equation:

$$\varepsilon = 1 - \left[\frac{1}{\rho_{pp}}(w_9 - w_6) + \frac{1}{\rho_b}(w_7 - w_9) \right] \left[\frac{w_2 - w_1}{(w_7 - w_6)\left(25 - \frac{(w_4 - w_2)}{0.9148}\right)} \right] \qquad (47)$$

The precision error in the weight measurements, W_1, W_2, W_4, W_6, W_7 and W_9 are all accurate to 3 d.p. (this is a hung error on the scales due to fluctuations). So in terms of a value the precision is ± 0.0005 g.

The precision in the numerical values for the densities, ρ_{pp}, and, ρ_b, and the value of the density of the oil, 0.9148, used in the calculations is not known and so ignored. The

precision in the accuracy of the quoted volume of the density bottle, 25ml, is estimated at 1% equating to ± 0.25cm^3.

To find the overall precision error the individual errors are combined in quadrature. In order to do this it needs to be done in stages as some of the errors need to be combined using their absolute values (where 2 values containing errors are added or subtracted) and some need to be combined using their fractional values (where 2 values containing errors are multiplied or divided). These stages in the error calculation are as follows (with the relevant equations from the stages in the porosity calculation on the r.h.s.):

$$\Delta_1 = \sqrt{(\Delta W2)^2 + (\Delta W1)^2} \qquad (48) \qquad : \qquad W_3 = W_2 - W_1 \qquad (49)$$

$$\Delta_2 = \sqrt{(\Delta W4)^2 + (\Delta W2)^2} \qquad (50) \qquad : \qquad W_5 = W_4 - W_2 \qquad (51)$$

Δ_3 = *error in bottle size* : estimated as 1% error = 0.25ml

$$\Delta_{Vo} = V_o \sqrt{\left(\frac{\Delta 2}{W_5}\right)^2} \qquad (52) \qquad : \qquad V_o = \frac{(W_5)}{\rho_{oil}} \qquad (53)$$

$$\Delta_4 = \sqrt{(\Delta 3)^2 + \left(\frac{V_o \Delta 2}{W_5}\right)^2} \qquad (54) \qquad : \qquad V_p = Vol_{bottle} - V_o \qquad (55)$$

$$\Delta_5 = \rho_p \times \sqrt{\left(\frac{\Delta 4}{V_p}\right)^2 + \left(\frac{\Delta 1}{W_3}\right)^2} \qquad (56) \qquad : \qquad \rho_p = \frac{W_3}{Vol_{bottle} - V_0} \qquad (57)$$

$$\Delta_6 = V_{pp}\sqrt{\left(\frac{0.000707}{W9-W6}\right)^2} \quad (58) \quad : \quad V_{pp} = \frac{W_9 - W_6}{\rho_{pp}} \quad (59)$$

$$\Delta_7 = V_b\sqrt{\left(\frac{0.000707}{W7-W9}\right)^2} \quad (60) \quad : \quad V_b = \frac{W_7 - W_9}{\rho_b} \quad (61)$$

$$\Delta_8 = \sqrt{(\Delta W7)^2 + (\Delta W6)^2} \quad (62) \quad : \quad W_8 = W_7 - W_6 \quad (63)$$

$$\Delta_9 = V_g \times \sqrt{\left(\frac{\Delta 5}{\rho_p}\right)^2 + \left(\frac{\Delta 8}{W8}\right)^2} \quad (64) \quad : \quad V_g = \frac{W_8}{\rho_p} \quad (65)$$

$$\Delta_{10} = \sqrt{(\Delta 9)^2 + (\Delta 6)^2 + (\Delta 7)^2} \quad (66) \quad : \quad Vol_{pores} = V_g - V_{pp} - V_b \quad (67)$$

$$\Delta_{11} = \varepsilon \times \sqrt{\left(\frac{\Delta 10}{Vg - Vpp - Vb}\right)^2 + \left(\frac{\Delta 9}{Vg}\right)^2} \quad \varepsilon = \frac{V_g - V_{pp} - V_b}{V_g} \quad \{(68)\} \quad (69)$$

As the precision in the weights W_1, W_2, W_4, W_6, W_7 and W_9 are all 0.0005 then the values of the errors Δ_1 Δ_2 and Δ_8 are all 0.000707.

The precision error, Δ_4 in the volume of powder calculated from the density bottles is ± 0.2501 cm^3.

When the precision error in the volume of the powder is used to calculate the precision error in the density, Δ_5, it is found to have an average precision error of ± 0.8894 g/cm^3 with a standard deviation in the error of 0.9730. The minimum and maximum errors are ± 0.0171 g/cm^3 and ± 4.5869 g/cm^3 respectively.

It was not possible to combine the individual values of the precision error, Δ_5, with their respective values in the subsequent binder contents results (due to difficulty in linking the data together) so the average error of 0.8894 was carried through.

The precision error in the volume of the $CaCO_3$ and Binder are ± 0.000262 and ± 0.000647 respectively. The error in the volume of the granules based on the average precision error for the density is variable with an average error of ± 0.2807 cm^3. Using actual precision errors in the volume of the granules and the errors in the volumes of $CaCO_3$ and Binder the overall precision error in the porosity was calculated. The equation for the porosity, Δ_{11}, uses the actual porosity in its calculation (but this gives negative errors in some cases, which is just as meaningless as the negative porosity values.) To find the average precision error in the porosity the absolute values of the precision errors were averaged, this gives a final average precision error for the porosity of ± 0.4055 with a standard deviation of 0.027.

The random error in the porosity values is more difficult to determine as there are not many values upon which to determine the standard deviation. The standard deviation for each batch of granules was determined (in most cases this was based on 2 values as only three batches of granules had enough data for 4 or more values of the calculated porosity). It was decided to ignore the sets only using 2 values as these were based on a single density bottle test and would not be truly representative of the random error caused by several density bottle tests. The following batches BN/04/01 (106-212), BN/04/11 (106-212) and BN/04/X2 (106-212) were used to calculate the average standard deviation in the spread of the porosity values. The standard deviations were 0.0907, 0.5336 and 0.001061 respectively. The average random error in the porosity is ± 0.2085 with a standard deviation in the estimate of the error of 0.2852.

From this analysis, and the differences between the porosity values of batches that only have two values, the precision error is more dominant than the random error. However there is not enough data to satisfactorily determine the random error.

The error in the porosity values is thus: ± 0.4055

This error is massive and swamps any differences between different sets of granules, which have calculated porosities of less than 1%. What this error says is that a granule that is calculated to have a porosity of 1% could plausibly actually have a porosity of 41% because of the precision of the measurements in the stages taken to find the porosity. This throws serious doubt onto the credibility of any of the relationships between properties and porosity. This would also explain why some researchers in the literature find contradictory results for strength to porosity relationships, especially if they have not followed such a rigorous analysis of the error.

11.6.8 Summary of Errors (estimated errors – rounded off)

Granule Size Distribution	=	? Undeterminable errors		
Abrasivity	=	Random error	=	± 68,000 μm^2
Strength	=	Precision error	=	± 4.5 (% of value)
Moisture = 0.78% by mass	=	Random error	=	± 1.19 % (by mass)
Binder Content	=	Random error	=	± 1.42 % (by mass)
Porosity	=	Precision error	=	± 40.55 % (by vol.)

Note: The errors for Moisture, Binder Content and Porosity are all absolute values by mass or volume of granule. The error for strength is a variable value; a percentage of the quoted value.

12 Results

The results database includes the data from the testing that was accurate, traceable and relevant to the batches produced using the High Shear Granulator. Because of the wide variety of testing and the subsequent analysis (data manipulation and averaging) a lot of effort was put into trying to get a first sweep of results, in other words at least 1 piece of data relevant to every required result / plot. There is very little repetition of results from the testing, this is for two reasons: firstly the complexity of the testing, secondly it was not possible to reproduce any of the batches of granules – none of the experimental recipe and processing combinations made 2 batches the same. Where an experiment was incorrectly carried out or a result could not be properly traced it was discarded before being added to the database. Other extreme high or low values are analysed statistically to determine their 95% confidence limits and thus the range over which their average value should fall if the test was repeated to determine whether any expected trend lines fall within this range.

12.1 Data for the plots

Enough data and results were generated to produce some form of most of the desired plots described in section 10.2.2, but not all these plots show anything useful. Only those plots that are meaningful or show anything useful (in terms of a trend existing / not existing or to show inaccuracies in an experimental method) are shown.
Most of the plots show averages of data; the data from individual batches is averaged, for example all the strength measurements for Batch BN/04/01 are averaged together to give a single strength value for plotting. The plots that were produced are shown in appendix I. Plots 1-39 (where data was available) are described in section 10.2.2. Plots 40 onwards show various other data and trends mostly from property to processing parameter relationships. The numbering of the plots is consistent with the description of desired plots given in section 10.2.2 and the queries used in the database (see data file on disk).

Plots where not enough data was recorded are not discussed.

12.1.1 Abrasivity versus Static Strength

Plot 1 shows the relationship between Abrasivity and Static strength. Each point represents the average of the average abrasive wears (from single abrasion plates) for a single batch against the average FCalc value for that batch. Only data for the size range

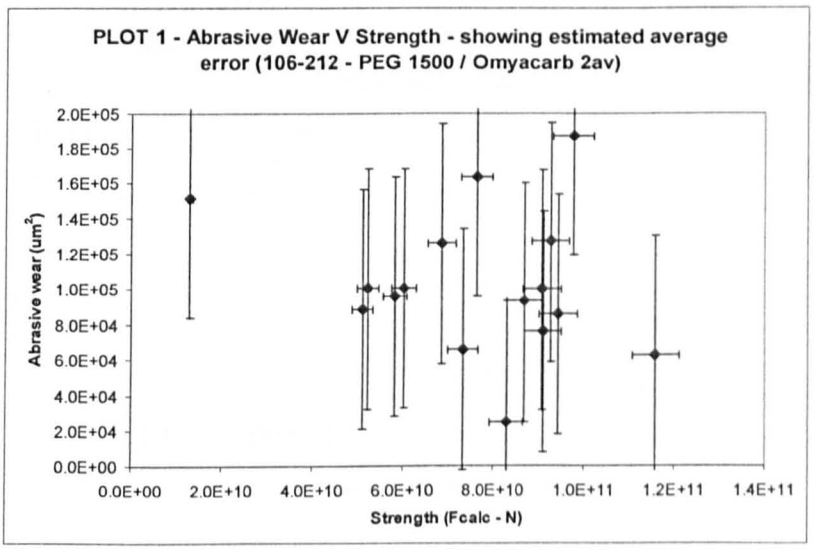

106-212 μm made from PEG 1500 and Omyacarb 2av is shown. This means that the granules are materially the same; so any change in the abrasivity is connected to the strength and not other variables. The different binder types and particle types will blur the strength values and maybe the abrasion values (as shown later).

The data is very scattered. There is no relationship between Abrasivity and static strength. The vertical error bars on the abrasive wear show the estimated average random error of ± 68,000 μm^2. The horizontal error bars on the strength show the estimated precision error as ± 4.5% of the value.

The strength quoted here is the strength of a structure, granule, and is the estimated load at failure (rather than a strength of the material which would be a stress, and would require a conversion factor on FCalc).

Plots 2 and 3 show the relationship between static strength and abrasivity for sizes 106-212um and 212-300um respectively. These plots include all the data, including batches made with different primary particles and binder.

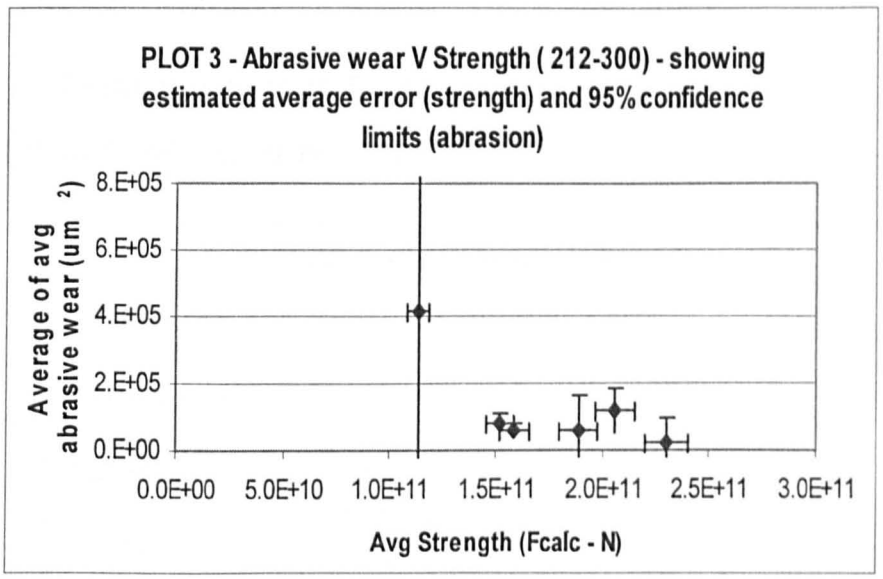

Plot 3 shows that when the 95% confidence limits are taken into account there is no trend between abrasivity and static strength for granules in the size range 212-300 μm. Plot 2 shows there is no trend between static strength and abrasivity for granules in the size range 106-212 μm.

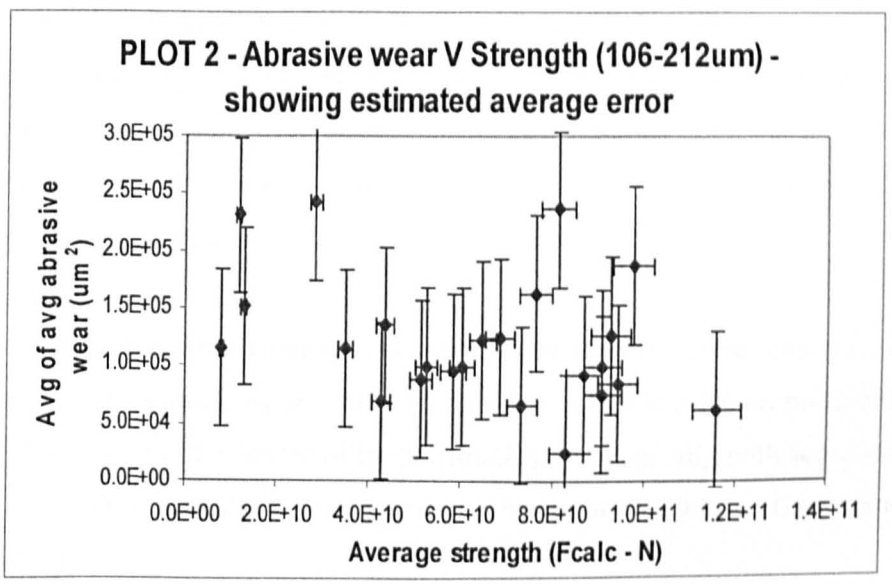

Ignoring the single point on Plot 3, that is possibly a statistical blip, there appears to be no change in the range of abrasivity as granules get stronger with size. If the single point is not a statistical blip, then difference between Plot 2 and 3 shows that smaller granules are less abrasive for a given strength.

12.1.2 Abrasivity versus Size

Plot 4 and 5 show the relationship between abrasivity and granule size.

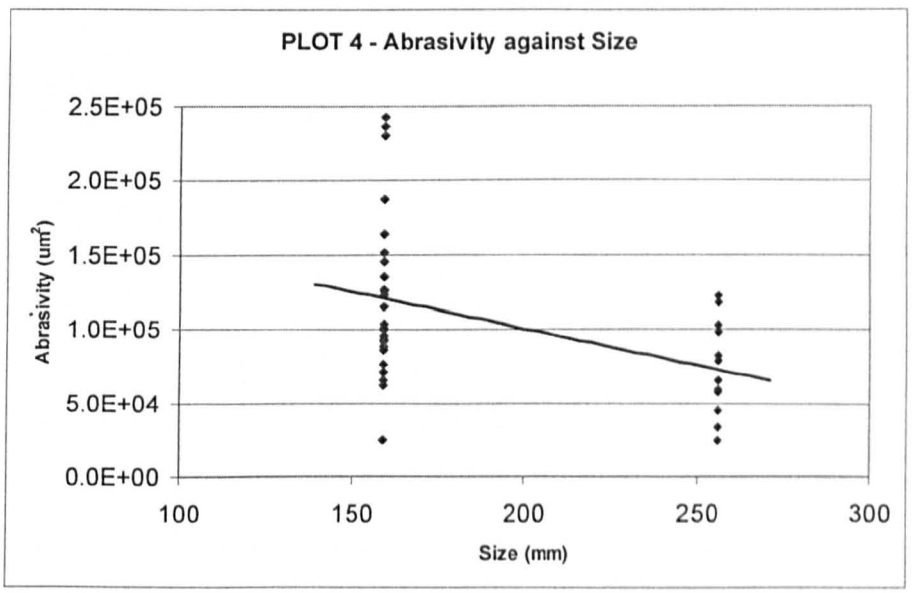

For granules taken from all batches in the size ranges 106-212 μm and 212-300 μm there is a trend for abrasivity to reduce with size (this is based on the average abrasivity of all granules at 106-212 and the average abrasivity of all granules in the cut 212-300). Individual error bars have not been added to Plot 4 as they obscure the information displayed by the data points.

When individual granule batches are considered over this size range (unfortunately only between two size values) they generally all conform to this indirect proportionality (11 out of 13 batches), but the degree of proportionality varies greatly with some granules showing direct proportionality. The error on the abrasivity means that these trends could be anomalous.

When batch BN/04/X3B is considered over a wider size range, Plot 5, there is no obvious relationship between size and abrasivity for size cuts 106-212, 212-300 and 300 -355 – the spread is easily accounted for by the errors in abrasivity. Granules in the size 63-106um are more abrasive and this is including the error.

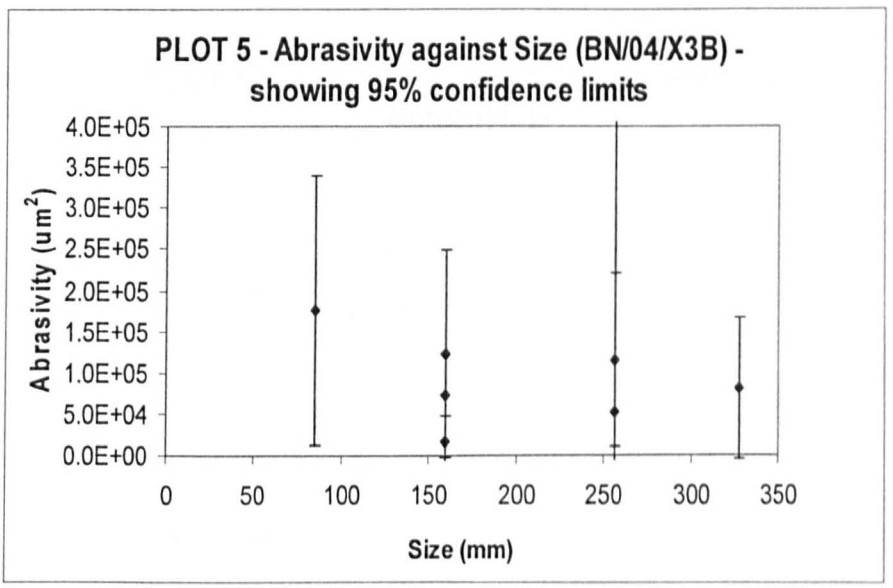

Statistically it is possible that no trend exists because the 95% confidence limits are so large. However the upper and lower bounds of the range in which the likelihood of a further data set would fall consistently decreases in value as the size gets larger, meaning that there is a trend for abrasivity to decrease with size. It also appears that the rate of decrease in abrasivity with size also decreases as the size increases.

12.1.3 Binder Content relationships

Plots 12 and 13 show there is no clear relationship between abrasivity and binder content of the final granules. Plot 12 includes granules from the size range 63-106 μm and 212-300 μm (it does not include error bars because they obscure too many of the data points).

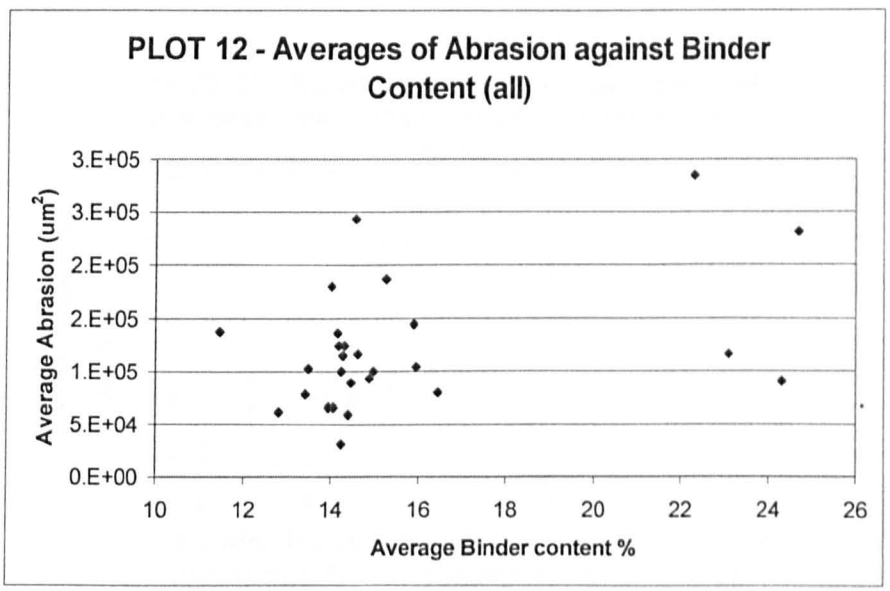

Plot 13 shows error bars showing the estimated average error in the abrasion and the binder content, although the error bars obscure a lot of the detail there is still no relationship between abrasion and binder content.

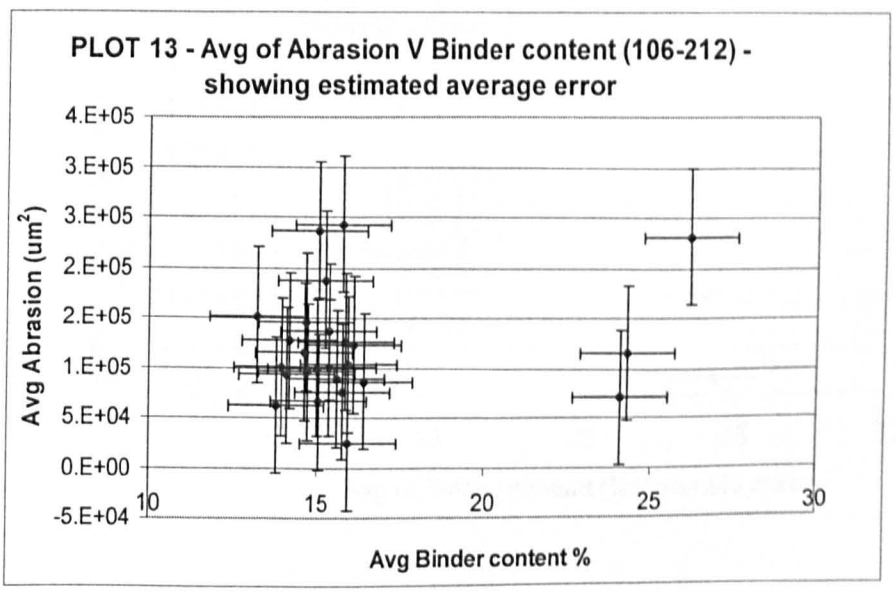

When the binder content of the final granules is plotted against the formulation parameter, binder ratio, we get the expected proportional relationship, Plot 52, however there are a few groups of results that have a standard deviation range that doesn't fall onto the trend line. These results could be because of errors in the measurements of the binder content (because not enough successful data was collected) or because of a real variation in binder content with granule size within those batches.

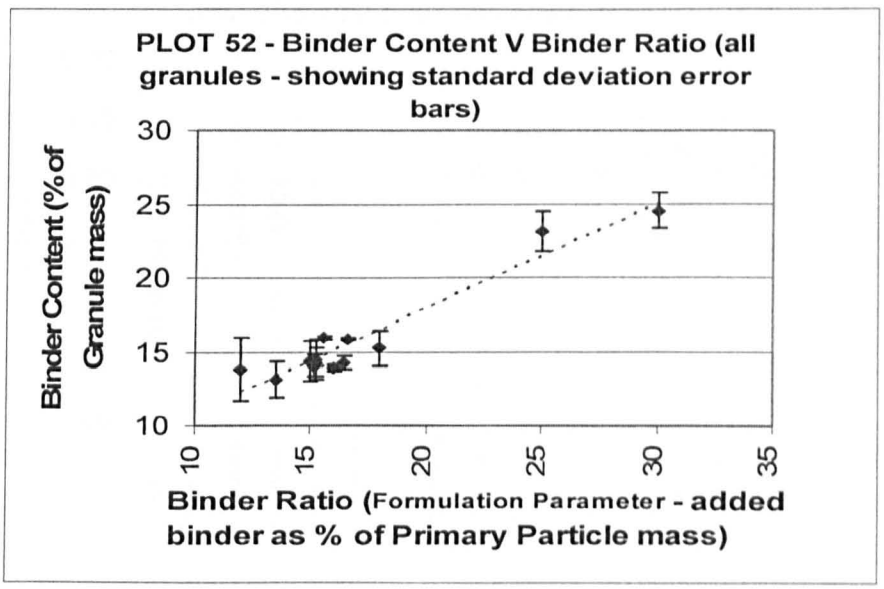

Plot 21 shows there is no relationship between static strength and binder content

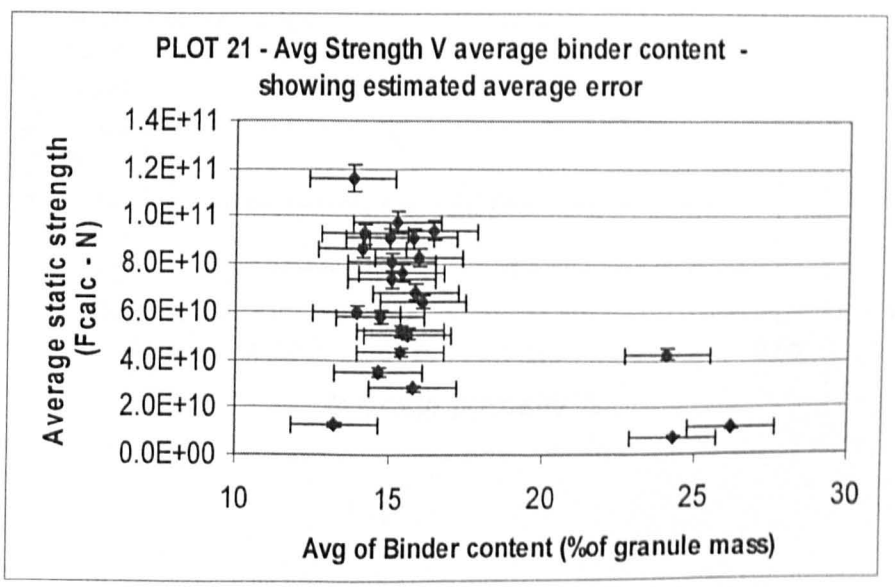

12.1.4 Porosity relationships

Plot 26 and 31 show the massive precision error present in the porosity data, this makes it impossible to comment on an possible relationships between porosity and other granule properties or between porosity and processing / formulation parameters.

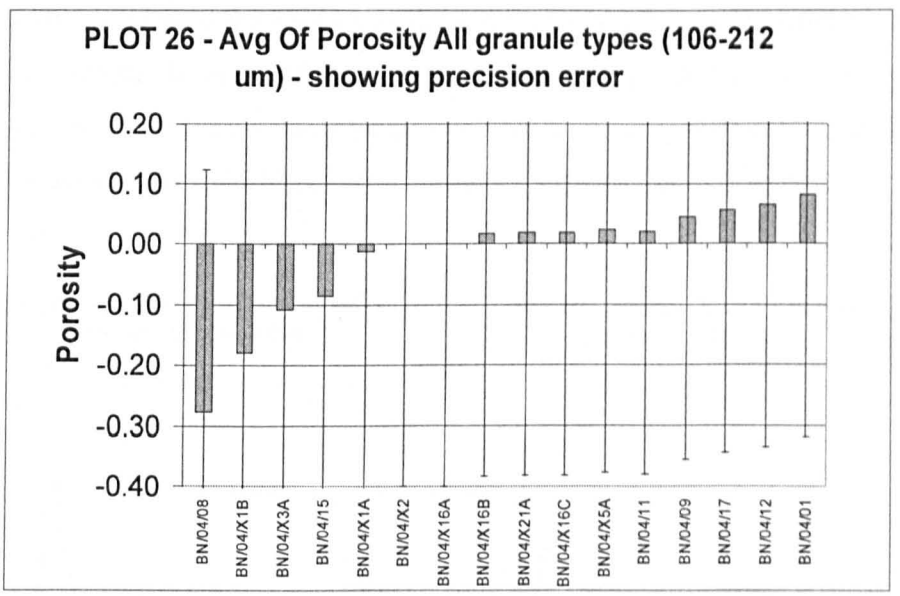

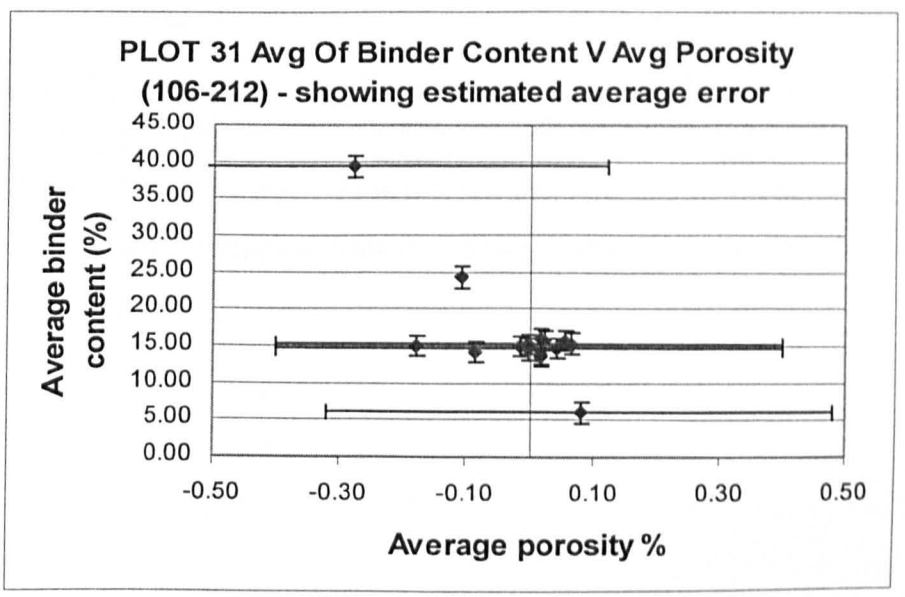

12.1.5 Granule size distribution relationships

As already described in the errors section the reliability of the size distributions generated using the Camsizer is very low (Plot 55 is an example of this), however some of them seem to have produced viable size distributions (plot 54) but it is not certain which size distributions are accurate and which are false. What was observed from the granulation process is that, visibly to the naked eye, there was nearly always a large spread in the sizes of the granules formed and that only 1 granule batch produced granules that seemed uniform in size, BN/04/X15C (this batch didn't produce very many microgranules and it couldn't be repeated even using exactly the same processing and formulation conditions).

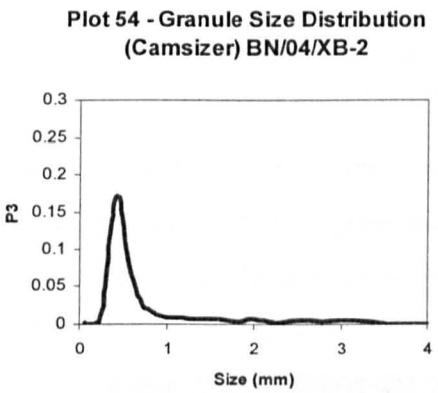

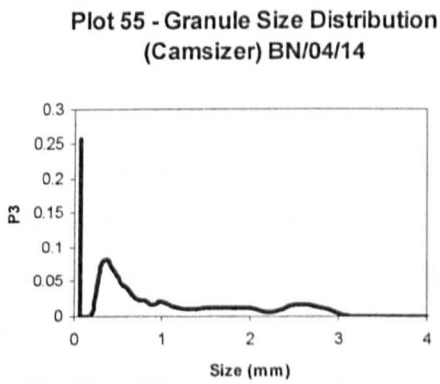

Plots 54 and 55 showing GSD's – note the spike at very small sizes on Plot 55 caused by combining sieved sizes <63microns with inaccurate Camsizer data.

Lots of the "successful" batches used in this research produced more caking on the sides of the granulator, on the impellor blade and on the chopper than granules of any sort see figure 47 below.

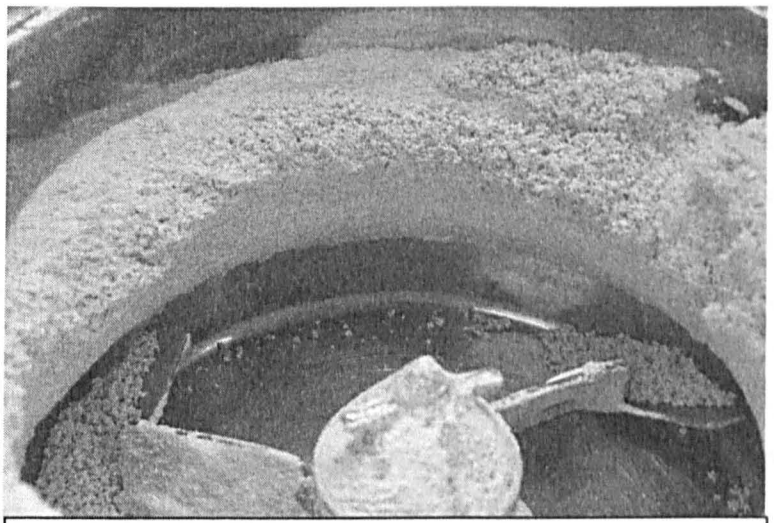

Figure 47 – showing caking on the walls of a batch, some granules have formed and are still in the mixing zone others are stuck in the "cake"

Quite often there would be a combination of caking, powdery granules (which it is assumed contains a lot of un-granulated powder and possibly very small granule fragments) and a few large snowballed granules that are easily identifiable with the naked eye. This is shown in the photo below of batch BN/04/X1B (figure 48).

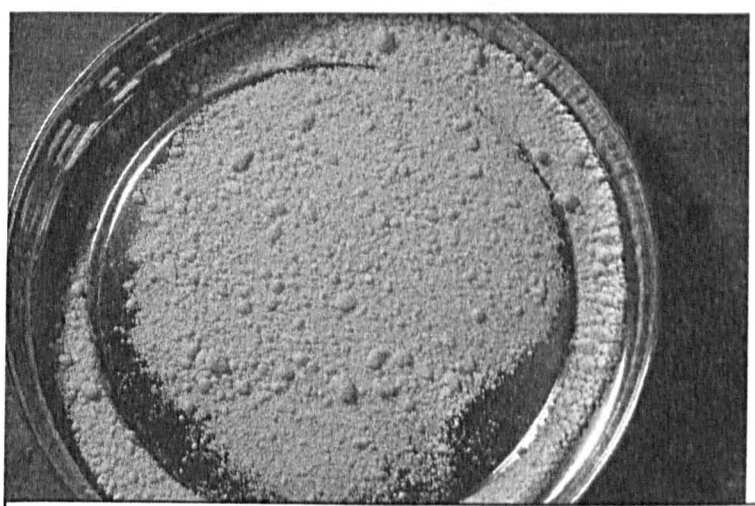

Figure 48 – showing snowballs and fine powder BN/04/X1B

It is only when a batch is sieved that the granules of the size of interest are visible. Not a single batch produced a significant amount of granules in the size portions of interest.

12.1.6 Strength Relationships

Most of the strength relationships have been covered in the previous sections. Section 12.1.1 shows that there is no relationship between abrasivity and static strength. Section 12.1.3 shows that there is no apparent relationship between binder content and the errors in the porosity means it is impossible to tell if there is the expected inversely proportional relationship between porosity and strength. It should be noted that even though Plot 21 showed no relation between strength and binder content, in reality this conclusion is probably wrong due to the errors measuring both the strength and the binder content combined with the fact that when strength is plotted against binder ratio (which is shown to be related to binder content) in the next section a relationship does exist.

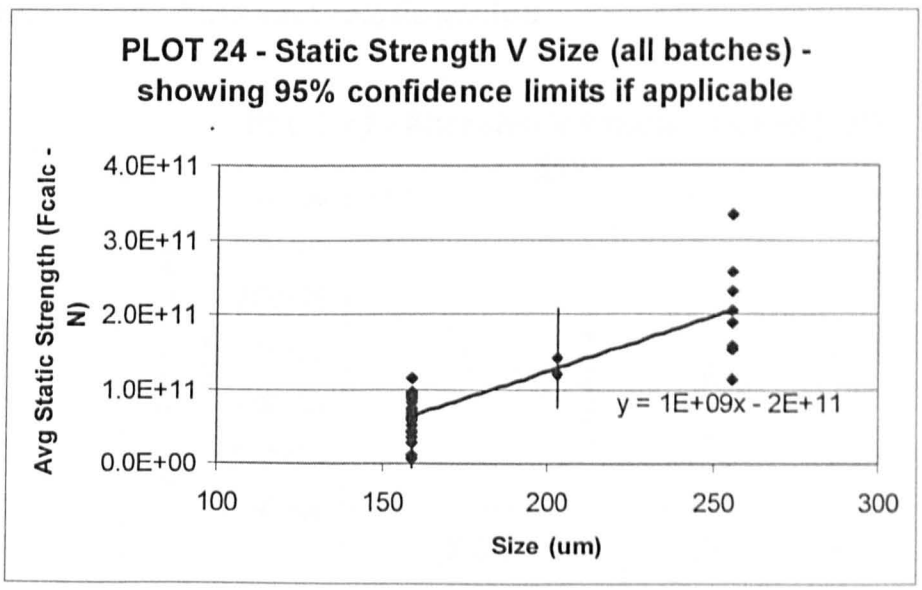

Plot 24 shows the relationship between static strength and size. Error bars showing 95% confidence limits have been added where enough data is present (for 2 data points in the size range 106-212 μm and 1 data point in the range 106-300 μm). There was not enough data in the 212-300 μm range to calculate 95% confidence limits. All the data points in the smallest size category fall just within the 95% confidence limits (obscuring the error bars on the graph). The trend has a gradient of $1x10^9$ which is the multiplier in the Aurbach equation relating strength to particle size (assuming the exponent is 1 – which would give the linear trend seen).

12.2 Property to Processing and Formulation Parameter relationships

Relationships were investigated to determine if there are simple relationships between the way a granule is made and what it is made from to the various granule properties.

The granule properties considered are: Abrasivity, Static strength and Porosity. These were each compared to the formulation and processing parameters: Impellor Speed, Run Time, Primary Particle Type, Binder Ratio.

12.2.1 Abrasion relationships

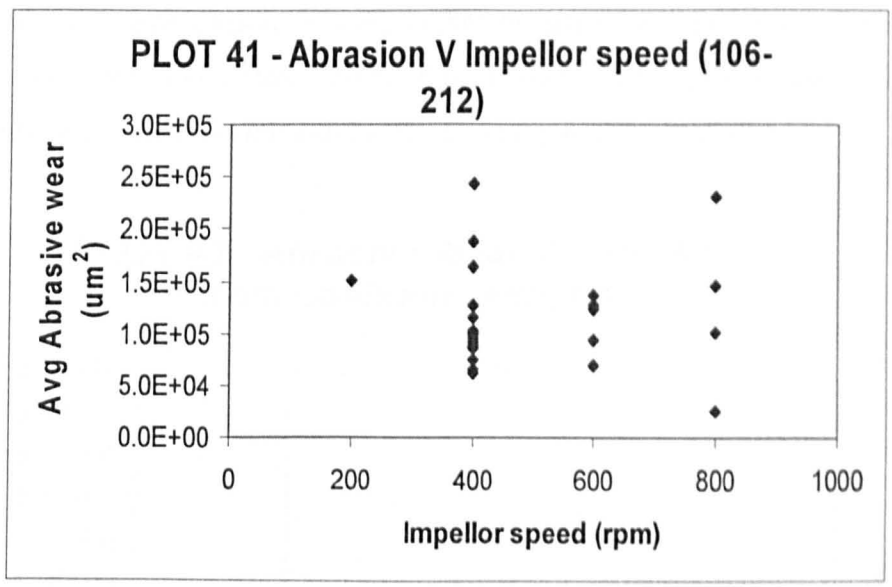

The Abrasivity was found to be unrelated to the Impellor speed for granules of the size 106-212um (Plot 41) and there was a no trend for 212-300um granules (Plot 40). When 95% confidence limits are plotted for the 1 anomalous result for 212-300 μm granules at an impellor speed of 400rpm it is seen that it is possibly a statistical error as there is nothing different between in the way those granules were made (BN/04/08).

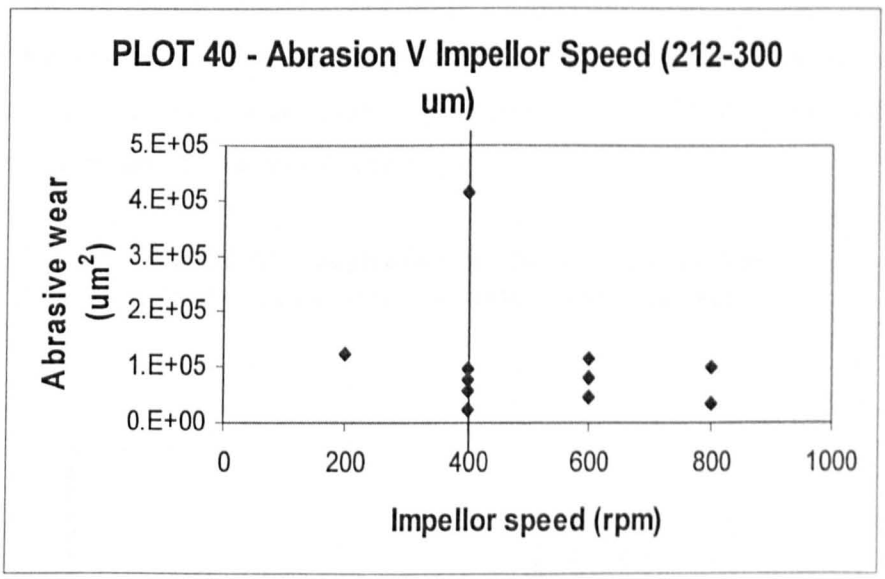

The effect of run time on abrasion is sown in Plot 43, there was only 1 data point for each time and the abrasivity was steady for a run time of 20minutes, 60minutes and 120 minutes with a run time of 30 minutes having a slightly higher abrasivity.

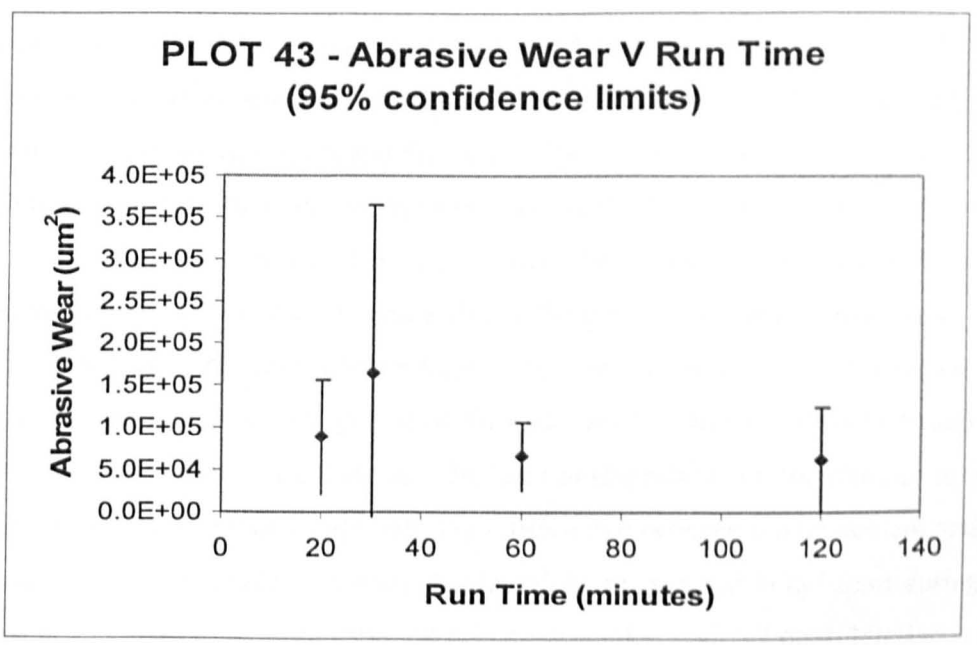

The higher value is probably due to error as there is no mechanistic reason why the abrasivity should increase and then decrease. The results relate to size cut 106-212 from

batches made using the same experimental protocol with only the run time changed. When error bars showing 95% confidence limits are added it is seen that the unusual high result at 30 minutes has a large range of confidence, thus it is likely to be a statistical variation and abrasivity has no relation to run time.

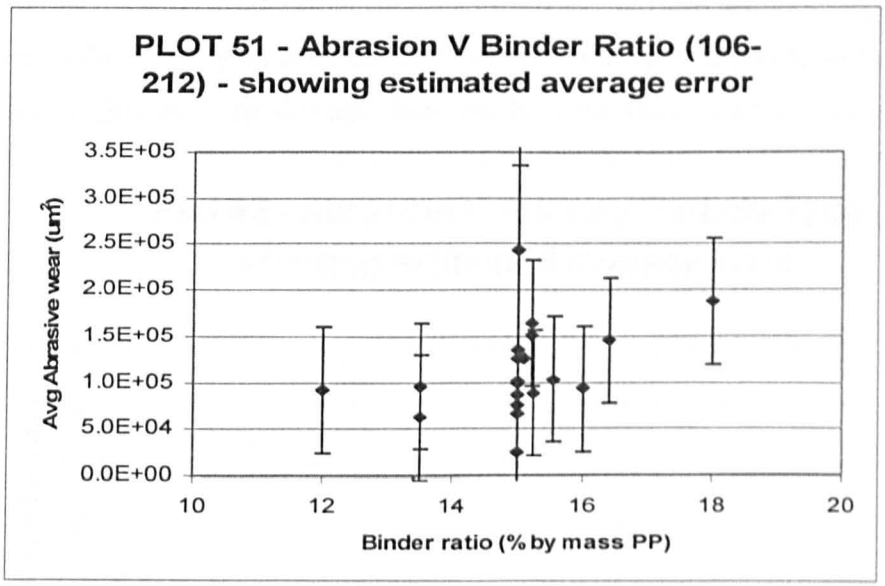

The abrasivity appears to be unrelated to the binder ratio (Plot 51), possibly with a slight trend to become more abrasive with increasing binder content but this is probably due to the errors in the measurements and the lack of data for the outlying binder ratios. The error bars show the estimated average error and the 95% confidence limits for the single high and single low value with a binder ratio of 15% (these have confidence limits of ± 323,000 μm^2 and ± 311,000 μm^2 respectively) Data points for some batches were removed because they used different types of binder or used primary particles which needed higher binder ratios to granulate. Granules made with PVP, PEG 1000 and PEG 6000 were removed because they need different binder ratios to form granules in the size range considered and thus would hide any relationship between binder content and abrasivity. Granules made with liquid binder might be expected to fall apart during abrasion. Granules made with different primary particles were not considered as it is believed that primary particle material is the main factor affecting abrasion. When these batches are included the abrasivity is unrelated to the binder content, so if there is a

relationship between binder content and abrasivity it is affected by the other processing and formulation variables.

Only 2 different types of primary particle, both $CaCO_3$, produced results from the experiments used for the database. There is no difference between the abrasivity caused by granules of the different types of $CaCO_3$ (Plot 42); this is not surprising as the primary particles are roughly the same size and shape and have the same material properties.

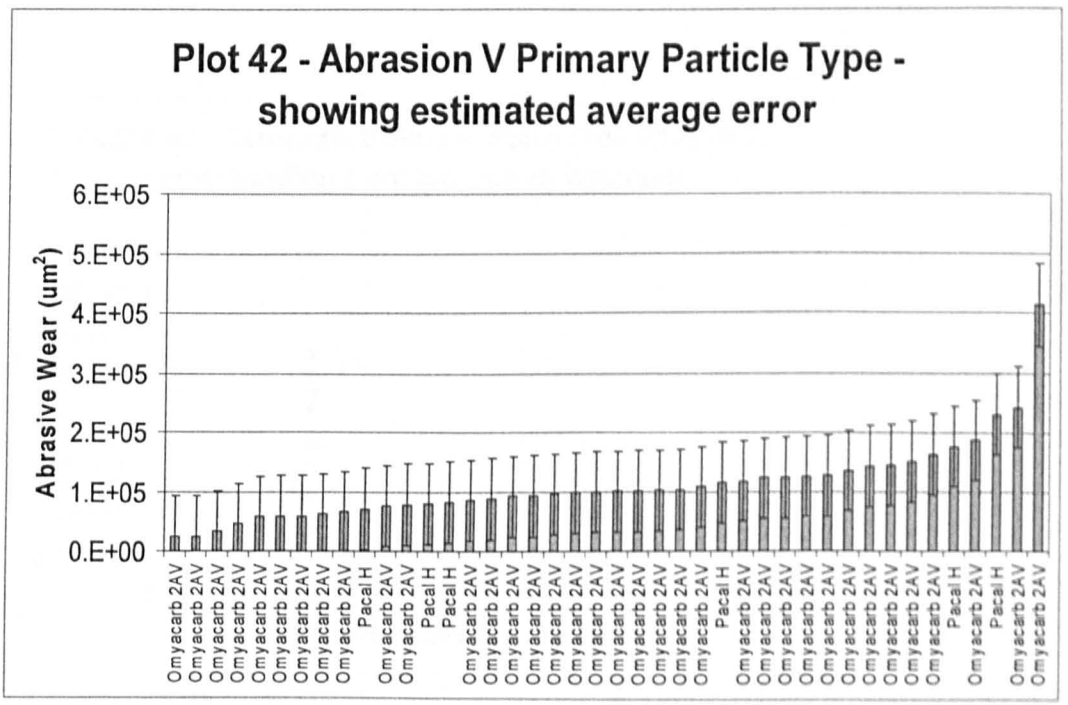

12.2.2 Strength

The relationship between Static Strength and binder ratio is very interesting. When the static strength is plotted against the binder ratio for granule sizes 106-212μm for all batches (Plot 44) there is a trend for the strength to be inversely related to the binder ratio (error bars are not shown as they add no value as the graph is just to illustrate how dramatic an effect on certain properties confounding and compounding variables can have).

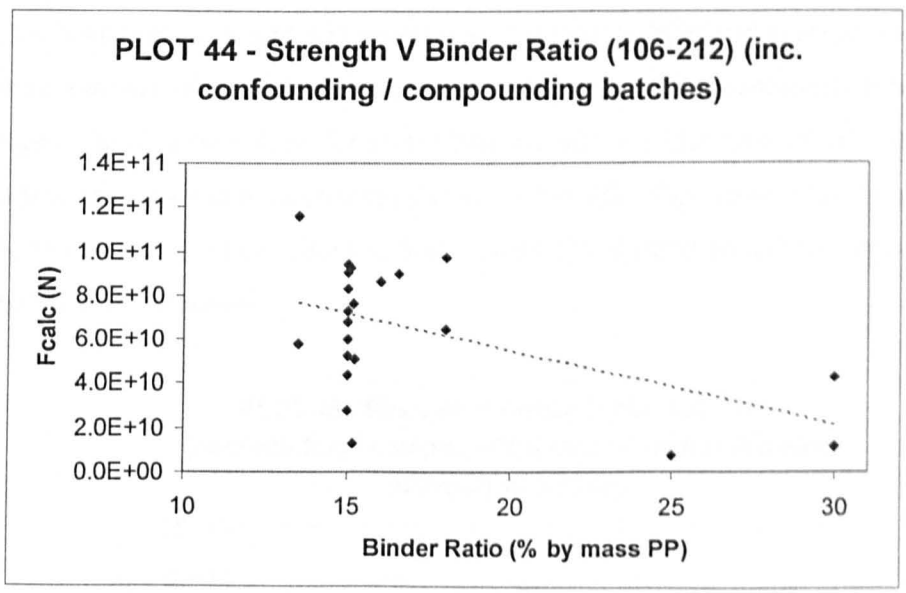

When batches made using PEG 1000 are removed the static strength of granules at that binder ratio increase – this is because the PEG 1000 is liquid at room temperature and thus is able to flow within a granule during compression and has less resistance to deformation. Therefore binder type affects the relationship between the binder ratio and the static strength. Other confounding batches were removed from the data: such as those made with PEG 6000 and those made with Pacal H (all of which need a higher binder ratio to granulate), batches made with an impellor speed of 200 (which have a very low strength), Batch X21A which has a high run time (giving it a high strength), Batch 19 which has a short run time (giving it low strength) and Batch 12 which was made using melt-in addition (which is the equivalent of a short run time due to the lag time required

to melt the binder before consolidation can start). When all these batches were removed from the plot (and they corresponded to the confounding and compounding batches), as shown in Plot 45 and 45b there is a clear reversal in the relationship between static strength and binder ratio.

Plot 45 shows the data points for each batch with error bars showing the standard deviations of the data within the strength tests of that batch, as it stands it would not be fair to say that a trend exists because the trend line would only cut the range of errors of some of the data points. However as all the theoretically confounding and compounding batches have been removed it is acceptable to group together and average results from different batches with the same binder ratio and produce 95% confidence limits of those averages. This has been done for all the batches with a binder ratio of 15% (none of the other binder ratios had enough data) shown in Plot 45b. This shows that the average value drops nicely onto the trend line and that a proportional trend does in fact exist between binder ratio and strength.

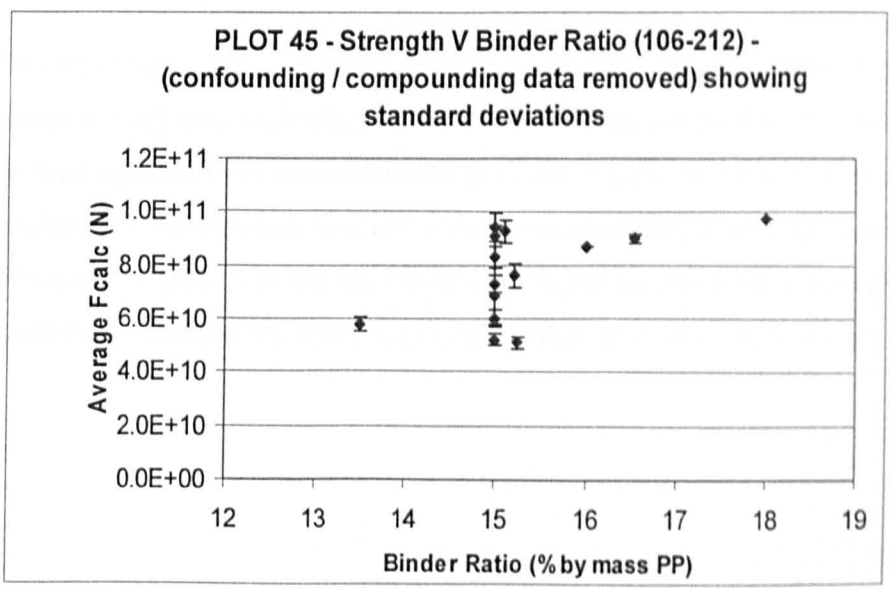

This highlights the importance of predicting qualitative effects of processing and formulation parameters accurately – the novel consolidation theory developed in section 7.3 allows this.

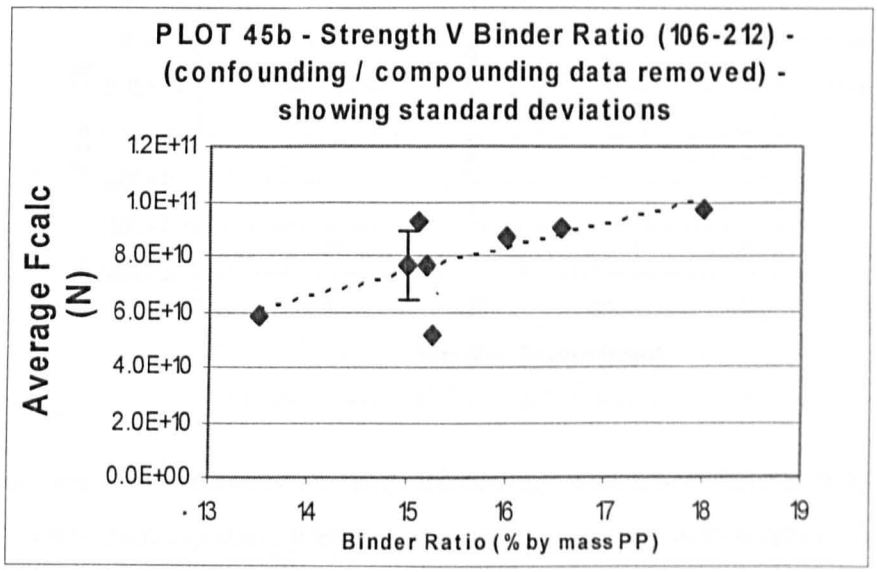

The effect of impellor speed on static strength is limited to the 106-212um size cut because not enough data was collected at other sizes to be useful. Plot 46 shows that at this size there appears to be no relationship between strength and impellor speed when all the granules are taken into account, this is due to confounding and compounding effects of other variables. Error bars are not shown on this plot as they would obscure the data points and do not add any value for determining whether or not a trend exists.

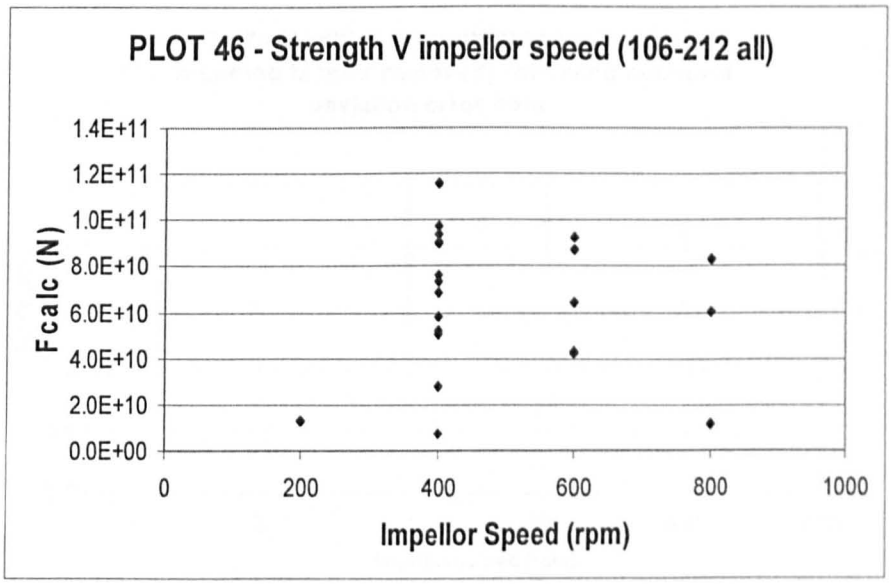

When granules from batches BNX2 and BN/04/X1A, which both have high binder ratios (already seen to increase static strength), were removed along with batches with variations on the run time and different binder types a bell shaped trend appeared; Plot 47 shows that the static strength increases with impellor speed (error bars showing standard deviations have been added). Short run times were removed because they will have weak granules for a given impellor speed and longer run times will have stronger granules (due to the extent of consolidation). Liquid binder is removed because it will be weaker.

An impellor speed of 200 r.p.m produces very relatively weak granules and then the data appears to form a hyperbola with the peak near an impellor speed of 600 r.p.m. At the highest impellor speed of 800 r.p.m the static strength drops and is similar to that produced at 400 r.p.m. For the 2 batches made using liquid binder (PEG 1000) there is also an increase in strength from the batch made at 400 r.p.m and the batch made at 600 r.p.m.

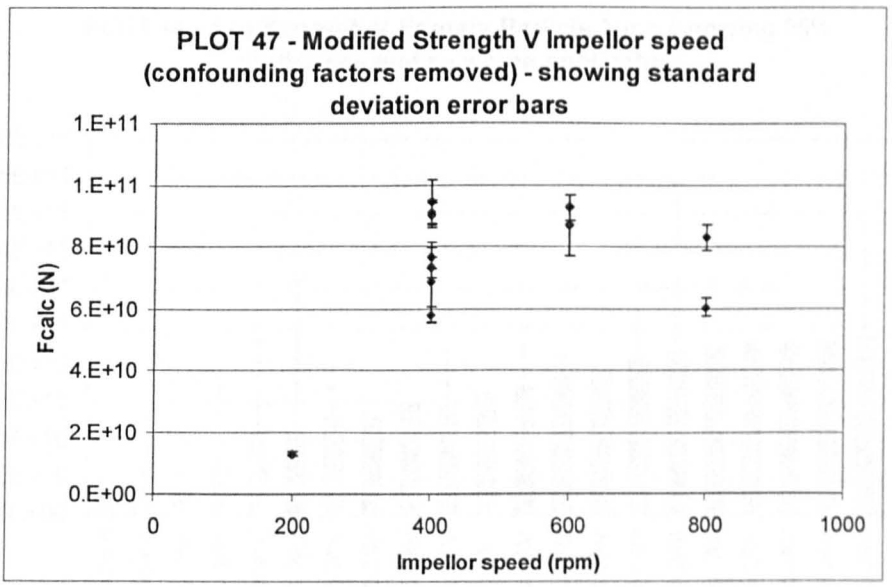

Plot 48 shows that the primary particle type affects the strength of the granule, but this is only based on 2 types of $CaCO_3$. Pacal H, the precipitated Calcium Carbonate, is weaker than the crushed Calcium Carbonate of OmyaCarb 2AV. The primary particle type seems to have a stronger influence than any other of the processing and formulation parameters on the granule strength. The error bars show that the low measured values of strength for Omyacarb could possibly be lower than they should be and the large error on the high value of Pacal H suggests that it could be higher than it should be – however not enough data for Pacal H (or other material) to say conclusively.

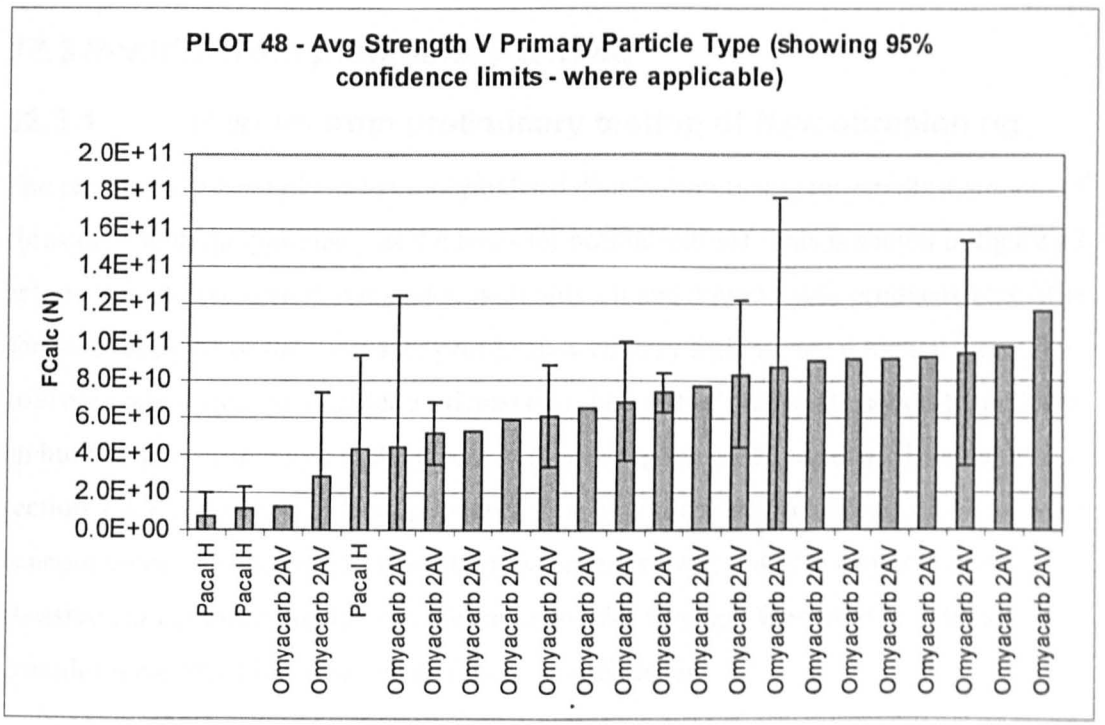
PLOT 48 - Avg Strength V Primary Particle Type (showing 95% confidence limits - where applicable)
FCalc (N)
2.0E+11
1.8E+11
1.6E+11
1.4E+11
1.2E+11
1.0E+11
8.0E+10
6.0E+10
4.0E+10
2.0E+10
0.0E+00
Pacal H
Pacal H
Omyacarb 2AV
Omyacarb 2AV
Pacal H
Omyacarb 2AV
Omyacarb 2AV
Omyacarb 2AV
Omyacarb 2AV
Omyacarb 2AV
Omyacarb 2AV
Omyacarb 2AV
Omyacarb 2AV
Omyacarb 2AV
Omyacarb 2AV
Omyacarb 2AV
Omyacarb 2AV
Omyacarb 2AV
Omyacarb 2AV
Omyacarb 2AV
Omyacarb 2AV
Omyacarb 2AV

12.3 Results from preliminary testing

12.3.1 Results from preliminary testing of New abrasion rig

The results have been plotted as a normalised distribution (using the smallest amount of abrasion – with no granules – as the basis for normalisation). This is shown in figure 48 below. It is clearly seen that abrasion with only oil and counterbody produces very little abrasion, analysis of the wear scar profile showed very little wear - it looked more like polishing when examined under a microscope. The rest of the results are quite muddled up but this is probably due to the errors in measuring the profile as described earlier (see section 7.4.2 – rejection of Knoop indent) , however there is a trend that $CaCO_3$ powder is about twice as abrasive as wessalith powder on its own. $CaCO_3$ powder is more abrasive than granules made from the same powder whereas Wessalith powder and granules have about the same abrasiveness as each other.

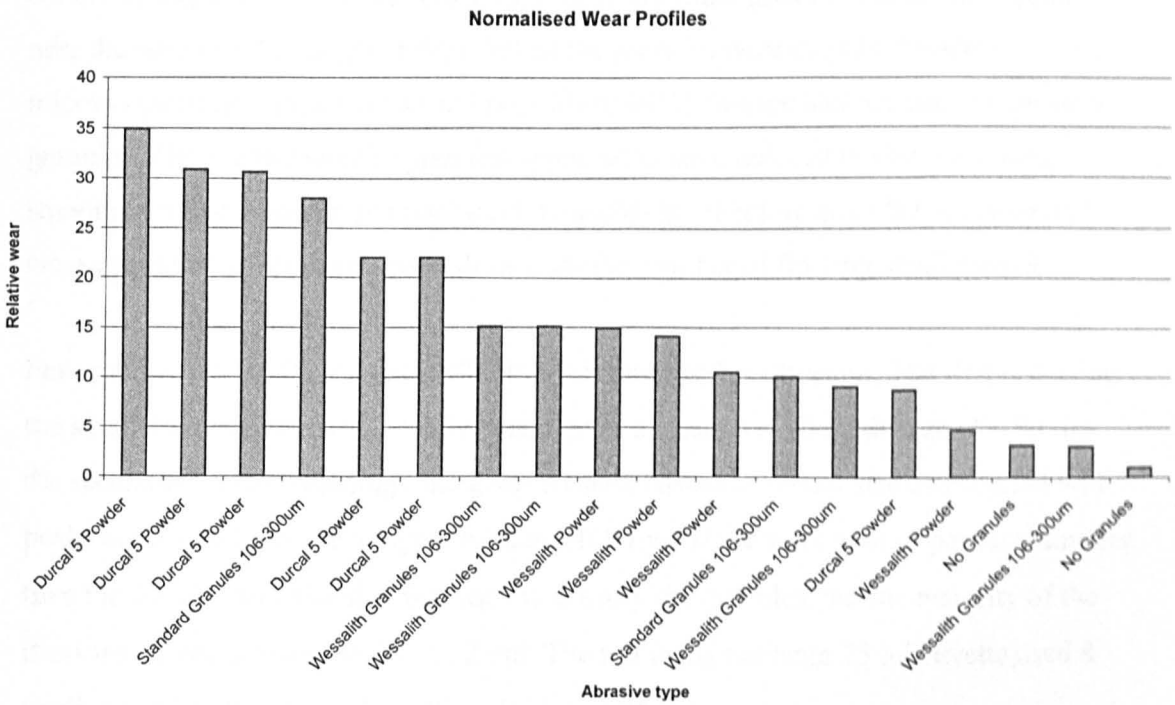

Figure 48 – showing normalised wear data for preliminary abrasion testing

12.3.2 Results from testing abrasion of toothbrush and granule breakage

The PMMA sample plates were examined before abrasion and no scratches were present on any of the plates. After abrasion all the sample plates had scratches and grooves running parallel to the direction of the brush strokes. The sample plate that was brushed with oil only had grooves similar to those produced on the plate brushed with granules for the same loading. The thickness and depth of grooves appeared to increase with loading, although this was difficult to tell using the 2-dimensional microscope.

The dry granules, before oil was added, were a mixture of sizes and looked like large rough spheroid granules aggregated with smaller angular granules attached to their surfaces. After oil was added most of the smaller granules detached from the larger spheroid granules leaving the larger granules appearing smooth.

In all tests granules were pushed to each end of the sample holder, with large granules collecting together close to the brushing region and small granules collecting together near the edges of the sample holder. When the granules were examined under a microscope after abrasion it was not possible to tell if damage had occurred to the large granules. The smaller angular granules appeared to have reduced in size, becoming smoother, rounder and more translucent. Granules in oil before and after abrasion that were examined under microscope show a similar number of floating small particles.

For granules having their size distribution measured before abrasion: The first test using the small 6 ml cuvette used 2 readings and gives a (mass based) mode size of ~ 90 μm, the second test used 6 readings and gives a (mass based) bi-modal size distribution with peaks at 90 – 100 μm and a higher peak at ~160 μm. There were a lot of particles smaller than the 63 μm sieve size that was used to classify the granules, but the majority of the mass was in the size region 60 – 112 μm. The test using the large 25 ml cuvette used 8 readings and gives a (mass based) mode size of 85 μm.

For granules having their size distribution measured after abrasion: The first test using the small 6 ml cuvette used 7 readings, after the initial stirring the sample was left to settle and 2 further readings were taken. After the 3rd reading the sample was re-stirred and 4 further readings were taken. Based on the readings taken immediately after stirring the

mode size was 90 – 100 μm. The readings taken as the sample settles show a reducing mode size with time suggesting that larger particles are settling out faster than the smaller particles. The second test using the small 6 ml cuvette used 7 readings and gives a mode size of 90 – 100 μm, a few of the readings gave bi-modal distributions with a second smaller peak at 160 μm. The test using the large 25 ml cuvette used 8 readings and gives a mode size of ~ 90 μm.

When all the tests are taken together there is no obvious difference between the size distributions before and after abrasion

13 Discussion – Results Analysis

13.1.1 Abrasivity versus Static Strength

There is possibly a slight inversely proportional relationship between abrasivity and static strength. There is a lot of scatter in the results and it is not a definitive trend, it is quite possible that the large errors in both the abrasivity and the static strength have created this trend (a no relationship situation was shown to be statistically possible). Gabbott, et al., [122] shows that uniaxial confined compression using the Adams, et al., [85] model, and alternatives, are not always reliable. Gabbott suggests that single granule compression should be used as an alternative, however this is not appropriate for this work as it is has not been possible to successfully isolate individual granules in the size ranges of interest; the uniaxial bulk compression remains the best estimate of granule strength. Assuming that the trend between abrasion and static strength does exist it is most likely to be explained by stronger granules being more consolidated and rounded and thus the granules will tend to roll more in the abrasion process with subsequently lower transfer of energy and abrasion of the substrate surface. Also if breakage of the granules occurs there will be less breakage for higher strength granules and therefore less sharp angular fragments produced and thus less abrasion – but analysis of the granules before and after abrasion suggests that breakage does not occur and that the only damage to the granules is a smoothing of the surface so the reduction in abrasion due to strength is more likely to be due to higher strength granules being more rounded.

13.1.2 Abrasivity versus Size

The results from Plot 4 show that abrasivity decreases with size. Plot 5 (showing effect of size within a single granule experimental batch) contradicts this and shows no trend but very small granules are more abrasive. This is believed to be because the abrasivity of granules is not dominated by the properties of the granule but rather the properties of the primary particles. In preliminary tests it was found that the abrasivity (measured on the Lissajous abrasion rig) was more dependent on the material of the primary particles than the size of granules. This is sensible because shape is a major influence on the abrasivity of a particle, with spherical particles being the least size dependent. Smaller granules are

the least spherical having a much smaller number of primary particle forming them and these primary particles form sharper angles at the surface: less rounded granules => more abrasion. Larger granules contain a lot more particles and a lot more binder, this combined with the fact that as spheres increase in size the angle at the point of contact between them and an abraded surface decreases mean that the contact is smoothed.

13.1.3 Static strength as a function of processing and formulation parameters

The static strength is proportional to the binder ratio, but this is not a simple relationship as it is affected by other processing and formulation parameters. Changing the binder type changes the relationship between strength and the binder ratio, this is clear from the results of static strength for granules made using PEG 1000 which is liquid at room temperature. Liquid binder will decrease the strength because it allows the primary particles to move and the whole granule to deform plastically, so as well as affecting the value of FCalc it also affects the mechanism and behaviour of compression. The effect of using a longer chain polymer is unclear; a higher binder ratio of PEG6000 was needed to make the powder granulate, but the single useful result was weaker than standard granules made with the same binder ratio. This could be because PEG6000 requires a higher temperature to remain soluble and might solidify within the high shear mixer more rapidly (before sufficient consolidation occurs thus reduces the relative strength) or because of its higher viscosity it requires more agitation for a given consolidation. A low impellor speed of 200 r.p.m. (using standard PEG 1500 binder) gave a low strength relative to the standard impellor speed for a given binder ratio and this is interpreted again being the result of less agitation leading to less consolidation and thus a weaker granule. The opposite sort of effect occurs in Batch X21A which had a long run time so it was more consolidated; this explains why it had a higher relative strength than standard granules even though it had the same binder ratio and binder type. A shorter run time giving a relatively weaker granule confirms this theory. The melt-in experiment also confirms this in a round about way, because there is a time lag whilst heat is transferred from the powder to the binder before the binder is completely melted the onset of

consolidation is later than if molten binder is sprayed or poured into the granulator. It is supposed that the binder that is stripped off the outside of the melting PEG particles can and will start to consolidate granules as soon as it is removed, but because the number of granules consolidating in this way starts off very low (compared to molten binder addition) then at the point of sampling (30 mins) there is either still un-melted PEG in the powder bed or PEG that melted from the core of the PEG particles has not had time to consolidate properly and weakens the overall strength of a sample under compression. This all supports the consolidation curve theory (section 7.3); Granule porosity is related to static strength with more porous granules being weaker, thus as granules consolidate (and thus get less porous) they become stronger. So stronger granules can be seen as indicative of denser granules, and thus consolidation, when you consider the batches that show positive trends between processing parameters such as run time and impellor speed (both of which are expected to increase the agitation rate constant (section 7.3.2.5) which in turn leads to greater consolidation and thus less porosity and therefore stronger granules) this is exactly what happens.

The relationship between static strength and impellor speed shows that as the impellor speed increases the static strength of the granules increases, this is the same with wet binder and solid binder. This is because the agitation rate constant is increased and leads to greater consolidation for a given run time and this in turn means less porous granules, which are known to be stronger. The fact that the same trend is true for wet binder (PEG 1000) is probably because in the high shear mixer the behaviour of the granule and its consolidation will be similar to solid binder (PEG 1500), because both are liquid in the granulator due to the high temperature keeping the solid PEG molten – it is only after cooling that the solid PEG solidifies. It is supposed that the pores within the wet binder granules are stable enough to remain after cooling and no more consolidation of the granule occurs due to the liquid PEG flowing within the granule until the granules have additional forces applied in the static compression tests. The peak in the granule strength as a function of impellor speed (Plot 47) is probably because at higher speeds the shearing forces are greater and there is probably more breakage of granules occurring within the granulator; only granules strong enough to survive that force survive. At the highest impellor speed the formed granules will have suffered a greater number of

impacts and it has been noted in other work (Han, et al., [67]) that repetitive loading and unloading of a particle (such as repetitive collisions) weakens the structure of the particle – thus making it weaker.

The primary particle type seems to have a very large influence on the static strength of the granule. Pacal H granules were notably weaker than granules made from Omyacarb 2AV even though they are both Calcium Carbonate, so it is probably not surface energy that is causing this shift in strength – more likely it is a combination of the mean size, size distribution and shape of the particles. Pacal H has a much tighter spread of sizes and the particles are probably more uniform in shape due to being crystallized. The rough shapes combined with the ratio of size between the small particles in Omyacarb 2AV to the large particles means that the packing structure will probably be denser, but results from binder content show that those granules made with Pacal H use nearly twice as much binder to successfully granulate and the final granules have a binder ratio nearly twice that of granules made with Omyacarb 2AV. So the low strength is probably not due to the way that primary particles pack but the way the shape interacts with the binder – because for granules made with Omyacarb 2AV a higher binder content gives stronger granules so it cannot be the closeness of the packing because a high binder content implies less close packing. Thus it is assumed that rough surfaces and irregular shape of the primary particles increases the static strength. This partly agrees with Fu, [32] interpretation, in his PhD thesis, of the work by Knight, et al., [97], Iveson, et al., [7], Litster and Ennis, [26], Dries et al. and Johansen and Schaefer. They found that granules made from fine powder or wide-distributions were strong and not easy to deform. They believed this to be due to a decreasing particle size leading to an increased surface area per volume and increased inter-particle contacts (increasing frictional resistance to deformation and failure) – they also propose that it increases the resistance to consolidation during the granulation process because the average pore size through which the binder must be squeezed decreases. They also found shape affects strength with rounded particles and those with a narrow size distribution being weaker, due to the reduction of interlocking effects.

The comparison of primary particle type also shows that for Pacal H increasing impellor speed also produces stronger granules when it is changed from 400 r.p.m to 600 r.p.m, but the static strength drops again as the impellor speed increases further to 800 r.p.m – further supporting the parabolic relationship between strength and impellor speed.

There is no clear relationship between porosity and impellor speed, even when all the anomalous granule batches are removed. This is a surprise because there is a clear relationship between strength and impellor speed and it is known that strength is related to porosity – it would therefore be expected that as the impellor speed increases the granule porosity would decrease in line with the increasing strength of the granules. This supports the suggestion that the porosity measurement techniques used in this research are not accurate enough and that other relationships related to porosity should not be taken seriously.

13.2 Porosity measurements

It is clear from the error analysis of the porosity measurements and the fact that no trends between porosity and other granule properties or between porosity and processing / formulation parameters exists that the porosity data in this report cannot be relied upon. It was noted earlier that mercury porosimetry and helium pycnometry are not suitable for finding the porosity of granules and it has been shown from the results in this report that thermogravimetric analysis combined with density bottle analysis is not suitable either. As there appears to be no other alternative for finding the porosity of granules, it casts doubt onto the validity of work by other researchers who have related porosity to other granule properties and processing mechanisms, especially when there is no mention of the method by which the porosity was found and the care taken to ensure its accuracy. It is believed that a combination of mercury porosimetry and helium pycnometry is the most valid method for finding the porosity of relatively large granules where a clear transition from intra-granular pores to inter-granular pores can be drawn from the pressure volume curves, but it is not valid for microgranules. A combination of thermogravimetric analysis and density bottle analysis is the best way to analyse the

porosity of microgranules, but the precision and care at every step needs to be improved. The factors that provide the most error in this work are:

- The assumption that precision error on the density bottle volume was ± 1%
- Assuming the moisture content in the thermogravimetric analysis was constant and negligible
- Assuming that the oil completely wets the surface of the granules and does not leave air pockets trapped on the surface or flow into granule pores

There is nothing that can be done about the last one, but determining the exact error on the density bottle and using more accurate bottles if necessary and measuring the moisture content for every test would reduce the errors in the porosity values. The apparent systematic error in the calculated porosity values probably comes from the wetting of the oil or the value of the density for any of the components (oil, PEG 1500 binder or Calcium Carbonate).

13.3 Discussion of Preliminary testing on Abrasion Rig, toothbrush counterbody and granule breakage during abrasion.

The similarity in abrasion between Wessalith (Zeolite) granules and Wessalith powder is probably because the wessalith granules are very weak and break down into powder form and so are controlled by the abrasiveness of the primary particles – which happen to be not very abrasive. It appears that wessalith granules, wessalith powder and durcal 5 ($CaCO_3$) granules all have the same abrasivity. The reduction in abrasivity of the durcal 5 powder when it is granulated is because by mass there is less abrasive entities in the slurry and those that are there are less angular and rounded with the abrasive Calcium Carbonate primary particles partially smoothed by PEG binder at the granule surface and the shape of the granule as a whole being rounded meaning that it will tend to roll in the slurry rather than dig in to the surface of the substrate causing gouges and scratches.

Some sort of segregation process is occurring during abrasion to produce the separate groups of large and small granules at the end. It is possible that the bristles are filtering out the large particles and the smaller particles get carried along with the oil

(toothbrushes were used in the preliminary testing rather than a solid cloth covered block). This segregation makes it impossible to analyse the size distribution before and after abrasion using image analysis because the location of the image taken on the sample plate will affect the size distribution. The images of granules before and after abrasion (figure 44 and 45) suggest that some form of erosion of the granules is taking place, as all the granules (small and large) become rounded and surface smooth after abrasion. The presence of more very small particles after abrasion using the Unilever linear abrasion rig supports this and could be primary particles worn from the surface of larger granules. The presence of small particles before abrasion using the In-House abrasion rig could be caused by primary particles aggregated onto the larger granules that become dislodged when the oil is added, it is too difficult to tell whether the number of these small particles increases with abrasion indicating erosion or whether there is the same number. It is not clear what happens to the small angular granules that are present at the start of abrasion; these seem to become smaller, more rounded and more translucent. It is not believed that complete destruction of whole granules occurs as there were no sharp angular particles, which are indicative of breakage, at the end of the abrasion.

Wider scratches and gouges indicates that the more abrasion is occurring, however it is not clear whether this is due to increased abrasion from the granules or the bristles on the toothbrush. It is likely that the increased damage is due to the bristles as the pattern of the damage remains consistent with that caused by bristles and there is no evidence of increased damage to the granules with increased load. This is sensible as if the bristles are filtering the large granules and the small granules are getting swept along by the oil then they are not in a position to have the extra load transferred to them. Any granules that do get caught and dragged underneath a bristle tip will feel the increased load and possibly suffer greater damage and cause more abrasion in the PMMA surface (hence a possible explanation for the few deeper scratches), but the number of these granules will be small and any damage will be masked by the presence of many more un-damaged granules.

The size analysis of the granules before and after abrasion using the Sympatec was an attempt to quantify the damage to the granules, but this did not prove that the granules are

breaking or being eroded during abrasion. It did show that larger granules settle quickly in oil, thus the sampling method and measuring method need to be strictly controlled in order to get reproducible and comparable results.

13.4 The granulation process – making micro-granules

As can been seen from the results there is wide variety in the properties of the granules that were produced. No experimental recipe processing conditions was able to make reproducible granules. Within any given batch there was massive variation in the size and distribution of the granules, the amount of caking on the impellor, granulator walls and chopper, the amount of powder left ungranulated, the amount of snowballing and the properties of the granules within the size cuts of interest. The combination of equipment and experimental recipe used in this research is unsuitable for assessing the fundamental relationships that this research project set out to achieve. As none of the batches were reproducible it is not possible to rely on the observations relating processing parameters and formulation to end granule properties, especially as these properties were only measured on a small (very small in most cases) fraction of the total granules produced in the mixer. If these combinations were to be used in an industrial situation then there would either be a lot of wastage or a lot of recycling of fines and reprocessing / milling of coarse granules making it very energy intensive.

It is fundamentally flawed to attempt to relate the properties of the granules at the small scale attempted in this research. This conclusion has been reached because it has not been possible to find a single set of granulating conditions that produces reproducible granules, this alone suggests that the particular combinations of ingredients and conditions are in an unstable regime. Additionally consider that:

- The granules are made from a charge of powder having a particular size distribution – a spread of large and small particles.
- This spread of sizes also has an associated spread of shapes, and any particular small size cut from the primary particles distribution will have a related distribution of shapes.

- There is a limited number of particles that form a micro-granule, the smaller the gap between the size of the primary particles and the size of the final granule the greater the variation in size and shape of the formed granules due to the initial PPSD.
- The binder distribution, if it is sprayed on (accepted as the most uniform method of binder addition) will have a droplet size distribution which combines with the primary particles that they contact to give a nucleus size distribution, nucleus primary particle distribution and nucleus binder content distribution.
- As the spray-on addition (or melt-in and pour-on) does not happen instantaneously there will be a spread of start times for each of these different nucleus; so even if the nucleus size, particle content and binder content were identical (which is unlikely) it would not have the same start time and thus same consolidation behaviour.
- There is a spread in the flow patterns and the forces felt within the granulator. In an unstable system, such as the one being investigated, the flow patterns and the way different granules behave within those flow patterns is such that depending upon a granules state when it is at a certain point in the flow it will behave in different ways. At an extreme one can imagine a large granule being flung harder against the walls of the granulator (or other granules) and is thus more likely to deform on those contacts and pick up more material and grow in size (assuming it doesn't break) whereas the small powder doesn't get thrown with such force and flow currents take it into another part of the granulator flow pattern increasing the disparity between the small and large granules.

This suggests that designer microgranules are not possible using the uncontrolled starting conditions that are used in high-shear granulation. A much tighter control of the initial size distributions of powder, binder and wetting time would be required. These arguments do not detract from the value of doing the types of investigations performed in this research only that it should be done on granules of a much larger scale in relation to their primary particle sizes. Some workers have observed that at extended mixing times the effect of the addition method is reduced, Knight, et al., [87], whereas others give detailed analysis of how important the spray flux and the nucleation stage is on the granulation

process, Iveson, et al., [7]. It is proposed that these two ideas combine with what has just been said. That any granulation system and set of conditions can be thought of as falling into 3 stages or scales:

1. An "unstable" phase analogous to the turbulent fluid flow stage between turbulent fluid flow and laminar flow. This relates to the very early stages of granulation or certain combinations of equipment, processing and formulation.
2. A "transition" regime, this is where the granule output and properties are very spread out, but trends are beginning to appear and a certain degree of homogeneity can be seen. I believe this scale is linked to combinations that can be shown to have strong dependencies on the nucleation stage and the conditions of the binder addition.
3. A "stable" regime, this is where the granules are large or mature or the conditions are such that batches are very homogenous and easily reproducible. They will be largely independent of small fluctuations in addition method or state at the nucleation stage.

The 3rd scale / stage is the optimal to be operating at industrially as the process will be most stable and least prone to upstream fluctuations. However the 2nd regime offers the best for altering settings and conditions to generate designer granules. The first regime is no good at all as an industrial operating regime as the product would be constantly changing and there is no control whatsoever. In my opinion granulation is too complex and chaotic to ever hope to understand it well enough to make a truly designer granule using quantitative relationships, granulation should remain an art and the research should aim at producing useful generally applicable qualitative relationships.

Even in (apparently) well behaved systems where the granulation appears to be consistent granules of the same size from within a batch will have inherent variation in all sorts of properties. Even when granules of the same size are considered properties such as measured failure, Gabbott, et al., [122], and liquid solid ratio, Reynolds, et al., [24], will show variation.

It is not possible to make a batch of granules with a mean size smaller than or close to the size of the binder droplets and primary particles being used. By the very definition of granulation it involves combining several primary particles together and this means a size increase. In order to theoretically make microgranules less than 100 microns by conventional high-shear granulation requires the use of powders with a mean size of about 2 to 15 microns (because any larger and the powder starts to contain a significant amount of material near the 100 micron size), the problem with this is at such small sizes the fine powder aggregates electrostatically into clumps larger than 100 microns – it is assumed that these clumps could contact binder droplets and form ready made large granules, bigger than the desired size. This is not to say that granulation with small particles is not possible, it is possible to form large granules; but granulation to form small granules from very small primary particles is not possible. This is because instability in a granulation system is more likely if the relative size difference between the smallest and largest primary particles in the feed powder is large, small primary particles have large distributions relative to their smallest sizes, and if the desired granule size is close to the size of the binder droplets.

14 Conclusion

14.1 Failure Distribution Model

The failure distribution model is suitable for predicting the failure rate of dense granules based on granule size and impact velocity. The Weibull equation accurately describes the experimental distribution of impact failures.

The theoretical distributions of impact failure can be found by:

1. Conduct static compression tests
2. fit data using modified Aurbach equation (4)
3. Calculate the critical normal impact velocity eqn. (10)
4. Use the critical normal impact velocity and impact angle to find the c-parameter eqn (9).
5. Use the Weibull equation (8) to find the failure distribution.

A fairly good agreement between the theoretical critical velocity calculated using eqn 10 . and values obtained from impact experiments supports the applicability of the theory.

14.2 Granule Strength

Granule static strength is suitable for predicting impact failure / impact strength, but it has not been proven suitable for predicting abrasive strength.

Granules of a given size from a batch will fail by different mechanisms – at least 4 different failure curves were observed, this is due to the heterogeneous nature of the granules and assumed to be due to a distribution of cracks and flaws.

The Adams, et al., [85] model, used in this work, for estimating static compression strength from uniaxial bulk compression of multiple granules is unreliable and, without single granule compression to determine the multiplication factor, can only give relative

strengths (FCalc). It is however the best model available for comparing the relative strengths of granules which are too small to test by crushing individually.

Porosity does relate to the strength of a granule and that as porosity increases the granule strength decreases – this is indirectly backed up by the results in this research when the qualitative predictions and inter-relationships that the Granule Compaction theory allows are applied.

A lot of the static strength relationships and abrasion relationships are dependent on the combination of size and number. Individually, larger particles can withstand larger loads and are more abrasive than smaller particles. But when tested by constant mass larger particles appear weaker and less abrasive because of the way that strength scales to the surface area (or cross sectional area) whereas mass and number scale to the volume.

No direct evidence of granule breakage has been seen in any of the high-shear granulation experiments used in this research.

Liquid binders are weaker than solid binders for the same binder content.

The static strength is directly proportional to the binder ratio. But confounding and compounding factors such as run time, PEG type, primary particle type and impellor speed have a greater effect; when these are taken into account they can reverse the trend and make static strength appear to be inversely proportional to binder ratio. It is this authors' conclusion that static strength is really related to the porosity, because all of these factors (including binder ratio) ultimately affect the porosity. It is generally accepted that a more porous granule is weaker.

Increasing impellor speed increases the static strength of granules. (caused by increased compaction) – But there appears to be a limit to this effect after which the strength starts to decrease.

Extending the run time increases the static strength of granules. (caused by increased compaction)

The primary particle type affects the strength. Granules made from Pacal H appear to be weaker than those made from Omyacarb (precipitated $CaCO_3$ and crushed $CaCO_3$ respectively). This is even when higher impellor speeds are used and thus the porosity of the Pacal H should be very low increasing their strength (which it does but not enough to come close to the strength of the ground $CaCO_3$). As there is not a chemical difference in the surface of the 2 particles it is assumed that the irregular shape of the ground Omyacarb is what gives it a greater strength.

14.3 Granulation – Processing Parameters

The formulation and processing parameter conditions chosen as the model for this research are not suitable for producing granules consistently. It is concluded that any set of formulation and processing parameter conditions can be thought of as falling into 1 of 3 granulation regimes:

- An "unstable" phase analogous to the turbulent fluid flow stage between turbulent fluid flow and laminar flow. This relates to the very early stages of granulation or certain combinations of equipment, processing and formulation.
- A "transition" regime, this is where the granule output and properties are very spread out, but trends are beginning to appear and a certain degree of homogeneity can be seen. I believe this scale is linked to combinations that can be shown to have strong dependencies on the nucleation stage and the conditions of the binder addition.
- A "stable" regime, this is where the granules are large or mature or the conditions are such that batches are very homogenous and easily reproducible. They will be largely independent of small fluctuations in addition method or state at the nucleation stage.

Extended run times reduce the effects of the initial nucleation conditions, negating the differences between binder addition methods.

Higher impellor speeds lead to greater granule consolidation.

Longer run times lead to greater granule consolidation.

14.4 Granulation – Formulation Parameters

It is believed that the distribution of different sized particles in the Primary Particle size distribution leads to the formation of heterogenous granules. A larger distribution leads to more heterogenous granules. The same is true for the binder content distribution within granule nucleus' as a result of non-uniform distribution, the binder addition method affects this initial distribution.

It is theorised that it is possible to control granule properties from the initial granule formulation and processing conditions, but in practice this is very difficult (and was not possible in this research). Smaller primary particles are less stable than larger particles – they either stay as a fine powder or snowball uncontrollably into larger granules. It is believed that for small primary particles (as used in this research) there is a fine line between too little binder (so the powder remains a powdery mess) and too much binder (resulting in the run-away snowball granulation), this is because once a granule consolidates to the point where it is saturated and surface wet there are likely to be lots of other granules in the same situation and when 2 saturated granules collide and stick they produce a larger granule with even more surface saturation.

Wessalith (Zeolite) primary particles are less abrasive than Calcium Carbonate primary particles.

The effect of moisture should be considered in future work. It is believed that varying moisture content is a possible explanation for the irreproducibility of batches following identical experimental protocol. A series of tests using identical batch recipes need to be

performed where the moisture content is rigorously controlled in order to determine whether it really is such an important influence on whether granulation is successful or not.

Increasing the binder ratio increases the granule strength.

14.5 Granules – Properties

Granules are heterogenous in nature; in terms of porosity, binder content, abrasive strength and static strength. This heterogeneous nature comes from the multiple start points due to a size distribution of primary particles, a size distribution of the binder that is applied to those primary particles and the distribution of relative start times for nucleation.

Granules of a given size from a batch will fail by different mechanism – at least 4 different failure curves were observed, this is due to the heterogeneous nature of the granules and assumed to be due to a distribution of cracks and flaws.

Shape and material are likely to be the most important factors affecting the amount of abrasive wear.

14.6 Granules – Property to Property relationships

NO relationships with porosity could be found directly due to the errors in the porosity test method and the small sizes being used. Several other property to property relationships were limited by the amount of suitably sized material that could be produced by the granulation and sieving processes.

It is possible to relate impact strength to static strength, but it appears no such relationship exists between abrasive strength and static strength. However there appears to be some sorts of trends; the abrasivity of smaller granules has a smaller dependency on static strength than larger granules. Larger granules having a given strength are more abrasive than smaller granules at the same strength.

There is no clear relationship between binder content and abrasivity.

There appears to be no relationship between static strength and binder content.

14.7 Granules – Property to Processing / Formulation relationships

Increasing impellor speed increases the static strength of granules. (caused by increased compaction)

Extending the run time increases the static strength of granules. (caused by increased compaction)

Higher impellor speeds lead to greater granule consolidation.

Longer run times lead to greater granule consolidation

The material (primary particles) used to make the granules affects the abrasivity. Granules made from Wessalith (zeolite) are the least abrasive, precipitated calcium carbonate (PacalH) is just as abrasive as crushed calcium carbonate (Omyacarb and Durcal) of the same size.

Liquid binder produces weaker granules than solid binder.

Binder content of the formed granules is proportional to the initial binder ratio.

There is no relationship between impellor speed and abrasivity.

The static strength appears to be directly proportional to the binder ratio. But confounding and compounding factors such as run time, PEG type, primary particle type and impellor speed have a greater effect; when these are taken into account they can

reverse the trend and make static strength appear to be inversely proportional to binder ratio. It is concluded that static strength is really related to the porosity, because all of these factors (including binder ratio) ultimately affect the porosity. A more porous granule is weaker.

14.8 Experimental Techniques

It has been shown that several test procedures that were, and are, being used should be reconsidered in the light of this work, including:

- The Knoop indent approach to measuring abrasive wear
- Use of the Camsizer to get size distribution for particles less than 150 microns
- Porosity measurements using Mercury Porosimetry and Helium Pycnometry
- Porosity measurements using thermogravimetric analysis and density bottles
- Thermogravimetric analysis of binder content whilst ignoring moisture

It was found that certain properties of microgranules that were assumed to be easily measurable are extremely difficult:

- Porosity of granules <100 microns
- Sieving and isolating granules <100 microns
- Individual static strength tests on granules <100 microns
- Isolating individual granules
- Image analysis less than 100 microns (determining what is binder and what is primary particles within a granule)
- Granule size distributions less than 100 microns

Mercury Porosimetry and Helium Pycnometry were not suitable for determining the porosity of micro-granules, and extreme care must be taken to ensure the accuracy of thermogravimetric analyses of porosity. This author doubts the validity of some previous research relating porosity to granule strength, specifically small granules and where the method of determining the porosity is not detailed.

The porosimetry experiments in this research are not reliable enough to show any trends relating porosity to other granule properties or processing parameters. There is a slight inversely proportional trend between binder content and porosity, but this is because the binder content values are used in the calculations for the porosity values.

The Knoop indent method on Perspex is not an accurate method for determining the abrasive wear of granular material or material that causes very small amounts of wear. The error caused by variation in judging the ends of the indent silhouette are significant.

The alternative abrasion test designed and developed in this research has not been proven conclusively to be a better or worse test than the Knoop indent method – further testing to determine the true random error in the technique would be needed.

When testing particles, specifically dosing the tests by added mass, care must be taken to interpret the relationships with size correctly. Individually, larger particles can withstand larger loads and are more abrasive than smaller particles. But when tested by constant mass larger particles are weaker and less abrasive because of the way that strength scales to the surface area or cross sectional area whereas mass and number scale to the volume.

Sieving is the rate determining step in this research; the granules of interest are so small and cause complications such as sliming, aggregation and breakage during sieving which all increase the time required to produce a suitable mass of sample for further testing. Sliming was occurring on sieves 212 μm and below.

The granules on any given sieve will include granules smaller than the sieve mesh size due to aggregation and incomplete sieving, but they will not include any granules larger than the upper mesh size (unless the particles are needle-like in nature or the sieve is damaged).

The Camsizer was not being used properly or it is not accurate enough to deal with small particles in the approximate range 63-750μm. It is thought there is a systematic error

caused by the presence of small fines (left on the particles due to sliming and aggregation) – these fall through the Camsizer and "stick" to both the glass screen and other particles increasing the apparent size that is measured by the Camsizers cameras.

It is difficult to assess the validity of the new abrasion testing technique using granules, because granulation cannot significantly affect any of the properties that affect abrasion except to make the abrasive process largely particle independent.

The experimental design used in this report to reduce the total number of tests from over 5 million to a few thousand was necessary to make the research manageable; however it does mean that a lot of the trends are based on very little data. Any of the trends quoted in this report should be tested further in individual studies in order to reduce the random errors associated with the lack of data.

Very few of the granules dosed onto an abrasion sample plate are involved in the abrasion process – most of them are pushed to the ends out of the way and are not re-entrained into the abrasion process. The granules that do remain cause abrasive wear.

Moisture content tests should be performed in parallel to every set of binder content tests as it is believe that moisture content can add a significant error to the binder content and this is carried through to any porosity calculations based on density bottles and thermogravimetric analysis.

Errors

Below is a list of the errors associated with the various test techniques and whether that error is due to the precision of the test or random errors.

Granule Size Distribution	=	Unknown and undeterminable errors		
Abrasivity	=	Random error	=	± 68,000 μm^2
Strength	=	Precision error	=	± 4.5 (% of value)
Moisture = 0.78% by mass	=	Random error	=	± 1.19 % (by mass)
Binder Content	=	Random error	=	± 1.42 % (by mass)
Porosity	=	Precision error	=	± 40.55 % (by vol.)

Note: The errors for Moisture, Binder Content and Porosity are all absolute values by mass or volume of granule. The error for strength is a variable value; a percentage of the quoted value.

14.9 Abrasion

Granule static strength is suitable for predicting impact failure / impact strength, but it does not appear suitable for predicting abrasive strength. However there appears to be some sorts of trends; the abrasivity of smaller granules has a smaller dependency on static strength than larger granules. Larger granules having a given strength are more abrasive than smaller granules at the same strength.

Granulation has limited application as an approach to controlling the abrasivity of particles or a system. The primary particles appear to have a greater influence on the abrasive wear than any other formulation parameter or processing conditions. Granulation is a suitable method of reducing the abrasivity of a system, by forming primary particles into large, strong spheres the abrasive nature is reduced because spherical particles roll over the surface and transfer less abrasive energy.

Toothbrush heads should not be used as a counterbody in abrasion testing as the bristles on the brush cause more abrasion than any of the abrasive particles being tested (on PMMA).

A jay-cloth covered metal block causes insignificant abrasion by itself (on PMMA).

The Knoop indent method on Perspex is not an accurate method for determining abrasive wear, but the alternative designed for this research has not been proven to be any more effective. The theoretical application of the Knoop indent is sound, it is the just the practical application that is flawed due human judgement involved in gauging the ends of the indents.

Although the dimensional analysis of the abrasion testing is incomplete it describes an important parameter: abrasive energy. The analysis shows that the abrasion process can be interpreted by an undefined equation relating this abrasive energy to another energy term (probably the energy required to cause failure) and to another term which is effectively the number of granules. This analysis highlights the problem with comparing abrasion tests of different granules simply using the same added mass and operating conditions (of the abrasion rig). Granules (or particles) will not be being tested on a "like for like" basis, instead different masses of granules will have to be added depending upon their density and size. However the dimensionless equation that allows this "like for like" testing has not been determined and in the absence of anything better dosing by constant mass will have to do. Experiments on a "like for like" basis have the advantage that different granules could be categorised by their relative efficiency at transferring the inputted abrasive energy into wear of the surface, rather than the cruder categorisation of amount of wear produced (which is a lumped dependency).

Damage to granular material during abrasion is probably by attrition and erosion of the surface rather than fracture failure.

When granulated material is used in the abrasion tester any abrasive wear is not likely to be controlled by material properties, it is more likely to be controlled by the operating conditions such as added mass, abrasion time, downward load, abrasion speed and counterbody and substrate properties.

The nature of the surface and substrate combined with the nature of the particle affect the amount of abrasive wear. Particle shape and hardness affect abrasion. Granulation cannot significantly affect any of the properties that affect abrasion except to make the abrasive process largely particle independent.

More granules => more abrasion
Smaller granules => more abrasion (when dosed by constant mass)

Very few of the granules dosed onto an abrasion sample plate are involved in the abrasion process – most of them are pushed to the ends out of the way and are not re-entrained into the abrasion process. The granules that do remain cause abrasive wear.

There appears to be no relationship between binder content and abrasivity.

There appears to be no relationship between impellor speed and abrasivity.

There appears to be no relationship between granulation run time and abrasivity.

The material (primary particles) used to make the granules affects the abrasivity. Granules made from Wessalith (zeolite) are the least abrasive, precipitated calcium carbonate (PacalH) is just as abrasive as crushed calcium carbonate (Omyacarb and Durcal) of the same size.

Wessalith (Zeolite) powder and granules made from Wessalith are less abrasive than Calcium Carbonate powder and granules made from Calcium Carbonate.

This author believes that shape and material are the most important factors affecting the amount of abrasive wear.

The abrasivity of a granule appears to be largely independent of how the granulator is operated; it is dependent on the primary particle material, the shape of the granule and the size of the granule (but the dependence on size decreases with increasing sphericity).

14.10 Granule Compaction / Porosity

The Granule Compaction theory in this research, although being incomplete and not rigorously tested, forms a mechanistic model for consolidation of a granule and its internal granule. This provides a coherent interpretation of formulation and processing parameters, consistent with existing literature, which allows useful qualitative predictions to be made. More importantly, when applied sensibly to a series of results such as the relationship between strength and binder ratio it can prevent incorrect interpretation of the results by allowing confounding and compounding effects to be taken into account (as shown in the transformation from a indirectly proportional trend in Plot 44 to a directly proportional relationship in Plot 45).

The compaction theory indirectly backs up the relationship that decreasing porosity (by compaction) increases strength. It shows qualitatively how things such as increasing impellor speed and increasing run time, which both increase strength, decrease the porosity by granule compaction.

A model has been proposed to represent the reduction in porosity of a granule with time and secondly the subsequent consolidation and squeezing out of binder to form surface wet granules. The model allows the theoretical prediction of the amount of binder on surface wet granules as a function of time, Eqn. (21). This model allows qualitative predictions of how changes in the granulation process and formulation will affect the consolidation rate and final surface wetness.

Further work needs to be done on the Granule Compaction Theory, specifically:

1. Confirming that the algorithm for packing spheres is correct and useful
2. Establishing how the packing factor, length term and binder thickness term can be determined for use in the general equation for interparticle space

3. Designing specific experiments to test the theory of internal granule compaction

The granule compaction theory is useful for making qualitative predictions about how a particular granulation batch will evolve when changes are made to the existing recipe and ingredients; it is not possible to make predictions about how a completely new recipe and ingredients will granulate.

Higher impellor speeds lead to greater granule consolidation.

Longer run times lead to greater granule consolidation.

Granule consolidation eventually leads to surface wetness (assuming enough binder is present).
Surface wet granules leads to snowballing.

The interparticle space, B_v, of a regular packing arrangement of spheres can be described by a generic equation in terms of an arrangement factor, k', the sphere diameter, d', and the binder thickness, a'.

$$B_v = 1 - \frac{k' d'^3}{(d' + a')^3} \qquad (13)$$

The factor, k', for body-centred cubic packing $k' = \pi\sqrt{3}/8$ and for a tetrahedral control volume (approximation based on tetrahedrons being approximated to pyramids within an Icosahedron) $k' = \pi\sqrt{2}/5$.

14.11 Results Database

Not enough results were produced to satisfactorily determine the random errors associated with the property tests.

The labelling system is very effective. Every result from a single test has a unique ID and this allows results to be easily traced back to the originating batch, this also allows data

from several different tests to be linked together in relationships in the database. This is powerful as an analytical tool. Not only can any data be listed within a single test procedure to determine the variations, but it can be linked to any other granule property with the ability to selectively analyse the results based on the processing and formulation parameters used to make the different batches. This means that compounding and confounding data can be easily identified and removed from a trend – for example the strength against binder content trend was reversed when data points associated with liquid binder were removed.

The linked data tables are all set-up for easy data entry and designed to allow the maximum amount of variation in studies to be carried out without the relationships and queries becoming too impractical and unwieldy. Every table has its own forms for data entry and because they are linked to the master High-Shear Granulation table the pull-down menus reduce the possibility of data entry errors – it is not possible to enter granule property test data for a batch unless the batch details (formulation and processing conditions) have been entered in the master table.

The database is transferable to other projects. The way the database is set up allows data from many different researchers to be entered and compared on a "universal" dataset. This makes increases the value of an individual data set as it can be compared directly to a lot more information in order to get general trends or the queries can be easily set so that only trends from within their dataset are compared.

A major limitation of the database is: there is no option to use 2 feed powders or 2 feed binders, however it would be a fairly simple task for a researcher to either copy the database and add new columns (which would limit the usefulness of the database as the new data would not be comparable to other data) OR they could combine the information on the 2 powders into a single column and put the necessary ratios in the special procedures box.

14.12 General

The formulation and processing parameter conditions chosen as the model for this research are not suitable for producing granules consistently. We were not able to reproduce a single batch following any of the sets of conditions listed in the Experiments table of the results database, appendix H, (experiments consistently produce smearing, or snowballs with a few experimental conditions but that is rather pointless). It is concluded that any set of formulation and processing parameter conditions can be thought of as falling into 1 of 3 granulation regimes:

1. Unstable
2. Transition
3. Stable

It is believed that a granulation batch either falls completely within one of these 3 categories and that stable and transition regimes exhibit a bit of instability in certain size classes within the batch. Reynolds, et al., [24] data shows an unstable region between 200 and 400 microns within his batch of granules.

This work has not found all the property to property relationships that are required to use granulation to make designer granules; however this research did manage to identify several relationships and provides a tool (in the form of the database) to find the rest.

Granulation still remains a "black art" and is likely to remain so. This research shows that granulation is very system specific in terms of actually getting stuff to granulate in the first place and the properties of the granules that are produced. Trends from one system are applicable to others but not in the quantitative manner required to produce designer granules but in a qualitative manner allowing general predictions.

The difference between agglomeration and aggregation needs to be distinguished. Many researchers in the literature interchange the two, but there is a difference (see definitions in the appendix) and the properties of a particular group of particles will depend upon whether they are true granular agglomerates or granular aggregates. Microgranules, of the size dealt with in this research, have a tendency to aggregate by electrostatic attraction

and weak binder bridges making them appear larger than they are and affecting the results of size dependent analyses.

The chopper should not be called a chopper because it doesn't chop anything, a better name would be a redistributor.

Using a mixture of water and PEG as a binder for Calcium Carbonate is not possible; the $CaCO_3$ dissolves in the water and leaves a slurry mess in the high-shear mixer.

The Rota-Junior (high-shear granulator) used in this research was initially believed to be damaged or not functioning correctly (the result being smearing on the walls and underneath the impellor blade), but it is now believed that the granular batch reproducibility issues relate to the other equipment (such as sprayer) and more likely due to the combination of formulation parameters used.

Acknowledgements

This thesis would not have been possible without the support and encouragement of my friend and supervisor Dr. Agba Salman, without his support I would probably have abandoned this work long before the end.

Thanks go to Unilever for the financial support of this research and specifically to Matthew Pickles for his ideas and guidance in the early stages of the work and for arranging the initial placement using the specialist equipment at the Unilever Port Sunlight research facilities.

I would also like to thank all my friends and family who encouraged me and kept me sane during my research and the writing up period.

I would specifically like to thank Jin Sheng Fu for passing on his knowledge in the early parts of my research and enabling me to get off to a flying start.

Special thanks has to go to Bob Sochon, Sellasi Dorvlo and Seth Ong. The help with conducting experiments that these three gave me in the summer of 2004 enabled me to produce enough meaningful results on which to base my work.

Chris Turner and Stuart the technicians deserve thanks for their patience and work they did on making and maintaining the experimental rigs.

Thanks go to Dr. Rob Dwyer-Joyce from the Mechanical Engineering department for his helpful advice on tribology and the pleasant manner of our meetings.

Finally I would like to thank all those people who are too numerous to name personally who I have worked with and offered tit-bits of advice and kept the personal and social side of my research fun and exciting.